



NTNU – Trondheim
Norwegian University of
Science and Technology

Laboratory investigation on salt migration and its effect on the geotechnical strength parameters in quick clay mini-block samples from Dragvoll

Rikke Nornes Bryntesen

Geotechnology

Submission date: July 2014

Supervisor: Bjørge Brattli, IGB

Co-supervisor: Arnfinn Emdal, BAT
Tonje Eide Helle, Statens Vegvesen

Norwegian University of Science and Technology
Department of Geology and Mineral Resources Engineering

TGB4930 Engineering Geology and Rock Mechanics, Master thesis,
spring 2014

Rikke Nornes Bryntesen

Laboratory investigations on salt migration and its effect on the geotechnical strength parameters in quick clay mini-block samples from Dragvoll

Background

Addition of salt as ground improvement in quick clay was studied in the sixties and seventies. Various types of salt and their effect on the mechanical behaviour of the clays were tested concluding that potassium chloride is the most effective salt. An increase of both the undisturbed and the remoulded shear strength was evident as well as an increase of the liquid limit. A recent laboratory study at NTNU carried out in 2012 confirms these findings. The previous studies only consider the impact from the changes in the geochemical environment. However, storage of samples has a great impact on the mechanical properties as well.

This master thesis is a laboratory study on how the mechanical properties in mini-block samples extracted from Dragvoll are affected as they are stored over several weeks in a) de-aired distilled water and b) fully saturated potassium chloride solution.

Content

The master thesis consists of:

- 1) A literature study focusing on
 - a. the influence of mineralogy and geochemistry on geotechnical properties
 - b. the impact of storage on the geotechnical properties
- 2) Laboratory work
 - a. index testing, atterberg limits, triaxial and oedometer testing
 - b. salt content and pH
 - c. bulk and clay mineralogy by XRD analysis
- 3) Discussion about the causes of changes in the geotechnical properties with special emphasis on how big portion is a result of storing, and how big portion may be as a result of the geochemical changes in the clay.

Based on the experience from this work, the student shall come up with recommendations for further work.

Organizing

The thesis is part of the research program «Naturfare – infrastruktur, flom og skred (NIFS)» a collaboration between the Norwegian Public Roads Administration, the Norwegian government's agency for railway services and the Norwegian Water Resources and Energy Directorate. External supervisor is Tonje Eide Helle, the Norwegian Public Roads Administration.

Extent and hand in

The thesis has an extent of 30 points – i.e. equivalent of one semester.

The work is to be handed in as a technical report with introduction and formulation of the problem, literature of relevant mechanisms, and presentation of obtained results. Clear conclusions and proposed further study will be credited.

The thesis is to be handed in digitally, as set forth by the Department of Geology and Mineral Resources Engineering.

Submission date

14th July 2014

Bjørge Brattli

Professor

Department of Geology and Mineral Resources Engineering

Acknowledgment

This master thesis is written at the Norwegian University of Science and Technology in a collaboration with the Norwegian Public Roads Administration. The work was carried out during spring 2014.

I would like to thank my supervisors Bjørge Brattli and Arnfinn Emdal for there help and discussions when needed, and for making it possible to write this thesis, as a collaboration between the Department of Geology and Mineral Resources Engineering and the Department of Civil and Transport Engineering. A special thanks is directed to Tonje Eide Helle for help, discussions and guides, especially during the last period.

Gratitude is also directed to all staph at the geotechnical department, for there help with this thesis. Especially Helene A. Kornbrekke, Jan Jøland for there guidance in the laboratory work. And Gunnar Winther, Anders S. Gylland and Einar Husby for the tremendous work of extracting the mini block samples in difficult conditions and for their guidance and explanations in the field.

I would also like to thank Laurentius Tjihuis for his help during preparations, analysis and interpretation of XRD analysis.

Finally I would like to thank family and friends for support and feedback on the report, especially Bent Even, Anne Kathrine and my mother, Heidi.

Abstract

Investigations of the effect of salt diffusion as ground improvement of quick clay is important to provide a clear understanding of the method, to be able validate the potential of commercial use. Previous extensive investigations by laboratory work has been carried out. Laboratory investigations of salt migration lead to extended storage time for the clay samples, as diffusion in clays is considered a slow process.

The objective of the work is to analyze the effect of KCl diffusion in relation to potential weathering and storage effects. The effect is analyzed in the laboratory with regards to both geotechnical properties, variations in pH and salinity. A literature study of previous findings related to salt migration and storage effects on both geotechnical properties and geochemistry, is also considered.

A series of mini block samples are submerged in cells containing deaired, ionized water and deaired, KCl solution. The samples are stored in the cell in a time period from 42 to 102 days. The samples are investigated in the laboratory to provide results relating to undisturbed and remoulded strength parameters, compressibility and general geotechnical properties. pH and salinity is also recorded. The findings are compared to a detailed depth profile of reference parameters, from a previous investigation done on mini block samples from the same bore hole. Tests are also carried out in sections throughout the water and salt treated clays, to map changes with regard to the time dependent diffusion and weathering.

The results indicated a general increase in peak undrained shear strength for the samples stored in KCl solution, approximately 50% of the observed general increase is also observed in the clay stored in water. A minor increase of plasticity limit is seen in both the water and salt treated samples. The comparison between sections for each sample show no clear deviations between the sections. Further, results from the salt migrated samples confirm the findings from previous investigations.

The samples are to some extent effected by weathering, in particular the peak undrained shear strength resulting from triaxial tests. However, the geotechnical properties observed after salt migration are changed to such an extent that the clay show a completely different behavior. The same distinct change is not observed in the clays only exposed to potential weathering.

The comparability between the samples are however, considered to be relatively low due to inhomogeneity in the soil profile and varying storage time prior to testing and cell installation. Loss of samples during sampling also lead to occasional large distance in depth, between the compared results.

Sammendrag

Undersøkelser av effekten av saltdiffusjon som grunnforsterkning i kvikkleire er viktig for å gi en klar forståelse av metoden og for å validere potensialet i kommersiell bruk. Grundig forskning ved laboratoriearbeid er tidligere blitt utført. Ved laboratorieundersøkelser av saltmigrering må leireprøver lagres over lang tid, ettersom diffusjon i leire er ansett som en langsom prosess.

Formålet med arbeidet er å analysere effekten av KCl diffusjon i forhold til potensiell forvitring og lagringseffekt. Effekten blir analysert i laboratoriet med hensyn til både geotekniske egenskaper, variasjoner i pH og saltinnhold. Litteraturstudie av tidligere funn knyttet til saltmigrering og lagringseffekter av både geotekniske egenskaper og geokjemi er også vurdert.

En serie miniblokkprøver er innstallert i henholdsvis avluftet, ionisert vann og avluftet KCl-løsning, i spesiallagde lagringsceller. Prøvene blir lagret i cellene i et tidsrom på 42 til 102 dager. Prøvene er undersøkt i laboratoriet for resultater knyttet til uforstyrret og omrørt styrke, kompressibilitet og generelle geotekniske egenskaper. Resultatene blir sammenlignet med en detaljert dybdeprofil av referanseparametre, fra en tidligere undersøkelse utført på mini blokkprøver fra samme borehull. Forsøk er også utført i seksjoner gjennom den vann- og saltbehandlede leiren for å kartlegge endringer med hensyn til den tidsavhengige diffusjon og forvitringen.

Resultatene indikerte en generell økning i maksimal udrenert skjærstyrke for prøvene lagret i KCl-løsning, omtrent 50 % av den observerte generelle økningen ble også observert i leire lagret i vann. En liten økning av plastisitetsgrensen er sett i både vann- og saltbehandlede prøver. Sammenligningen mellom seksjoner for hver prøve viser ingen markante avvik mellom seksjonene. Videre bekrefter resultatene av de saltmigrerte prøvene liknede funn observert i tidligere undersøkelser.

Prøvene blir til en viss grad påvirket av forvitring, særlig maksimal udrenert skjærstyrke fra triaksial test. Imidlertid er de geotekniske egenskapene, observert etter saltmigrering, forandret i en slik grad at leiren viser en helt annen oppførsel. De samme endringene er ikke observert i leire kun utsatt for potensiell forvitring.

Sammenlignbarheten mellom prøvene er imidlertid ansett for å være relativt lav på grunn av inhomogenitet i jordprofilet og varierende lagringstid før testing og celleinstallasjon. Tap av prøver under prøvetaking førte også til varierende avstand i dybden mellom de sammenlignede resultatene.

Contents

Acknowledgment	i
Abstract	iii
Sammendrag	v
1 Introduction	3
2 Theory	5
2.1 Quick clay	5
2.2 Mineralogy	6
2.3 Influence of pore water chemistry on clay particles	8
2.3.1 Electric double layer	8
2.3.2 Cation exchange capacity	10
2.3.3 Preliminary study of salt treatment in quick clay	11
2.3.4 Effect of weathering in quick clay	17
2.4 Storage effects in clay	17
2.4.1 Effect of aging on geotechnical index properties of clay	18
2.4.2 Effect of aging on undrained shear strenght	20
2.4.3 Effect of aging on consolidation	22
2.4.4 Impact of aging on pore water chemistry	24
3 Dragvoll research site	27
3.1 Background geology	28
4 Sampling	31
4.1 Mini block sampler	31
5 Preparations and previous investigations	33
5.1 Previous investigation	33
5.2 Preparations	34
6 Method	37
6.1 Block sample sectioning	37

6.2	Methodology	40
6.2.1	X-ray diffraction analysis (XRD)	40
6.2.2	Geochemistry	41
6.2.3	Geotechnical index tests	43
6.2.4	Oedometer	46
6.2.5	Triaxial test	47
7	Results	51
7.1	Observations	51
7.2	Grain size distribution	53
7.3	XRD	54
7.4	pH and pore water salt content	55
7.5	Geotechnical index results	58
7.5.1	Unit weight	59
7.5.2	Water content and Atterberg limits	59
7.5.3	Falling cone	63
7.6	Oedometer results	66
7.7	Triaxial test results	71
7.8	Summary of results	83
8	Discussion	89
9	Conclusion	97
10	Further investigation	99
	Bibliography	101
A	Salt content conversion chart	107
B	Samples	109
C	XRD Results	113
D	Oedometer tests on reference samples	127
E	Oedometer tests on samples stored in water and KCl solution	145
F	Triaxial test on reference samples	159
G	Triaxial test on samples stored in water and KCl solution	167
H	Oedometer comparison	189

List of Figures

2.1	Silicone-oxygen tetrahedral sheet [30]	6
2.2	Magnesium or aluminium oxygen octahedral [30]	7
2.3	Assembly of sheets and unit layers of phyllosilicates [30]	7
2.4	Illustration of the diffuse electric double layer [59]	8
2.5	Illustration of the effect of pore water ion concentration on the diffuse double layer [46]	9
2.6	The effect of ion concentration on inter particle repulsion [59]	10
2.7	Effects of different salts at varying concentrations on remolded shear strength in illite- and chlorite dominated clays [33]	12
2.8	Recorded influence of salt concentration on sensitivity, remoulded and undrained shear strength, water content and liquid and plastic limit [4]	13
2.9	Reduction of liquid limit by leaching of salty pore water. The circle represents the natural water constant of the clays. a) Clay prior to leaching, b) clay after leaching	13
2.10	Recorded changes in a depth profile after installation of salt wells at a quick clay location [11]	14
2.11	Increase in preconsolidation pressure by weathering and salt migration, respectively [5]	16
2.12	Relationship between yield stress and pH at constant water content of clay at different concentrations of NaCl (salinity) [58]	16
2.13	Recorded influence of dry crust and weathering zone at a quick clay location [5], based on [32]	17
2.14	Moisture loss of London clay during storage, using different sealing methods [10]	18
2.15	Influence of storage time on geotechnical index tests [25]	19
2.16	Loss of peak undrained shear strength in triaxial test results by internal swelling [37] (data from Bjerrum [6] NGI [35])	20
2.17	Effect of storage time on normalized s_u on samples obtained using different sampling methods [37]	21
2.18	Influence of storage time on preconsolidation pressure and modulus number [48]	22

2.19 Recorded changes in preconsolidation after 511-542 days, relative to fresh samples [37] (data from [18])	23
2.20 Effect of storage time in days on undrained strength from triaxial tests and preconsolidation pressure, respectively, on different sample quality. Modified [2]	24
2.21 Storage effects, in months, on remoulded strength, liquidity index and pH, relative to pore water ion concentration [26]	25
2.22 Direct relation between cation concentration and remoulded shear strength [26]	26
3.1 Test location and salt diffusion research area at Dragvoll [9]	27
3.2 Sedimentary map of the Dragvoll area. Modified [39]	28
3.3 Stages of sedimentation environment in the Dragvoll area depending on sea level by isostatic uplift	29
3.4 Cross section of the central Dragvoll area [14]	30
4.1 The different elements indicated on the mini block sampler [9]	32
4.2 Handling of the extracted sample (Photo: Rikke N. Bryntesen)	32
5.1 Illustration of cell assembly and installation of mini block samples	34
6.1 Cutting station for mini block samples (Photo: Rikke N. Bryntesen)	37
6.2 Sectioning of an ideal mini block sample	38
6.3 X-ray diffractometer and HCl test	40
6.4 Example result of interpreted output of the X-ray diffractometer	41
6.5 Dimensions of sections in the geochemistry layer	42
6.6 Illustration of triaxial equipment [9]	47
6.7 Illustration of the stepwise consolidation phase in triaxial tests	48
6.8 Equipment for triaxial specimen preparation. (Photo: Rikke N. Bryntesen)	49
7.1 Shells and stones found in the mini block samples (Photo: Rikke N Bryntesen)	51
7.2 Discoloration in the mini block sample periphery (Photo: Rikke N Bryntesen)	52
7.3 Discoloration and water migration in silt layers (Photo: Rikke N Bryntesen)	52
7.4 Results from hydrometer test on grain size distribution in the depth profile and resultant clay content with depth [9]	53
7.5 Change in pH in section 1, 2 and 3, for reference samples and samples stored in water and KCl solution	57
7.6 Index tests from reference samples, describing the depth profile [9]	58
7.7 Assembly of recorded unit weight, presented with depth	59
7.8 Variations in water content and Atterberg limits, between the sections, of water treated samples	60
7.9 Variations in water content and Atterberg limits, between the sections, of salt treated samples	60

7.10 Assembly of all results of water content and Atterberg limits, presented for each section	61
7.11 Summation of results of water content and Atterberg limits in each sample, presented with depth	62
7.12 Sum of resultant liquidity and plasticity index for each sample	63
7.13 Variations in undrained and remoulded shear strength and sensitivity, between the sections, of water treated samples	64
7.14 Variations in undrained and remoulded shear strength and sensitivity, between the sections, of salt treated samples	64
7.15 Variations in undrained and remoulded shear strength for each section within the samples	65
7.16 Sum of results over each sample, of undrained and remoulded shear strength and sensitivity presented with depth	65
7.17 Illustration of interpretation method for preconsolidation pressure	66
7.18 Illustration of modulus number in the NC range and OC deformation modulus	66
7.19 Illustration of consolidation coefficient, a value is chosen at a desired stress level. In this thesis at the in situ vertical stress	66
7.20 Assembly of stress strain results from the reference samples (data from [9])	67
7.21 Assembly of stress strain results from samples stored in water	68
7.22 Assembly of stress strain results from samples stored in KCl solution	68
7.23 Comparison of the stress strain results from reference samples and samples stored in water and KCl solution	69
7.24 Preconsolidation pressure and OCR results from each storage method, presented with depth	70
7.25 Modulus number in the NC range and OC deformation modulus results from each storage method, presented with depth	70
7.26 Interpretation of triaxial tests	71
7.27 Q-p plot of the reference samples (data from [9])	72
7.28 NTNU plot of the reference samples (data from [9])	73
7.29 Stress strain plot of the reference samples (data from [9])	73
7.30 Triaxial tests with calibration error	74
7.31 Q-p plot of samples stored in water	75
7.32 NTNU plot of samples stored in water	76
7.33 Stress strain plot of samples stored in water	76
7.34 Q-p plot of samples stored in KCl solution	77
7.35 NTNU plot of samples stored in KCl solution	78
7.36 Stress strain plot of samples stored in KCl solution	78
7.37 Assembly of triaxial results for each sample treatment, at depths between 3 and 5 m	79

7.38 Assembly of triaxial results for each sample treatment, at depths between 4 and 5 m	79
7.39 Assembly of triaxial results for each sample treatment, at depths between 5 and 6 m	80
7.40 Assembly of triaxial results for each sample treatment, at depths between 7 and 9 m	80
7.41 Peak and residual undrained shear strength from triaxial tests, presented by depth	82
A.1	108
C.1 Bulk XRD result	114
C.2 Bulk XRD result	115
C.3 Bulk XRD result	116
C.4 Bulk XRD result	117
C.5 Bulk XRD result	118
C.6 Bulk XRD result	119
C.7 Bulk XRD result	120
C.8 Bulk XRD result	121
C.9 Bulk XRD result	122
C.10 Clay fraction XRD result	123
C.11 Clay fraction XRD result	124
C.12 Clay fraction XRD result	125
H.1 Comparison of storage method, preconsolidation pressure	190
H.2 Comparison of storage method, preconsolidation pressure	191
H.3 Comparison of storage method, preconsolidation pressure	192
H.4 Comparison of storage method, preconsolidation pressure	193
H.5 Comparison of storage method, preconsolidation pressure	194

List of Tables

2.1	Cation exchange capacity of common clay minerals. Modified [15] based on [30]	11
5.1	Outline of tests and storage time	33
5.2	Outline of tests, storage time and diffusion time	35
6.1	Descriptions and location of tests for each mini block sample	39
7.1	Bulk mineralogy in the depth profile	54
7.2	Mineralogy of the clay fraction	54
7.3	Results from pH conductivity analysis in reference samples	55
7.4	Results from pH conductivity analysis in samples stored in water and KCl solution	56
7.5	Assembly of peak and residual undrained shear strength the the percent reduction from peak, for each treatment method.	81
7.6	Summarized results from index, pH and conductivity analysis	84
7.7	Summarized results from oedometer tests	86
7.8	Summarized triaxial test results	87
B.1	Mini block samples before and after cell storage (photo: Rikke Nornes Bryntesen and Tonje Eide Helle)	109

Chapter 1

Introduction

The research program «Naturfare – infrastruktur, flom og skred (NIFS)» is a collaboration between the Norwegian Public Roads Administration, the Norwegian government's agency for railway services and the Norwegian Water Resources and Energy Directorate. The research program consist of seven projects. This master thesis is part of the quick clay project, related to stabilizing of quick clay.

Stabilization methods of slopes in quick clay areas can be challenging. Based on investigations carried out in the 60- and 70-ties, quick clay can be stabilized by the addition of salt. Various types of salt and the related effect on the mechanical behavior of the clays were tested. Potassium chloride was concluded to be the most effective in relation to stability and diffusion time. Significant increase of both the undisturbed and the remoulded shear strength were evident, as well as an considerable increase of the liquid limit. Despite promising results, the method was considered expensive and time consuming. Thus, salt migration as ground improvement is not used today. New installation methods are considered to be more efficient and less expensive. Hence, further study of the effect of salt diffusion is needed.

A recent laboratory study at NTNU, carried out in 2012, confirms the results obtained in the previous studies. However, the studies only consider the impact from the changes in the geochemical environment. Storage and weathering effects on the mechanical properties, related to laboratory investigations on salt migration are not considered.

Laboratory investigation of quick clay from Dragvoll, an quick clay area known by the local geotechnical community, were carried out as part of a study of the initial geotechnical and chemical conditions in the depth profile. The study was performed as part of a project assignment, carried out by the author. The laboratory tests was carried out on undisturbed samples extracted using the NTNU developed mini block sampler. Several of the extracted mini block samples were used in this master thesis. The area is also related to research of salt migration by salt well installation, a research carried out by Ph.D. candidate Tonje Eide Helle.

In this thesis a review of previous findings and the theory behind salt migration as ground improvement, including influence of mineralogy and geochemistry on geotechnical properties, is carried out. Where the effect of storage time and weathering in relation to both geochemistry and geotechnical properties are considered.

An overview of the geological conditions in the area as well as a rough description of sampling method is described. Including descriptions of preparations and analysis methods.

Laboratory investigations including index testing, triaxial compression test and CRS oedometer tests. And also measurements of pH and pore water salinity are carried out on samples stored in fully saturated potassium chloride solution and samples stored in distilled water, both in a close to anaerobic environment. Analysis of bulk and clay mineralogy are also included. The results are compared to reference samples, tested as part of the project assignment carried out by the author, and presented and discussed. Conclusions and proposed further investigations are included.

Chapter 2

Theory and literature study

2.1 Quick clay

Clay consist of particles with grain size less than 0.002 mm and is, by NS3007 [40] defined as soil consisting of more than 15% clay fraction. Clay originate from mineral grains in bedrock, degraded by natural processes of mechanical erosion and weathering.

During the last ice age, vast quantities of soil was degraded, transported and deposited in the seawater by glaciers. When clay is deposited in salt water the particles flocculates and create an open grain structure with salty pore water. Ions in the salty pore water cause strong electrochemical attraction forces between the particles [52]. Isostatic uplift caused elevation of the marine clay above the littoral zone, exposing the marine clay to fresh water infiltration in the form of precipitation and ground water flow. Thus, causing leaching of the salty pore water [16]. Leaching of the ion rich pore water in marine clay is a slow process due to the low hydraulic conductivity of the sediment. Acceleration of ion leaching is to be expected in clay containing thin layers of slit or sand due to the higher hydraulic conductivity in the respective layers. Clays around Trondheim, Norway are usually silty clays with silty layers, consisting of 20-50 % clay [52].

Quick clay is defined as a clay with remoulded shear strength (s_r) below 0,5 kPa [34].

Natural seawater normally has a salt content of about 35 g/l. The pore water salinity of which a clay can be defined as quick has been discussed. However, Torrance [56] concludes that below a limit of 2-5 g/l the attractive forces between the clay particles is sufficiently weakened for the clay to be defined as quick.

According to Torrance [56], there are several aspects influencing the development of quick clay in addition to reduction of pore water salt content. These include:

- Low activity minerals must dominate minerals in the sediment. For clay minerals, this include illite and chlorite.
- A high natural water content is required, consolidation after sedimentation of the clay must therefore be low or non-existing.
- Ion composition in the pore water is of great importance in the formation of quick clay.

2.2 Mineralogy

The clay minerals are structured as plane sheets and belong to the mineral family phyllosilicates. These minerals are assembled by arrays of tetrahedral- or octahedral sheets. The tetrahedral sheet consist of stacked silicone-oxygen tetrahedral, assembled as illustrated in Figure 2.1. While, the octahedral sheets are assembled by magnesium or aluminium oxygen octahedral Figure 2.2. The tetrahedral- and octahedral- arrays or sheets are assembled by shearing of oxygen atoms or hydroxyls, respectively. The assembly of sheets, stacked parallel to each other, resulting in plate like clay minerals are displayed in Figure 2.3. Characterized by the assembly of arrays and how the clay mineral structure is held together defines the various clay minerals [30].

Isomorph substitution, replacement of the silicon in the tetrahedral layer or aluminium in the octahedral layer with small atoms, usually of lower valence, within the mineral arrays changes the property of the minerals. Replacement of atoms of high valence to lower valence causes a net negative charge in the mineral layers in turn creating negatively charged clay particles [59]. To compensate for this negative charge, layers of water molecules and/or compensating cations or positively charged sheets are formed between the mineral layers [30].

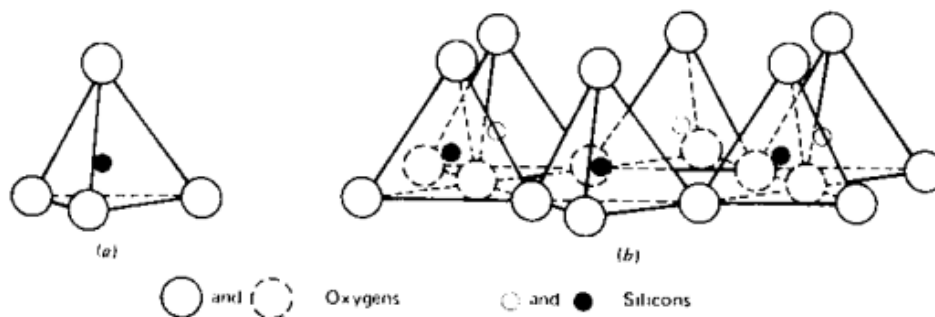


Figure 2.1: Silicone-oxygen tetrahedral sheet [30]

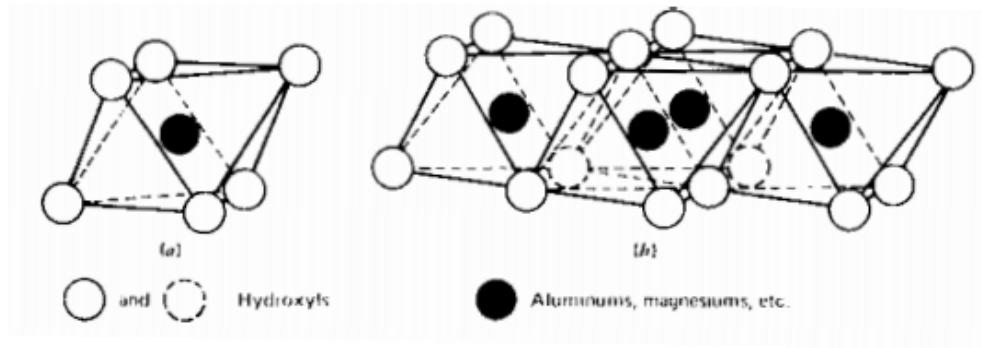


Figure 2.2: Magnesium or aluminium oxygen octahedral [30]

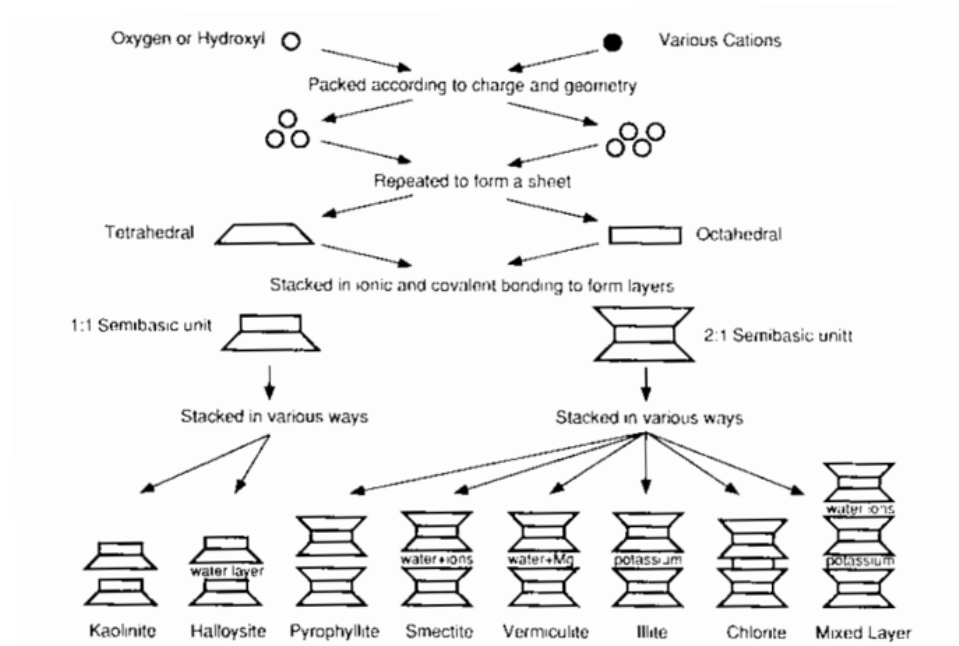


Figure 2.3: Assembly of sheets and unit layers of phyllosilicates [30]

Investigations by Berry and Jørgensen [3] and Emdal et al. [12], documented the normal mineral content in most sensitive Norwegian clays, including quick clays. The clays are usually dominated by chlorite, illite, muscovite, feldspar, and quartz. Where, chlorite and illite are clay minerals. Illite is essentially mechanically disintegrated muscovite i.e. smaller particles of muscovite, and may therefore be difficult to distinguish.

2.3 Influence of pore water chemistry on clay particles

The environment of deposition is of significant importance for sediment properties and pore water ion composition within the sediment. The minerals within the sediment will remain stable in the depositional environment. Leaching changes in the pore water environment, inducing reactions within the system to regain equilibrium.

2.3.1 Electric double layer

Surface forces influence soil behavior when particle sizes is below 2 μm , i.e. clay particles. The unbalanced electrical surface forces and small particle size of clay induce repulsive and attractive forces between particles. These forces are hugely dependent on pore water composition [30]. The clay minerals are, as explained by Mitchell and Soga [30] and van Olphen [59], usually thin, plate shaped and negatively charged particles. In completely saturated soil, the negatively charged particles will attract counter-ions, oppositely charged ions, which forms a sphere around the particle. This “surface charge and compensating counter-ion charge, accumulating in the liquid in the neighborhood of the surface particles” is defined as the electric double layer. The counter ion sphere within the electric double layer is referred to as the diffuse layer [59]. Simultaneously as the cations are attracted to the negatively charged clay particle, anions are repelled. The electric double layer is displayed in Figure 2.4. As illustrated, a higher density of ions is expected close to the surface of the clay particle.

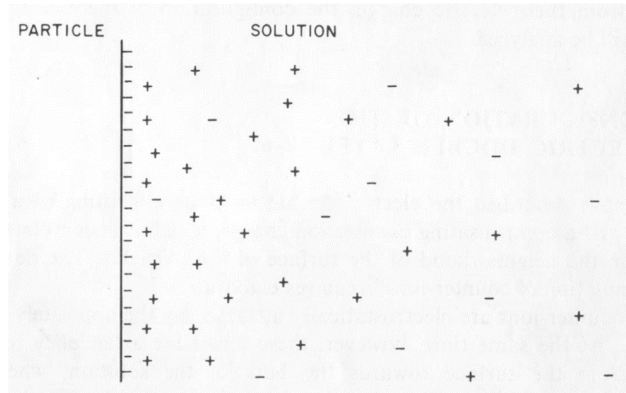


Figure 2.4: Illustration of the diffuse electric double layer [59]

The concentration of cations and anions, within the diffuse layer, decrease and increase respectively with distance from the particle. The ion concentration, with respect to distance from the particle is displayed in Figure 2.5. The thickness of the diffuse double layer decreases and increases with ionic strength of the cations and anions within the pore water, respectively. Increase in ion concentration within the water phase decrease the thickness of the double layer due to reduced surface potential. Higher ion concentration in the pore water causes, as seen in Figure 2.5, a much higher cation concentration close to the particle surface but also a rapid decent in the concentration with distance. [30] [59]

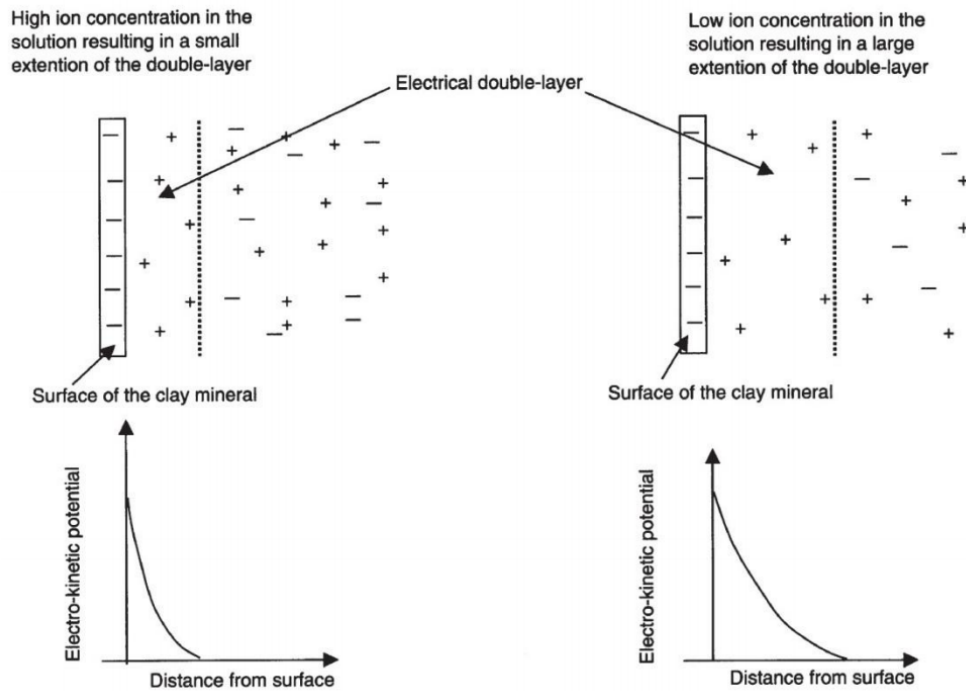


Figure 2.5: Illustration of the effect of pore water ion concentration on the diffuse double layer [46]

Two clay particles of close proximity will induce alterations within the diffuse layers and change the ion distribution within the layers, instigating repulsive energy between the particles. Thus, particles with compressed diffuse layers will have a shorter ranged repulsive energy between them. As displayed in Figure 2.6, the repulsive energy decreases as particle separation increases. Quick clay, which has a low salt concentration, will have a denser structure after remoulding as the low attractive forces reduces the flocculating ability. The attraction energy of the clay particles, which is generated by the van der Waals forces, does not depend on ion concentration in pore water, as displayed in Figure 2.6. [59] [30] [1]

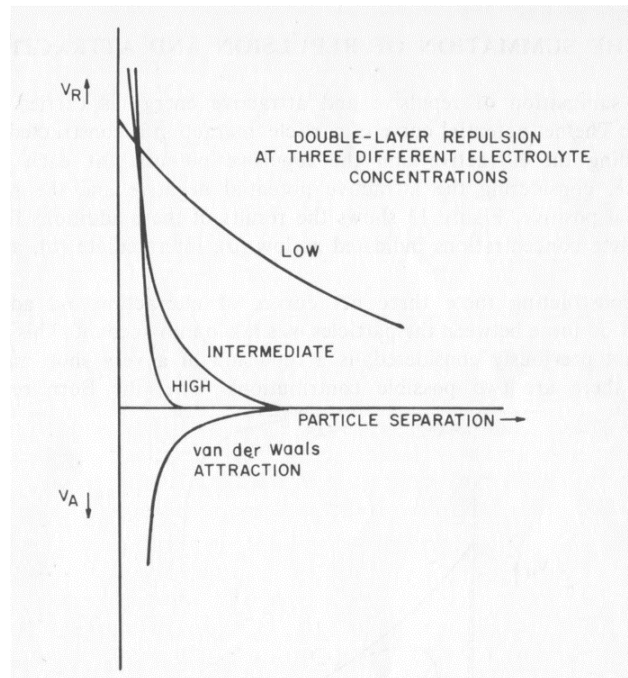


Figure 2.6: The effect of ion concentration on inter particle repulsion [59]

2.3.2 Cation exchange capacity

In most clay minerals, compensating cations can be exchanged by other cations available in the pore water. These cations are referred to as exchangeable cations [59]. A change of ion composition in the pore water may therefore encourage an exchange of cations. Cation exchange capacity (CEC) is the analytically determined amount of exchangeable cations in milliequivalents per 100 g of dry clay [59]. Even under saturated conditions, water cannot penetrate between the mineral layers of illite and chlorite, only the surface ions are available for exchange. Thus, illite and chlorite has low CEC [59]. Table 2.1 displays CEC of common clay minerals, CEC is also directly linked to specific surface area.

Table 2.1: Cation exchange capacity of common clay minerals. Modified [15] based on [30]

Clay mineral	Specific surface area [m^2/g]	CEC [$meq/100g$]
Kaolinite	10-20	3-15
Montmorillonite	50-120 (primary) 700-840 (secondary)	80-150
Illites	65-100	10-40
Vermiculite	40-80 (primary) 870 (secondary)	100-150
Chlorite		10-40

2.3.3 Preliminary study of salt treatment in quick clay

As set forth in the previous sections, the cations are of severe importance to the characteristics of a clay and therefor also to the geotechnical properties [30] [56]. The pore water of marine clays contain abundant amounts of sodium (Na^+) and is the dominant adsorbed cation. Lower amounts of magnesium (Mg^{2+}), calcium (Ca^{2+}) and potassium (K^+) with only small traces of iron (Fe^{2+}) and aluminum (Al^{3+}) are generally represented in the pore water of marine clays. Talme [53] and Soderblom [50] concluded that formation of quick clay not only depend on reduction of pore water salinity. Also, the composition of ions in the pore water is essential to the formation of quick clay. Investigations presented by Talme et al. [54] displayed low concentrations of Mg^{2+} and Ca^{2+} in quick clays, compared to non quick clay. Moum et al. [31] concluded that the sum of K^+ , Mg^{2+} and Ca^{2+} in the pore water effects the sensitivity. The Gouy theory predicts that the ions of higher valence is accumulated near the particle, therefor a higher concentration of cations of higher valence is found in the diffuse layer as opposed to the bulk pore water [59]. Which, support the order of replacing power of cations as proposed by Mitchell and Soga [30]: $Na^+ < Li^+ < K^+ < Rb^+ < Cs^+ < Mg^{2+} < Ca^{2+} < Ba^{2+} < Cu^{2+} < Al^{3+} < Fe^{3+} < Th^{4+}$. Further, the increase of shear strength observed by adsorption of cations is presented in the following order $Na^+ < Fe^{2+} \leq Mg^{2+} \leq Ca^{2+} < Fe^{3+} < K^+ < Al^{3+}$ [27]. The relation between different ione concentration and remoulded shear strenght, is displayed in Figure 2.7. The liquid and plastic limits are also hugely effected by cations in the pore water. The order of which different cations increase the Atterberg limits of clay is presented in the following order: $Na^+ < Fe(OH)_3 = Fe^{2+} = Mg^{2+} = Ca^{2+} < Fe^{3+} < Al^{3+} = K^+ < Al(OH)_3$ [28].

Studies performed by Bjerrum and Rosenqvist [7], provide confirmation of the leaching hypothesis. Leaching tests were performed on artificially sedimented clays, the results displayed a change in sensitivity from 5, increasing to 110 after leaching. A sample sedimented in fresh-water retained a sensitivity of 5 to 6. Changes in strength and sensitivity of a normally consolidated marine clay, subjected to leaching, were studied by Bjerrum [4]. The results showed an increase of sensitivity with decreasing pore water salt content. Both liquid limit, undisturbed and remoulded shear strength displayed a decreasing trend with decrease in pore water salinity, as presented in Figure 2.8. However, no significant changes in geotechnical properties were observed until a salt content of approximately 15g/l was reached. The survey displayed no changes in plastic limit, nor water content.

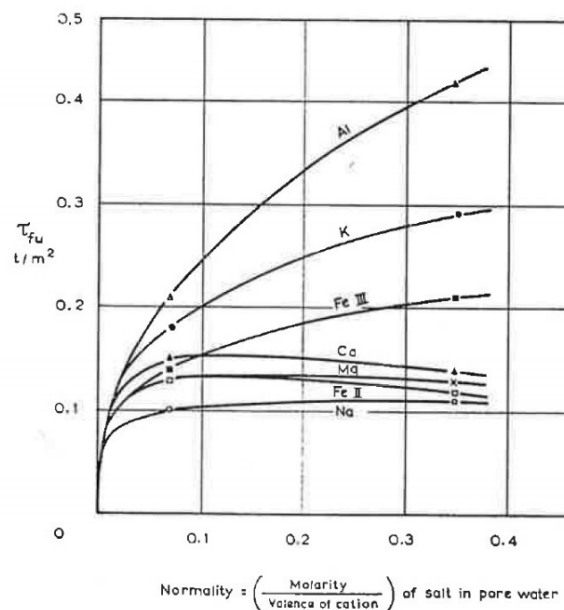


Figure 2.7: Effects of different salts at varying concentrations on remoulded shear strength in illite- and chlorite dominated clays [33]

A post-depositional decrease of liquid limit, during which the water content remains constant is therefore a requirement for quick clay development. Leaching of the salty pore water cause, as previously described, a reduction in liquid limit. The natural water content is therefore situated above the plastic range, i.e. the area between the plastic and liquid limit, after the reduction of pore water salinity, as illustrated in Figure 2.9. Thus, the clay behaves as a liquid if remoulded [57].

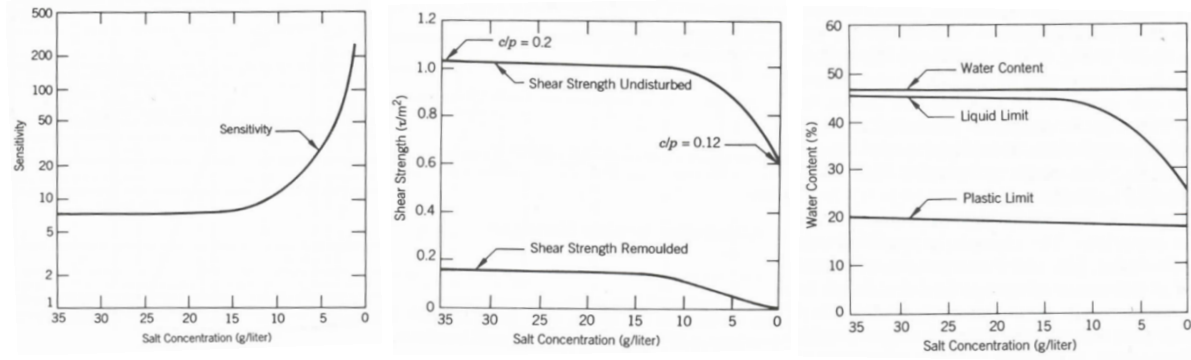


Figure 2.8: Recorded influence of salt concentration on sensitivity, remoulded and undrained shear strength, water content and liquid and plastic limit [4]

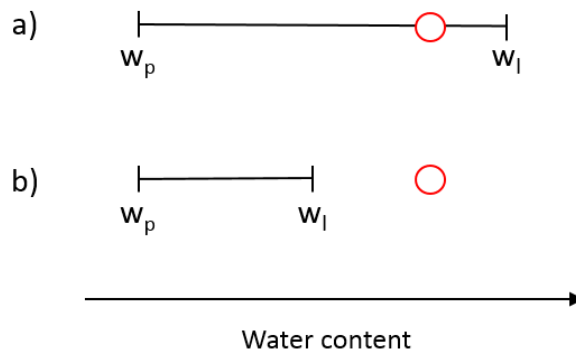


Figure 2.9: Reduction of liquid limit by leaching of salty pore water. The circle represents the natural water constant of the clays. a) Clay prior to leaching, b) clay after leaching

Several investigations of chemical remediation has been carried out using different salts and concentrations. According to the results presented in Figure 2.7, $AlCl_3$ has the greatest increase of remoulded shear strength[31]. However, $AlCl_3$ is only partially dissolved in the natural ground water in Norwegian quick clay due to the relatively high pH of approximately 8, normally seen in these clays. Potassium chloride is easily dissolved in the natural conditions of the water phase and show, as previously presented, a considerable effect on the remoulded shear strength. According to Moum et al. [33] the effect of KCl on remoulded shear strength is doubled relative to what is acquired from NaCl. The clay in which NaCl is used as chemical remediation would also eventually return to quick clay, with Na-dominated pore water of low salinity. By using KCl, the potassium salt will also eventually leach out but will leave behind a K-dominated clay with a sufficiently high liquid limit. Thus, quick clay is not likely to reoccur. Further, KCl will diffuse more rapidly in the sediment [31] and has the longest reach of diffusion into the clay, according to laboratory investigations [17].

Supply of K^+ , causing an increased K^+/Na^+ ratio, induce a collection of K^+ ions the clay surface, as K^+ has a higher replacing power, compared to Na^+ . The increase of K^+/Na^+ ratio will lead to an alteration of geotechnical properties of the clay. [5] [11]

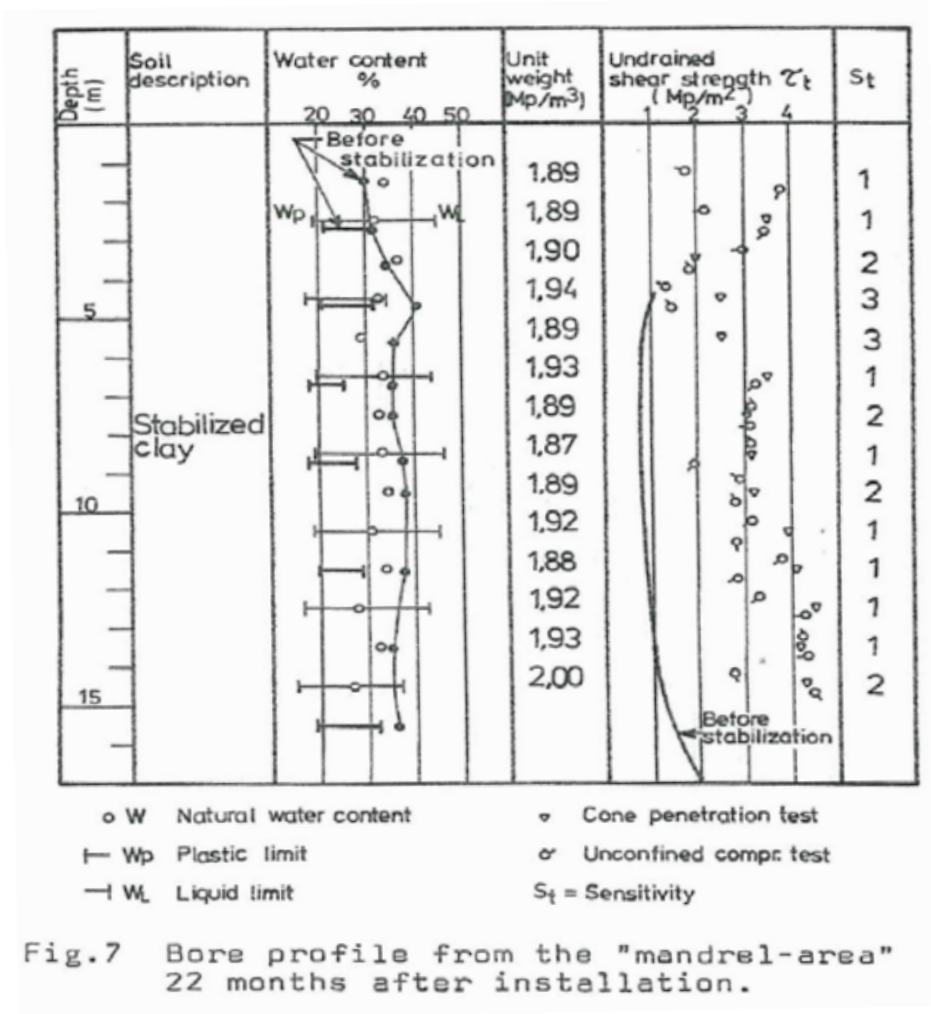


Figure 2.10: Recorded changes in a depth profile after installation of salt wells at a quick clay location [11]

Eggestad and Sem [11] installed salt wells, for KCl diffusion, for large-scale ground reinforcement of very sensitive, soft marine clay. 21 months after installation the shear strength had increased with a factor of approximately 2.3, 15 cm from the salt well. While, 80 cm from the well an increase of approximately 1.4 was observed. Figure 2.10 displays the resultant geotechnical index tests on undisturbed samples from the reinforced area, 22 months after salt well installation, compared to the initial condition. A clear alteration of the geotechnical properties was observed. The liquid limit was increased to above the natural water content. The natural water content decreased to some extent and the plastic limit slightly increased for most of the depth profile, resulting in increased plasticity. The remoulded shear strength increased with a factor of up to 4. After 3 years it was concluded that the average shear strength of the reinforced clay increased with 200% [11].

Experiments have shown that the preconsolidation pressure, p_c , of a clay can change by alterations in pore water chemistry. Replacing Na by K can increase p_c and the resistance to consolidation of the soil [23]. Investigations carried out by Bjerrum [5], proposed that the increase of plasticity and shear strength developed an increase of resistance against deformations. Undisturbed clay samples were permeated with K^+ rich water, and oedometer tests run on the samples displayed an increase in p_c from 360 to 560 kPa. In addition, the compressibility of the clay, exceeding the increased p_c , was reduced. Which, was related to the increased plasticity of the clay. As presented in Figure 2.11 a, the increased preconsolidation pressure highly relates to the increased undrained shear strength observed at increased K^+/Na^+ ration. The results of the oedimeter tests are presented in Figure 2.11 [5]. Torrance [55] also concluded that introduction of potassium and magnesium salts increased the consolidation resistance of the soil. The p_c can also be reduced during leaching. However, it may presumably be partially regained by secondary consolidation [55].

Observations state that pore water of high pH tend to disperse clay systems [29]. Increase of pH dissociate H^+ ions, and leads to enlarged negative charge of clay particles and thus increase inter particle repulsion. Positive charge will dominate the edges of clay particles for low pH, inducing enhanced flocculation. Acid attacks less stable minerals in the post-glacial marine clay, chlorite and carbonates, and release ions into the pore water. Thus, reduce inter particle repulsion and encourage flocculation of clay particles [58]. Chemical stabilization of quick clay by salt diffusion may decrease the pH of the material. Hence, the effect of pH on clays of varying pore water salinity was studied by Torrance and Pirnat [58]. Derived results are displayed in Figure 2.12. The results display, as expected, a reduction of yield stress with increasing pH for both concentrations of NaCl.

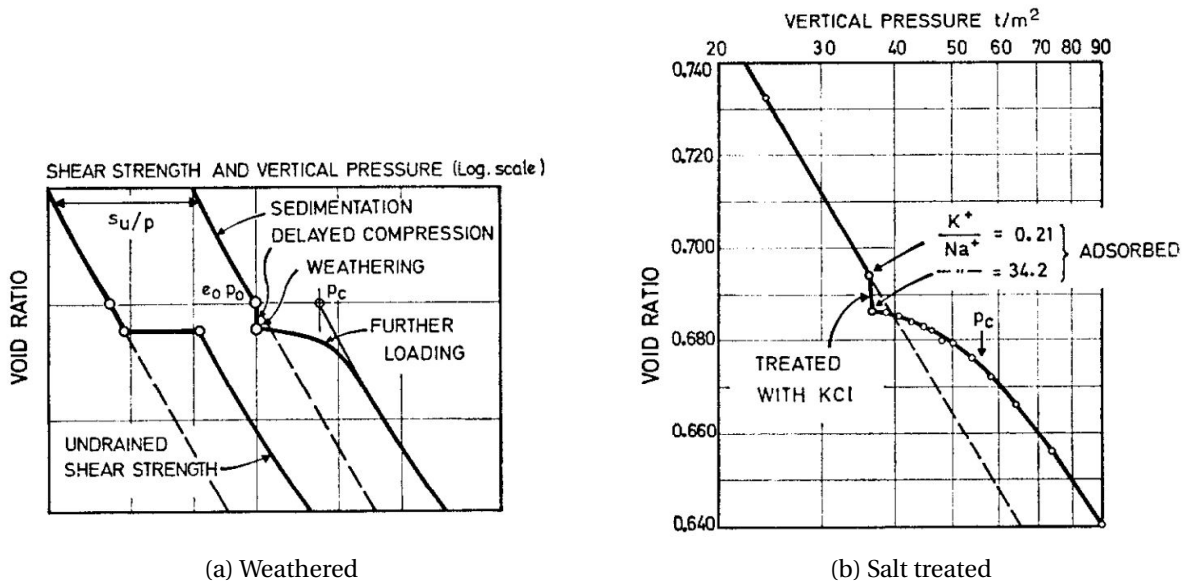


Figure 2.11: Increase in preconsolidation pressure by weathering and salt migration, respectively [5]

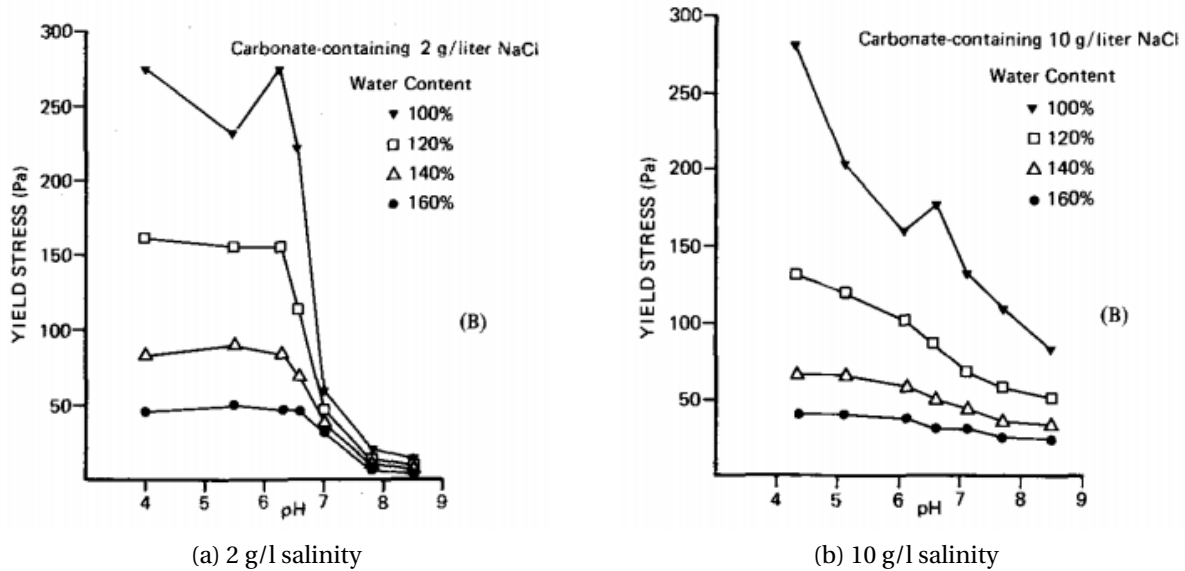


Figure 2.12: Relationship between yield stress and pH at constant water content of clay at different concentrations of NaCl (salinity) [58]

2.3.4 Effect of weathering in quick clay

As percolating rain water cause leaching of Na^+ , the rain water also contains dissolved O_2 and CO_2 . Where the supply of oxygen cause oxidation, forming acid and together with the carbon-dioxide, lowers the pH. At sufficantly low pH, disintegration of felspar, mica and chlorite commences, releasing cations of higher replacing order, which is adsorbed on the clay surface. The effect cause similar changes of geotechnical parameters as described by salt migration, such as increased preconsolidation pressure, as seen in Figure 2.11. Influence on index parameters are displayed in Figure 2.13. As the change is related to percolating water, the effect is reduced with depth [5]. The effect is explained further in section 2.4.4, as the in situ weathering is related to storage effects in quick clay.

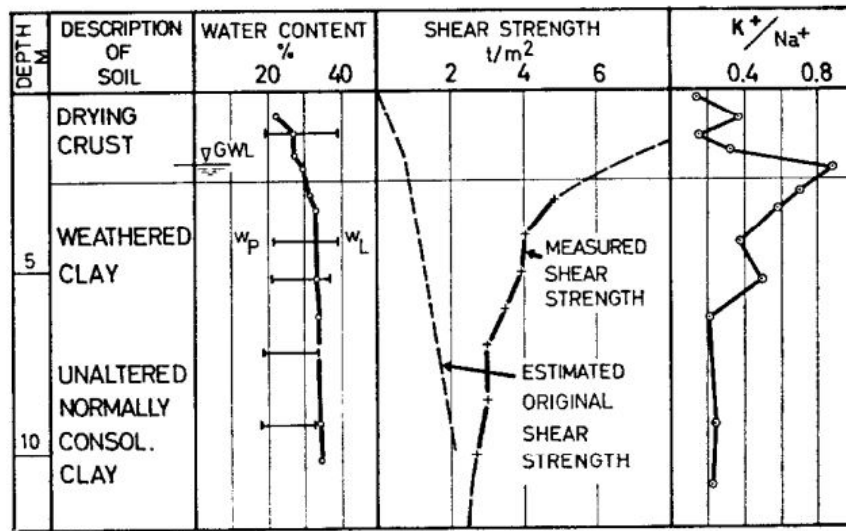


Figure 2.13: Recorded influence of dry crust and weathering zone at a quick clay location [5], based on [32]

2.4 Storage effects in clay

Several factors are related to post sampling disturbance and alterations of soil samples. Related to storage time, moisture loss and chemical alterations are the dominant mechanisms of soil sample disturbance [10].

2.4.1 Effect of aging on geotechnical index properties of clay

Migration of water and moisture loss will affect stored clay samples over time, the effect was first documented by Hvorslev [20]. Further studies based on storage effects of London clay with several approaches of sealing techniques were studied by Heymann [19] and displayed in Figure 2.14. Loss of moisture during storage, cause pore fluid suction. Which, may lead to an increase of the mean effective stress experienced by the samples during laboratory tests.

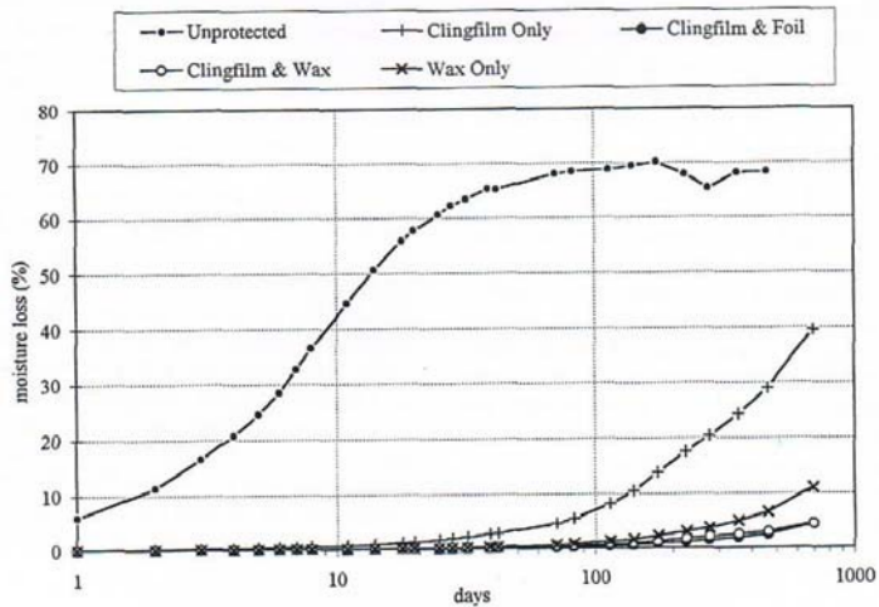


Figure 2.14: Moisture loss of London clay during storage, using different sealing methods [10]

Extensive study carried out by the Swedish Geotechnical Institute (SGI) documents the storage effect of Swedish clay. Tests were performed on portions of the recovered samples immediately after sampling, while the remaining samples were retained and stored for up to 750 days. The result show no decrease of water content in the clay samples. The survey indicated an increase of liquid limit, which by definition, results in a reduction of liquidity index. In addition, a general decrease in sensitivity was detected [18]. Previous investigations, performed by Leroueil et al. [24], show a relation between liquid limit and remoulded shear strength as expressed by equation 2.1, indicating that a decrease in liquid limit leads to an increase in remoulded shear strength (S_r), in kPa. Which is consistent with the results obtained in the SGI survey. The laboratory investigation of index parameters therefor indicated a reduction of both clay sensitivity and plasticity as a result of sample storage.

$$S_r = \frac{1}{(I_L - 0.21)^2} \quad (2.1)$$

An intensive survey by Lessard and Mitchell [26] was carried out to determine the effect of storage time on quick clay. Regardless of the storage procedure, an increase in remoulded shear strength and liquid limit, and a decrease in sensitivity and liquidity index was observed. Water content, plastic limit and undrained shear strength from falling cone test displayed no consistent deviations with storage time.

Studies carried out by Lessard [25], where quick clay was stored for up to 1 year, clearly display the same trend. Continually testing resulted in geotechnical properties as seen in Figure 2.15. The results stated that aging cause loss of quick clay characteristics [25] [26].

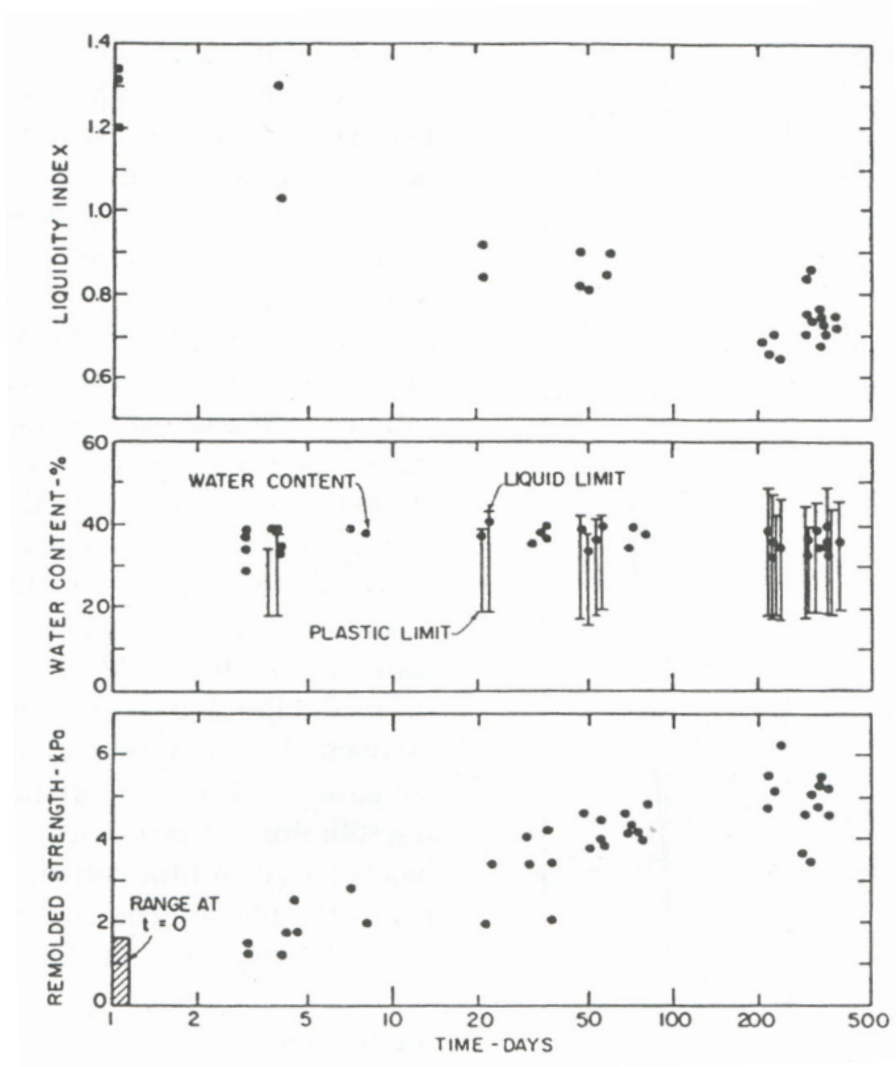


Figure 2.15: Influence of storage time on geotechnical index tests [25]

2.4.2 Effect of aging on undrained shear strength

Bjerrum [6] and NGI [35] performed Anisotropically Consolidated Undrained (CAU) triaxial tests on quick clay, immediately after sampling and after 2-3 days storage time. All samples were consolidated to the in situ stress condition. The tests, displayed in Figure 2.16, indicate a 13.5% reduction of the peak undrained shear strength (s_u) of the stored samples, relative to the samples tested immediately after sampling. The deviation was explained by increase of internal swelling with time [6].

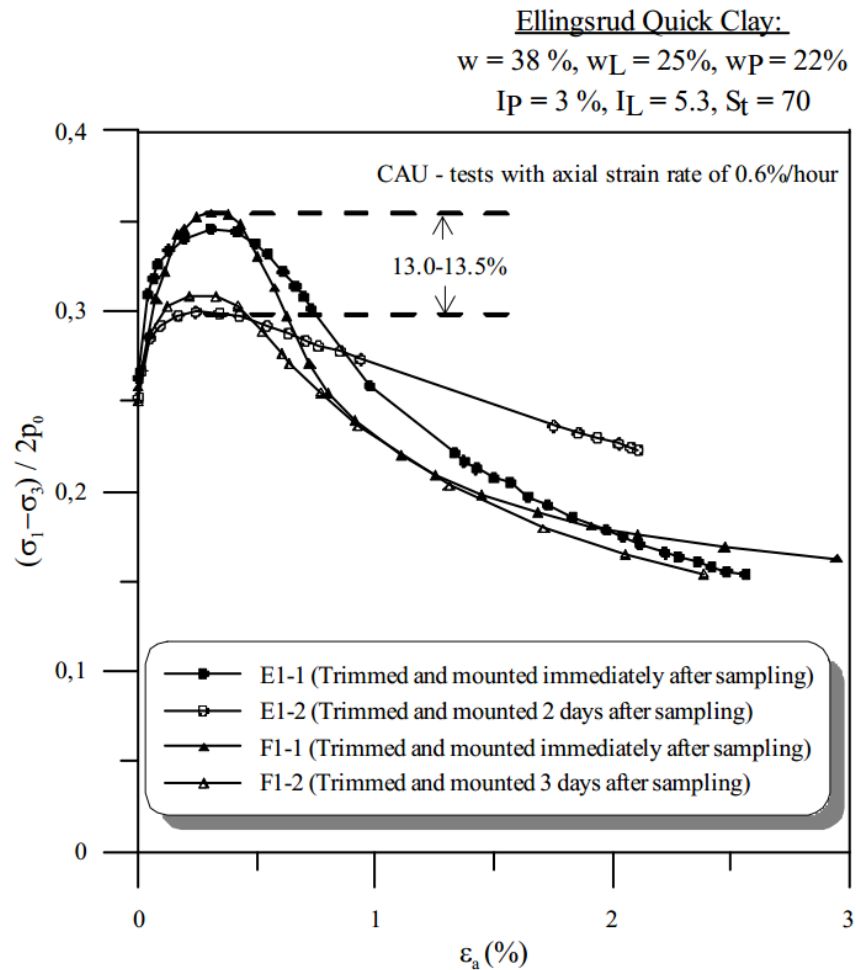


Figure 2.16: Loss of peak undrained shear strength in triaxial test results by internal swelling [37] (data from Bjerrum [6] NGI [35])

CAUc triaxial tests were performed by NGI on clay samples from various depths in Onsøy, Norway. The results were normalized with respect to in situ consolidation by NGI [37] and plotted with respect to storage time as seen in Figure 2.17. The block samples and 72 mm samples displayed a decrease in s_u of up to 5% and 10%, respectively. Results from 54 mm samples were considered unrealistic due to initial sample disturbance. Laboratory tests by Rochelle et al. [47] in block samples stored in a humid environment for several years, also displayed a decrease in s_u after storage time.

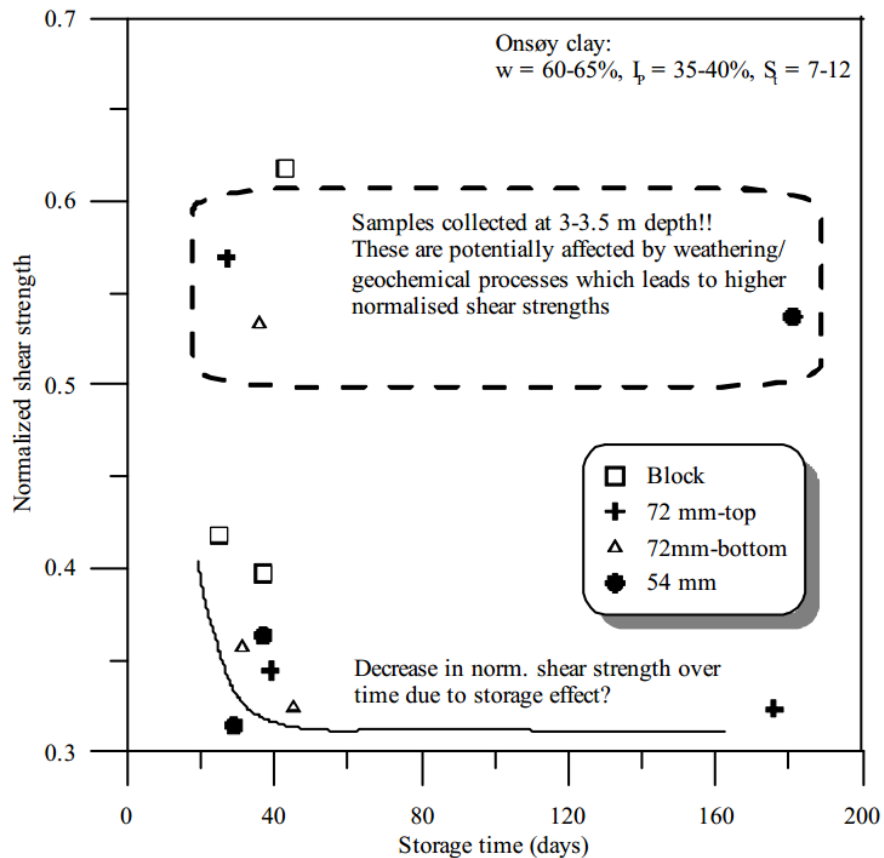


Figure 2.17: Effect of storage time on normalized s_u on samples obtained using different sampling methods [37]

2.4.3 Effect of aging on consolidation

Bozozuk [8] analyzed consolidation results performed on a block sample of over consolidated, sensitive marine clay. The tests displayed a decrease in preconsolidation pressure (p'_c) of 4.8% in samples stored between 2 and 17 months. Laboratory investigations by Rømoen [48] also show a decrease in p'_c after 2-3 weeks storage time. The tests also displayed a decrease of modulus number (m), as illustrated in Figure 2.18.

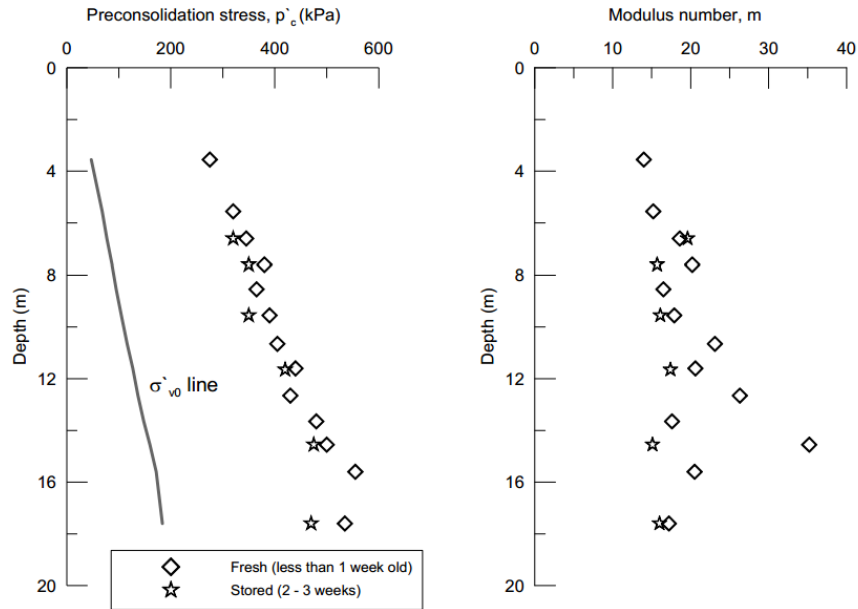


Figure 2.18: Influence of storage time on preconsolidation pressure and modulus number [48]

During the study performed by SGI, presented above in section 2.4.1, several Constant Rate of Strain (CRS) oedometer tests were performed immediately after sampling and after 18 months of storage time. The results were presented by the percent change in effective preconsolidation stress as displayed in Figure 2.19, and indicated a tendency of decrease in p'_c with time. However, several studies of the effect of storage time on the compressibility of clays, performed by Rochelle et al. [47] and NGI [36] indicated no clear deviation of p'_c of the stored samples, relative to specimen tested immediately after sampling.

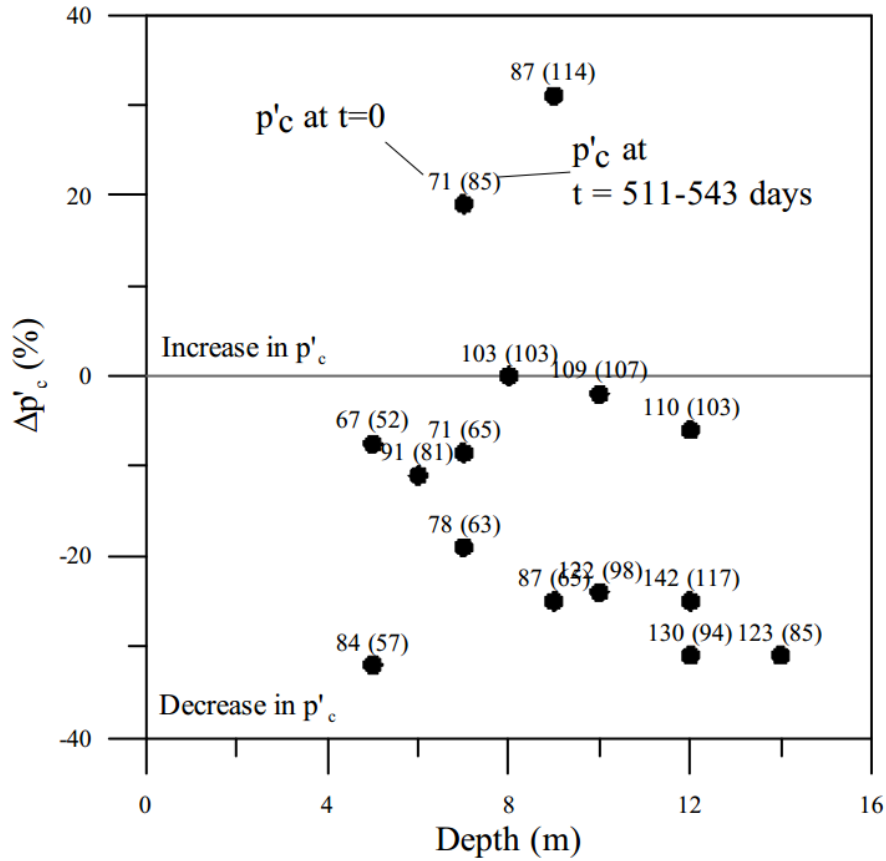


Figure 2.19: Recorded changes in preconsolidation after 511-542 days, relative to fresh samples [37] (data from [18])

A comprehensive study by Arman and McManis [2] resulted in distinct correlations between degradation of s_u and p'_c with specimen storage time and initial sample quality. The correlation is clearly illustrated in the results from the laboratory investigations, displayed in Figure 2.20 a and b. The block samples do not deteriorate with an increasing rate after 10 days, as observed in the 71 mm and 127 mm chore samples.

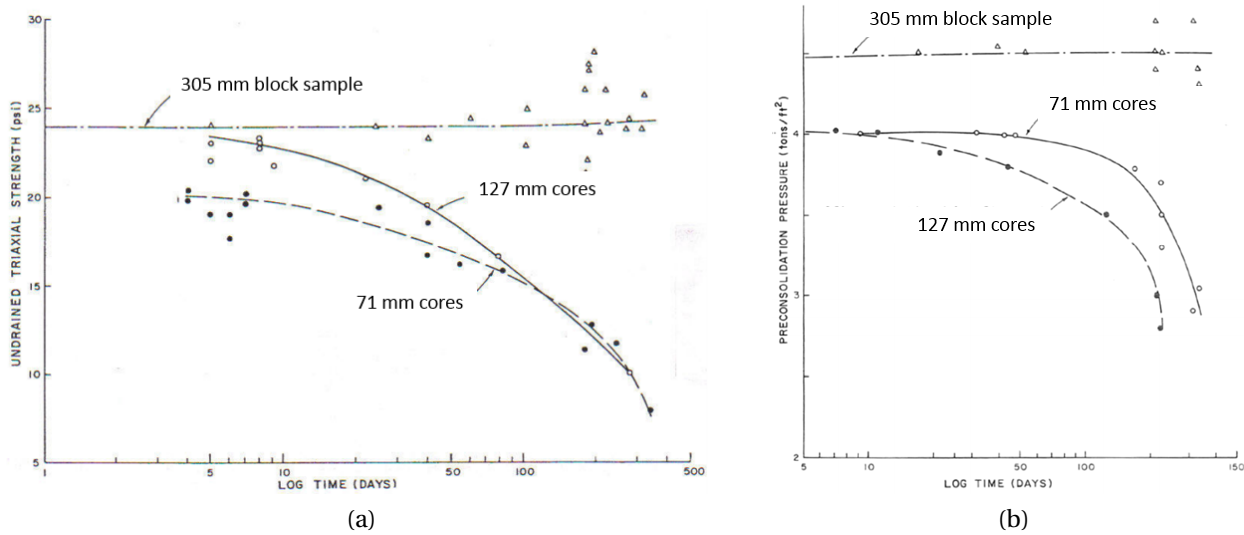


Figure 2.20: Effect of storage time in days on undrained strength from triaxial tests and preconsolidation pressure, respectively, on different sample quality. Modified [2]

2.4.4 Impact of aging on pore water chemistry

Changes of geotechnical properties in clay during aging must be seen in relation to changes in the chemistry. The study performed on LaBaie quick clay, by Lessard and Mitchell [26], presented in section 2.4.1, displayed results of geochemical changes in relation to aging. The results of geotechnical parameters and pore water chemistry are displayed in Figure 2.21. The investigation revealed an increase of pore water salinity and concentrations of divalent cations in the pore water and a decrease in pH with sample storage time. These changes reduce the extent of the electrical double layer and thus the particle repulsion in the clay. Hence, the geochemical changes are responsible for the increase of remoulded shear strength and decrease of I_L . As seen in Figure 2.22, the remoulded shear strength correlates with both the concentrations of divalent cations and total cations. The increase of Atterberg limits on stored clay sample in a study by Bjerrum and Rosenqvist [7], was related to an observed increase in potassium ions in the pore water.

The method of storage does not affect the correlations between remoulded shear strength and cation concentrations. However, it affects the required time for the chemical changes to occur [30].

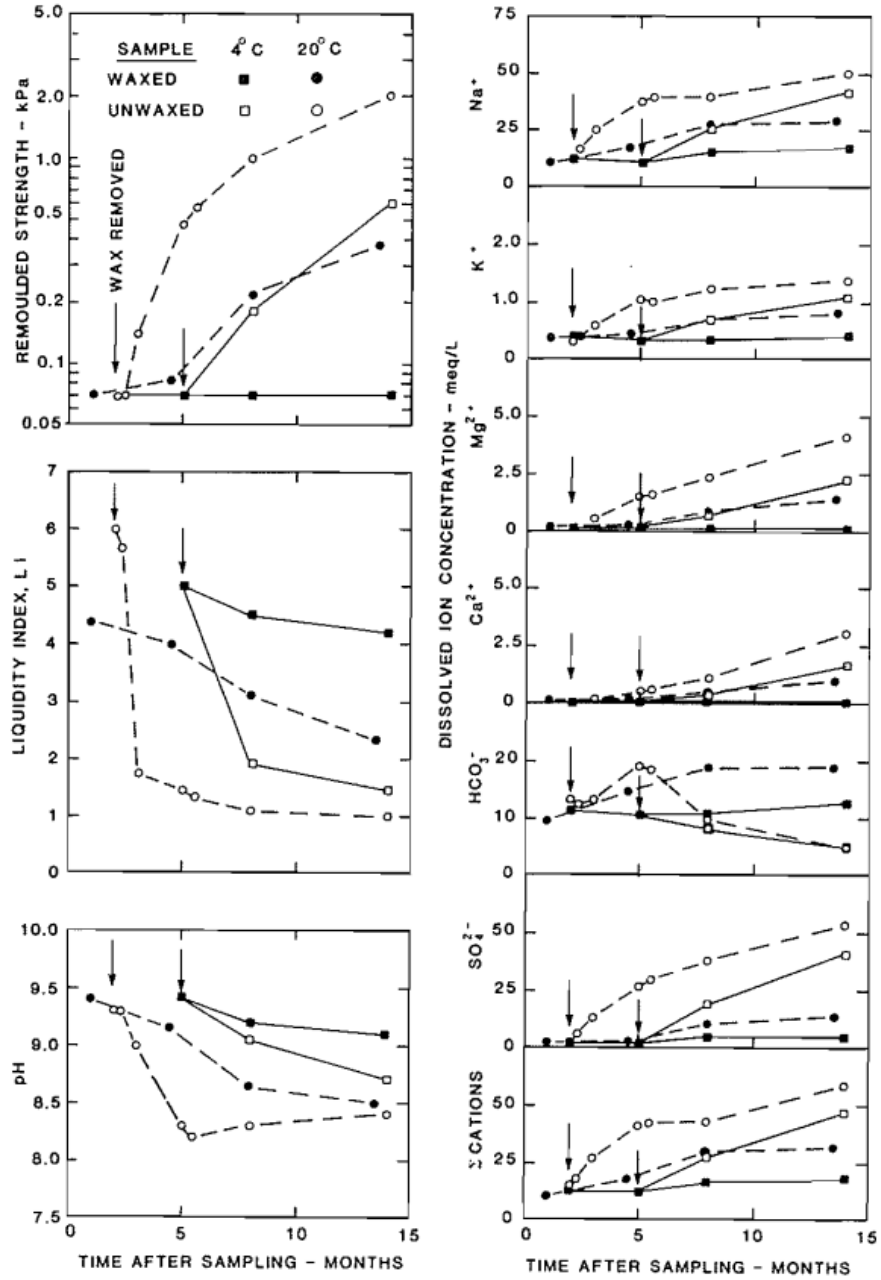


Figure 2.21: Storage effects, in months, on remoulded strength, liquidity index and pH, relative to pore water ion concentration [26]

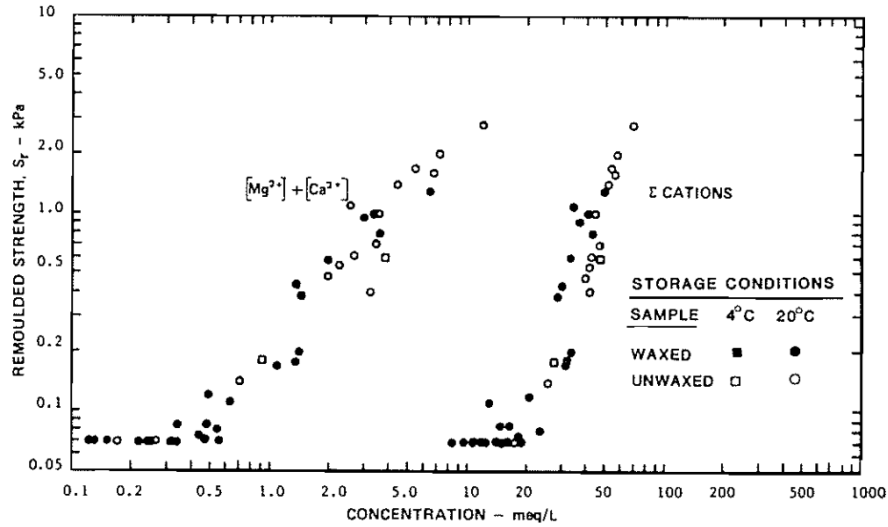


Figure 2.22: Direct relation between cation concentration and remoulded shear strength [26]

The observed chemical changes of quick clay are related to “the change from anaerobic to aerobic state and the accompanying changes in the microbial activity” as described by Söderblom [51]. Oxygen causes organic matter to oxidize to form carbonic acid, and oxidation of pyrite to form sulphuric acid and ferric hydroxide. A slow transformation of $Fe(OH)_3$ to $FeO - OH$ may cause brownish discoloration of the clay. Thus, oxidation cause the decrease in pH, seen in Figure 2.21. Sulphuric acid cause chemical weathering of calcite, releasing Mg^{2+} and Ca^{2+} in the pore water, which cause an exchange of absorbed cations on the clay particles. Thus, Na^+ and K^+ ions are released in the pore water, inducing an increase of pore water salinity [30].

Chapter 3

Dragvoll research site

Located east of central Trondheim, Norway, the Dragvoll area is displayed by the map in Figure 3.1. The salt diffusion research area by Ph.D. candidate Tonje Eide Helle is located within the marked area. Sampling for this thesis is done from 2 different bore holes within the indicated location, approximately 5 m apart. Sampling is carried out using the NTNU mini block sampler.

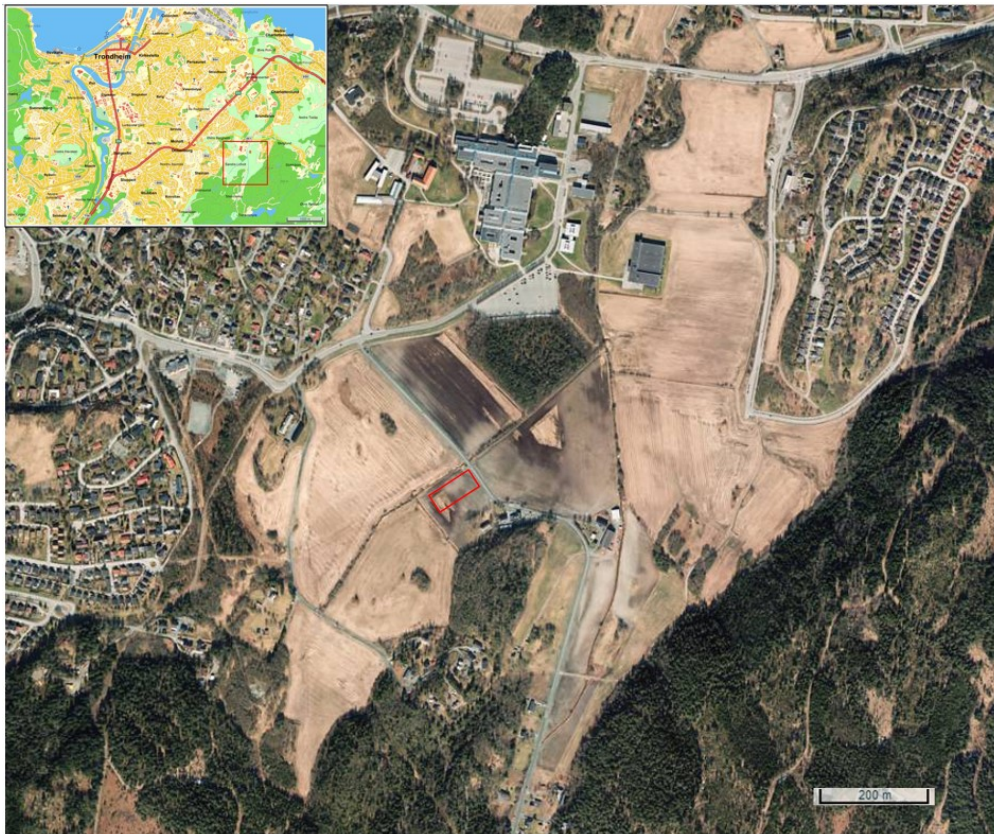


Figure 3.1: Test location and salt diffusion research area at Dragvoll [9]

3.1 Background geology

When inspecting the Dragvoll campus area today a series of low hills, covered with thin moraine layers and marine shore deposits, are surrounding the lower laying, flat area consisting of thick marine deposits and peat. A sediment map of the area is displayed in Figure 3.2. In the northern region the terrain falls and slopes toward the fjord, but as seen in Figure 3.2, a ridge of marine shore deposits act as a dam and provides a basin shaped area [14]. As seen from the map, the area is located close to the marine limit. The surrounding bedrock in the area consists mostly of greenstone and green schist [38].

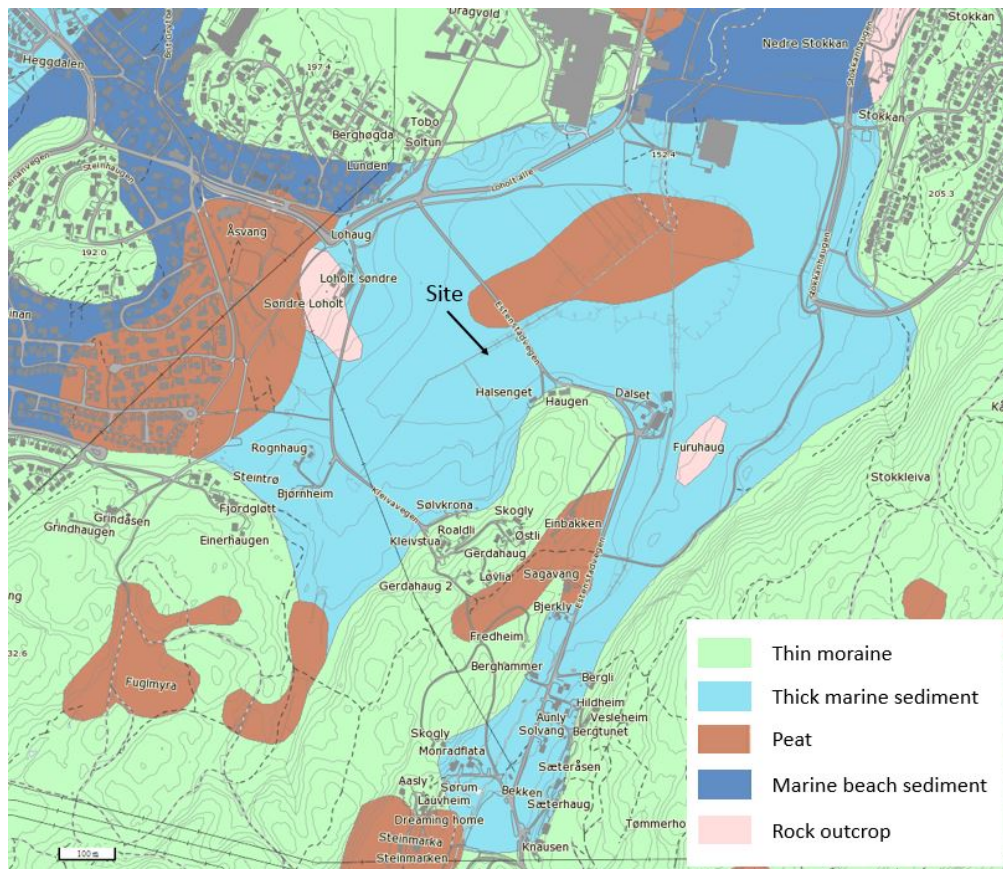


Figure 3.2: Sedimentary map of the Dragvoll area. Modified [39]



Figure 3.3: Stages of sedimentation environment in the Dragvoll area depending on sea level, a) water level at its highest, b) brackish water stadium, c) fresh water lake stadium, d) swamp and peat stadium. [9] (based on [13])

Carbone 14 dating is done to map the last deglaciation process in the Trondheim fjord area. It is estimated that the Dragvoll-Stokkan area was ice-free approximately 11 500 years ago. Due to a climatic setback the ice returned but only reached the edge of the Dragvoll area in the period 11 000-10 500 years before present (BP). Over time, the heavy overburden of the ice sheet had pressed down the land providing an elevated sea level and a marine limit as high as 178 m above the current sea level as displayed in Figure 3.3, a [13]. During the deglaciation extensive amounts of silt and clay sediments, nearly 50m deep, were deposited within the basin as marine sediments, recognised as glacial marine clay with shell bearing top layers [14]. As the ice retrieved, an elevation of land caused a gradually drop in the littoral zone. Approximately 10 000 years BP the sea level reached a point where the area is only in contact with the fjord during high tide, resulting in a saline lake covering the area as displayed in Figure 3.3, b. A rapid melt down of the residual ice caused a prompt isostatic uplift resulting in a rapid drop of sea level over the next 1 000 years, separating the area from the fjord and turning the saltine lake into a freshwater lake (Figure 3.3, c). Resulting in limnic sediment deposited over the marine clay. Erosion of the marine shore sediment section in the north, drained the lake and turned the area into a swamp as seen in Figure 3.3, d (9 000-8 500 years BP), creating peat layer on top of the stratigraphy [13]. Figure 3.4 displays a Vest- East going cross section of the central Dragvoll area displaying the rough stratigraphy of the area with approximately 6m of peat and limnic sediments covering the 50m of marine clay with high silt content [14]. The properties of the marine clay in the area has been altered with time and is today considered a quick clay [12].

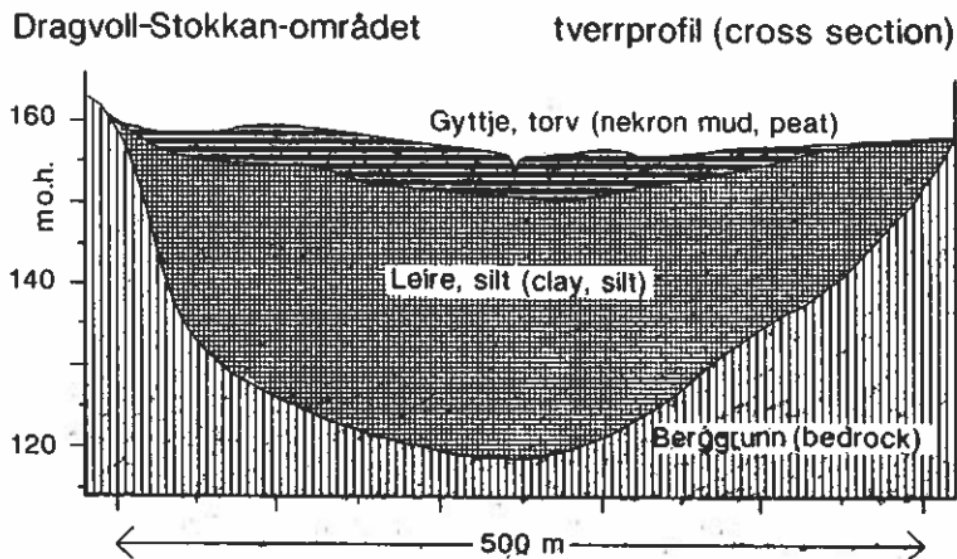


Figure 3.4: Cross section of the central Dragvoll area [14]

Chapter 4

Sampling

Soil sampling for geological and geotechnical investigations were performed in the area indicated in Figure 3.1, chapter 3.

4.1 Mini block sampler

The newly developed Mini Block sampler, created by the Geotechnical Division of the Norwegian University of Science and Technology, NTNU, is used for the extraction of undisturbed samples for geotechnical laboratory tests. The design is similar to the Sherbrook Block sampler, described in detail by Karlsrud et al. [22]. The main differences between Sherbrook and the Mini Block sampler includes:

- The Mini Block sampler carves cylinder shaped blocks with a sample diameter of 160mm and height of 250mm. The smaller size enables the sampler to fit between the front forks of the bore rig.
- The rotation direction is changed to match the rotation of traditional bore rigs.
- The release mechanism for the knives are changed and is easily triggered before the sample is extracted.

The sampling process for the mini block sampler starts with augering down to the desired depth, after which a cylinder is inserted to prevent sidewall material from entering the borehole. The mini block sampler is inserted and pressurized water is used to cut the soil as the sampler rotates and slowly moves downward. When the desired level is reached, the bore rig is stopped and the water supply is cut off. A weight is dropped on the release mechanism to activate the knives, as indicated in Figure 4.1. Thereafter the sampler is rotated to ensure detachment between the sample and underlying soil before it is carefully extracted.



Figure 4.1: The different elements indicated on the mini block sampler [9]



(a) Sample



(b) Sealing method

Figure 4.2: Handling of the extracted sample (Photo: Rikke N. Bryntesen)

The sample is cleaned for excess, disturbed soil with flowing water and the knives are bent back in position while the sample is positioned with care on a prepared pedestal, as seen in Figure 4.2. The sample is extensively wrapped in plastic foil and placed in a specially designed casing. After extraction, the mini block samples are stored in a cool environment, preferably of high humidity to reduce evaporation from the sample.

Chapter 5

Preparations and previous investigation

5.1 Previous investigation

Laboratory investigations on mini block samples of Dragvoll clay were carried out by Bryntesen [9]. An overview of the mini block samples with storage time is presented in Table 5.1. The samples were sealed with plastic foil, covered with a plastic bag with a damped cloth inside, and stored at approximately 7°C.

Table 5.1: Outline of tests and storage time

Bore hole	Block sample	Sampling date	Opening date	Days stored	note
1	3.0-3.25 m	25.9.13	3.10.13	8	Stored in 20°C
2	3.0-3.25 m	4.10.13	16.10.13	12	
2	3.25-3.5 m	4.10.13	14.10.13	10	Stored in 20°C
1	3.75-4.0 m	25.9.13	13.10.13	18	
2	4.0-4.25 m	4.10.13	18.11.13	45	
2	4.5-4.75 m	4.10.13	25.11.13	52	
1	5.0-5.25 m	27.9.13	1.10.13	4	
1	6.0-6.25 m	30.9.13	11.10.13	11	
2	7.7-7.95 m	30.10.13	27.11.13	28	
2	8.45-8.7 m	5.11.13	8.11.13	3	
2	8.7-9.0 m	8.11.13	12.11.13	4	

5.2 Preparations

Investigations of salt migration through quick clay is prepared for eight mini block samples. Four of the samples are to be subjected to diffusion of salt, while the remaining four is used as reference with regard to storage effect and weathering.

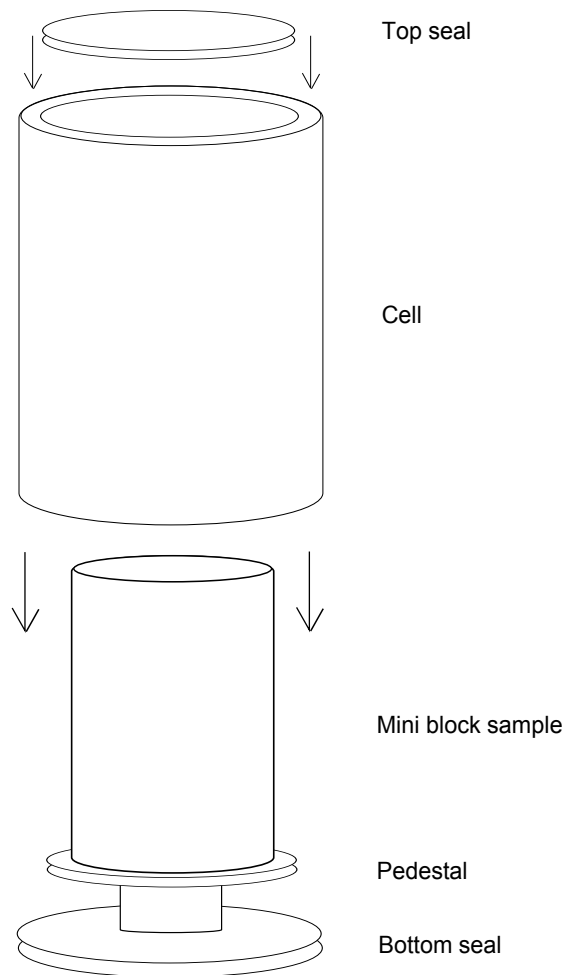


Figure 5.1: Illustration of cell assembly and installation of mini block samples

The mini block samples are placed in custom made diffusion cells, as seen in Figure 5.1. First, the pedestals holding the mini block samples are fitted with a bottom seal. Four of the samples are prepared for salt migration by removing the plastic foil covering the sample. Plastic foil is kept on the remaining samples to limit the extent of potential mechanical weathering. The cell is carefully directed over the block sample and fixed to the bottom seal. Large quantities of water is deaired by pressure boiling and saturated with N_2 gas before the water is transferred into the cell, using utter care not to disturb the sample or mix air into the liquid. Thereafter, Potassium chloride (KCl) is added to the four cells prepared for salt migration. Enough KCl salt is used to ensure saturated conditions for each cell at room temperature, i.e. $> 344\text{g/L}$ solid KCl . The cells must contain enough deaired, N_2 saturated KCl solution or water to cover the mini block sample. Cling wrap is placed over the water KCl solution, removing all trapped air, before the top seal is positioned on top of the plastic foil. Both the top and bottom seals are made air- and watertight using artificial grease. The cells, containing the samples, are stored in a cold environment of approximately 7°C .

Table 5.2 displays an overview of diffusion and storage time with information of approximate in situ depth of the samples. Pictures of the samples pre- and post cell storage are displayed in appendix B.

Table 5.2: Outline of tests, storage time and diffusion time

Salt / Water	Block sample	Sampling date	Date installed in cell	Opening date	Days stored regular	Days stored in cell
Salt	3.5-3.75 m	4.10.13	4.12.13	15.1.14	61	42
Water	3.75-4.0 m	4.10.13	4.12.13	20.1.14	61	47
Salt	4.25-4.5 m	4.10.13	4.12.13	4.2.14	61	62
Water	4.75-5.0 m	24.10.13	4.12.13	10.2.14	41	68
Salt	5.05-5.3 m	24.10.13	4.12.13	18.2.14	41	76
Water	5.55-5.8 m	24.10.13	4.12.13	24.2.14	41	82
Salt	7.45-7.7 m	30.10.13	4.12.13	10.3.14	35	96
Water	8.2-8.45 m	30.10.13	4.12.13	16.3.14	35	102

Opening of the mini block samples, from the storage cells, is done by separating the cell from the bottom seal, draining the water or KCl solution. For salt migrated samples potential precipitated salt with a few mm soil is carefully removed using a spatula.

Chapter 6

Laboratory methods

6.1 Block sample sectioning

Block samples are prepared for laboratory tests by carefully dividing the block sample using string wire and a custom-made station, seen in Figure 6.1, to slice the mini block with utter precision.

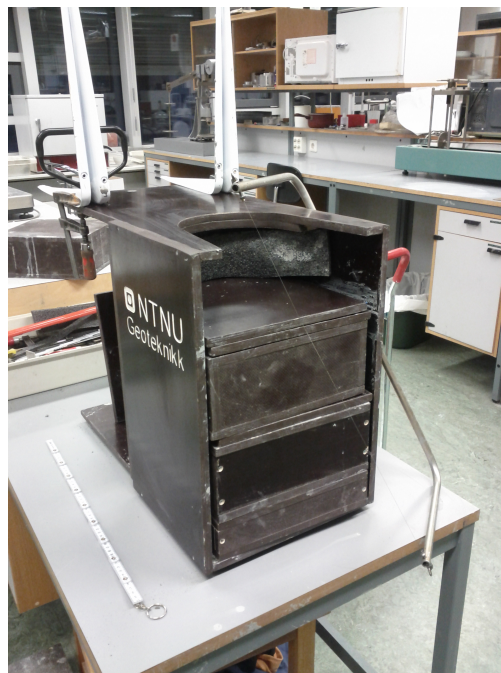


Figure 6.1: Cutting station for mini block samples (Photo: Rikke N. Byrntesen)

After opening, the mini block samples are divided as illustrated by Figure 6.2. Which, also display dimensions of an ideally sized mini block sample. The sectioning is carried out quickly after opening. All sections that cannot be tested immediately is wrapped in plastic foil and wet towels and stored in approximately 7°C to prevent loss of water content and delay oxidation of the clay sample. Table 6.1 describes and illustrates the procedure of sample sectioning of each layer in the block sample. The samples are to be tested as described in the table. However, execution may be limited due to variations in block sample size and quality.

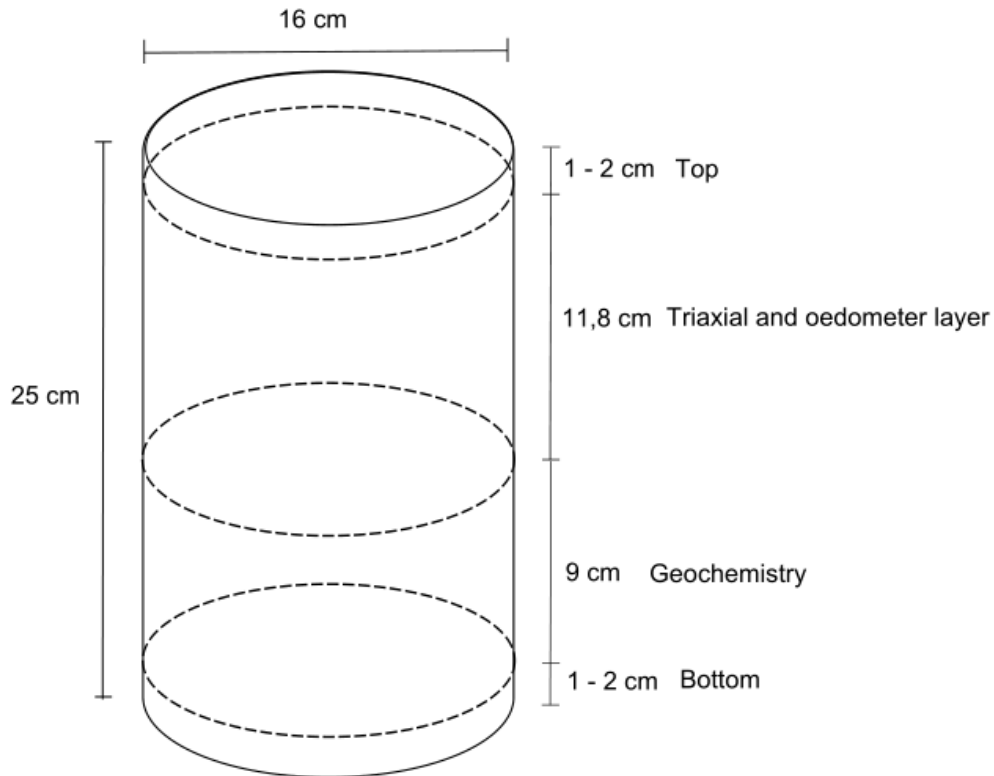


Figure 6.2: Sectioning of an ideal mini block sample

Table 6.1: Descriptions and location of tests for each mini block sample

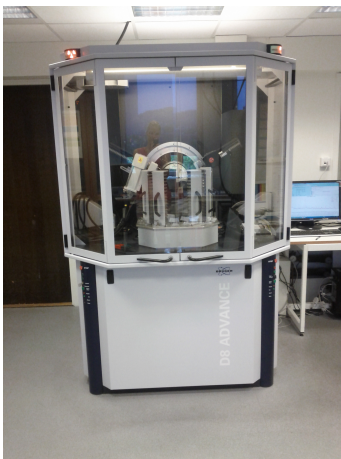
Layer	Tests	Illustration
Top	<p>In case of material shortage in geochemistry layer, the top layer may replace section 3 below:</p> <ul style="list-style-type: none"> • Falling cone test • Water content • Atterberg limits 	
Triaxial and oedometer	<ul style="list-style-type: none"> • 3 CRS oedometer tests • 2 triaxial tests • Water content and unit weight for each oedometer and triaxial sample 	
Geochemistry	<p>For each section:</p> <ul style="list-style-type: none"> • Falling cone test • Water content • Atterberg limits • Cation exchange capacity • Pore-water chemistry • Temperature and pH as indicated 	
Bottom		

6.2 Methodology

6.2.1 X-ray diffraction analysis (XRD)

Material for X-ray diffraction analysis (XRD) was set aside and stored during the project assignment, fall 2013 [9]. The XRD analysis is conducted on dried oedometer material throughout the depth profile. The bulk mineralogy is analysed using the following procedure. Dried samples are first coarsely grinded, thereafter the clay goes through the secondary grinder, a Sibteknik laboratory disc mill, obtaining grain size of the material below 6 μm . Between each sample preparation, the instruments are systematically cleaned with ethanol. After the required grain size is obtained, the material from each sample is carefully evened out on a dish and marked.

The clay sized fraction is analyzed by mixing ungrinded clay sample with distilled water and adding the mixture to a cylinder. Sedimentation is allowed for 15 hours and 52 min, after which the upper 20 cm of the water and clay mixture is collected and the water is filtered out. A thin film of the sample is transferred to a glass plate, ready for analysis.



(a)



(b)



(c)

Figure 6.3: X-ray diffractometer used in the XRD analysis in a) and b). HCL testing of the clay in c) (Photo: Rikke N Bryntesen)

XRD analysis on both the clay fraction and the bulk samples is conducted using Bruker D8 Advance, seen in Figure 6.3 a and b. The analysis for each sample is logging for approximately 1 hour and 20 minutes. The output of the recording is illustrated by the blue “graph” displayed in Figure 6.4. After recording is complete, the result of each sample is analysed using the mineral detection computer programme Difrac.eva. Each mineral is interpreted by specific combinations of peaks in the obtained graph. Thereafter the content of each mineral is calculated using the computer program Topas, creating an interpretation as seen in Figure 6.4. In tests where calcite is detected a portion of the material is tested with 1 mole HCl to verify the presence of calcite, illustrated in Figure 6.3 c. The samples of the clay sized fraction are glycol treated to corroborate the absence or presence of swelling clay minerals such as smectite.

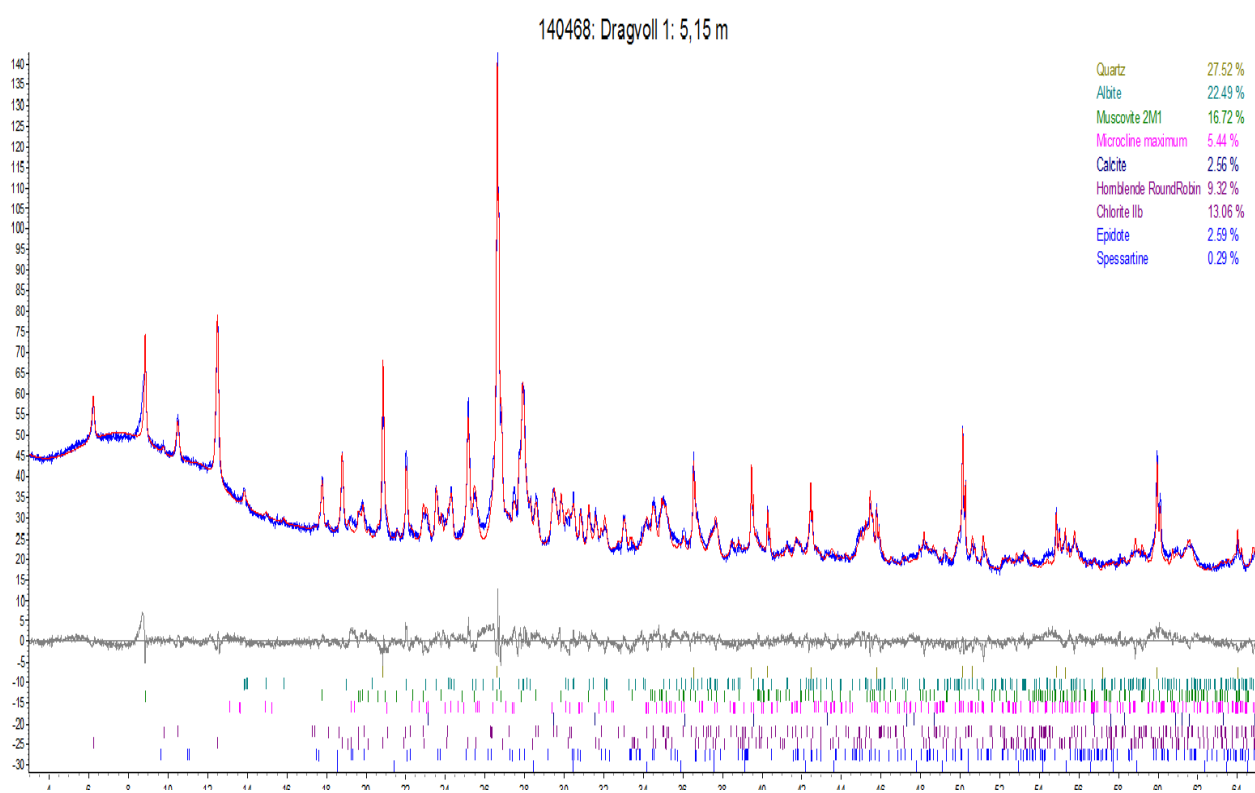


Figure 6.4: Example result of interpreted output of the X-ray diffractometer

6.2.2 Geochemistry

An overview of the tests done on the geochemistry layer is provided above. After opening the sample in the laboratory, sections within the geochemistry layer are marked with dimensions as seen in Figure 6.5.

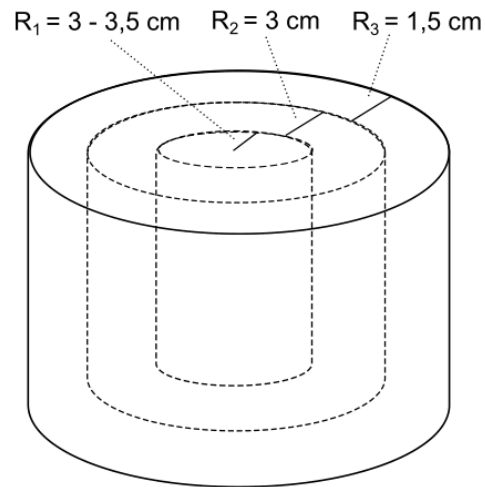


Figure 6.5: Dimensions of sections in the geochemistry layer

Temperature and pH measurements are recorded as illustrated in Table 6.1 section 6.1, recording the temperature using a thermometer, penetrated 1-2 cm into the clay from the top of the sample. The temperature is then entered into the pH-meter computer and the electrode of the pH meter is inspected to ensure it is clean and saturated with 3 mol KCl solution. Thereafter the electrode is penetrated into the clay in the same manner as the thermometer. After the measurement is complete, the electrode is thoroughly rinsed with distilled water. The sequence is repeated for each section in the geochemistry layer.

For each section within the geochemistry layer, four 15 ml containers are filled with clay. Care is taken not to remould the clay when inserting it into the containers as separation of pore water is problematic on remolded clay samples. The samples are centrifuged for 20-45 minutes with 4000 rpm. After centrifugation is complete, the separated pore water is extracted and filtered through a $0.45 \mu\text{m}$ syringe filter. The pore water is thereafter tested for salinity, determined by measuring electric conductivity in of the pore water. Conductivity meter CDM 2d is used. The remaining pore water is stored in a freezer until further testing can take place.

Material with mass $> 150 \text{ g}$, from each of the sections is stored in a freezer for CEC analysis.

6.2.3 Geotechnical index tests

Density

Determination of natural density, wet density, of the clay is done with a small cylinder of known volume, according to manual 14.425 [60]. Equation 6.1 and 6.2 are used to determine density and unit weight respectively. In this thesis, the density was determined using the odometer steel ring of known volume, due to clay shortage.

$$\rho = \frac{m_s + m_w}{V} = \frac{m}{V} \quad (6.1)$$

$$\gamma = \frac{(m_s + m_w)g}{V} = \frac{mg}{V} \quad (6.2)$$

m_s = Mass of solid particles [g]

m_w = Mass of water [g]

m = Total mass of sample [g]

V = Total volume of sample [m^3]

g = Gravity ($9.81 m/s^2$)

Water content and Atterberg limits

The natural water content of the specimen is to be tested as quickly as possible, after the mini block sample is opened in the laboratory. The procedure is performed in accordance with NS8013 [43], and calculated using equation 6.3.

$$w = \frac{m_w}{m_s} = \frac{m - m_s}{m_s} 100\% \quad (6.3)$$

The liquid limit can be determined by using the falling cone method or the Casagrande method, described in NS8002 [42] and NS8001 [41], respectively. In this thesis, the test is conducted using the falling cone method [42].

Liquid limit determined by falling cone test is done with the falling cone apparatus on a remoulded sample. The liquid limit is defined, in the test, as the water content of the sample at which a 60 g cone with an angle of 60° penetrates the clay by 10 mm. For further explanation of the method and corrections for deviations of cone penetration, reference is made to NS8002 [42].

Determination of plastic limit is done by taking 10-20 g of material and rolling it using a flat hand against a glass surface. When the clay crumbles at a diameter of 3-4 mm, the plastic limit is reached, and the sample is collected. The water content at this stage corresponds to the plastic limit of the material.

The plasticity index I_p , calculated using equation equation 6.4 is defined as the range of which the natural water content can lie for a clay to show plastic behaviour. Liquidity index I_L describe the relation between the natural water content and the plastic range and is defined by equation 6.5.

$$I_p = w_l - w_p \quad (6.4)$$

$$I_L = \frac{w - w_p}{w_l - w_p} \quad (6.5)$$

w_l = Liquid limit [%]

w_p = Plastic limit [%]

Falling cone

The falling cone apparatus is used on a specimen to evaluate the undrained shear strength by analysing the depth of cone penetration through an undisturbed sample by gravitational force alone. Remoulded shear strength is determined by falling cone penetration through a remoulded sample. Based on results of the described methods, the sensitivity of the soil is determined by equation 6.6.

$$S_t = \frac{S_u}{S_r} \quad (6.6)$$

S_u = Shear strength [kPa]

S_r = Shear strength [kPa]

S_t = Sensitivity [-]

For correlation between cone penetration and shear strength, along with extensive description of the procedure, reference is made to NS8015 [44].

Salinity

Pore water salinity is determined by measuring electric conductivity of pore water expelled by centrifugation of a sample, as described above. Conductivity meter type CDM 2d measuring the conductance. The calibration chart, displayed in appendix A, is used to convert conductance to total salt content in g/l. The calibration is valid up to 55 g/l with a solution temperature of 25°C.

6.2.4 Oedometer

The oedometer test is used for deriving the load history of the soil. The test simulates a one-dimensional deformation, which is a simplified simulation of in situ deformation of soil.

The oedometer tests are prepared and run as set forth in NS8018 [45]. Equipment used is also as presented in the standard. A steel ring of known volume and weight is used to cut the sample, by weighing the sample within the ring, the density can be calculated as described above, in equation 6.1 and 6.2. Thereafter the ring, containing the clay sample, is mounted in the oedometer. One-way drainage is applied with pore pressure measurements at the base of the sample. For accurate pore pressure measurements, it is essential to use de-aired water only as air-bubbles will act as springs while pressure is applied. Thus, also the filters must be saturated in deaired water.

Constant Rate of Strain (CRS), a Continuous Loading (CL) test procedure is used, where a top cap is forced down with a constant displacement rate of 5 $\mu\text{m}/\text{min}$. It is assumed a parabolic pore pressure distribution over the sample height. Hence, the average effective stress is calculated using equation 6.7. The deformation modulus, a measure of a soils resistance to deformation, is calculated using the basic definition as seen in equation 6.8. Coefficient of consolidation, a measure of the time rate of consolidation, is estimated using equation 6.9.

$$\sigma' = \sigma - \frac{2}{3}u_b \quad (6.7)$$

$$M = \frac{d\sigma'}{d\varepsilon} \quad (6.8)$$

$$c_v = \frac{d\sigma'}{dt} \frac{[H_0(1 - \varepsilon)]^2}{2u_b} \quad (6.9)$$

u_b = Recorded pore pressure at the base of the sample [kPa]

σ = Pressure applied by cap [kPa]

H_0 = Initial hight of sample (20mm)

ε = Strain [-]

The preconsolidation pressure, the maximum pressure a soil sample has previously experienced, is inspected visually by the Janbu [21] method.

6.2.5 Triaxial test

Shear strength of a soil can be estimated using the triaxial test. The test is performed in accordance with Vegvesen [60], with a triaxial cell and equipment as displayed in Figure 6.6.

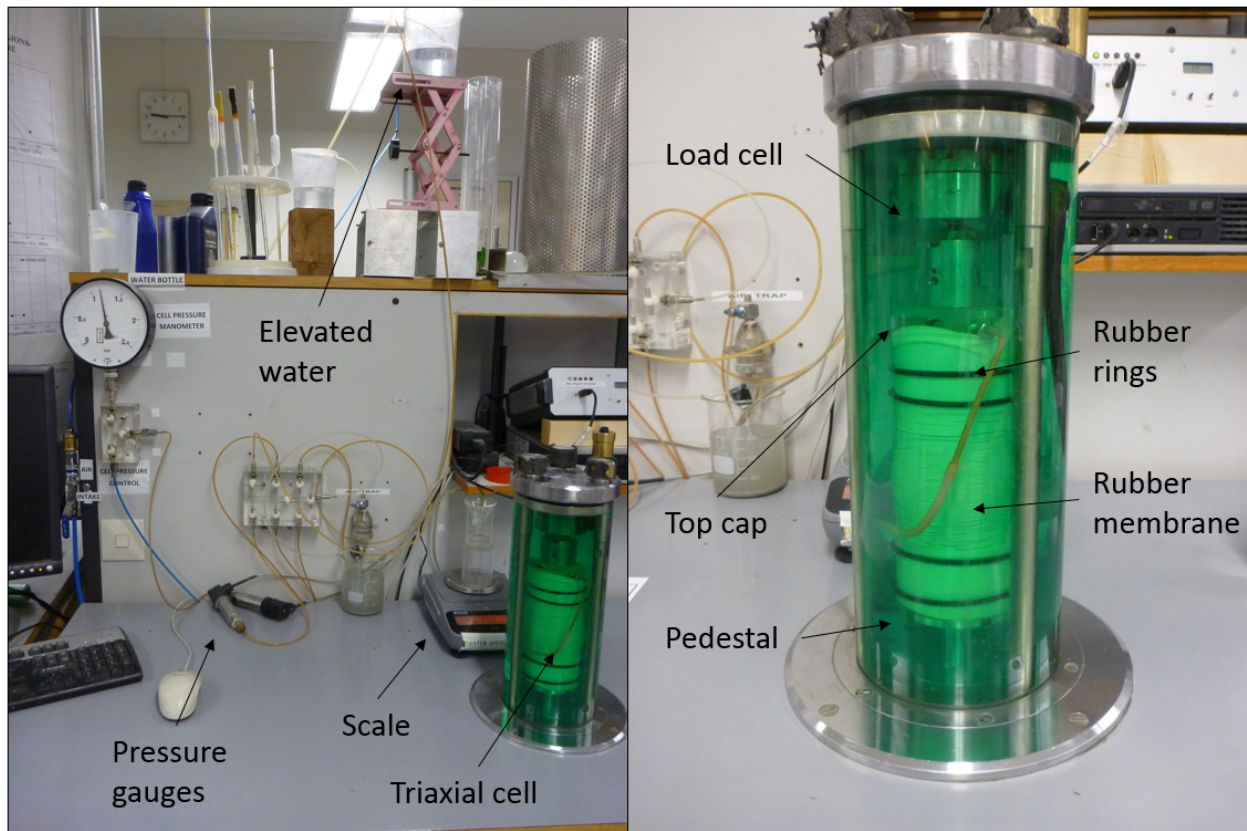


Figure 6.6: Illustration of triaxial equipment [9]

In this thesis an active Anisotropic Consolidation, Undrained test (CAUa) is performed on all the triaxial tests. The consolidation phase is carried out using stepwise consolidation with four steps as illustrated in Figure 6.7. For each step the consolidation remains constant for 1 hour, the sample is then consolidated for 12 hours after reaching the final step. The stepwise procedure is to prevent the soft, sensitive clay from collapsing under consolidation. The share phase is conducted using a strain rate of 1.5 %/hour. The consolidation phase of the triaxial test is based on the theory of simulating the in situ stress conditions in ground and thereafter evaluating the resistance against additional applied axial load. First, the in situ stress conditions are calculated based on equation 6.10 and 6.11. For this thesis a conservative earth pressure coefficient of 0.7 is used along with the assumption of ground water in terrain. For each mini block sample, where possible, triaxial tests are to be preformed with a consolidation phase according to p'_0 - and $1.1p'_0$ - consolidation, in the respective order of priority.

$$p'_0 = \sigma'_{v0} = \gamma d - \gamma_w h_w \quad (6.10)$$

$$\sigma'_h = K'_0 \sigma'_{v0} \quad (6.11)$$

d = Depth of sample, ground surface and down to the middle of the sample [m]

h_w = Height of water column above sample [m]

K'_0 = Earth pressure coefficient [-]

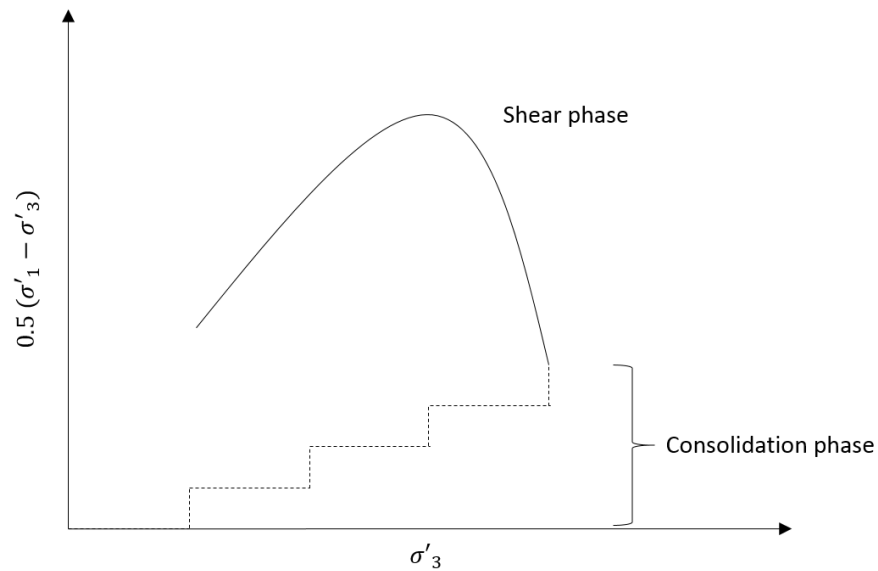


Figure 6.7: Illustration of the stepwise consolidation phase in triaxial tests

As the test performed on mini block samples must be hand carved, to obtain the cylinder shape appropriate in triaxial tests with a diameter of approximately 54 mm. The appropriate length of 100 mm is cut by using a standard cradle at NTNU. The cradle and tools for triaxial specimen preparation are displayed in Figure 6.8.



Figure 6.8: Equipment for triaxial specimen preparation. (Photo: Rikke N. Bryntesen)

Mounting of the sample preformed as illustrated in Figure 6.6. The sample is placed on the pedestal with de-aired filters on top and bottom. A saturated filter paper is attached to the cylinder surface, acting as drainage paths. A rubber membrane is carefully fitted around the sample and sealed on the top cap and the bottom pedestal using rubber rings and grease. As equipment leakage has been a problem in several of the triaxial tests, the mounting of the sample evolved to the use of three rubber rings on both top and bottom along with an extra, shorter, rubber membrane over the pedestal and bottom part of the sample. Together with the use of vast amounts of grease. Further, using the drainage pipes in the apertures, de-aired water is injected inside the rubber membrane, filling it with water and to ensure removal of all air bubbles. The load cell and the cell chamber is mounted and tightened, and the chamber is filled with water applying an isotropic cell pressure of 10 kPa on the sample. The filters are flushed with water to remove air. The sample is elevated until contact between load cell and top cap is reached. To remove the excess water in the rubber membrane, due to the previous saturation within the rubber membrane, the valves are opened and the consolidation phase is started with a confining pressure of 10 kPa for 10 minutes without logging. Thereafter the consolidation is started by increasing the cell pressure and axial pressure in 4 equal steps, as described above. When the desired consolidation stress condition is reached, it is kept constant for 12 hours. During which the confining pressure squeeze water out of the sample. The expelled pore water is recorded on a scale.

After 12 hours of consolidation the share phase can be started, after flushing the filters to remove residual air in the system. In the share phase for undrained conditions, the drainage valves are closed and the pore pressure within the sample is recorded along with deformation, applied cell pressure and vertical force. Calculations using the recorded data is carried out using the below equations.

$$A_a = A_0 \frac{\frac{1-\Delta V}{V_0}}{\frac{1-\Delta V}{3V_0}} \quad (6.12)$$

$$\sigma_1 - \sigma_3 = P \frac{1-\varepsilon}{A_a} \quad (6.13)$$

$$\varepsilon = \frac{\delta}{h_0} \quad (6.14)$$

$$\varepsilon_v = \frac{\Delta V}{V_0} \quad (6.15)$$

$$\tau = \frac{\sigma_1 - \sigma_3}{2} \quad (6.16)$$

$$\sigma' = \sigma - u \quad (6.17)$$

$$\Delta u = \Delta \sigma_m - D \Delta \sigma_d \quad (6.18)$$

$$\sigma_m = p' = \frac{1}{3}(\sigma'_1 + 2\sigma'_3) \quad (6.19)$$

$$\sigma_d = q = \sigma'_1 - \sigma'_3 \quad (6.20)$$

ΔV = Volume of expelled pore water

V_0 = Initial volume of specimen (232 cm³)

h_0 = Initial height of specimen

u = Pore pressure [kPa]

σ_1 and σ_3 = Vertical and horizontal applied pressure [kPa]

D = Dilatancy parameter [-]

ε_v = volumetric strain

Chapter 7

Results

7.1 Observations

During laboratory investigation of the quick clay samples observations were made with regard to visual changes in clay, layering and presence of shells and drop stones. Figure 7.1 displays drop stones and shells found inside the salt migrated mini block sample D4.25-4.5m.

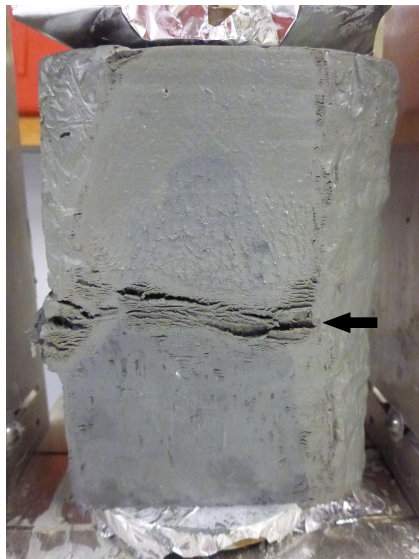


Figure 7.1: Shells and stones found in the mini block samples (Photo: Rikke N Bryntesen)

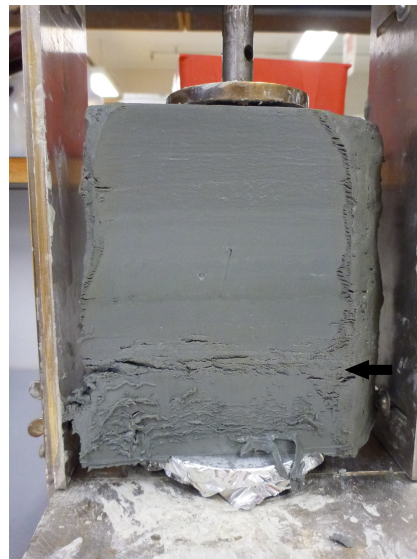
Figure 7.2 displays a freshly cut mini block sample, clearly showing color change ranging approximately 1 cm from the outer edge of the sample, towards the center. A clear distinguish between the original color and the color change is displayed in the figure. The sample was stored for 45 days in approximately 7°C, covered with plastic foil, after sampling.



Figure 7.2: Discoloration in the mini block sample periphery (Photo: Rikke N Bryntesen)



(a) Stored in air, sealed with plastic foil



(b) Stored in KCl solution

Figure 7.3: Discoloration and water migration in silt layers (Photo: Rikke N Bryntesen)

A silt layer, indicated with an arrow, is displayed in the clay specimen in Figure 7.3 a. The color change at the outer parts of the sample is represented in the silt layer, throughout the sample, and affecting the clay surrounding the layer. The sample was stored in 7°C for 52 days after sampling, covered in plastic foil. Figure 7.3 b display a sample with a silt layer indicated by the arrow. The sample was stored in 7°C , wrapped in plastic foil for 35 days, after which the sample was stored in deaired KCl solution for 96 days. No distinct area of discoloration was evident in the sample.

7.2 Grain size distribution

The hydrometer analysis results from the reference samples, and the resultant clay content is plotted with depth, as displayed in Figure 7.4. The hydrometer analysis is done as part of the project assignment [9]. The figure show a clay content of 24-28% in the upper part of the profile, increasing to approximately 38% in the deeper parts.

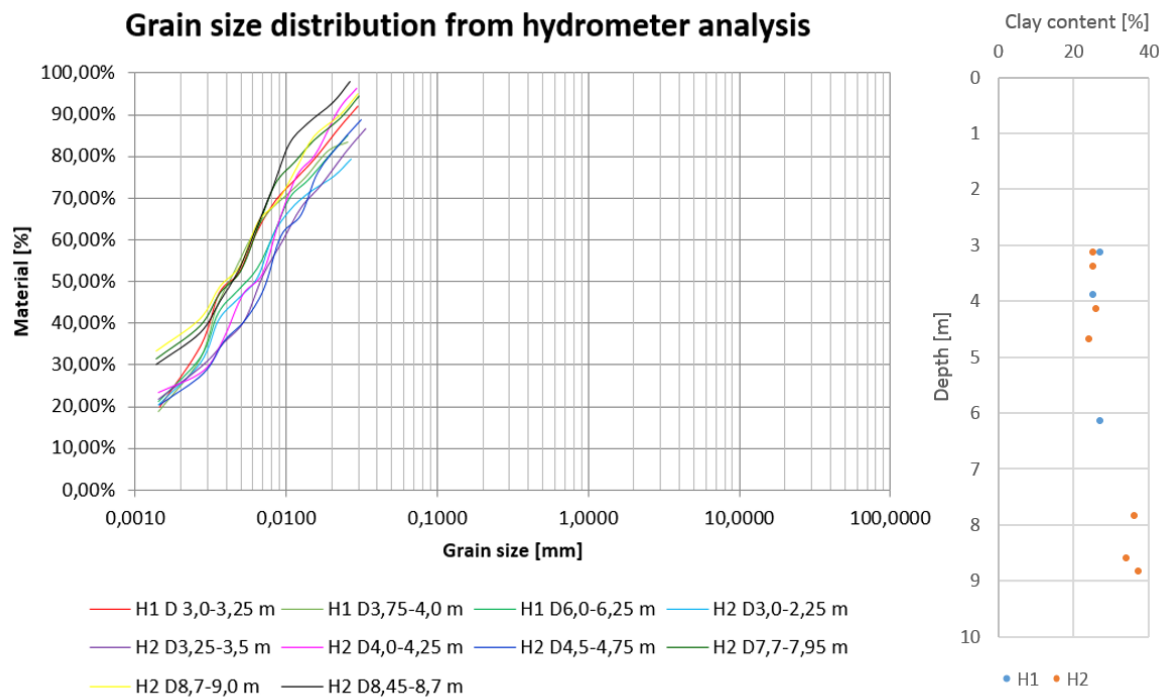


Figure 7.4: Results from hydrometer test on grain size distribution in the depth profile and resultant clay content with depth [9]

7.3 XRD

Bulk mineral content of the quick clay, analyzed using XRD, is presented in Table 7.1 throughout the investigated depth profile.

The results show no distinct variations between bore hole 1 and 2. A general decrease of quartz content with depth and lower calcite content at the upper part of the profile is observed from the resultant bulk mineralogy.

Table 7.1: Bulk mineralogy in the depth profile

Depth [m]	Bore hole 1		Bore hole 2						
	5.15	6.1	3.13	3.34	4.16	4.67	7.88	8.55	8.91
Quartz [%]	27	26	28	31	31	28	24	24	26
Albite [%]	22	21	22	23	21	21	21	21	22
Muscovite [%]	16	17	16	16	16	16	17	17	15
Chlorite [%]	13	12	13	13	13	13	13	13	13
Hornblende [%]	9	10	8	9	7	9	10	10	10
Microcline [%]	5	5	5	3	6	6	7	6	6
Epidote [%]	2	2	2	2	2	2	2	2	2
Calcite [%]	2	3	1	<1	<1	2	3	3	3
Spessartine [%]	<1	<1	<1	<1	<1	<1	<1	<1	<1

Detailed mineralogy for the clay sized fraction of the quick clay is presented in Table 7.2.

Table 7.2: Mineralogy of the clay fraction

Depth [m]	3.34	7.88	8.91
Muscovite [%]	30	34	34
Biotite [%]	13		
Albite [%]	16	14	13
Quartz [%]	13	11	15
Chlorite [%]	10	16	14
Hornblende [%]	4	10	10
Microcline [%]	11	9	7
Calcite [%]		4	4
Illite [%]	2	1	<1

Output results for bulk and clay XRD analysis are displayed in Appendix C.

7.4 pH and pore water salt content

The results of the recorded pH, pore water conductivity and total pore water salt content are presented for each section at all recorded depths, and given in context with storage time. The center section is defined by section 1, middle by section 2 and the edge section by section 3, as illustrated in Table 6.1, section 6.1.

Result of pH measurements of the reference samples are displayed in Table 7.3. Conductivity measurements of expelled pore water, converted to salinity is also included in the table.

Table 7.3: Results from pH conductivity analysis in reference samples

Mini block sample	Depth [m]	Section [-]	pH [-]	T [°C]	Conductivity [mmho]	Salt content [g/l]	Storage time regular [days]
3.25-3.5m	3.39	3	8.09	9	0.76	0.76	12
3.25-3.5m	3.39	2	8.19	8	0.75	0.75	12
3.25-3.5m	3.39	1	8.23	7	0.75	0.75	12
4.0-4.25m	4.12	3	8.4	9	0.85	0.85	45
4.0-4.25m	4.12	2	8.48	7	0.78	0.78	45
4.0-4.25m	4.12	1	8.58	7	0.74	0.74	45
4.5-4.75m	4.63	3	8.77	9	0.8	0.8	52
4.5-4.75m	4.63	2	8.74	9	0.74	0.74	52
4.5-4.75m	4.63	1	8.66	8	0.71	0.71	52
7.5-7.75m	7.83	3	9.11	10	0.73	0.73	28
7.5-7.75m	7.83	2	9.04	9	0.73	0.73	28
7.5-7.75m	7.83	1	9.06	9	0.73	0.73	28
8.7-9.0m	8.87	1	9	6	0.56	0.56	4

Table 7.4 displays results of the recorded pH and pore water conductivity for both samples stored in KCl solution and in water. The salinity of salt migrated samples are not presented. As the recorded conductivity of the salt treated samples exceeds the reach of the conductivity to salinity conversion chart.

Table 7.4: Results from pH conductivity analysis in samples stored in water and KCl solution

Salt/ Water	Mini block sample	Depth [m]	Section [-]	pH [-]	T [$^{\circ}C$]	Conduc- tivity [mmho]	Salt content [g/l]	Storage time regular [days]	Storage time cell [days]
Salt	3.5-3.75m	3.62	3	7.05	9	165		61	42
Salt	3.5-3.75m	3.62	2	6.94	9	161		61	42
Salt	3.5-3.75m	3.62	1	6.92	9	161		61	42
Water	3.75-4.0m	3.88	3	8.05	8	0.74	0.74	61	47
Water	3.75-4.0m	3.88	2	8.27	8	0.72	0.72	61	47
Water	3.75-4.0m	3.88	1	8.23	8	0.72	0.72	61	47
Salt	4.25-4.5m	4.39	3	7.33	9	112.5		61	62
Salt	4.25-4.5m	4.39	2	7.4	8	107.5		61	62
Salt	4.25-4.5m	4.39	1	7.35	8	100		61	62
Water	4.75-5.0m	4.85	3	8.30	8	0.8	0.8	41	68
Water	4.75-5.0m	4.85	2	8.65	7	0.75	0.75	41	68
Water	4.75-5.0m	4.85	1	8.68	7	0.75	0.75	41	68
Salt	5.05-5.3m	5.19	3	7.45	10	142.5		41	76
Salt	5.05-5.3m	5.19	2	7.4	9	141		41	76
Salt	5.05-5.3m	5.19	1	7.41	9	139		41	76
Water	5.55-5.8m	5.68	3	8.65	14	0.67	0.67	41	82
Water	5.55-5.8m	5.68	2	8.85	9	0.7	0.7	41	82
Water	5.55-5.8m	5.68	1	8.87	9	0.7	0.7	41	82
Salt	7.45-7.7m	7.58	3	7.8	10	150		35	96
Salt	7.45-7.7m	7.58	2	7.72	9	150		35	96
Salt	7.45-7.7m	7.58	1	7.65	9	150		35	96
Water	8.2-8.45m	8.32	3	8.98	4	0.77	0.77	35	102
Water	8.2-8.45m	8.32	2	9.08	4	0.75	0.75	35	102
Water	8.2-8.45m	8.32	1	9.09	4	0.7	0.7	35	102

The variation of pH over the different sections, and comparison between different treatment methods are illustrated in Figure 7.5. Results of the samples stored in KCl solution displays an average decrease in pH of 1.2, relative to the reference samples and the water treated samples. The result show a fairly consistent pH over the sections for the reference samples. However, samples stored in water display a distinct reduction in pH for the edge section of the sample (section 3). Salt migrated samples show indications of increased pH for the edge section. Results fro the reference samples indicate a consistent increase in pH with depth. The numbers located on the left side of the figures indicates the storage time in storage cells and in regular conditions, with brackets around the regular storage time. The reference samples only display the regular storage time.

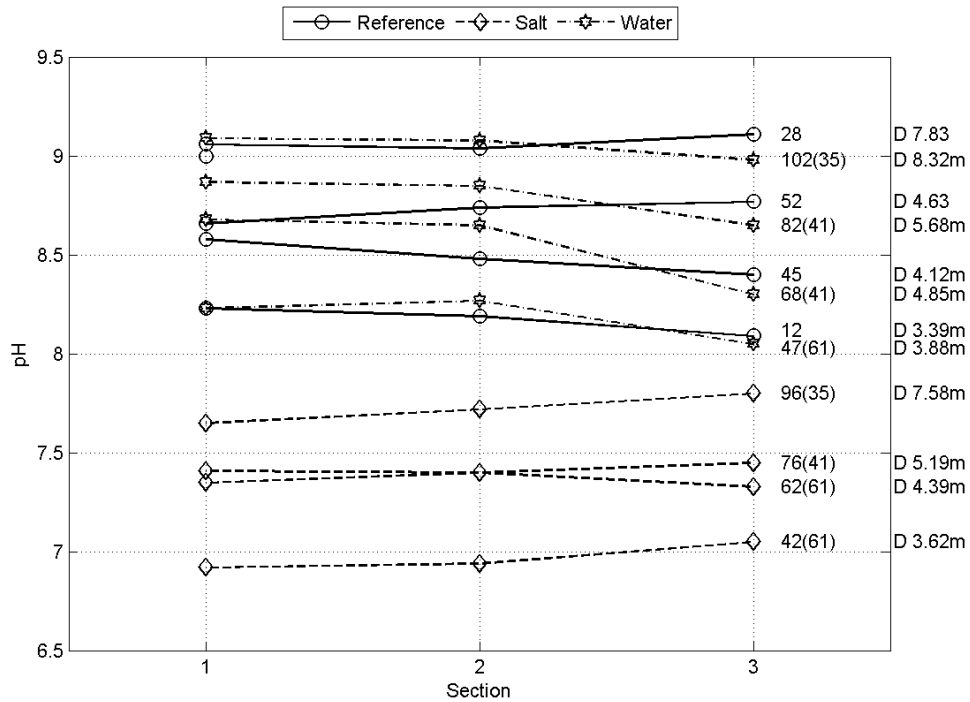


Figure 7.5: Change in pH in section 1, 2 and 3, for reference samples and samples stored in water and KCl solution

7.5 Geotechnical index results

Index results of reference samples, carried out as part of the project assignment by Bryntesen [9], are displayed in Figure 7.6. Thus, the figure describes the in situ conditions and initial condition, related to the water and salt treated samples.

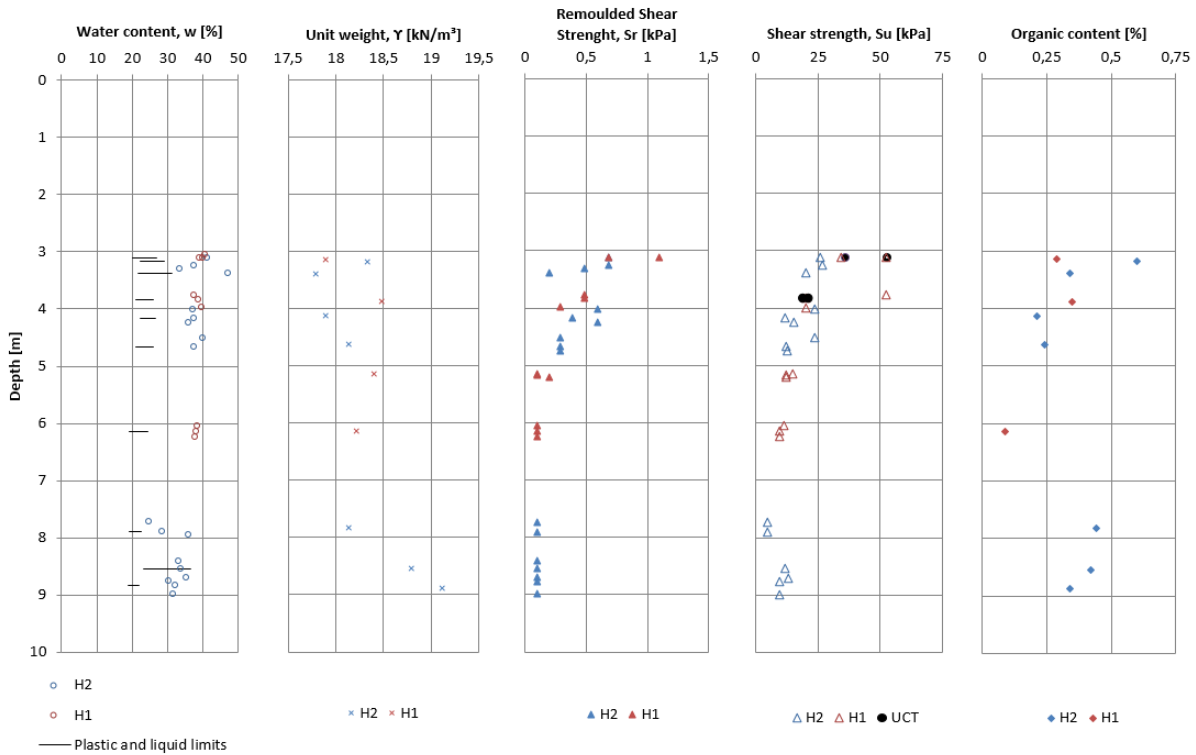


Figure 7.6: Index tests from reference samples, describing the depth profile [9]

7.5.1 Unit weight

Correlations between clay storage method and unit weight is presented in Figure 7.7. An average increase of approximately 0.7 kN/m^3 is observed for the samples exposed to salt migration, relative to the samples stored in water and reference samples.

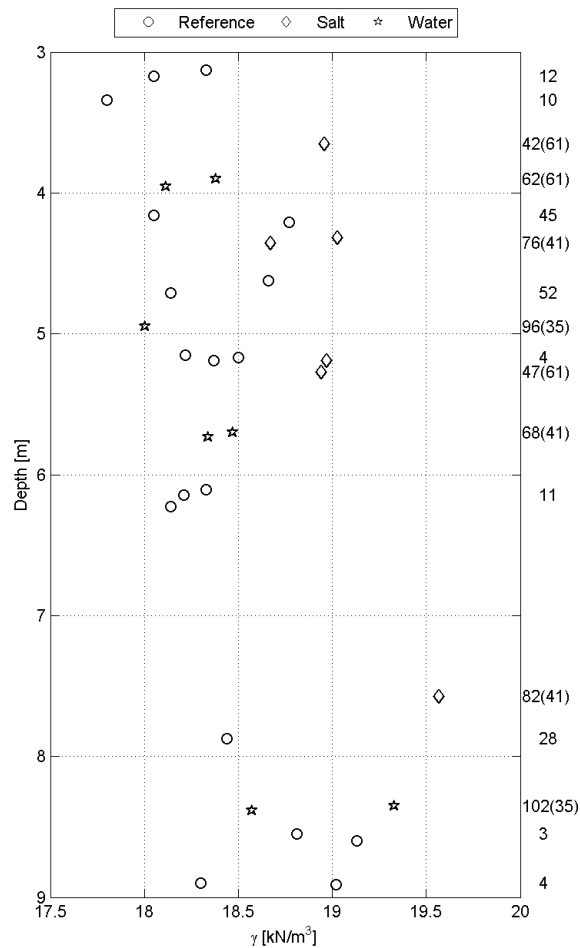


Figure 7.7: Assembly of recorded unit weight, presented with depth

7.5.2 Water content and Atterberg limits

Resultant water content and Atterberg limits of the samples stored in deaired water and KCl solution are displayed in Figure 7.8 and 7.9, respectively. The diagrams display deviations between the sections in each mini block sample.

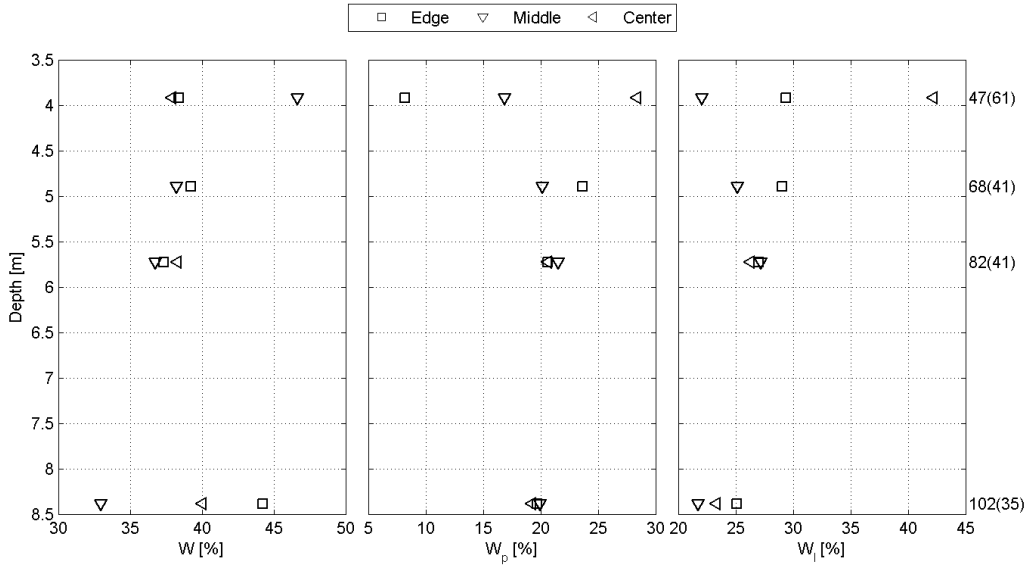


Figure 7.8: Variations in water content and Atterberg limits, between the sections, of water treated samples

As displayed in Figure 7.8, the results of water content and Atterberg limits are generally consistent for all sections. However, some larger deviations are presented. Results of the liquid limit display a trend of higher values recorded in the edge section.

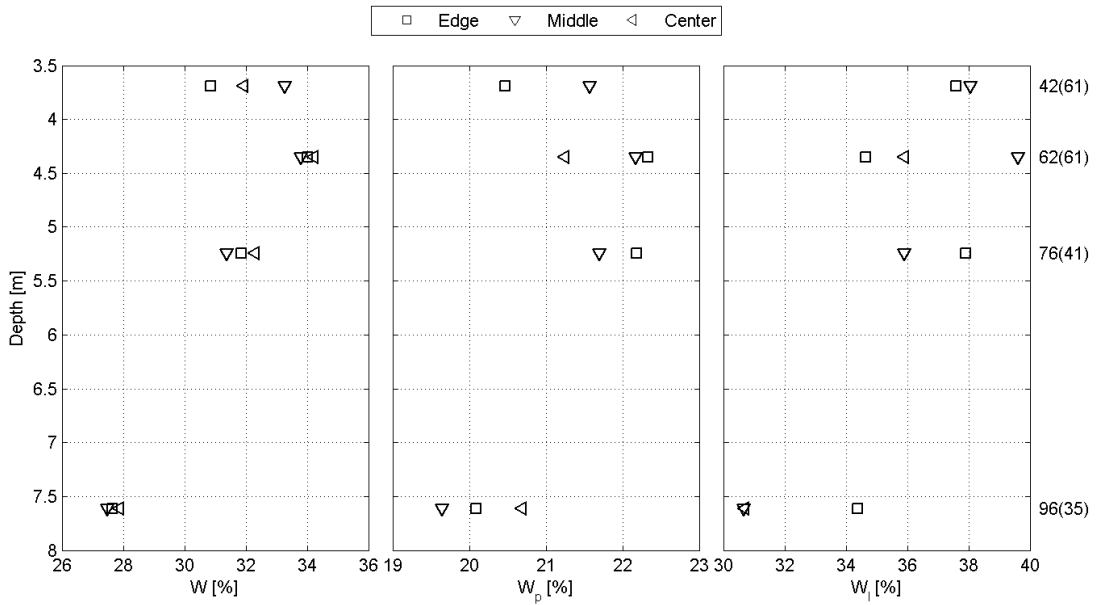


Figure 7.9: Variations in water content and Atterberg limits, between the sections, of salt treated samples

The results, seen in Figure 7.9, display only minor deviations throughout each KCl treated mini block sample. Water content of the center section display a water content a fraction higher, compared to the surrounding sections.

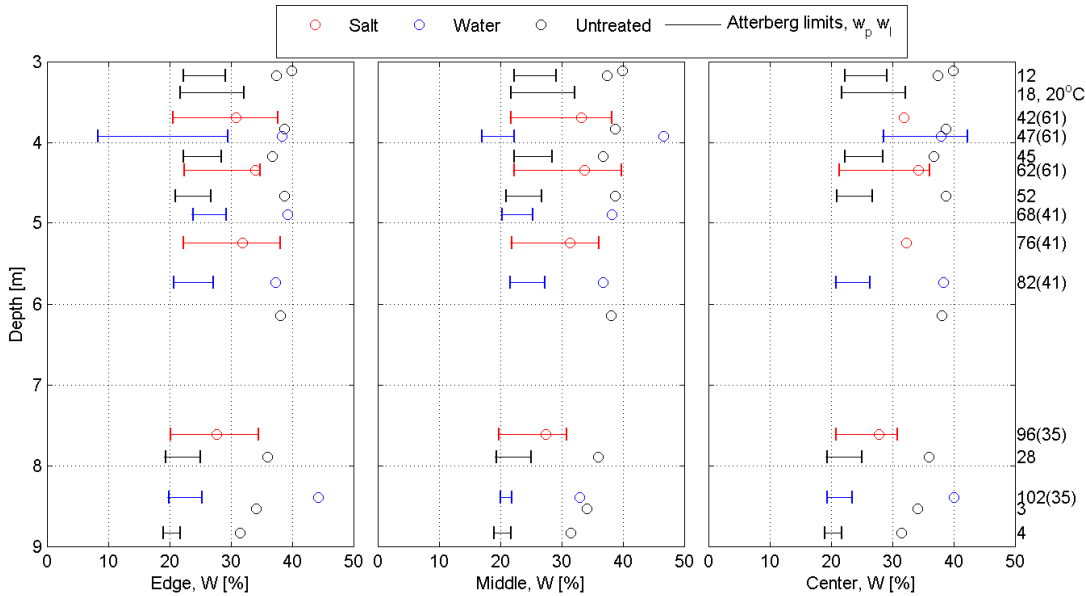


Figure 7.10: Assembly of all results of water content and Atterberg limits, presented for each section

Results of the different sections are displayed in Figure 7.10, assembled with results from the reference samples. The results display few variations through the sections.

As no significant correlations are detected, the sum of the results for each section are presented in Figure 7.11. Results of samples exposed to salt migration display a general reduction in water content, relative to samples stored in water and reference samples. The figure indicate significantly increased liquid limits for the salt treated clay samples. A general increase in plastic limit for samples stored in both water and KCl solution, relative to the reference samples, is also evident in the results. The changes induce changes in both liquidity- and plasticity index, as seen in Figure 7.12. Salt diffusion increase the plasticity index from what is defined as low plasticity, in the water and reference samples, to medium plasticity. The liquidity index also display a distinct decrease, relative to the water and reference samples.

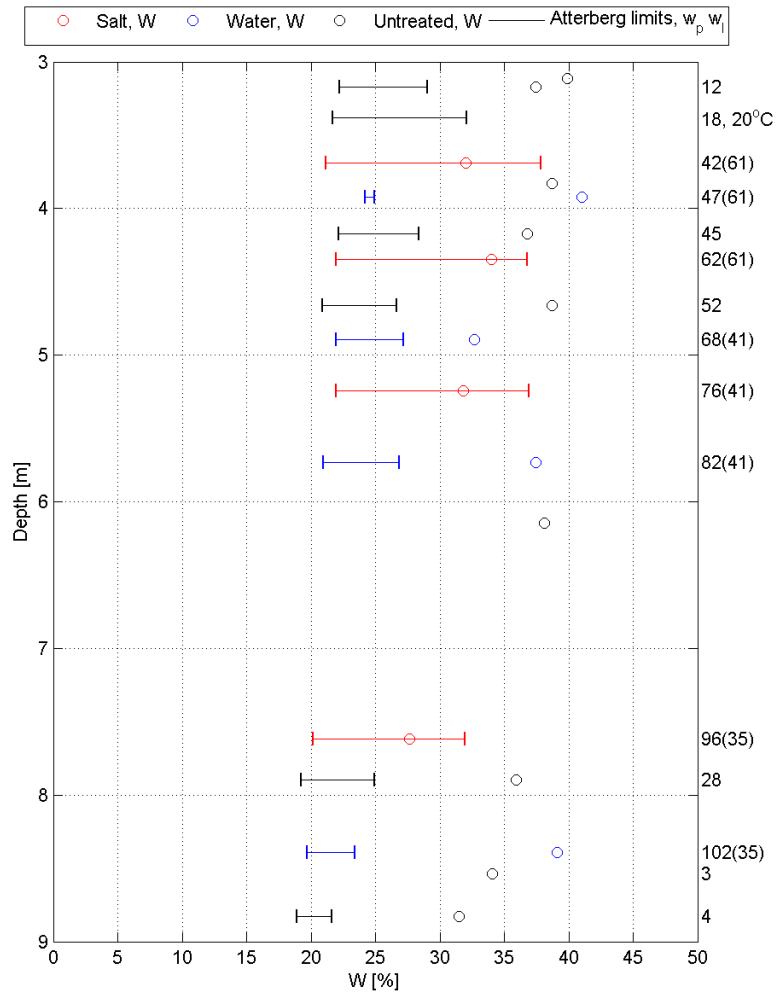


Figure 7.11: Summation of results of water content and Atterberg limits in each sample, presented with depth

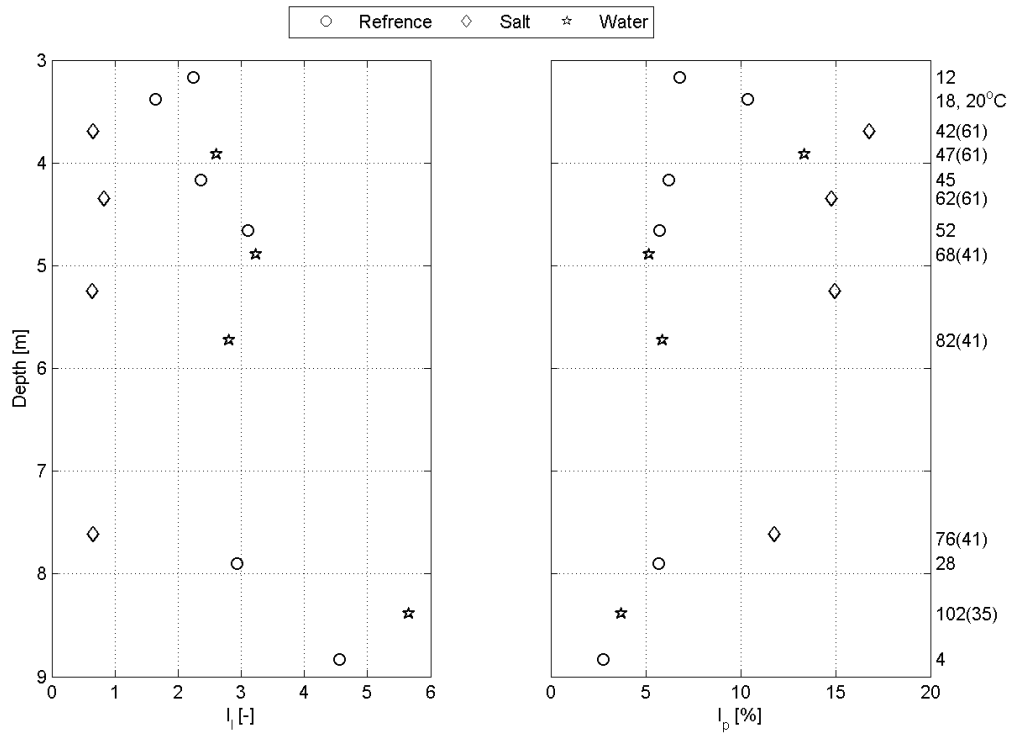


Figure 7.12: Sum of resultant liquidity and plasticity index for each sample

7.5.3 Falling cone

Figure 7.13 display results of falling cone tests on the samples stored in water cells. Results of the falling cone test on KCl treated clay samples are illustrated in Figure 7.14. The edge section display a general lower undrained shear strength compared to the middle and center sections, for the samples exposed to salt migration. No other distinct trends are recognized.

Figure 7.15 display the resultant undrained and remoulded shear strength for each section, assembled with results from the reference samples. Some results from the center and middle sections are not included due to limited material to conduct the tests in these sections. Further, no distinct deviations are observed across the sections.

Due to limited variation across the sample sections, the sum of the results form each mini block sample is presented in Figure 7.16. The presented results display a distinct increase of approximately 10 kPa for undrained and 4 kPa for remolded shear strength, for the KCl treated clay. No distinct variation is observed between the water treated and reference samples. The increase in remoulded strength lead to reduced sensitivity for the salt migrated clay, as seen in the results. KCl diffused samples display a low sensitivity, relative to the water and reference samples, which are classified as very sensitive, based on the results and Sandven et al. [49].

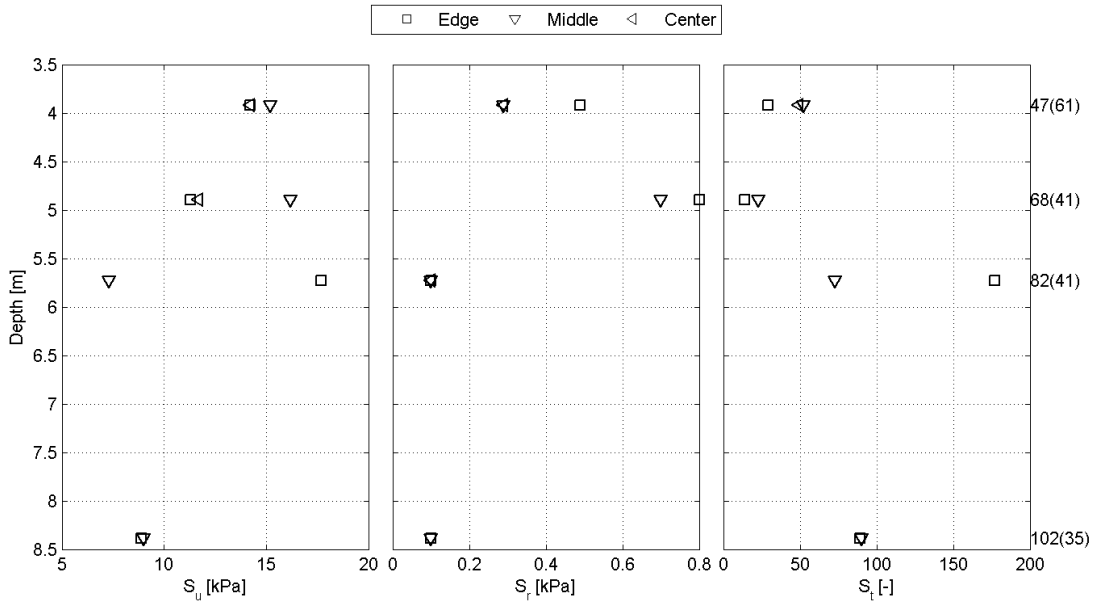


Figure 7.13: Variations in undrained and remoulded shear strength and sensitivity, between the sections, of water treated samples

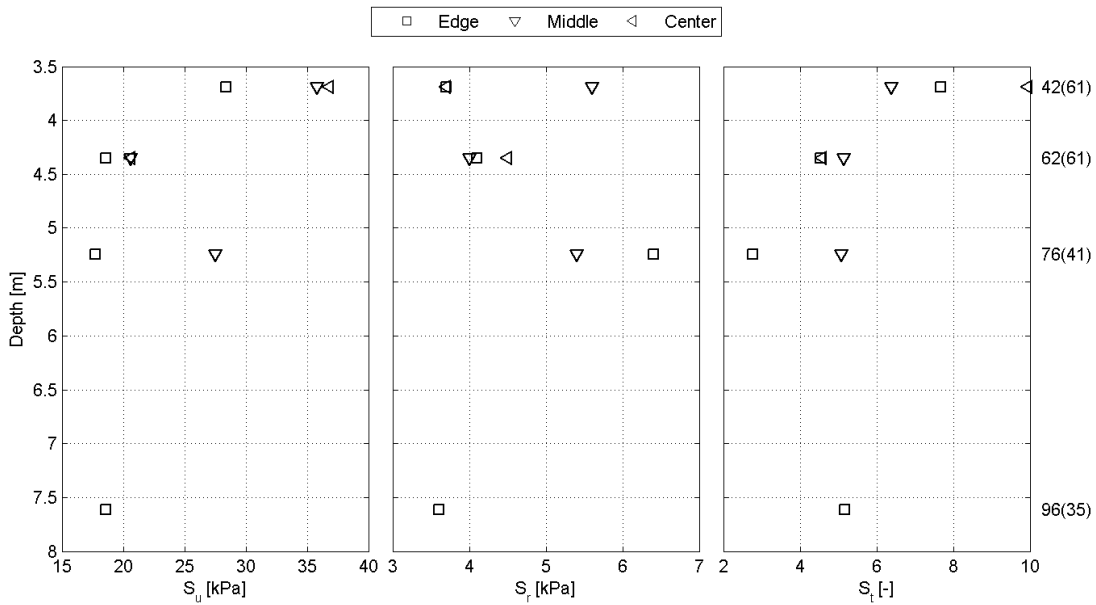


Figure 7.14: Variations in undrained and remoulded shear strength and sensitivity, between the sections, of salt treated samples

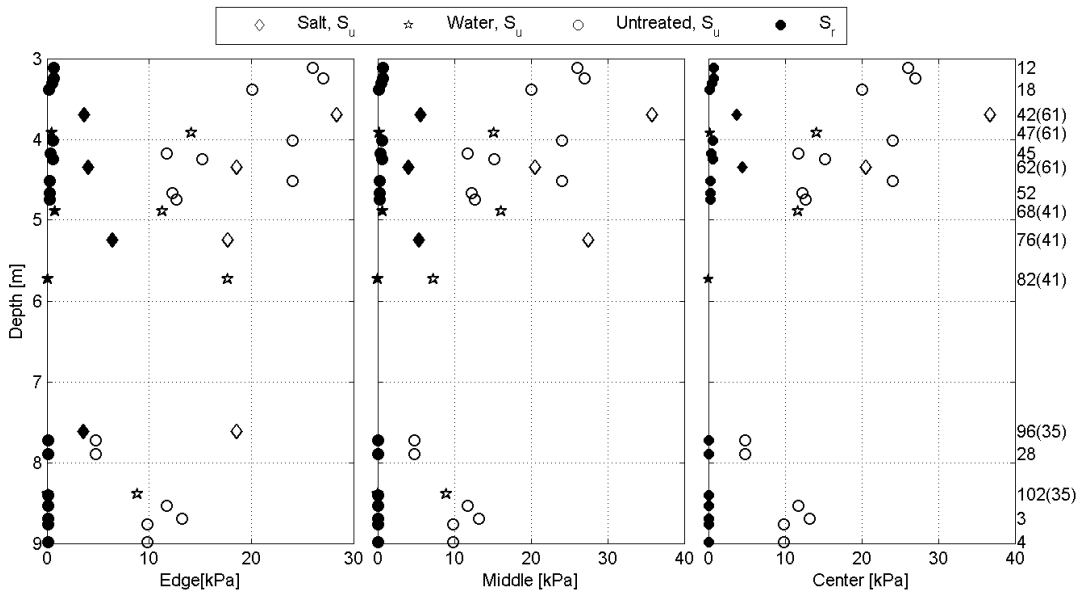


Figure 7.15: Variations in undrained and remoulded shear strength for each section within the samples

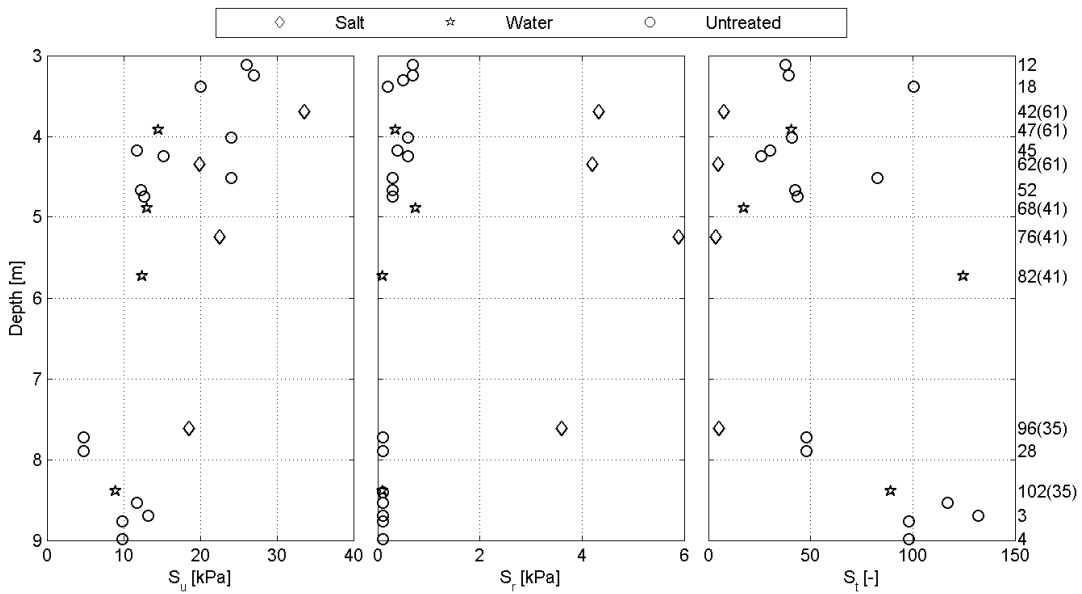


Figure 7.16: Sum of results over each sample, of undrained and remoulded shear strength and sensitivity presented with depth

7.6 Oedometer results

Oedometer results are interpreted as illustrated in Figure 7.17, 7.18 and 7.19.

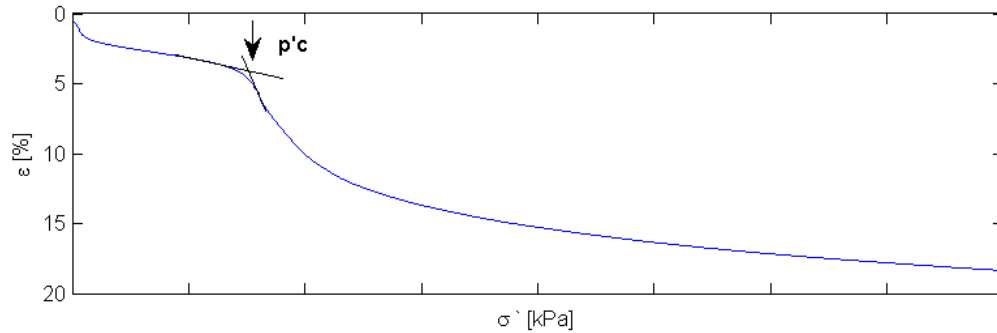


Figure 7.17: Illustration of interpretation method for preconsolidation pressure

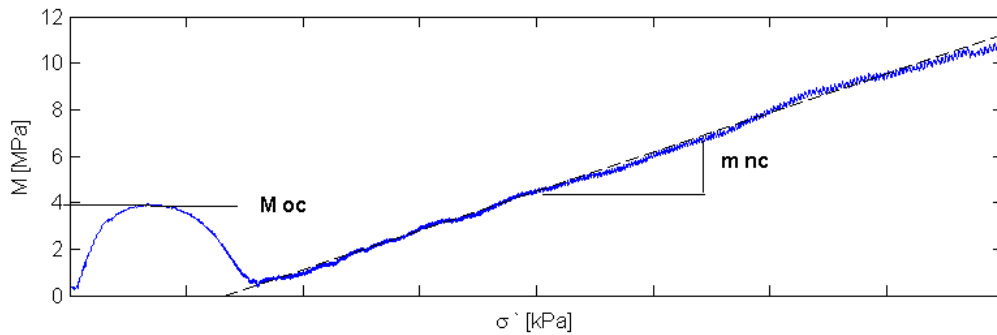


Figure 7.18: Illustration of modulus number in the NC range and OC deformation modulus

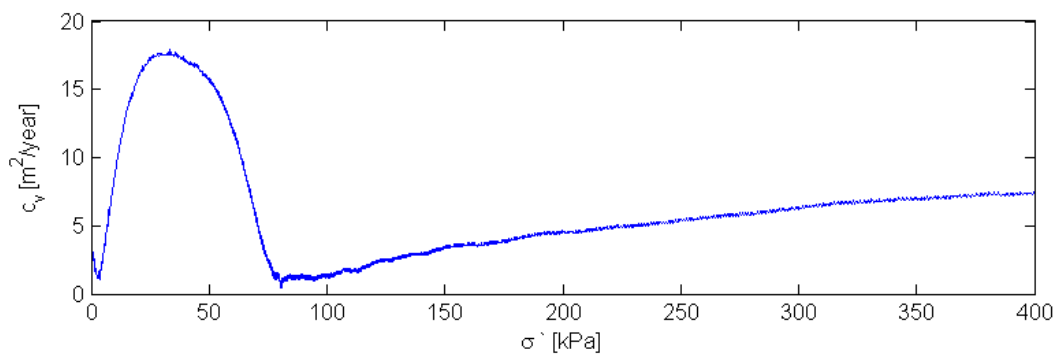


Figure 7.19: Illustration of consolidation coefficient, a value is chosen at a desired stress level. In this thesis at the in situ vertical stress

Results of the CRS oedometer tests are displayed in the following. Detailed results of each salt and water treated samples are included in Appendix E. For further details of results on untreated clay, reference is made to Bryntesen [9] and Appendix D. The results for all CRS tests performed on untreated clay is displayed in Figure 7.20, indicating a preconsolidation pressure between 70 and 75 kPa for most parts of the depth profile. Storage time, in days, prior to testing is indicated in the legend with the exact depth of each specimen.

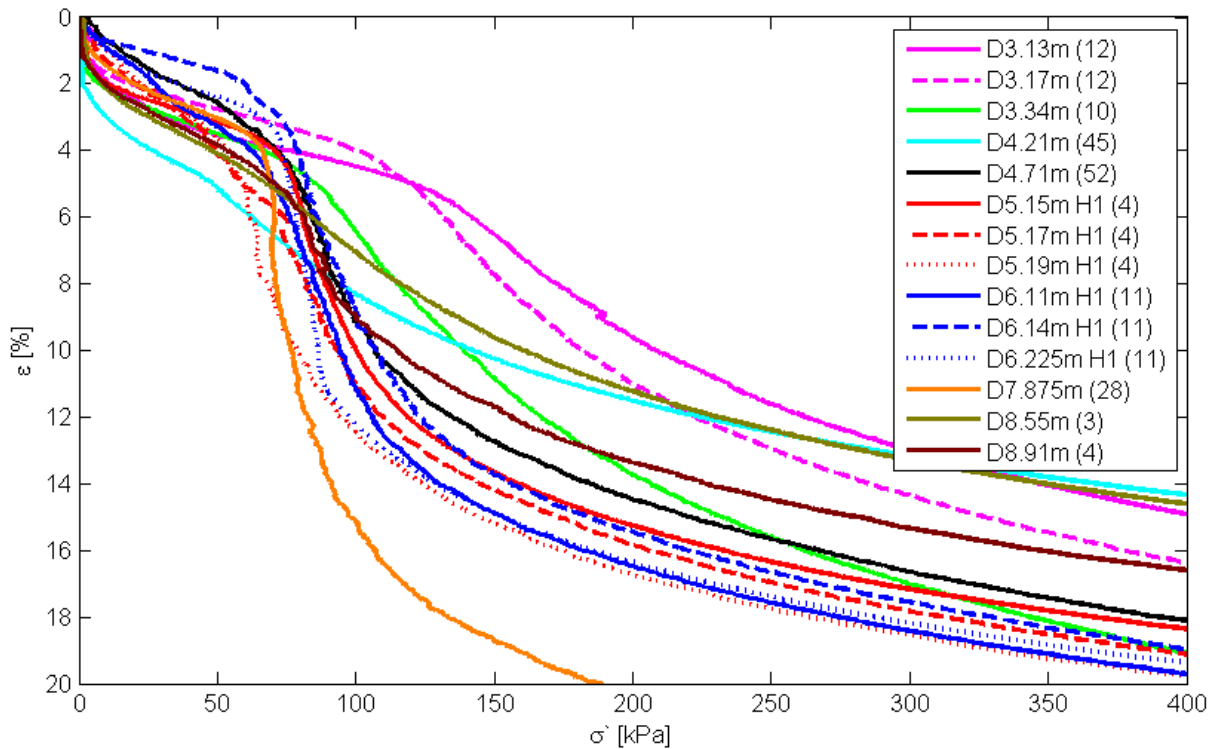


Figure 7.20: Assembly of stress strain results from the reference samples (data from [9])

Figure 7.21 and 7.22 displays effective vertical stress vs strain curves for water and salt treated samples respectively. Storage time, in days, in the cell and prior to cell installation is indicated in both plots. The results indicate a preconsolidation pressure of approximately 70-80 kPa for the water treated clay. Whereas the salt treated clay show a preconsolidation pressure of 80-120 kPa.

Some results are excluded from the plots due to problems with the apparatus during testing. Faulty results are included in Appendix E. The result at depth 5.705 m in Figure 7.21 was stopped by a power breakage, however the result show indications of a preconsolidation pressure, before the test was stopped, and is therefore included in the results. By comparing the untreated samples with the water and salt treated samples, the indication of preconsolidation pressure is generally less visible for the salt and water treated samples.

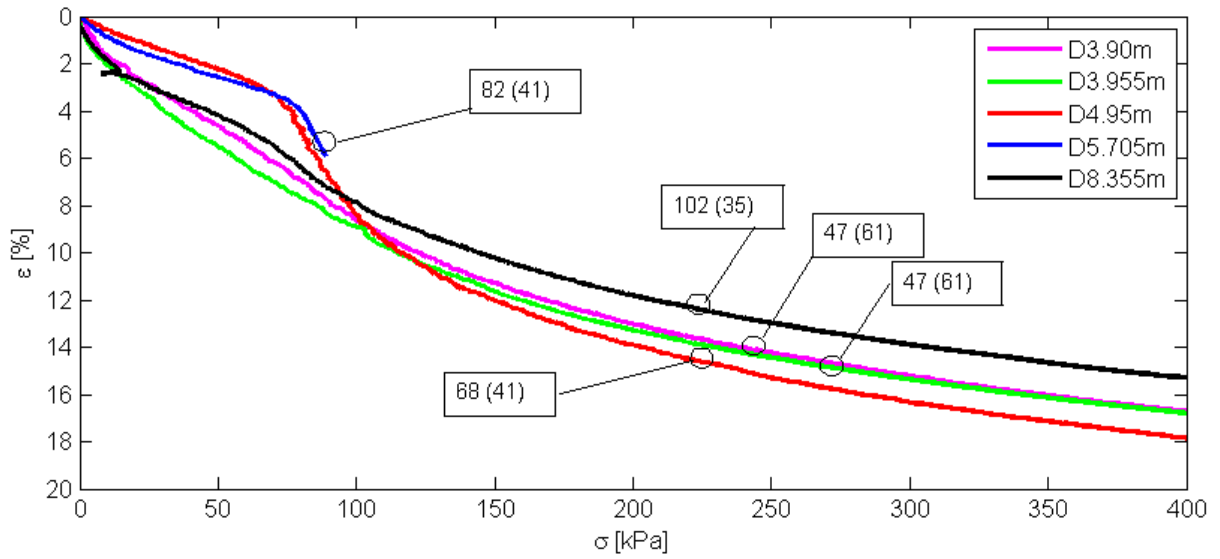


Figure 7.21: Assembly of stress strain results from samples stored in water

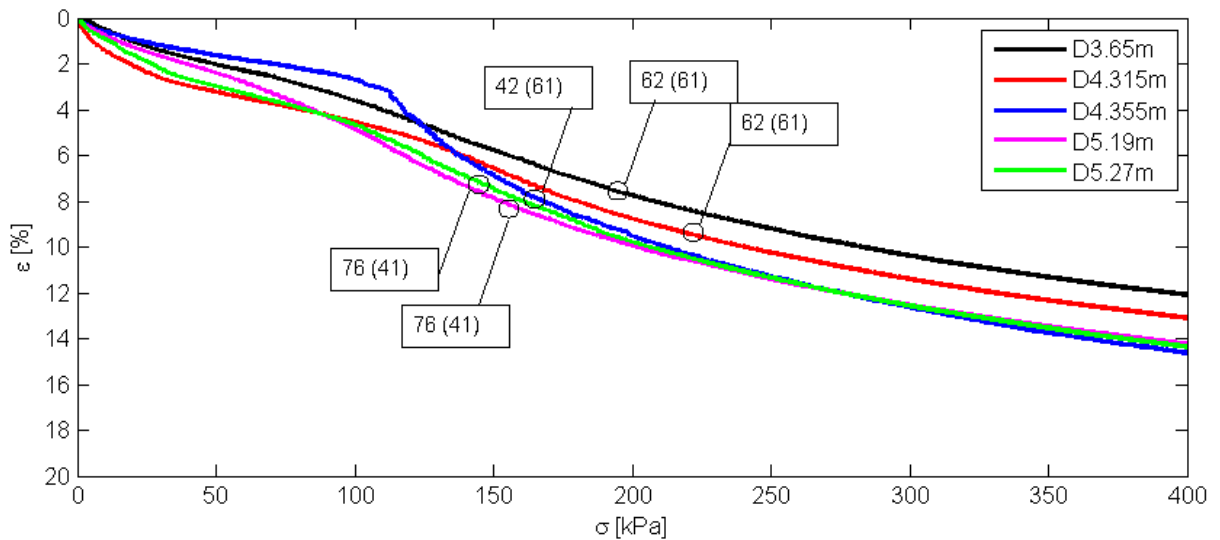


Figure 7.22: Assembly of stress strain results from samples stored in KCl solution

Figure 7.23 displays correlations of preconsolidation pressure between the salt migrated sample, the sample stored in water and the reference sample. The arrows indicate the preconsolidation pressures for each treatment method. The observed results display no deviation between the salt treated sample and the reference sample. However, an increase of approximately 40 kPa is observed for the salt migrated sample. Further comparison between the sample treatment from the oedometer tests results are displayed in Appendix H.

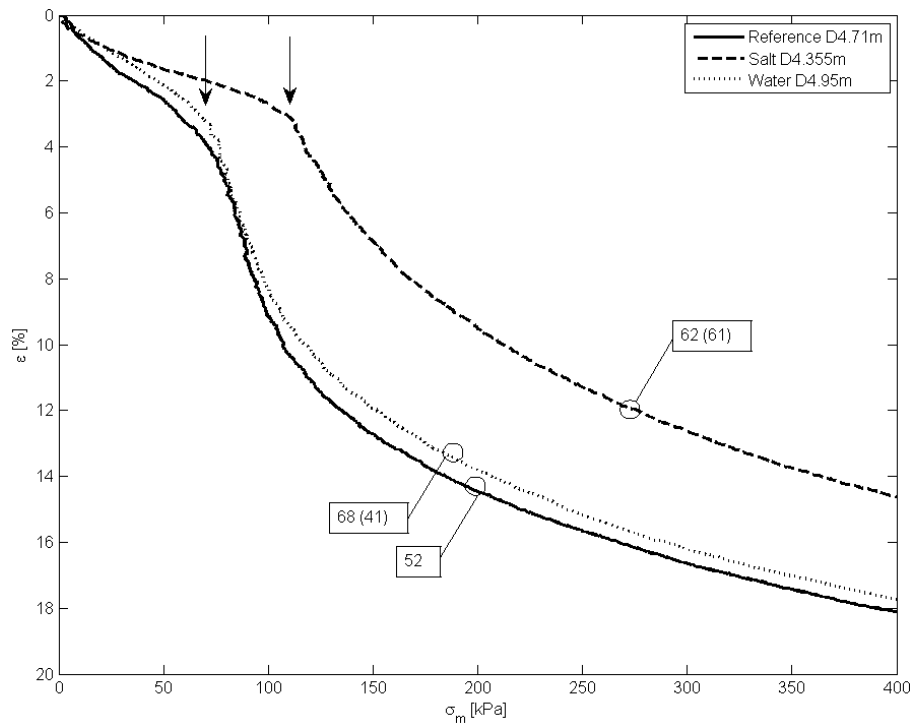


Figure 7.23: Comparison of the stress strain results from reference samples and samples stored in water and KCl solution

The same trend is displayed for all the samples, as seen in Figure 7.24. Deviations of OCR for all the differently treated samples are also presented in the figure.

Figure 7.25 display modulus number, m and consolidation coefficient, c_v , with depth. The figure displays a trend of decrease of the modulus number for the salt migrated sample, relative to the water treated and reference samples. A gentle decrease can also be observed in the water treated samples. The consolidation coefficient display generally consistent results in relation to storage method, however a large increase is observed in two of the salt treated samples.

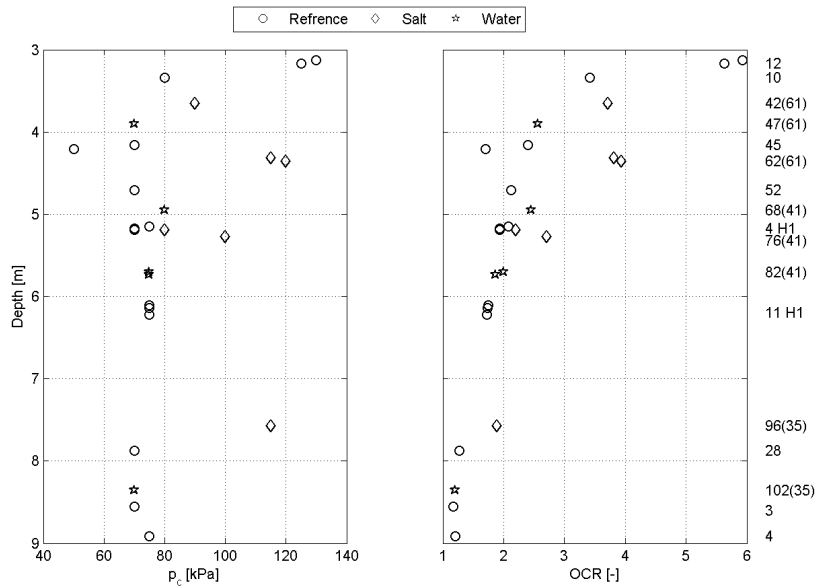


Figure 7.24: Preconsolidation pressure and OCR results from each storage method, presented with depth

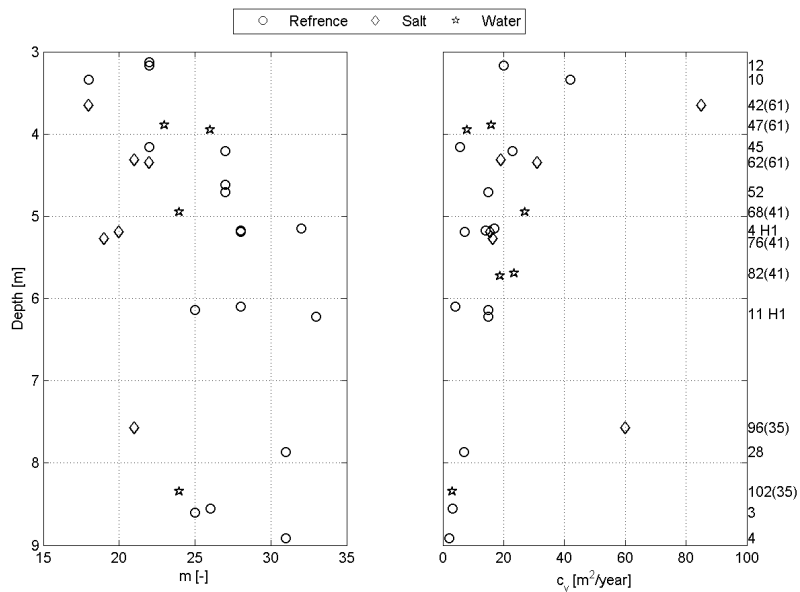


Figure 7.25: Modulus number in the NC range and OC deformation modulus results from each storage method, presented with depth

7.7 Triaxial test results

Interpretation of the triaxial results are illustrated in one of the reference samples, seen in Figure 7.26.

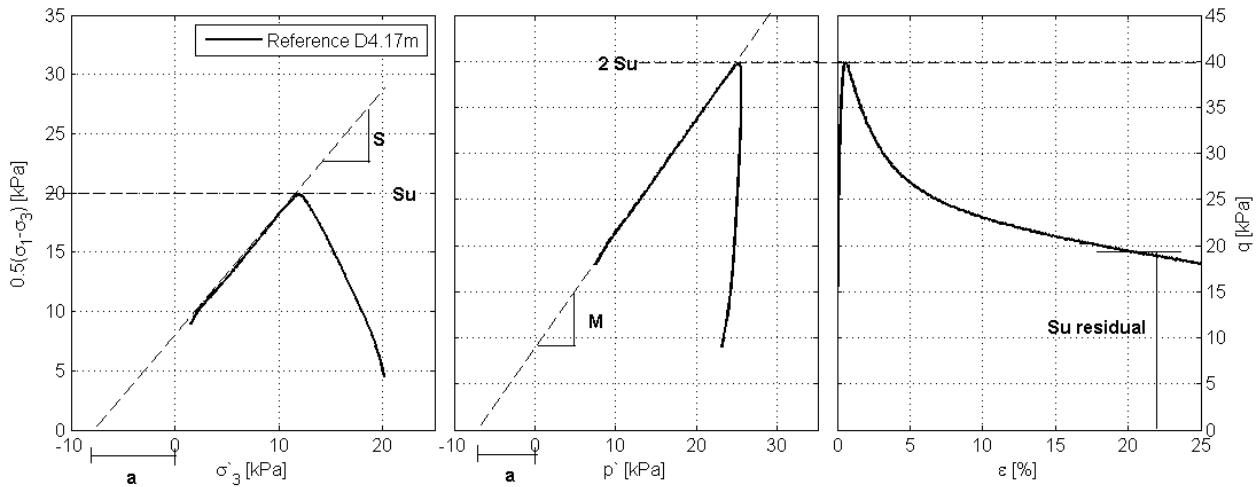


Figure 7.26: Interpretation of triaxial tests

Triaxial tests carried out on samples of several depths from the Dragvoll area as part of the project assignment [9], are used as reference results of the untreated clay. The results of the triaxial tests are displayed in Figure 7.27, 7.28 and 7.29, as q-p plot, NTNU plot and stress strain plots respectively. The storage time is indicated for each test in the figures. Some results were considered to be flawed due to disturbance and operator error during testing and are therefore not included in this thesis. Detailed plots are presented in Appendix F. For further detail and discussion of the results, reference is made to Bryntesen [9].

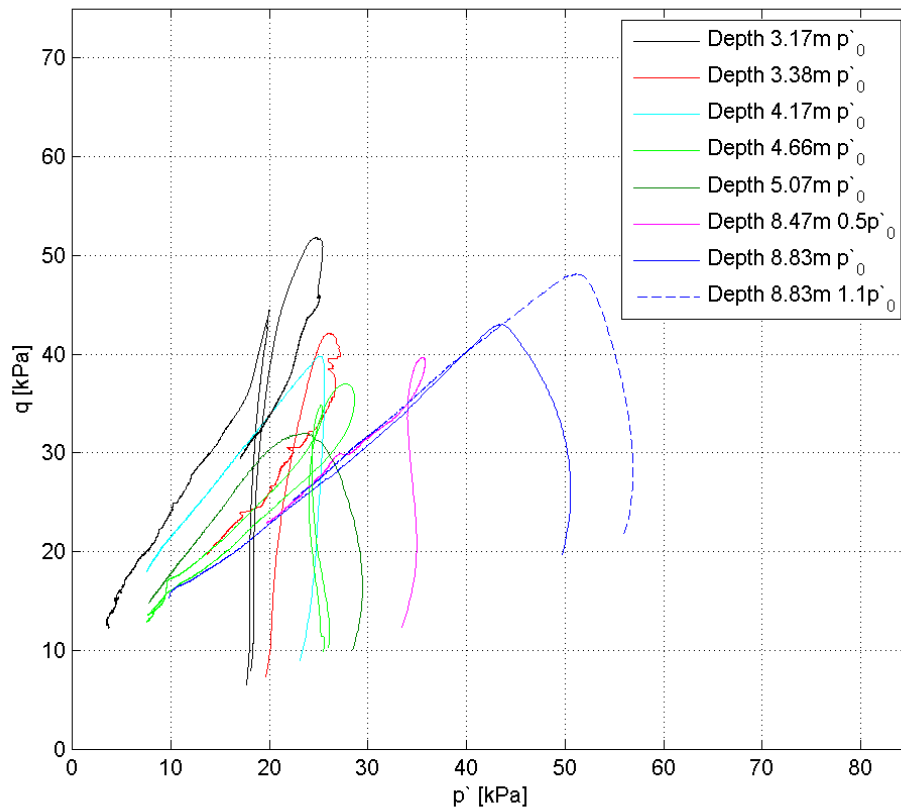


Figure 7.27: Q-p plot of the reference samples (data from [9])

The results displayed in Figure 7.27 and 7.28 indicates friction angles from 35° and down to 23° and an attraction of approximately 7.5 kPa, for the upper part of the profile. Friction angles of roughly 31° and attraction of 11kPa is registered in the deeper part of the profile.

The stress strain plot, Figure 7.29, displays peak and residual undrained shear strength. The residual undrained shear strength is estimated at the point of 20% strain. Results of peak and residual undrained shear strength for all samples are presented in Table 7.5, bellow.

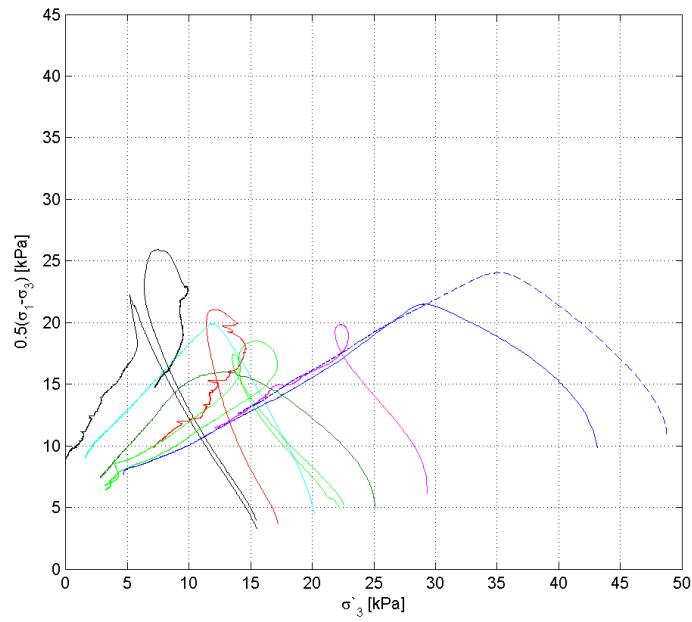


Figure 7.28: NTNU plot of the reference samples (data from [9])

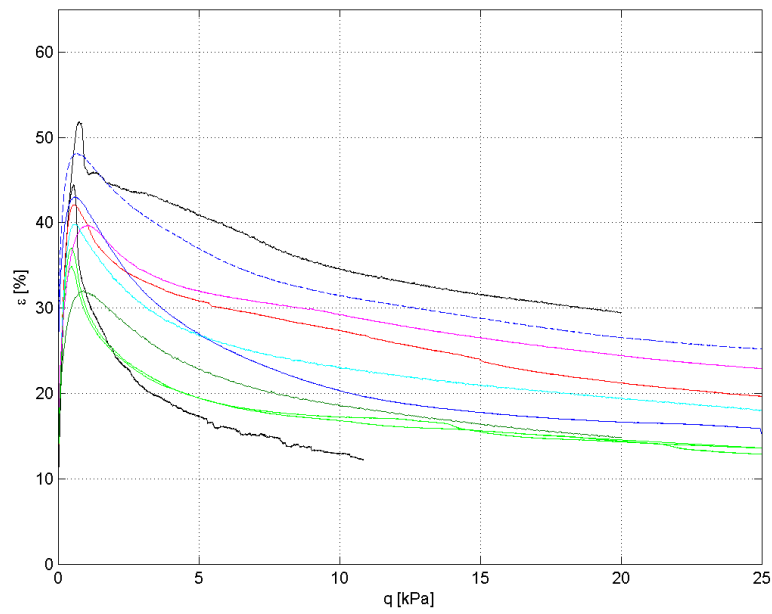


Figure 7.29: Stress strain plot of the reference samples (data from [9])

All triaxial tests performed on KCl and water stored samples are presented individually in Appendix G. Q-p plots of triaxial tests carried out on mini block samples stored in water and KCl solution are plotted in Figure 7.30 a and b, respectively. After the laboratory work was conducted, abnormalities for several of the triaxial results were observed between the tests conducted on the two different triaxial cells. Further investigation proved that the tests carried out on triaxial cell number two, provided a cell pressure half of what was displayed in the equipment. The vertically applied force displayed the correct value. Thus, the tests were consolidated using a too low vertical stress unrealistically low vertical to horizontal stress ratio, K_0' . The results of the tests are displayed in Figure 7.30 a and b, were the results of the tests consolidated to the wrong level is indicated. As seen, the results indicated a generally lower attraction and peak undrained shear stress for the wrongly consolidated specimen relative to the tests considered to be correct. The tests that were run with a deviation in consolidation are therefore excluded in the following.

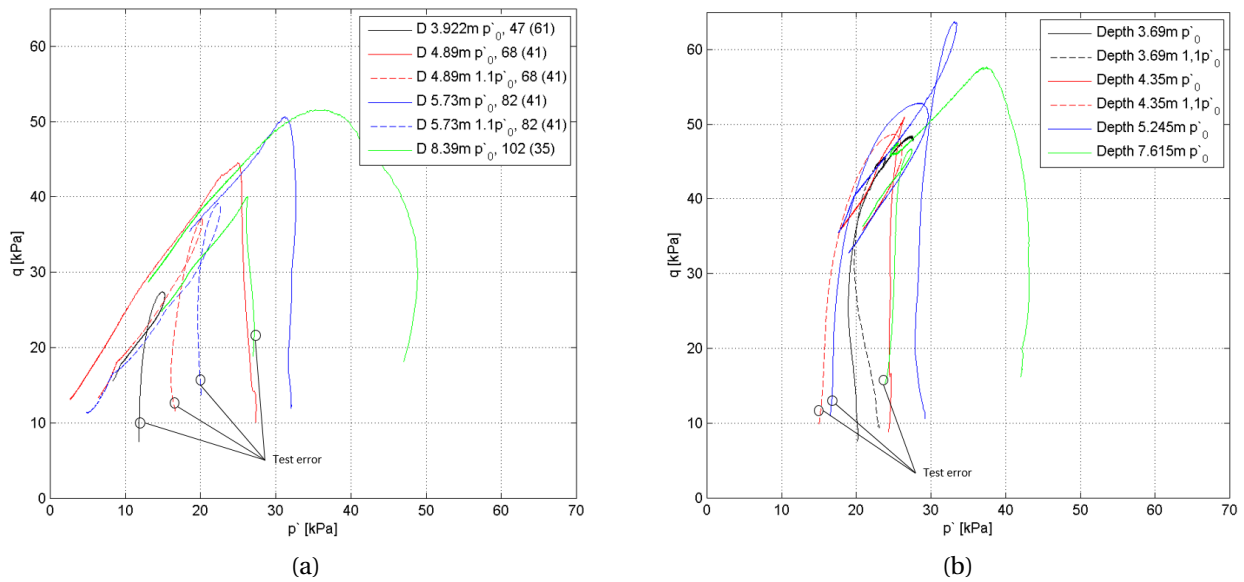


Figure 7.30: Triaxial tests with calibration error

Results from triaxial tests, consolidated to the correct level and performed on block samples stored in water are displayed in the q-p plot, NTNU plot and stress strain plot in Figure 7.31, 7.32 and 7.33 respectively.

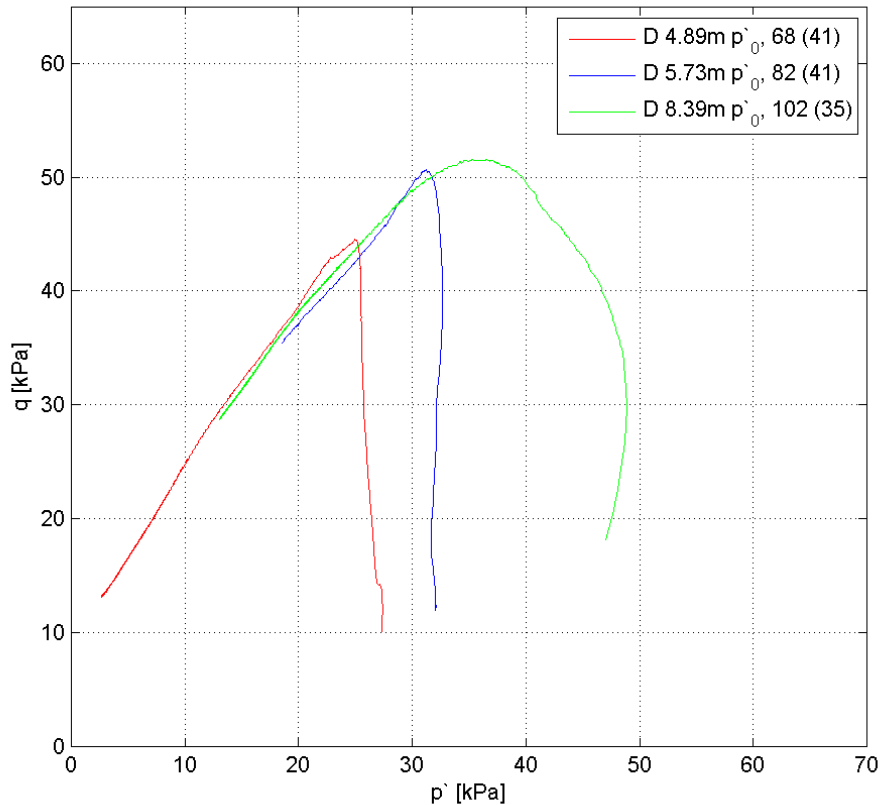


Figure 7.31: Q-p plot of samples stored in water

The results presented in Figure 7.31 and 7.32 indicate friction angles of approximately 31° and attraction of approximately 10 kPa for the deeper parts of the profile, with an attraction and friction angle of 15 kPa and 28° respectively, for the deeper part of the profile.

Stress strain plot displayed in Figure 7.33, indicates the residual and peak strength of specimen stored in water. The triaxial test for the specimen at depth 5.73m was interrupted by a power breakage.

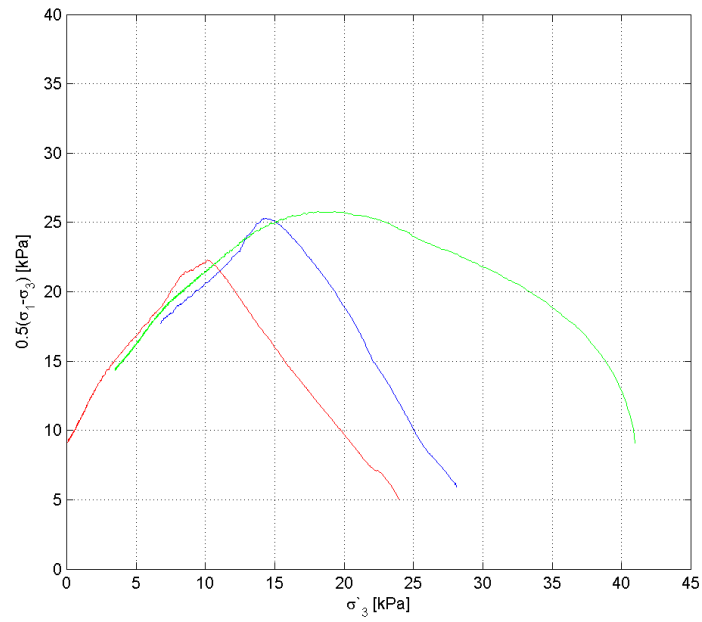


Figure 7.32: NTNU plot of samples stored in water

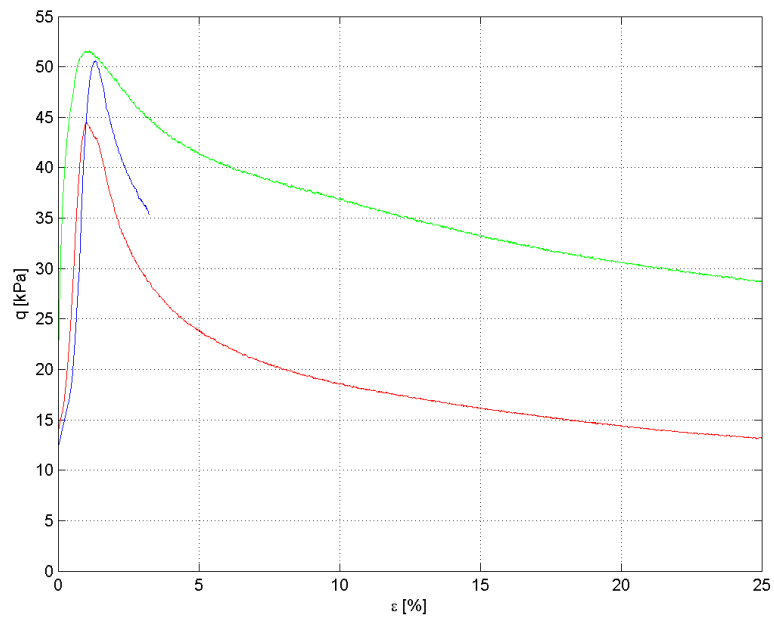


Figure 7.33: Stress strain plot of samples stored in water

Results from triaxial tests, consolidated to the correct level and performed on block samples stored in KCl solution are displayed in the q-p plot, NTNU plot and stress strain plot in Figure 7.34, 7.35 and 7.36 respectively.

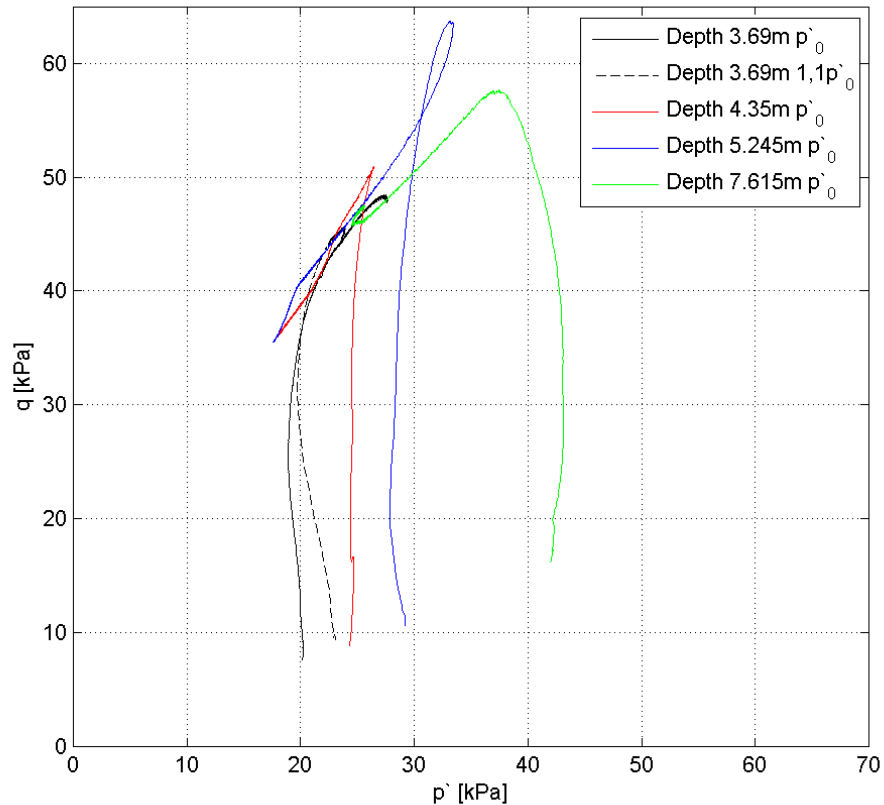


Figure 7.34: Q-p plot of samples stored in KCl solution

Figure 7.34 and 7.35 show friction angles and attraction for the upper part of the profile of $30-32^\circ$ and 12.5 kPa, and 27° and 18 kPa in the lower part of the profile.

Stress strain plot displayed in Figure 7.36, indicates residual and peak strength of specimen stored in KCl solution.

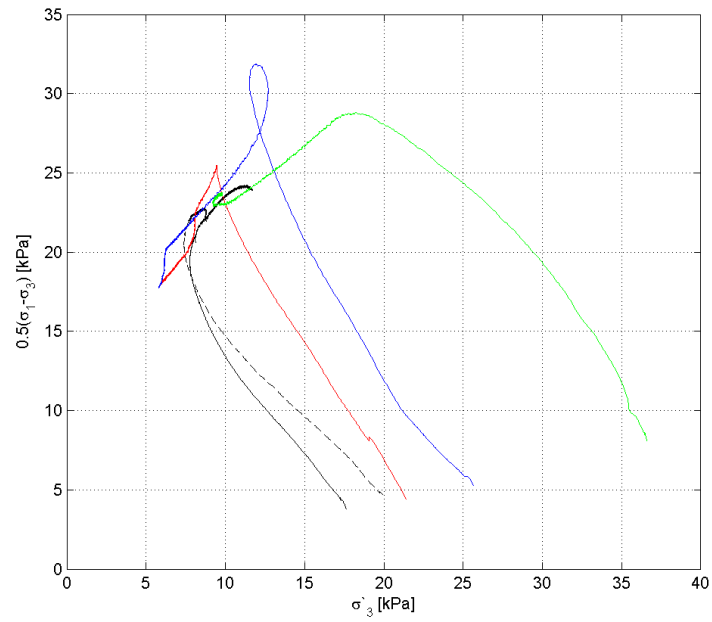


Figure 7.35: NTNU plot of samples stored in KCl solution

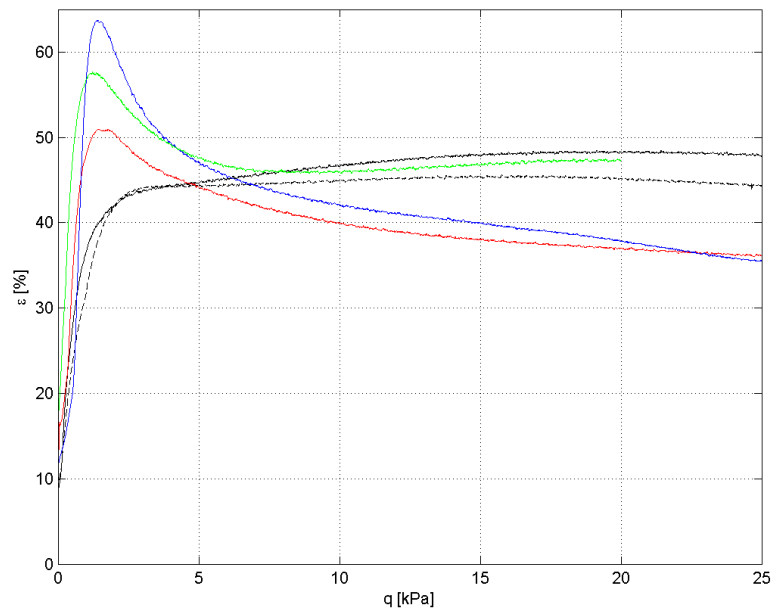


Figure 7.36: Stress strain plot of samples stored in KCl solution

Figure 7.37 to 7.40 display assembled triaxial test results for the different sample treatments. The displayed results are of close proximity in depth and only the results considered to be reliable are included in the assembly. The storage time for each sample is included in the legend. Due to the limited number of reliable triaxial results for some of the storage methods, some are presented in different assemblies.

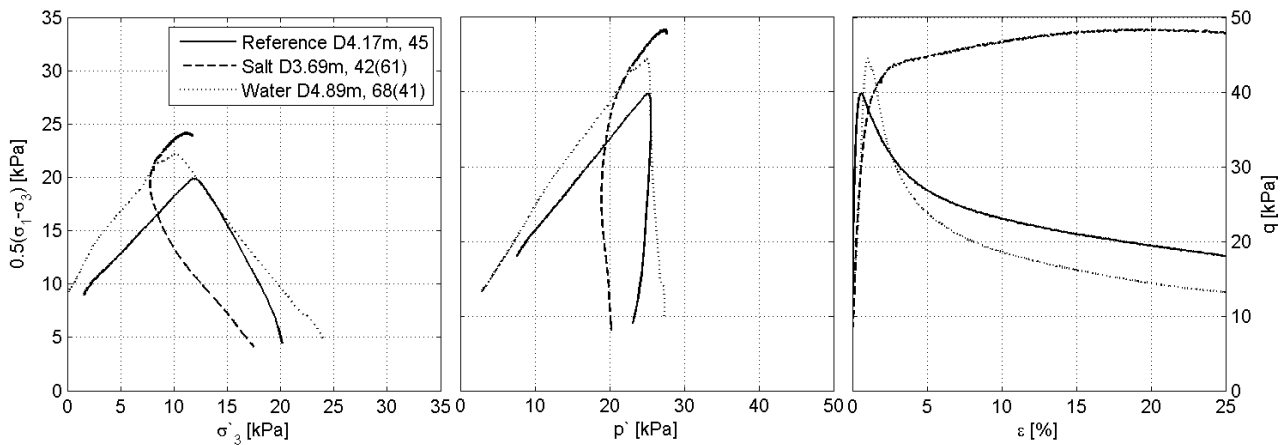


Figure 7.37: Assembly of triaxial results for each sample treatment, at depths between 3 and 5 m

Figure 7.37 displays the correlation between the storage methods of the top of the investigated profile. An increase in undrained shear strength with increased strain is evident for the salt migrated sample, thus the sample dilates. Both the sample stored in water and the reference sample show strain softening, where the clay is weakened with increased strain.

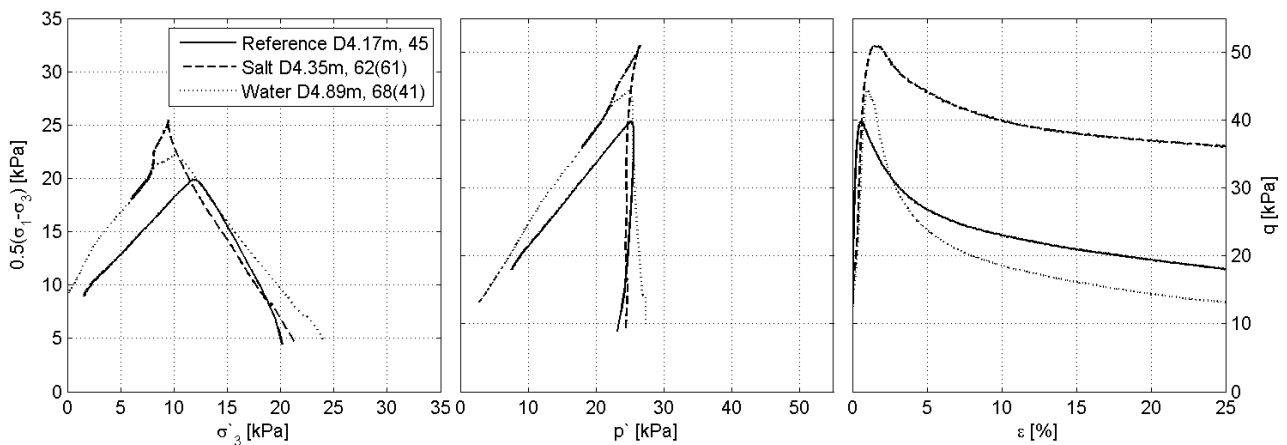


Figure 7.38: Assembly of triaxial results for each sample treatment, at depths between 4 and 5 m

Samples acquired from lower parts of the profile only indicate some tendency of dilatancy at failure, however the results show strain softening with increased strain, as seen in Figure 7.38 and 7.39.

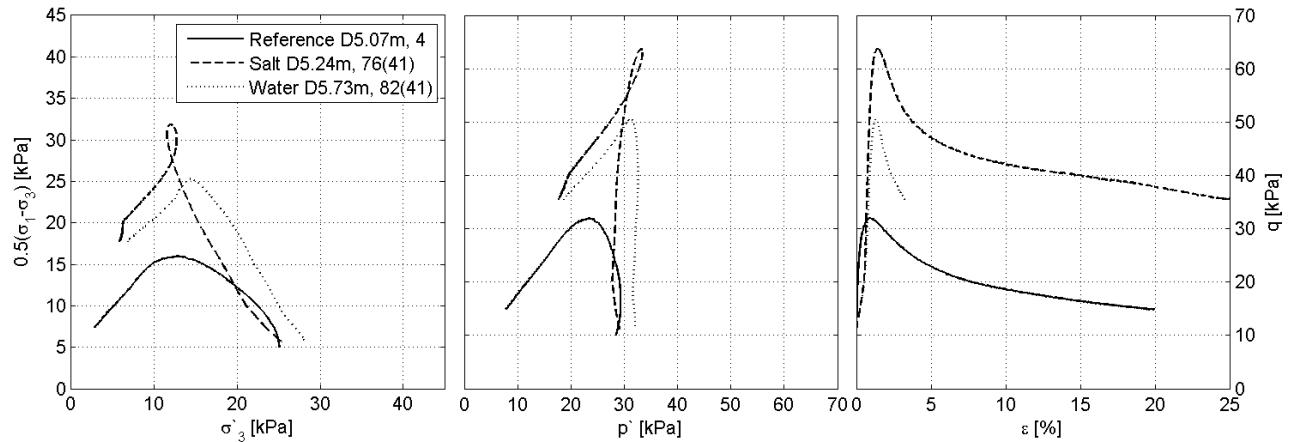


Figure 7.39: Assembly of triaxial results for each sample treatment, at depths between 5 and 6 m

Figure 7.40 display the correlations between the storage methods at the deepest part of investigated profile. Neither of the samples show tendencies of dilatancy at the point of failure. However, the KCl treated sample partially dilates with increased strain, after the point of failure.

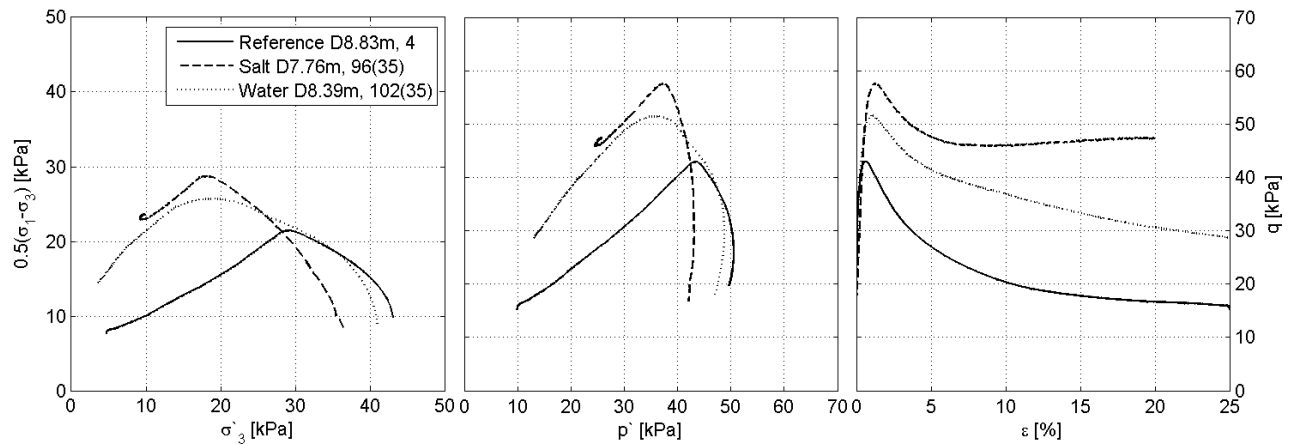


Figure 7.40: Assembly of triaxial results for each sample treatment, at depths between 7 and 9 m

The tests generally show less strain softening for the salt treated samples, compared to the water treated and untreated samples. Further, all tests show an increase in undrained shear strength for the samples exposed to salt migration. A general increase of undrained shear strength is also evident for the samples stored in water.

Table 7.5: Assembly of peak and residual undrained shear strength the the percent reduction from peak, for each treatment method.

Treatment	Consolidation level [p'_0]	Depth [m]	Peak S_u [kPa]	Residual S_u [kPa]	S_u Reduction from peak [%]	Storage time [$days$]	Storage time, cell [$days$]
Refrence	1	3.17	25.9	14.8	43.0	12	
Refrence	1	3.17	22.2	-	-	12	
Refrence	1	3.38	21.0	10.6	49.5	10	
Salt	1	3.69	21.6	24.2	-12.0	61	42
Salt	1.1	3.69	21.8	22.6	-3.8	61	42
Refrence	1	4.17	19.9	9.7	51.1	45	
Salt	1	4.35	25.5	18.5	27.4	61	62
Refrence	1	4.66	17.4	7.2	58.9	52	
Refrence	1	4.66	18.5	7.2	61.0	52	
Water	1	4.89	22.3	7.2	67.7	41	68
Refrence	1	5.07	16.0	7.4	53.7	4	
Salt	1	5.245	31.9	18.9	40.6	41	76
Water	1	5.73	25.3	-	-	41	82
Salt	1	7.615	28.8	23.6	18.1	35	96
Water	1	8.39	25.8	15.3	40.7	35	102
Refrence	0.5	8.47	19.8	12.2	38.4	3	
Refrence	1	8.83	21.5	8.3	61.2	4	
Refrence	1.1	8.83	24.1	13.3	44.8	4	

Table 7.5 displays the peak undrained shear strength and residual undrained shear strength, at 20% strain, acquired from the triaxial tests. Also the percent reduction of undrained shear strength from peak to residual strength is included in the table. The salt treated samples show relatively little change between the peak and residual strength, relative to the salt and water treated samples. As seen in the above figures, peak and residual strength is increased for the salt treated samples and water treated samples, where the salt treated samples display the largest increase of strength. The trend is clearly presented in Figure 7.41, illustrating the resultant depth profile of peak and residual undrained shear strength.

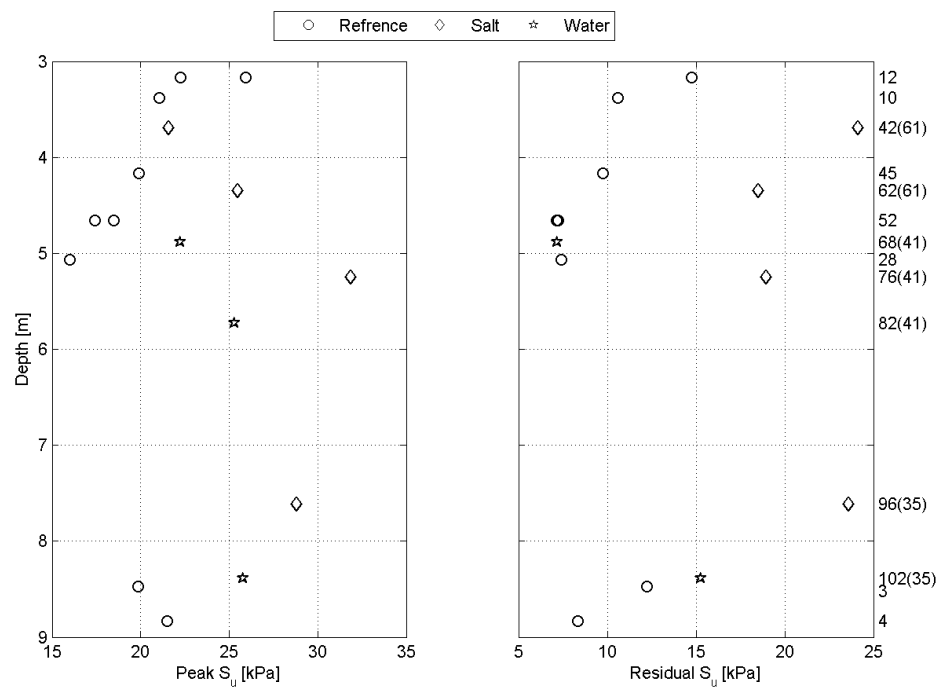


Figure 7.41: Peak and residual undrained shear strength from triaxial tests, presented by depth

7.8 Summary of results

Summary of the results of index, pH and pore water conductivity, oedometer and triaxial tests are displayed in Table [7.6](#), [7.8](#) and [7.8](#), respectively.

Table 7.6: Summarized results from index, pH and conductivity analysis

Salt/ Water/ Ref.	Bore hole	Block	Sec- tion	w [%]	w_l [%]	w_p [%]	I_l [-]	I_p [%]	s_u [kPa]	s_r [kPa]	s_t [-]	Conduc- tivity [mmoh]	pH [-]	Time reg. [days]	Time cell [days]
Ref.	2	3.0-3.25m	3	37.45	28.99	22.18	2.24	6.8	27	0.69	39.13			12	
Ref.	2	3.0-3.25m	2						26	0.69	37.68			12	
Ref.	2	3.0-3.25m	1											12	
Ref.	2	3.25-3.5m	3	38.7	32.05	21.67	1.64	10.38	20.1	0.2	100.5	0.76	8.09	10	
Ref.	2	3.25-3.5m	2									0.75	8.19	10	
Ref.	2	3.25-3.5m	1									0.75	8.23	10	
Salt	2	3.5-3.75m	3	30.85	37.5	20.47	0.61	17.13	28.4	3.7	7.68	165	7.05	61	42
Salt	2	3.5-3.75m	2	33.29	38.06	21.57	0.71	16.49	35.8	5.6	6.39	161	6.94	61	42
Salt	2	3.5-3.75m	1	31.92		21.41			36.8	3.7	9.95	161	6.92	61	42
Water	2	3.75-4.0m	3	38.39	29.4	8.18	1.42	21.21	14.2	0.49	28.98	0.74	8.05	61	47
Water	2	3.75-4.0m	2	46.68	22.07	16.88	5.74	5.19	15.2	0.29	52.41	0.72	8.27	61	47
Water	2	3.75-4.0m	1	37.92	42.19	28.41	0.69	13.78	14.2	0.29	48.97	0.72	8.23	61	47
Ref.	2	4.0-4.25m	3	36.78	28.33	22.13	2.36	6.2	24	0.59	40.68	0.85	8.4	45	
Ref.	2	4.0-4.25m	2						11.7	0.39	30	0.78	8.48	45	
Ref.	2	4.0-4.25m	1									0.74	8.58	45	
Salt	2	4.25-4.5m	3	34.02	34.64	22.33	0.95	12.31	18.6	4.1	4.54	112.5	7.33	61	62
Salt	2	4.25-4.5m	2	33.79	39.61	22.17	0.67	17.44	20.6	4	5.15	107.5	7.4	61	62
Salt	2	4.25-4.5m	1	34.22	35.92	21.25	0.88	14.67	20.6	4.5	4.58	100	7.35	61	62
Ref.	2	4.5-4.75m	3	38.73	26.63	20.88	3.10	5.75	12.7	0.29	43.79	0.8	8.77	52	
Ref.	2	4.5-4.75m	2						12.3	0.29	42.41	0.74	8.74	52	
Ref.	2	4.5-4.75m	1									0.71	8.66	52	
Water	2	4.75-5.0m	3	39.26	29.06	23.67	2.89	5.39	11.3	0.8	14.13	0.8	8.3	41	68

Continued on next page

Table 7.6 – Continued from previous page

Salt/ Water/ Ref.	Bore hole	Block	Sec- tion	w [%]	w_l [%]	w_p [%]	I_l [-]	I_p [%]	s_u [kPa]	s_r [kPa]	s_t [-]	Conduc- tivity [mmoh]	pH [-]	Time reg. [days]	Time cell [days]
Water	2	4.75-5.0m	2	38.23	25.18	20.14	3.59	5.04	16.2	0.7	23.14	0.75	8.65	41	68
Water	2	4.75-5.0m	1	20.53					11.7			0.75	8.68	41	68
Salt	2	5.05-5.3m	3	31.86	37.91	22.18	0.62	15.73	17.7	6.4	2.77	142.5	7.45	41	76
Salt	2	5.05-5.3m	2	31.38	35.9	21.7	0.68	14.2	27.5	5.4	5.09	141	7.4	41	76
Salt	2	5.05-5.3m	1	32.3								139	7.41	41	76
Water	2	5.55-5.8m	3	37.35	27.03	20.61	2.61	6.43	17.7	0.1	177	0.67	8.65	41	82
Water	2	5.55-5.8m	2	36.74	27.18	21.53	2.69	5.65	7.3	0.1	73	0.7	8.85	41	82
Water	2	5.55-5.8m	1	38.31	26.25	20.66	3.15	5.6		0.1		0.7	8.87	41	82
Salt	2	7.45-7.7m	3	27.64	34.37	20.09	0.53	14.28	18.6	3.6	5.17	150	7.8	35	96
Salt	2	7.45-7.7m	2	27.47	30.66	19.64	0.71	11.02				150	7.72	35	96
Salt	2	7.45-7.7m	1	27.88	30.70	20.69	0.72	10.01				150	7.65	35	96
Ref.	2	7.5-7.75m	3	35.95	24.89	19.19	2.94	5.7	4.8	0.1	48	0.73	9.11	28	
Ref.	2	7.5-7.75m	2						4.8	0.1	48	0.73	9.04	28	
Ref.	2	7.5-7.75m	1									0.73	9.06	28	
Water	2	8.2-8.45m	3	44.21	25.13	19.74	4.54	5.39	8.9	0.1	89	0.77	8.98	35	102
Water	2	8.2-8.45m	2	32.98	21.73	19.94	7.29	1.79	9	0.1	90	0.75	9.08	35	102
Water	2	8.2-8.45m	1	40.03	23.31	19.27	5.14	4.04				0.7	9.09	35	102
Ref.	2	8.45-8.7m	3						13.2	0.1	132			3	
Ref.	2	8.45-8.7m	2						11.7	0.1	117			3	
Ref.	2	8.7-9.0m	1	31.46	21.62	18.85	4.56	2.77	9.8	0.1	98	0.56	9	4	

Table 7.7: Summarized results from oedometer tests

Salt/ Water/ Ref.	Bore hole	Block	Depth [m]	σ'_{v0} [kPa]	w [%]	γ [kN/m ³]	σ'_c [kPa]	OCR [-]	M_{OC} [MPa]	m [-]	c_v [m ² /y]	e_v [%]	$\delta e/e_0$ [-]	Time reg. [days]	Time cell [days]
Ref.	2	3.0-3.25m	3.17	22.19		18.05	125	5.63	5	22	20	2.44		12	
Ref.	2	3.0-3.25m	3.13	21.91	38.70	18.33	130	5.93	6	22		2.19	0.04	12	
Ref.	2	3.25-3.5m	3.34	23.38	45.40	17.80	80	3.42	4	18	42	2.66	0.05	10	
Salt	2	3.5-3.75m	3.65	25.55	36.66	18.96	90	3.72	4	18	85	1.96	0.04	61	42
Water	2	3.75-4.0m	3.9	27.33	40.66	18.38	70	2.56	2	23	16	2.33	0.04	61	47
Water	2	3.75-4.0m	3.95	27.68	40.76	18.12			2	26	8	2.29	0.04	61	47
Ref.	2	4.0-4.25m	4.16	29.12	40.60	18.05	70	2.4	3	22	5.7	0.00	0.00	45	
Ref.	2	4.0-4.25m	4.21	29.47	35.50	18.77	50	1.7	2	27	23	1.95	0.04	45	
Salt	2	4.25-4.5m	4.35	30.48	40.48	18.67	120	3.94	6	22	31	2.27	0.04	61	62
Salt	2	4.25-4.5m	4.31	30.2	37.82	19.03	115	3.81	4	21	19.2	2.03	0.04	61	62
Ref.	2	4.5-4.75m	4.71	32.97	39.70	18.14	70	2.12	2	27	15	2.45	0.05	52	
Ref.	2	4.5-4.75m	4.62	32.38	35.40	18.66			3	27		0.00	0.00	52	
Water	2	4.75-5.0m	4.95	34.65	41.42	18.00	80	2.45	2	24	27	2.43	0.04	41	68
Ref.	1	5.0-5.25m	5.15	36.05	37.30	18.22	75	2.08	4	32	17	2.36	0.05	4	
Ref.	1	5.0-5.25m	5.17	36.19	39.20	18.50	70	1.93	2	28	14	2.50	0.05	4	
Ref.	1	5.0-5.25m	5.19	36.33	39.90	18.37	70	1.93	2	28	7.08	2.55	0.05	4	
Salt	2	5.05-5.3m	5.27	36.89	38.55	18.94	100	2.71	3	19	16.5	2.16	0.04	41	76
Salt	2	5.05-5.3m	5.19	36.33	38.04	18.97	80	2.2	3	20	15.5	2.12	0.04	41	76
Water	2	5.55-5.8m	5.7	39.93		18.47	75	2	3		23.5			41	82
Water	2	5.55-5.8m	5.73	40.14		18.34	75	1.87	4		19			41	82
Ref.	1	6.0-6.25m	6.1	42.74	39.30	18.33	75	1.75	3	28	4	2.58	0.05	11	
Ref.	1	6.0-6.25m	6.14	43	38.90	18.21	75	1.74	5	25	15	2.52	0.05	11	
Ref.	1	6.0-6.25m	6.22	43.58	41.10	18.14	75	1.72	4	33	15	2.46	0.05	11	
Salt	2	7.45-7.7m	7.57	53.02		19.57	115	1.89	3	21	60			35	96
Ref.	2	7.7-7.95m	7.87	55.13	43.70	18.44	70	1.27	3	31	7	3.04	0.06	28	
Water	2	8.2-8.45m	8.35	58.48	34.13	19.33	70	1.2	2	24	3.3	2.22	0.05	35	102
Ref.	2	8.45-8.7m	8.6	60.21	33.50	19.13			4	25		2.02	0.04	3	
Ref.	2	8.45-8.7m	8.55	59.85	35.00	18.81	70	1.17	2	26	3.2	2.02	0.04	3	
Ref.	2	8.7-9.0m	8.91	62.38	34.30	19.02	75	1.2	3	31	2.2	2.19	0.05	2	

Table 7.8: Summarized triaxial test results

Salt Water	Bore hole	Block	p'_0	Depth [m]	σ'_{v0} [kPa]	w [%]	γ [$\frac{kN}{m^3}$]	s_u [kPa]	s_u res. [kPa]	a [kPa]	$\tan\phi$ [-]	D [-]	ϵ_f [%]	ΔV [cm^3]	ϵ_v [%]	$\Delta e/e_0$ [-]
Ref.	2	3.0-3.25m	1	3.17	22.5	45.6	17.45	25.9	14.8	-	-	0.03	0.67	0.59	0.25	
Ref.	2	3.0-3.25m	1	3.17	22.5	-	17.24	22.2		5.8	0.73	0.04	0.7	0.52	0.22	0.004
Ref.	2	3.25-3.5m	1	3.38	23.6	-	-	21.0	10.6	2.8	0.58	0.09	0.66	0.8	0.34	0.006
Salt	2	3.5-3.75m	1	3.69	25.83	34.26	19.08	21.6	24.2	11.1	0.78	-0.08	2.5	1.18	0.51	0.010
Salt	2	3.5-3.75m	1.1	3.69	25.83	33.48	19.31	21.8	22.6	11.1	0.78	-0.34	2.5	1.55	0.67	0.014
Ref.	2	4.0-4.25m	1	4.17	29.19	38.4	17.2	19.9	9.7	7.2	0.61	0.18	0.46	1.03	0.44	0.009
Salt	2	4.25-4.5m	1	4.35	30.45	35.87	18.92	25.5	18.5	10	0.78	0.05	1.47	1.24	0.53	0.011
Ref.	2	4.5-4.75m	1	4.66	32.6	41.1	17.48	17.4	7.2	6.4	0.47	-	0.38	1.91	0.82	0.016
Ref.	2	4.5-4.75m	1	4.66	32.6	41.4	18.68	18.5	7.2	8.2	0.47	0.01	0.37	1.48	0.64	0.012
Water	2	4.75-5.0m	1	4.90	34.27	39.64	18.75	22.3	7.2	9.3	0.65	0.03	1.02	2.52	1.09	0.021
Ref.	1	5.0-5.25m	1	5.07	35	41	18.85	16.0	7.4	3.64	0.62	0.27	0.7	3.97	1.71	0.033
Salt	2	5.05-5.3m	1	5.25	36.72	34.26	19.52	31.9	18.9	13.3	0.59	-0.29	1.42	2.42	1.04	0.022
Water	2	5.55-5.8m	1	5.73	40.11		18.79	25.3		14.1	0.52	-0.09	1.33	1.38	0.60	
Salt	2	7.45-7.7m	1	7.62	53.31	30.68	19.90	28.8	23.6	18.1	0.5	0.1	1.23	3.22	1.39	0.031
Water	2	8.2-8.45m	1	8.39	58.73	34.27	19.48	25.8	15.3	16.7	0.49	0.17	1.12	-	-	
Ref.	2	8.45-8.7m	0.5	8.47	59.3	35.3	19.66	19.8	12.2	11.2	0.43	0.32	0.77	30.3	13.06	0.270
Ref.	2	8.7-9.0m	1.1	8.83	61.8	37.5	19.6	21.5	8.3	9.8	0.43	0.23	0.44	4	1.72	0.037
Ref.	2	8.7-9.0m	1	8.83	61.8	38.1	19.46	24.1	13.3	9.8	0.43	0.23	0.4	5.25	2.26	0.048

Chapter 8

Discussion

Properties of in situ depth profile

Based on visual observations, hydrometer analysis and NS3007 [40], the clay is defined as silty clay in the upper part to clay in the deeper parts of the profile. Horizontal silt layers, occasional drop stones, shells and shell fragments were also observed. The observations, supported by laboratory investigation, indicate a general inhomogeneity through the depth profile. Results of the reference samples from the oedometer test displayed high OCR values at around 3 m depth. Thus, the dry crust is assumed to reach down to approximately 3 m. Below what is considered the dry crust, the OCR is decreased to a level of approximately 1.3 at the depth of about 8 m. Hence, below 8 m the clay is considered normally consolidated. The over-consolidation of the samples in the upper part of the profile induce an undrained strength above the failure line and a tendency to dilate at the point of failure. Thus, creating the characteristic loops. The described effects may be related to a weathering zone. No triaxial or oedometer tests were carried out on untreated clay samples between 5 and 8 m in bore hole 2, due to high sample loss during sampling, in the respective area. The influence depth of the presumed weathered zone is therefore unknown. Reduction in recorded pH with depth and relatively higher remoulded shear strength in the upper part of the profile amplifies the theory of influence of weathering in the respective area. As described from previous investigations and theory, the influence of weathering is assumed to decrease with depth. Due to potential large local variations, only results from bore hole 2 is considered. Results of ion concentrations in the sampled pore water is expected to provide information related to the weathering zone.

Limitations

General limitations in the study of the effect of KCl migration, storage- and weathering effects are related to the high level of inhomogeneity, associated to both the weathering zone and layering, observed in the analyzed soil profile. The large deviations in storage time and the general inhomogeneity of the soil reduce the level of comparison between the clay samples. Thus, only consistent variations observed for the different treatments of the clay can be seen as conclusive.

As the mini block samples were installed in the storage cells, large amounts of KCl salt was added to ensure saturated solution. When the salt migrated samples were extracted from the cells, precipitated salt was observed, covering large portions of the mini block sample. The cell containing mini block sample D 7.45-7.7m displayed signs of leakage and was therefore placed in a water tank to slow down the leakage. When the cell was opened approximately one third of the water had drained out. Thus, the mini block sample was partially stored in KCl slurry.

For mini block samples stored in the deaired, distilled water, the surrounding plastic foil was not removed prior to cell installation. Thus, air trapped within the plastic foil is a possible error for all the samples. Due to potential increase in oxygen supply.

Observations

Observed color change on the mini block periphery is recognized as slow oxidation of $Fe(OH)_3$ to $FeO - OH$, described by Mitchell and Soga [30]. The reach of the discoloration seem to increase with storage time. The outer part of the samples are exposed to oxygen and is therefore easily affected by the oxidation. An observed silt layer indicated color change throughout the sample within the layer and some millimeters into the surrounding clay. Which, is probably due to the higher permeability of silt, relative to clay. Thus, the silt layer is more easily affected by migration of water and moisture loss and intrusion of air, i.e. oxygen. Causing accelerated oxidation in the respective area of the sample. The discoloration is slowed down after cell installation, due to the relatively anaerobic environment in the cell.

Mineralogy

The decrease of quartz with depth may be seen in relation with the increased clay content with depth, recorded by hydrometer analysis. The recorded calcite minerals are assumed to originate from shell fragments observed in the clay. Thus, the lower calcite content recorded in the upper layers may indicate absence or reduction of shell fragments.

The analysis of the bulk quick clay indicated low contents of clay minerals. In addition, results from the clay fraction displayed low contents of clay minerals. Which, can possibly be explained by the fact that the clay mineral illite is mechanically degraded muscovite. A distinction between muscovite and illite can therefore be problematic. Another explanation could be that the clay sized fraction contain relatively low contents of clay minerals and larger quantities of rock minerals, mechanically degraded to $< 2 \mu\text{m}$. The clay minerals detected in the minerals is of known low cation exchange capacity. Thus, a low cation exchange capacity is expected for the clay. Results from analysis of cation exchange capacity are therefore desired to confirm the assumption.

Muscovite and biotite are both minerals within the mica group, which can cause difficulty in distinguishing between the two minerals. Thus, the exact content of the different mica minerals are difficult to analyze.

The detected minerals are consistent with the minerals which are generally present in quick clay, based on previous investigations.

pH and pore water chemistry

The observed consistent increase in pH with depth can possibly be explained by decreasing influence from the surface, where the clay is affected by weathering, from water and oxygen. Thus, pH is decreased by increased acid in the pore water, formed by oxidation. Due to the described oxidation process a reduction in pH was expected in the edge section of the samples, relative to the center section. However, no distinct reduction in pH was observed for the outer parts of the section. Which is probably due to poorly calibrated pH-meter or by human error. Another explanation is that the samples must be stored over a longer period to induce observable pH changes. However, the visual, slow oxidation of $\text{Fe}(\text{OH})_3$ to $\text{FeO} - \text{OH}$, reached as far as 1 cm into the clay in the sampled stored in air for 45 days. The samples stored in deaired, distilled water show a consistent reduction in pH for the outer layer, indicating oxidation during water storage, thus oxygen has entered the cells. However, the result can also be explained by influence of the surrounding water, with an initial pH of 7 and possible leaching of ions from the clay pore water onto the surrounding distilled water. A generally consistent increase in pH, with average of 1.2 is indicated after salt diffusion. Based on previous investigations a decrease in pH in salt migrated samples was expected.

Results from the conductivity measurement indicate a pore water salt content below 1 g/l in the water treated and reference samples. Thus, the salinity is below the level which encourage quick clay development. As expected, a general increase of pore water conductivity is registered with increasing KCl diffusion time. However, the conductivity-meter is considered unreliable for analysis of highly conducting liquid, based on previous experience in the laboratory by Tonje Eide Helle.

Pore water chemistry analysis of the major ions, i.e. Na^+ , K^+ , Ca^{2+} , Mg^{2+} , Cl^- , SO_4^{2-} , NO_3^- and HCO_3^- , of the sampled pore water should be carried out to analyze the effect of storage time in air, water and KCl solution. And in turn, compare the chemical results to the geotechnical properties and variations observed from pH measurements. The concentration of K^+ is considered extra important as it can be used to analyze the diffusion process. And in addition relate the ion concentration to the change in geotechnical parameters.

Index tests

Laboratory investigations of index parameters displayed a general consistency in the results throughout the sections in the clay samples, which correlates with the pH recordings. Minor changes and trends are overruled by the general variability in the results. The general horizontal homogeneity within each sample is probably due to the extensive storage time. Minor deviations are related to operator error. Previous investigations state an evident increase of liquid limit with salt content, the the results obtained in this thesis display the same trend, relative to both the reference samples and the samples stored in water. No significant increase in the liquid limit was observed in the water treated samples, relative to the reference samples. The clear reduction of water content observed in the salt migrated samples is linked to the precipitated KCl surrounding the samples. Thus, inducing osmosis, extracting water from the sample. The minor increase of plastic limit, observed in the salt migrated samples are consistent with previous investigations. However, the same increase is evident in the water treated sample. Indicating that the increase is presumably caused by weathering alone. The results are however not conclusive due to inhomogeneity observed in the profile. Further investigations are recommended. The large increase of liquid limit induce and increase of plasticity index, which classify the water treated and reference values as low plasticity clay. The salt migration alters the clay properties to what is defined as medium plasticity clay. A decrease in liquidity index is also evident in the KCl migrated clay. However, the liquidity index is also related to water content, thus the presumed osmosis also affect the decrease of liquidity index.

The falling cone test display a general increase in undrained shear strength, of approximately 10 kPa, implying an approximate increase of 100%, observed after salt migration. The increase is related to the increased inter-particle strength of the clay, caused by the escalated ion concentration. The remoulded shear strength of the salt migrated sample indicated an average value approximately 40 times the remoulded strength obtained from the reference and water treated samples. The undrained and remoulded strength obtained from the falling cone test is however largely dependent on water content. Thus, the observed reduction in water content, in the salt migrated samples, also increase undrained, and especially the remoulded shear strength. The level of influence is indecisive, however the resultant strength increase is partially due to the reduced water content and should therefor be considered. The large increase of remoulded strength cause, by definition, a decrease in sensitivity. Thus, the salt migration alters the clay properties form a very sensitive clay in the lower region of the profile, resulting in a clay of low sensitivity. Previous investigations displayed an increase in remoulded shear strength and thus, a decrease in sensitivity due to aging. No increase in remoulded strength is evident in the water treated samples. Which, is probably related to storage time and good quality samples.

Oedometer

Oedometer results displayed a distinct, general increase of quasi-preconsolidation pressure of the salt migrated samples, relative to the water treated and reference samples. A distinct, general reduction of compressibility was also observed from the oedometer tests. The described trends are also concluded in previous investigations [5] [23] [55]. The increased preconsolidation pressure is related to the increased shear strength of the material. Whereas the increased modulus number of the normally consolidated area, i.e. the general compressibility at high stresses, is related to the increased plasticity, as set forth in by Bjerrum [5]. The increased preconsolidation pressure obtained in the KCl migrated samples, resultant from this thesis might relate to the increased unit weight of salt migrated samples. Where, results of density tests indicates a general increase in density, or unit weight, for the KCl treated sample. The observed increase may be related to the increased salt content in the pore water alone, as the added ions cause additional weight. In addition, a post sampling consolidation, due to osmosis during salt migration, causing compression of the clay, may also be a plausible explanation. The effect would also lead to increased preconsolidation pressure, compared to reference and untreated clay. However, reduced water content for salt treated clay was not reported in the previous investigations. Thus, the main effect causing the increased preconsolidation is related to increased shear strength. However, no conclusion can be drawn based on the results of this thesis, due to the unexpected reduction of water content in the respective samples. Theory predicts an increase in preconsolidation pressure caused by weathering. The results from water treated samples however, display no clear increase in preconsolidation pressure. Thus, for the cell storage time is not sustained for the required amount of time, based on the close to deaired environment in the cell, for the preconsolidation to be affected. Which, is confirmed by the pH results. No distinct decrease in compressibility was observed for the samples stored in water, relative to the reference results, which correlates with the low plasticity. The coefficient of consolidation is generally unaffected by the storage method. Two of the salt migrated samples do however display a considerable increase in the coefficient of consolidation, potentially caused by silt layers and increased silt content.

Triaxial test

Diffusion of dissolved KCl resulted in a general increase in s_u , is consistent with the previous investigations. The increase is related to the increased inter-particle bonding of the clay after infiltration of K^+ ions. The results indicated large variations in the undrained shear strength of KCl migrated samples, relative to the reference samples. The large variations are linked to the inhomogeneity of the soil profile in relation to layering, the deep influence of the in situ quick clay weathering and to KCl diffusion time. A general increase of undrained shear strength of the samples stored in water, relative to the reference samples, is also evident from the results. Based on theory, the increased undrained shear strength is most likely caused by weathering of the clay samples during cell storage. Approximately 50% of the increase of undrained shear strength observed in the KCl migrated samples, is also evident in the samples stored in water. Due to the high level of inhomogeneity. The exact ratio between increase in s_u for salt migrated samples and samples stored in water should be further investigated. A general increase of residual undrained shear strength is observed from the triaxial test results. The increase is related to the increase of remoulded shear strength observed in the clay and the decreased inter-particle repulsion of the clay. Reduction from peak undrained shear strength to the residual strength of the KCl migrated samples, is generally decreased relative to the water treated and reference samples. The water treated samples show no consistent increase in residual strength. The residual strength is related to the remoulded shear strength. Despite the increased residual strength and the plastically properties observed in the KCl migrated samples, some decrease from the peak to residual strength is present. Which, can be explained by high quality samples obtained using the mini block sample.

Chapter 9

Conclusion

Most of the obtained results, with regard to alterations related to salt migration, is equivalent to findings from previous investigations. Deviations in some of the results, obtained from the samples stored in water, related to storage time and weathering are evident. Thus, parts of the improvement of geotechnical properties, observed in the laboratory, is not related to salt diffusion alone. Weathering and aging may represent parts of the soil strengthening observed in the laboratory tests. The effects must be considered when considering the outcome of installation of the in situ ground improvement.

Relative to the reference samples, a significant decrease in pH is evident in the samples exposed to salt migration. No considerable change is recorded in the samples stored in water, however a minor but consistent decrease is observed in the periphery of the mini block samples.

A large increase is recorded in the liquid limit after salt migration. However, no significant increase is evident in the samples stored in water.

Minor increase in plastic limit is recorded for samples stored in both water and salt solution, relative to the reference samples. Thus, the alteration is potentially influenced by weathering alone. The recorded increase is however small, considering the general variability and inhomogeneity in the profile.

The significant increase of the liquid limit, combined with only minor increase in plastic limit, cause alteration in the clay property after salt migration. And thus alters the material properties of the clay, from low plasticity to medium plasticity clay. As no increase of liquid limit is evident for the sample stored in water, no alteration of the plasticity is obtained.

Results obtained from the falling cone test show increased undrained shear strength and significantly increased remoulded shear strength, in the salt migrated samples. Thus, the clay is altered from very sensitive clay to clay of low sensitivity. No such alteration is observed in the samples stored in water.

Oedometer test results display an increase in preconsolidation pressure in the salt migrated samples, relative to reference samples. No clear increase is evident in the samples stored in the water cell. However, the preconsolidation pressure is difficult to interpret in most of the results from samples stored in water cells, and partially in KCl solution cells. A decrease of compressibility, i.e. modulus number, is also evident in the salt migrated samples. No clear trend of decrease in compressibility is evident in the samples stored in water.

A distinct trend of increase of undrained shear strength, resultant from triaxial undrained compression tests, is evident in both salt migrated samples and samples stored in water. Due to inhomogeneity in the soil profile, a percent increase cannot be concluded. However, the general trend display that the samples stored in water display an increase of approximately half the increase resulting from the salt migrated samples, relative to the reference results.

A general increase in residual undrained shear strength, resultant from triaxial tests, is observed in the salt migrated samples. No deviations are evident in the residual strength between the water and reference samples.

Although some changes are seen in in the water treated samples. The complete alteration of clay property, as seen in salt migrated clay, is not evident in the weathered clay.

Analysis of cation exchange capacity in sampled clay and concentration of the major ions in the sampled pore water are recommended to correlate changes in the geotechnical parameters to the general geochemistry and especially potential variations of the pore water ion concentration.

Due to the varying storage time and considerable inhomogeneity observed in the profile, based on observations and initial tests, the tested samples are considered to have a low degree of comparability. Thus, only large variations are considered conclusive. The loss of water content in the samples exposed to salt migration, related to osmosis, alters the properties of the clay. And, is a considerable source of error. Further investigation to support or discard the conclusions made in this thesis is recommended.

Chapter 10

Further investigation

Potential further work include, perform analysis of major ions, i.e. Na^+ , K^+ , Ca^{2+} , Mg^{2+} , Cl^- , SO_4^{2-} , NO_3^- and HCO_3^- , on the sampled pore water and analyze cation exchange capacity of the prepared, sampled clay. Diffusion time can be analyzed by back calculation of the recorded concentrations.

To further investigate the effect of weathering during storage time, the method described in this thesis should be repeated with the following changes:

- A location of known homogeneity should be chosen as a research area. The samples should be collected from depths below a potential weathered zone. In the Dragvoll area it is recommended to extract the samples from below the minimum depth of 7 m.
- The samples should be tested and stored in the cell in a consistent order.
- The samples should be tested and installed in the allocated storage cells as soon as possible, preferably within 3-4 days after sampling. Which, will remove the extra variable of sample storage.
- The KCL solution should be pre-mixed with the desired KCL concentration, to remove the presumed osmosis effect observed from the clay slurry.
- Prior to cell installation the water content, Atterberg limits and falling cone tests should be performed on the samples allocated to salt migration or storage in water. The testing can be conducted on the top layer of each of these mini block samples.
- When the samples are extracted from the cell, each sample should be inspected with regard to potential layering and visible storage effects.
- For better comparison of undrained shear strength, the triaxial test results should be normalized.

Based on the above changes, the effect of ion concentration on the geotechnical properties can be analyzed in further detail.

As the clay minerals only represented minor portions of the clay fraction, an XRD analysis on the clay fraction can be repeated to conform the findings.

Bibliography

- [1] Appelo, C. A. J. and Postma, D. (2005). *Geochemistry, groundwater and pollution*. A. A. Balkema, 2nd edition.
- [2] Arman, A. and McManis, K. (1976). Effects of storage and extrusion on sample properties. *ASTM special technical publication*, (599):66–87.
- [3] Berry, P. W. and Jørgensen, P. (1971). Grain size, mineralogy and chemistry of a quick-clay sample from the ullensaker slide, norway. *Engineering Geology*.
- [4] Bjerrum, L. (1954). Geotechnical properties of norwegian marine clays. *Geotechnique*, 4:49–69.
- [5] Bjerrum, L. (1967). Engineering geology of norwegian normally-consolidated marine clays as related to settlements of buildings. *The 7th Rankine lecture. Geotechnique*, 17:83–117.
- [6] Bjerrum, L. (1973). Problems of soil mechanics and construction on soft clays and structurally unstable soils (collapsible, expansive and others). In *Proc. of 8th Int. Conf. on SMFE*, volume 3, pages 111–159.
- [7] Bjerrum, L. and Rosenqvist, I. (1956). Some experiments with artificially sedimented clays. *Geotechnique*, 6:124–136.
- [8] Bozozuk, M. (1971). Effect of sampling, size, and storage on test results for marine clay. *Sampling of Soil and Rock, STP*, 493:121–131.
- [9] Bryntesen, R. N. (2013). Block sample testing at dragvoll. *Project assignment, Norwegian University of Science and Technology*.
- [10] Clayton, C. (1999). Block sampling of soil: Some practical considerations. In *Geotechnics for Developing Africa: Proceedings of the 12th regional conference for Africa on soil mechanics and geotechnical engineering, Durban, South Africa, 25-27 October 1999*, volume 12, page 331. CRC Press.

- [11] Eggestad, A. and Sem, H. (1976). Stability of excavations improved by salt diffusion from deep wells. In *Sechste Europaeische Konferenz Fuer Bodenmechanik Und Grundbau*, volume 1.
- [12] Emdal, A., Long, M., Bihs, A., Gylland, A., and Boylan, N. (2012). Characterisation of quick clay at dragvoll, trondheim, norway. *Geotechnical Engineering Journal of the SEAGS and AGSSEA*, 43.
- [13] Hafsten, U. and Mack, G. (1989). Universitetsområdet på dragvoll gjennom 12 000 år. *Unit-Nytt*, pages 16–19.
- [14] Hafsten, U. and Mack, G. (1990). Den postglaciale landskapsutviklingen på dragvoll universitetsområde, trondheim. *Norsk geografisk tidsskrift*, 44:131–148.
- [15] Helle, T. E. (2013a). Clay minerals - mineralogy, pore water chemistry and geotechnical properties. *Fakultet for Ingeniørvitenskap og Teknologi, NTNU*.
- [16] Helle, T. E. (2013b). Saltdiffusjon som grunnforsterking i kvikkleire. *Norges vassdragsdrag og energidirektorat, NGL, Statens vegvesen og Jernbaneverket*.
- [17] Helle, T. E., Gjengedal, I., Emdal, A., Aagaard, P., and Høydal, Ø. (2013). Potassium chloride as ground improvement in quick clay areas - a preliminary study.
- [18] Henriksson, M. and Carlsten, P. (1994). Lagringstidens inverkan på prøver tagna med standardkolvprotogare. *Statens geotekniska institut*.
- [19] Heymann, G. (1998). The stiffness of soil and weak rock at very small strains. *PhD Thesis, University of Surrey, U.K.*
- [20] Hvorslev, M. J. (1949). Subsurface exploration and sampling of soils for civil engineering purposes.
- [21] Janbu, N. (1963). Soil compressibility as determined by oedometer and triaxial tests. In *European Conference on Soil Mechanics and Foundation Engineering*, volume 1, pages 19–25.
- [22] Karlsrud, K., Otter, R., and Gjelsvik, V. (2013). State-of-the-art: Blokkprøver.
- [23] Kenny, T. C. (1966). Shearing resistance of natural quick clays. *Ph. D. Thesis, Univ. of London*.
- [24] Leroueil, S., Tavenas, F., and Bihan, J.-P. L. (1983). Propriétés caractéristiques des argiles de l'est du canada. *Canadian Geotechnical Journal*, 20(4):681–705.
- [25] Lessard, G. (1978). *Traitement Chimique Des Argiles Sensibles D'Outardes 2*. PhD thesis, Université de Montréal.

- [26] Lessard, G. and Mitchell, J. K. (1985). The causes and effects of aging in quick clays. *Canadian geotechnical journal*, 22(3):335–346.
- [27] Løken, T. (1968). Kvikkleiredannelse og kjemisk forvitring i norske leirer. *NGI, Norwegian Geotechnical Institute*.
- [28] Løken, T. (1970). Recent research at the norwegian geotechnical institute concerning the influence of chemical additions on quick clay. *Geologiska Föreningen i Stockholm Forhandlingar*, 92(2):133–147.
- [29] Mitchell, J. K. (1976). *Fundamentals of Soil Behavior*. Wiley, New York.
- [30] Mitchell, J. K. and Soga, K. (2005). *Fundamentals of Soil Behavior*. John Wiley and Sons, Hoboken, NJ, 3rd edition.
- [31] Moum, J., Løken, T., and Torrance, J. K. (1971). A geochemical investigation of the sensitivity of a normally-consolidated clay from drammen, norway. *Geotechnique*, 21:329–340.
- [32] Moum, J. and Rosenqvist, I. T. (1955). Kjemisk bergart forvitring belyst ved en del leirprofiler. *Norsk geologisk tidsskrift*, 34(2/4):167–174.
- [33] Moum, J., Sopp, O. I., and Løken, T. (1968). Stabilization of undisturbed quick clay by salt wells. *Norwegian Geotechnical Institute*, 81:1–7.
- [34] NGF (2011). Veiledning for symboler og definisjoner i geoteknikk - identifisering og klassifisering av jord. *Melding nr 2*.
- [35] NGI (1971). Resultater av triaxialforsøk med 95 mm prøver av kvikkleirefra ellingsrud. *NGI-rapport 50306*.
- [36] NGI (1988). Soil investigation troll field, block 31/6. laboratory report. *NGI-report 882504-01*.
- [37] NGI (2013). The causes and effects of aging in quick clays. *NIFS-N.6.4.3*.
- [38] NGU (2013). Berggrunns kart. Available online at <http://www.ngu.no/no/hm/Kart-og-data/Berggrunn/>.
- [39] NGU (2014). Løsmasse kart. Available online at <http://www.ngu.no/no/hm/Kart-og-data/Losmasser/>.
- [40] NS3007 (1986). *Terminologi for løsmasser*. Norges Byggstandardiseringsråd (NBR), 1st edition.
- [41] NS8001 (1982). *Geoteknisk prøving. Laboratoriemetoder. Støtflytegrensen*. Norges Byggstandardiseringsråd (NBR), 1st edition.

- [42] NS8002 (1982). *Geoteknisk prøving. Laboratoriemetoder. Konusflytegrensen*. Norges Byggstandardiseringsråd (NBR), 1st edition.
- [43] NS8013 (1982). *Geoteknisk prøving. Laboratoriemetoder. Vanninnhold*. Norges Byggstandardiseringsråd (NBR), 1st edition.
- [44] NS8015 (1988). *Geoteknisk prøving. Laboratoriemetoder. Bestemmelse av udrenert skjærstyrke ved konusprøving*. Norges Byggstandardiseringsråd (NBR), 1st edition.
- [45] NS8018 (1993). *Geoteknisk prøving. Laboratoriemetoder. Bestemmelse av endimensjonale konsolideringsegenskaper ved ødometerprøving. Metode med kontinuerlig belastning*. Norges Byggstandardiseringsråd (NBR), 1st edition.
- [46] Rankka, K., Andersson-Skold, Y., Hulten, C., Larsson, R., Leroux, V., and Dahlin, T. (2004). Quick clay in sweden. *Swedish Geotechnical Institute report no 65*.
- [47] Rochelle, P. L., Leroueil, S., and Tavenas, F. (1986). A technique for long-term storage of clay samples. *Canadian Geotechnical Journal*, 23(4):602–605.
- [48] Rømoen, M. (2005). Evaluation of ground conditions and stability of the berg area in trondheim. *Project assignment NTNU*.
- [49] Sandven, R., Senneset, K., Emdal, A., Nordal, S., Janbu, N., Grande, L., and Kornbrekke, H. A. (2013). Geotechnics field and laboratory investigations. *Geotechnical Division*.
- [50] Soderblom, R. (1969). Salt in swedish clays and its importance for quick clay formation. *Swedish Geotechnical Institute (SGI)*, 22.
- [51] Söderblom, R. (1974). Aspects on some problems of geotechnical chemistry: Part iii. *Swedish Geotechnical Institute*, (55):452–468.
- [52] Sveinan, H., Janbu, N., Nesvold, J., Røe, Ø., and Skjelstad, L. (2002). Leirras, sett fra en geologisk og geoteknisk synsvinkel. *Hegra Historielag*.
- [53] Talme, O. A. (1968). Clay sensitivity and chemical stabilization. *Rapport (Statens institut for bygnadsforskning)*.
- [54] Talme, O. A., Pajuste, M., and Wenner, C.-G. (1966). Secondary changes in the strength of clay layers and the origin of sensitive clay. *Byggforskningsrådet*, 46.
- [55] Torrance, J. K. (1975). On the role of chemistry in the development and behavior of the sensitive marine clays of canada and scandinavia. *Canadian Geotechnical Journal*, pages 326–335.

- [56] Torrance, J. K. (1983). Towards a general model of quick clay development. *Sedimentology*, 30:547–555.
- [57] Torrance, J. K. (2012). Landslides in quick clay. *Landslides: Types, Mechanisms and Modeling*, pages 83–94.
- [58] Torrance, J. K. and Pirnat, M. (1984). Effect of ph on the rheology of marine clay from the site of the south nation river, canada, landslide of 1971. *Clays and Clay Minerals*, 32(5):384–390.
- [59] van Olphen, H. (1977). *An Introduction to Clay Colloid Chemistry*. John Wiley and Sons.
- [60] Vegvesen, S. (2005). *Laboratorieundersøkelser Håndbok R210*. Statens Vegvesen.

Appendix A

Salt content conversion chart

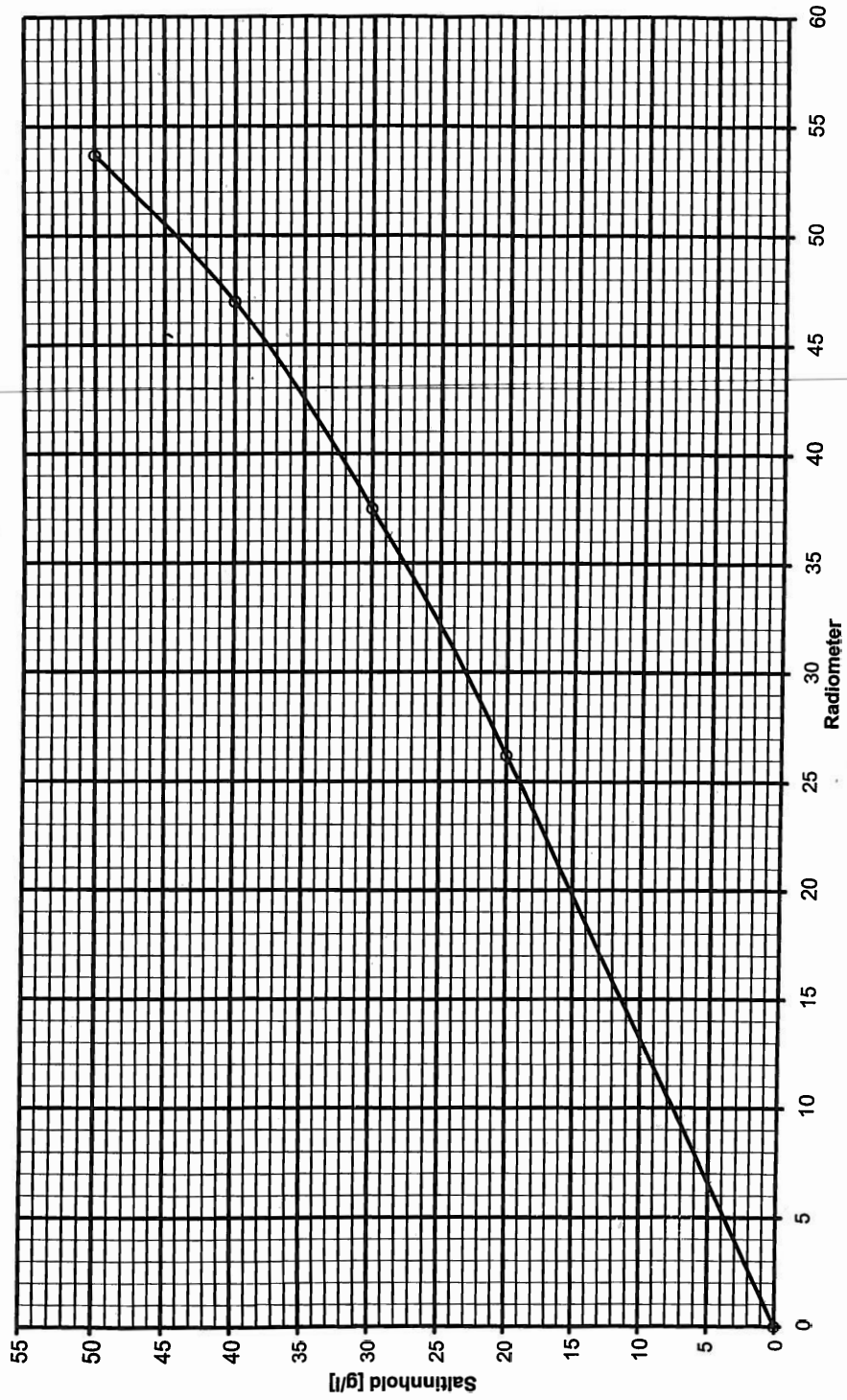





Figure A.1

Appendix B







Samples

Table B.1: Mini block samples before and after cell storage (photo: Rikke Nornes Bryntesen and Tonje Eide Helle)

Stored in	Mini block sample	Prior to cell installation	Extracted from cell
Salt	3.5-3.75 m	 <p>A cylindrical mini block sample wrapped in dark, crinkled plastic. A white label with handwritten text is attached to the bottom. The sample is sitting on a wooden surface in a workshop-like environment.</p>	 <p>The same cylindrical mini block sample, now heavily encrusted with white, crystalline salt deposits. A yellow measuring tape is visible to the left for scale.</p>
Water	3.75-4.0 m	 <p>The same cylindrical mini block sample, wrapped in dark, crinkled plastic. A yellow measuring tape is visible to the left for scale.</p>	 <p>The same cylindrical mini block sample, now heavily encrusted with white, crystalline salt deposits. A yellow measuring tape is visible to the left for scale.</p>

Continued on next page

Table B.1 – Continued from previous page

Stored in	Mini block sample	Prior to cell installation	Extracted from cell
Salt	4.25-4.5 m		
Water	4.75-5.0 m		
Salt	5.05-5.3 m		

Continued on next page

Table B.1 – Continued from previous page

Stored in	Mini block sample	Prior to cell installation	Extracted from cell
Water	5.55-5.8 m		
Salt	7.45-7.7 m		
Water	8.2-8.45 m		

Appendix C

XRD Results

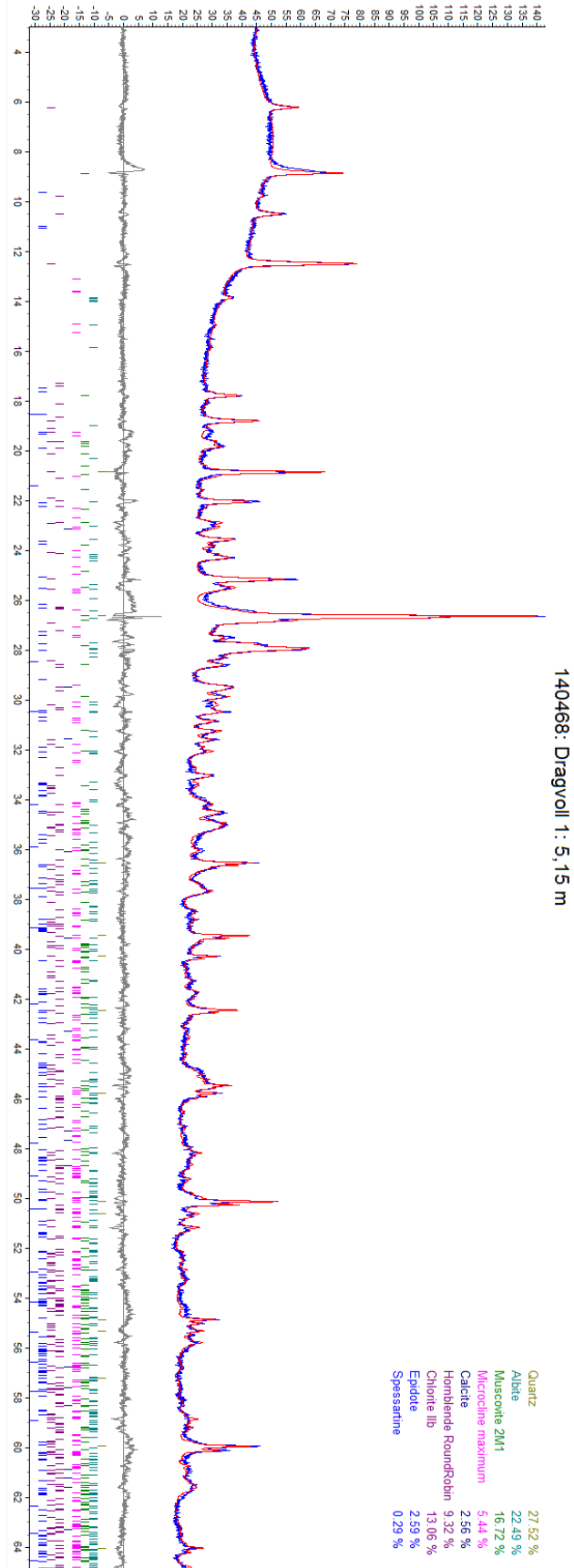


Figure C.1: Bulk XRD result

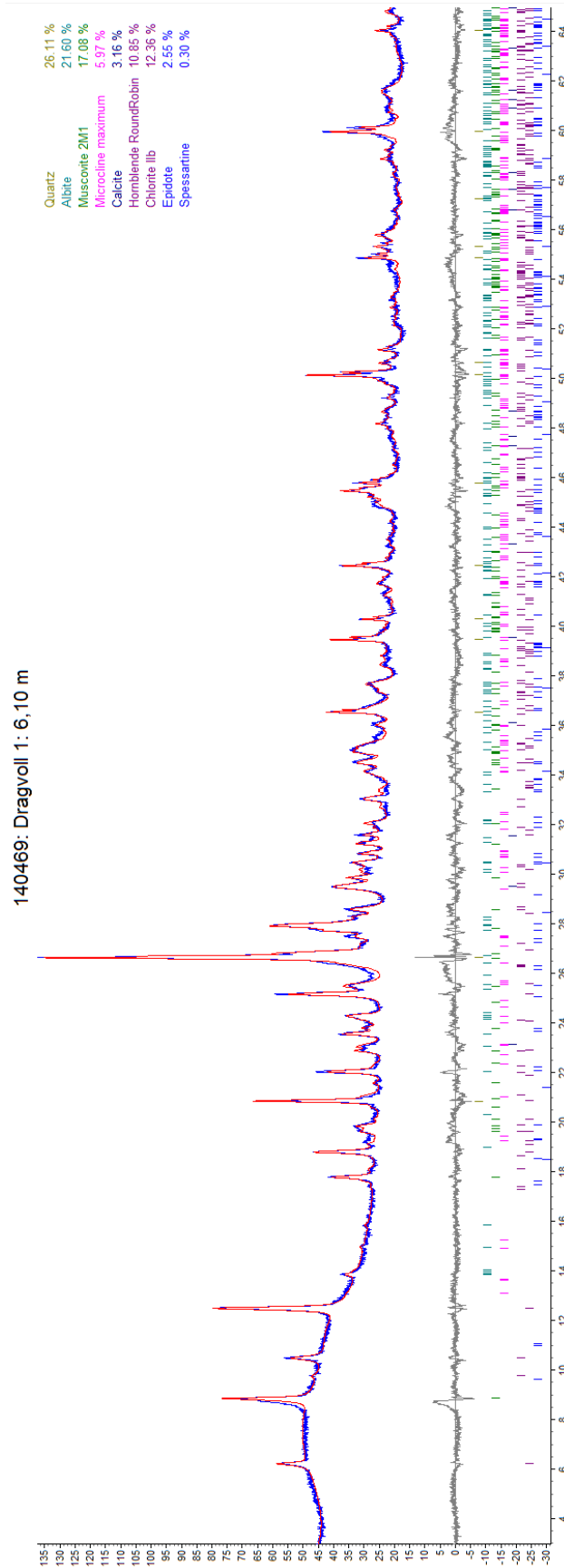


Figure C.2: Bulk XRD result

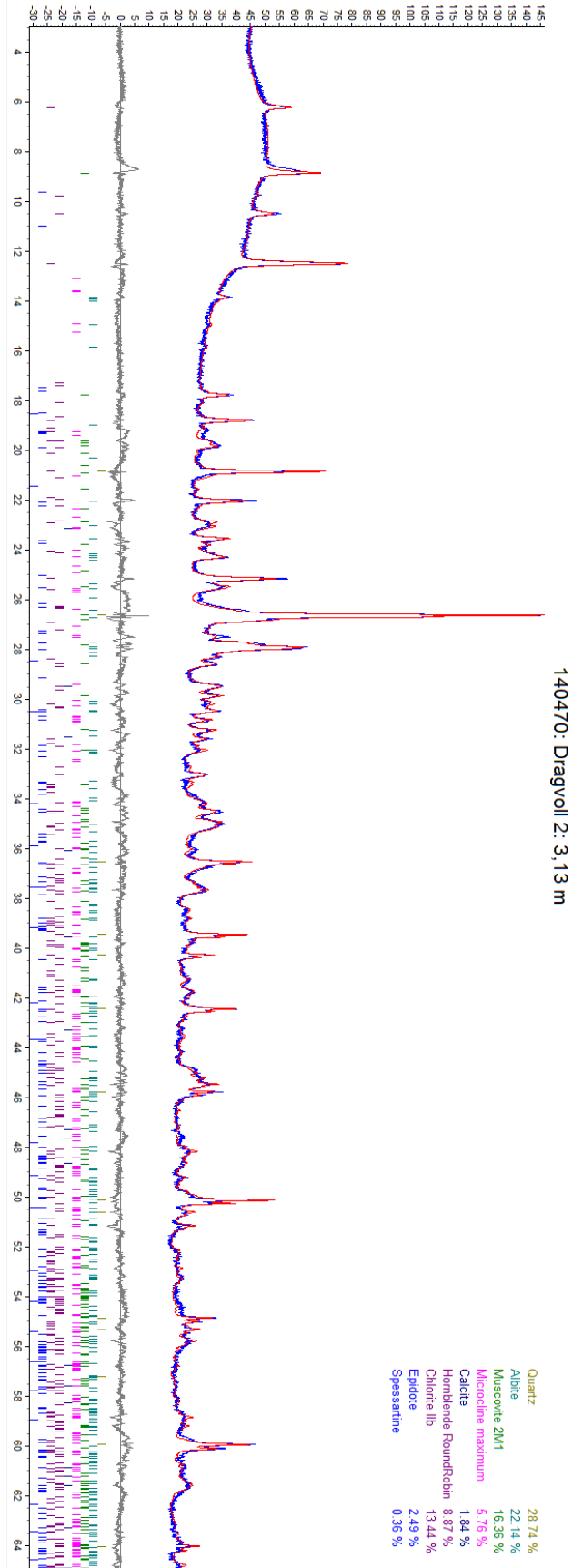


Figure C.3: Bulk XRD result

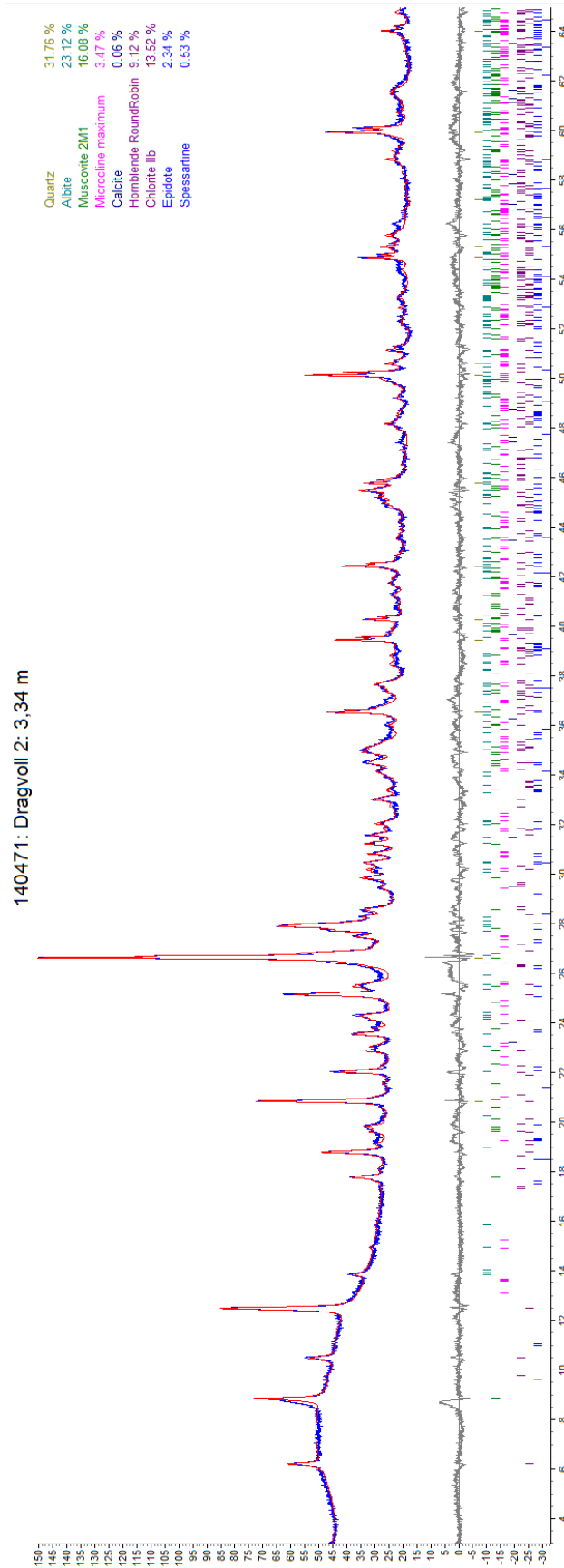


Figure C.4: Bulk XRD result

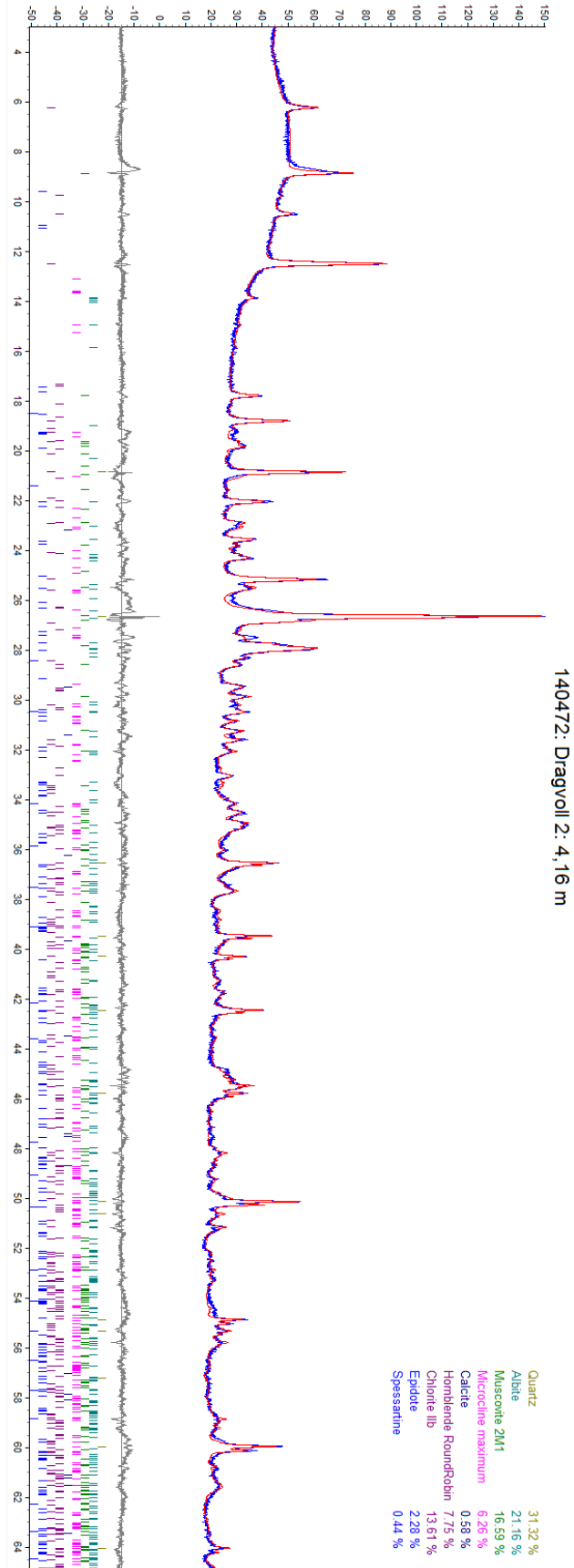


Figure C.5: Bulk XRD result

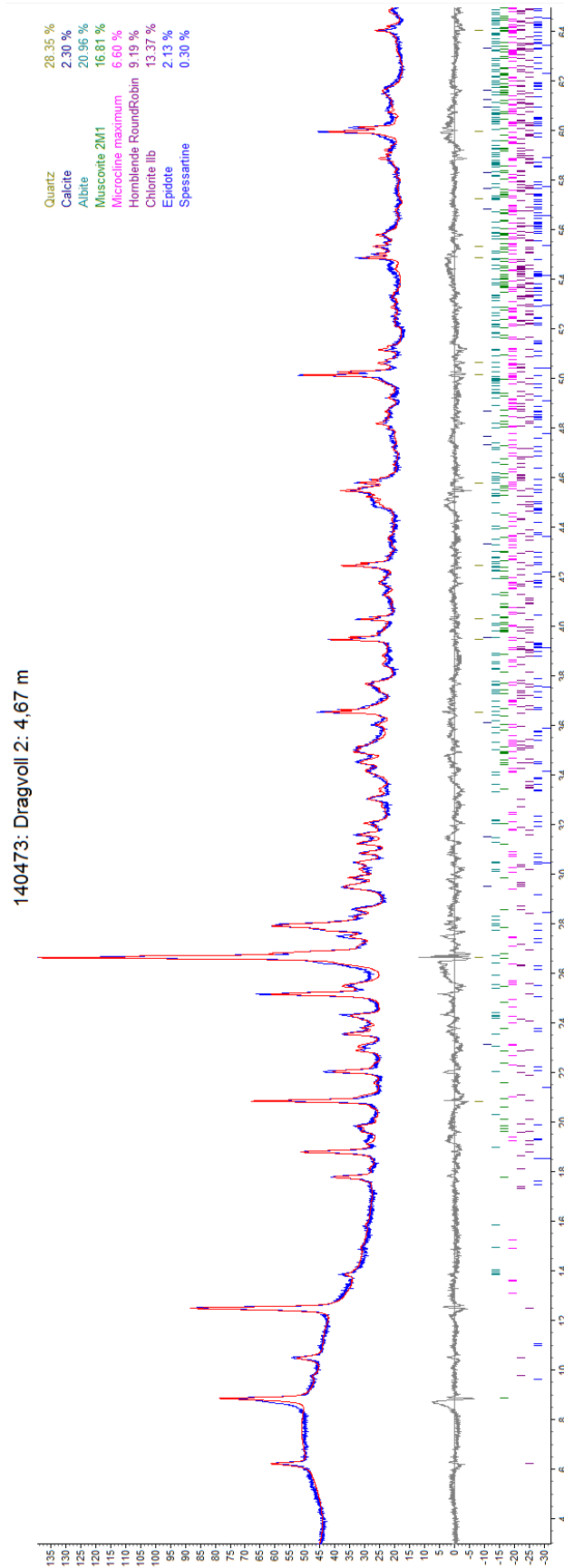


Figure C.6: Bulk XRD result

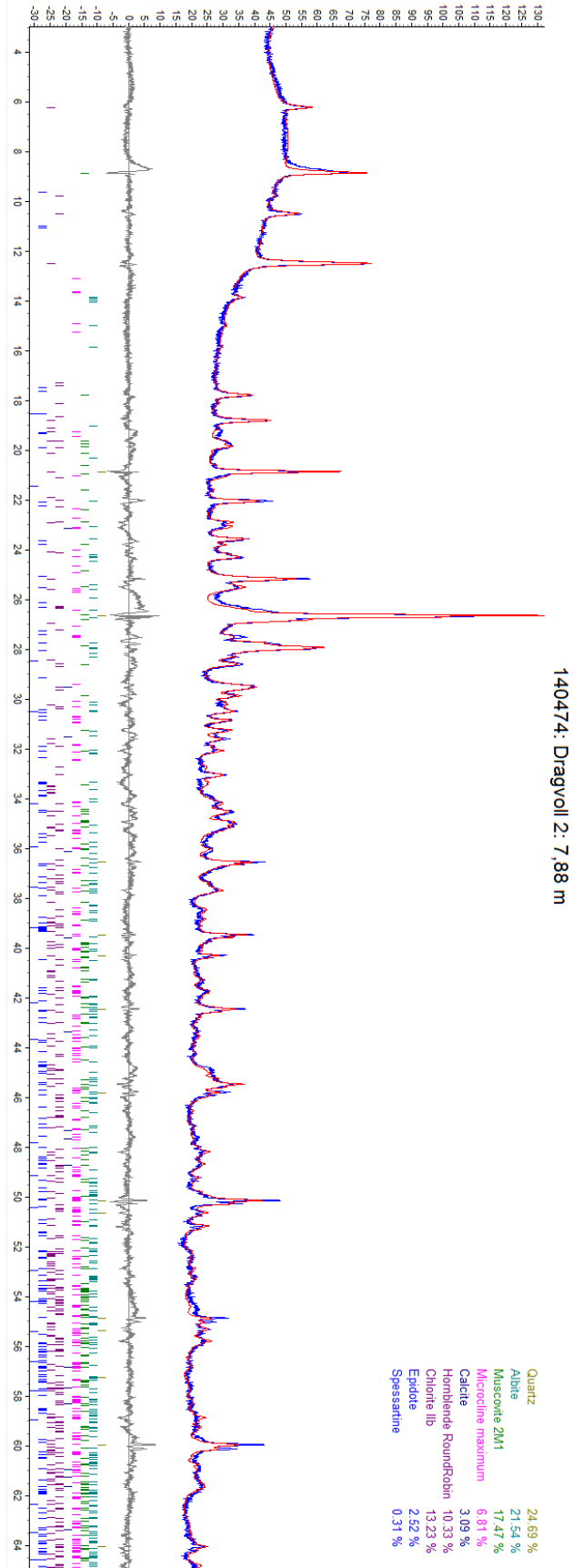


Figure C.7: Bulk XRD result

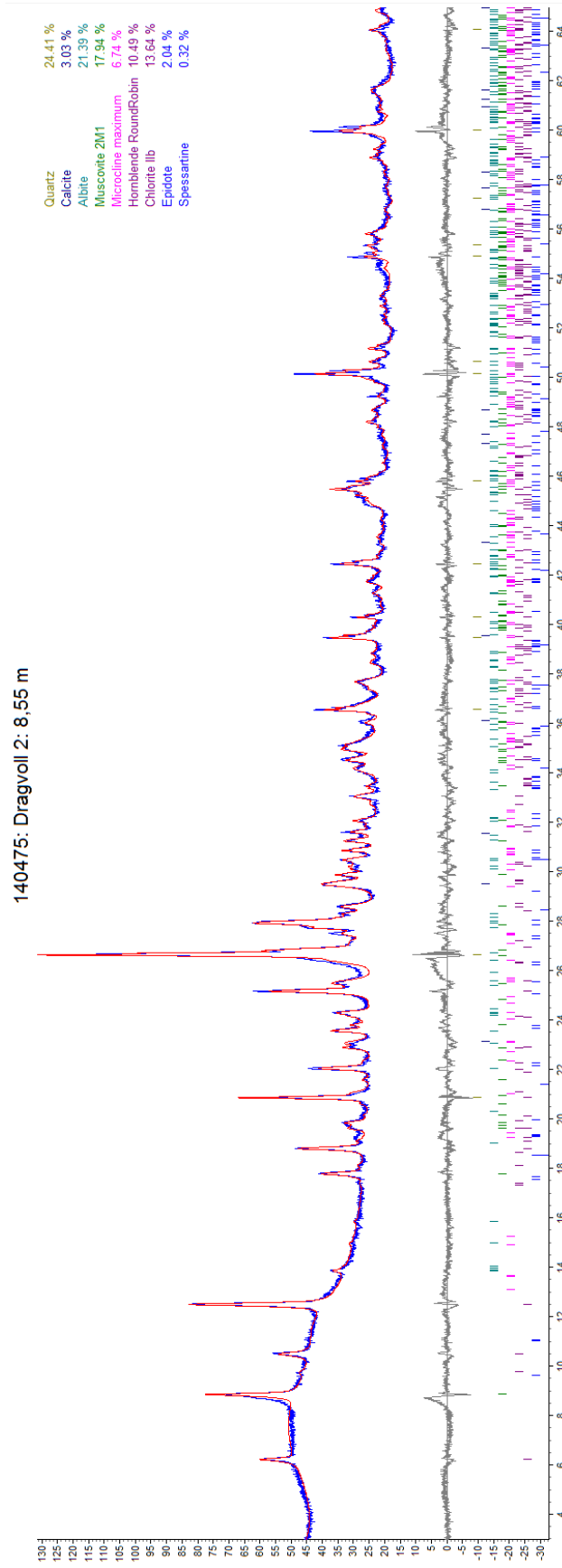


Figure C.8: Bulk XRD result

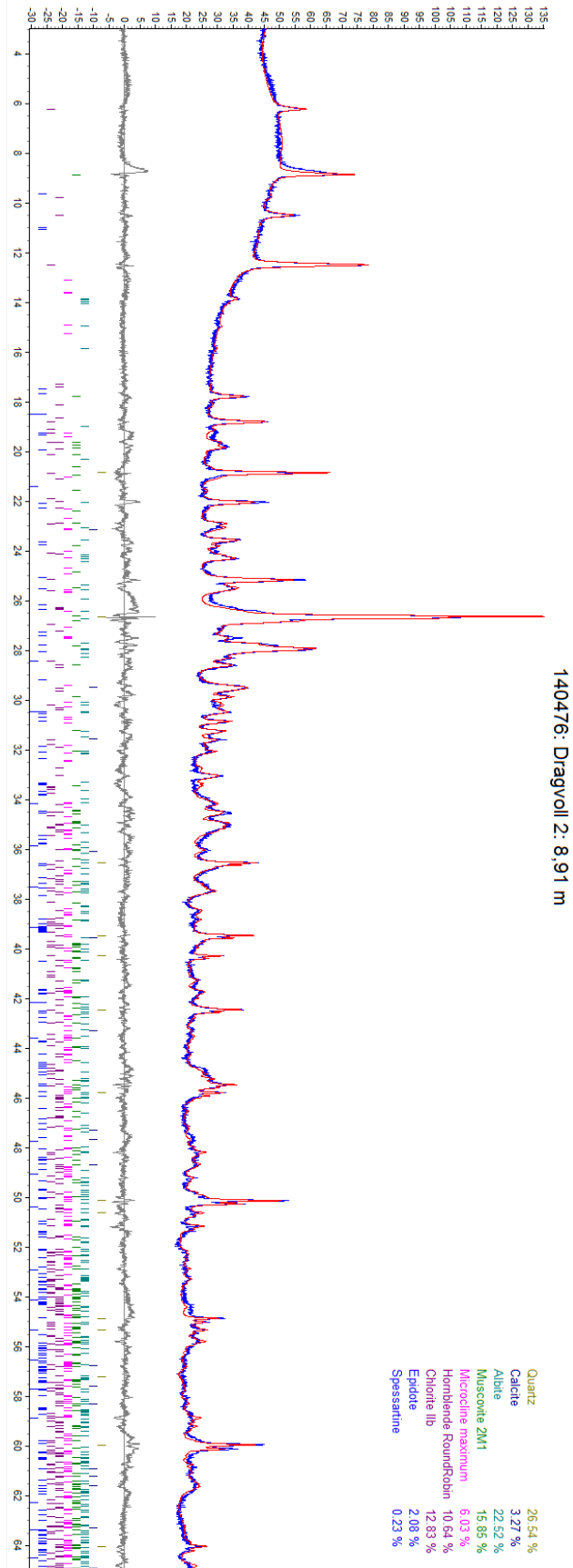


Figure C.9: Bulk XRD result

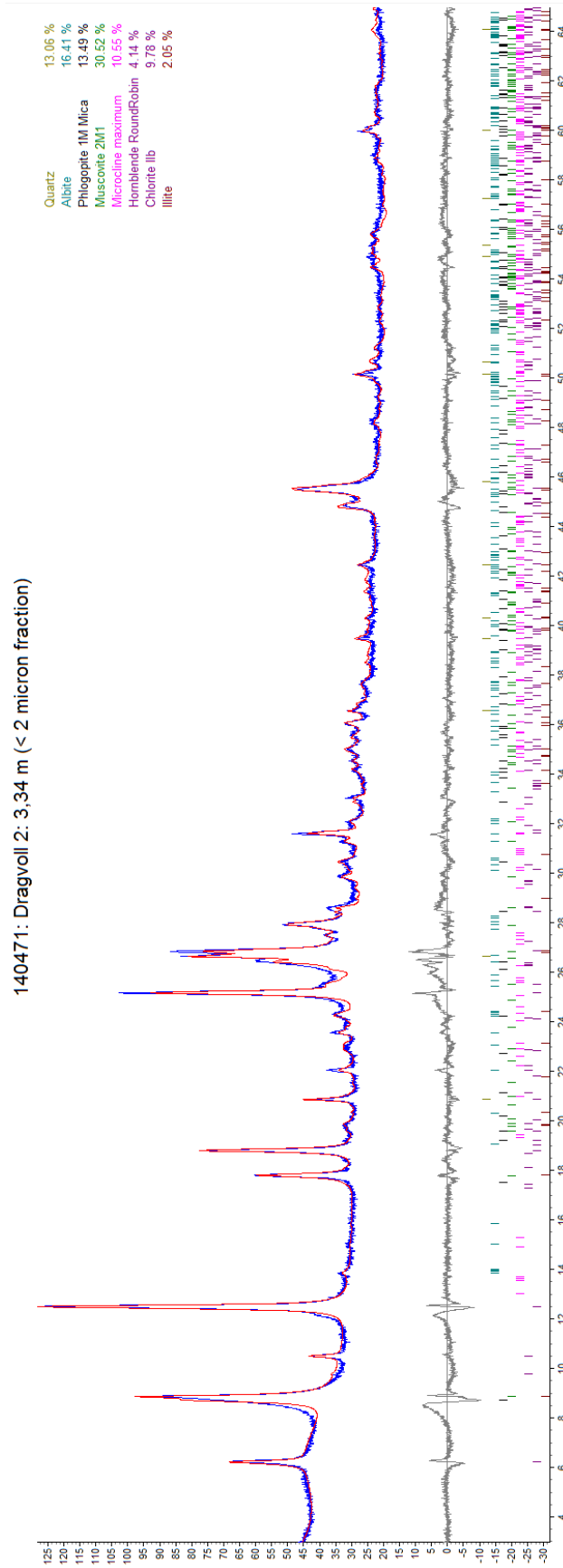


Figure C.10: Clay fraction XRD result

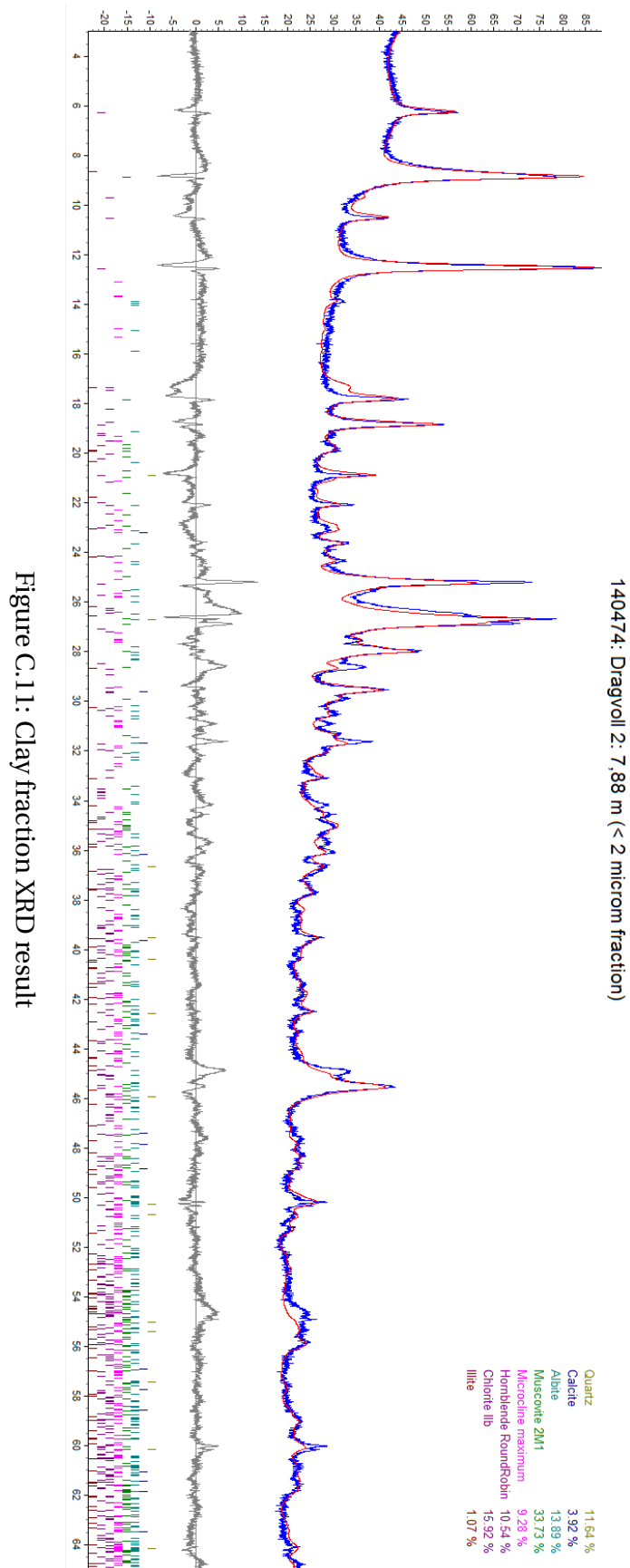


Figure C.1.1: Clay fraction XRD result

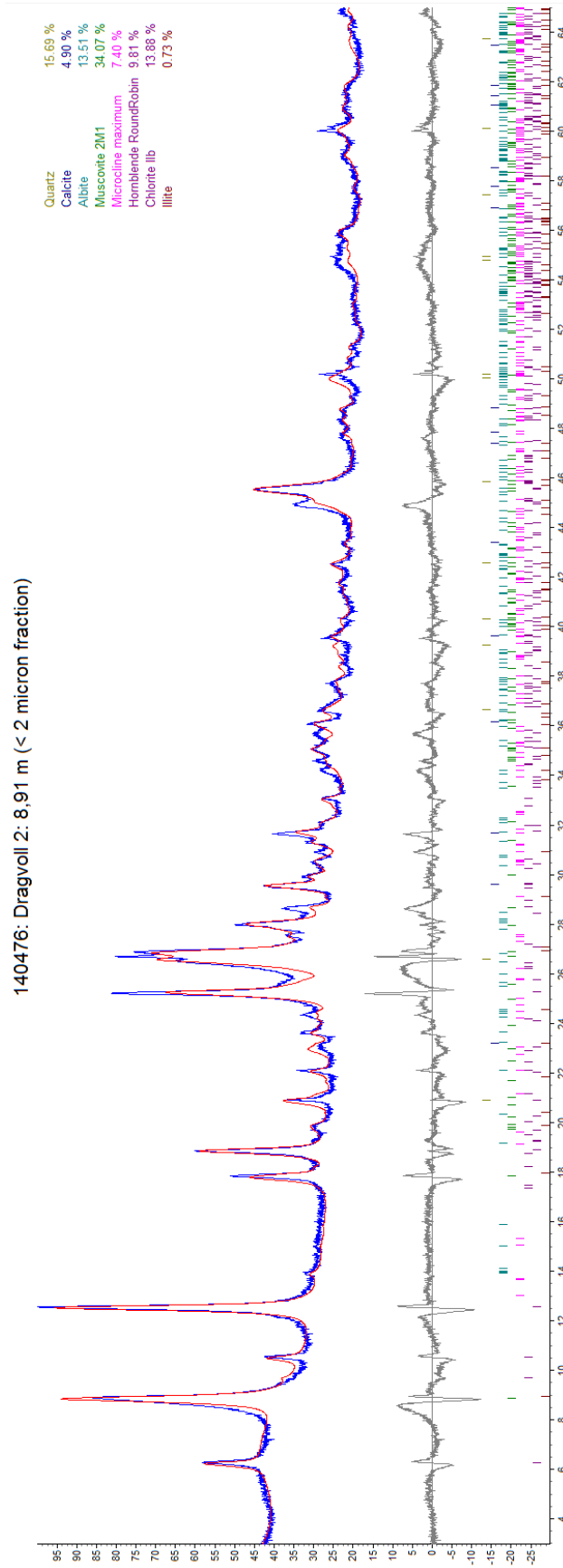


Figure C.12: Clay fraction XRD result

Appendix D

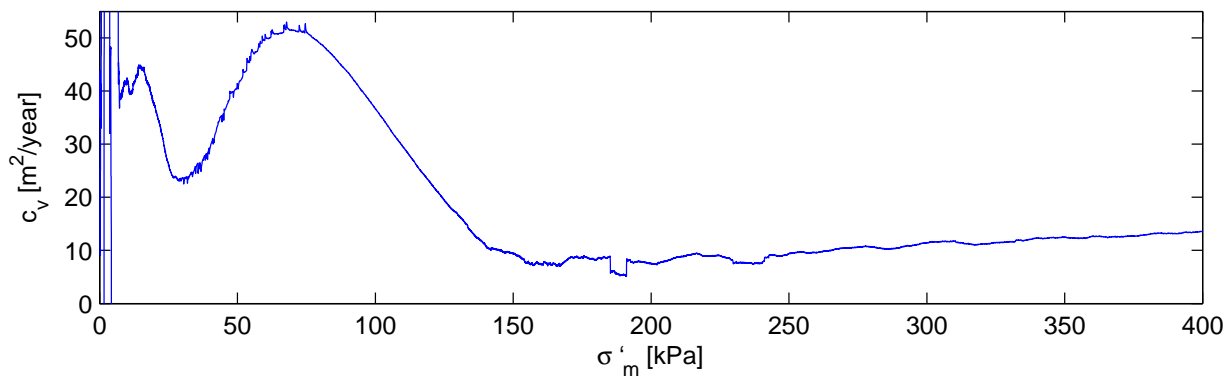
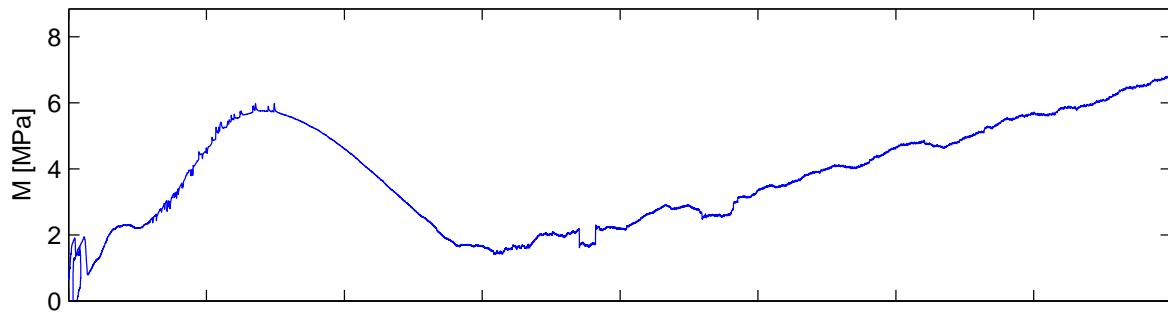
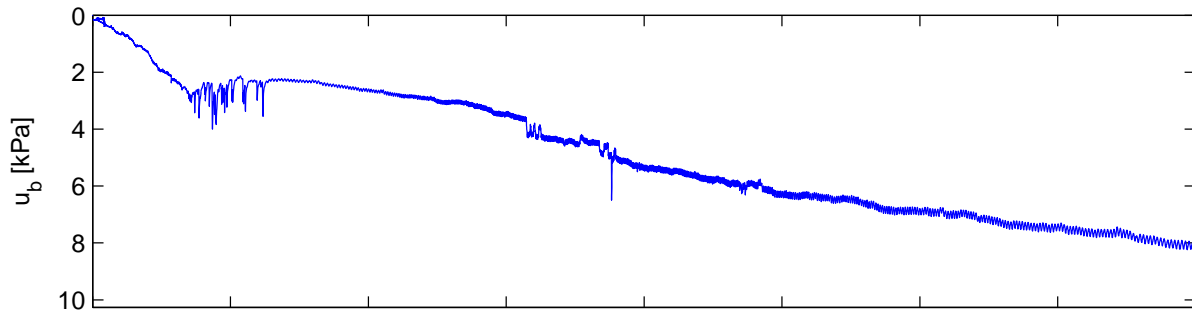
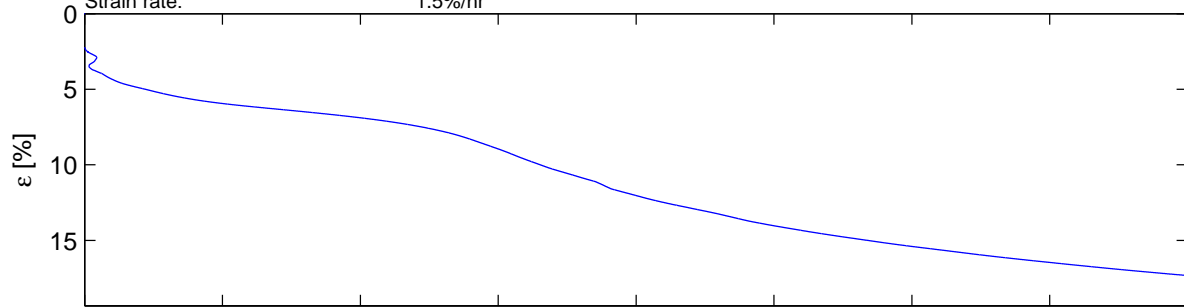
Oedometer tests on reference samples

All plots taken from Bryntesen [9].

Dragvoll CRS

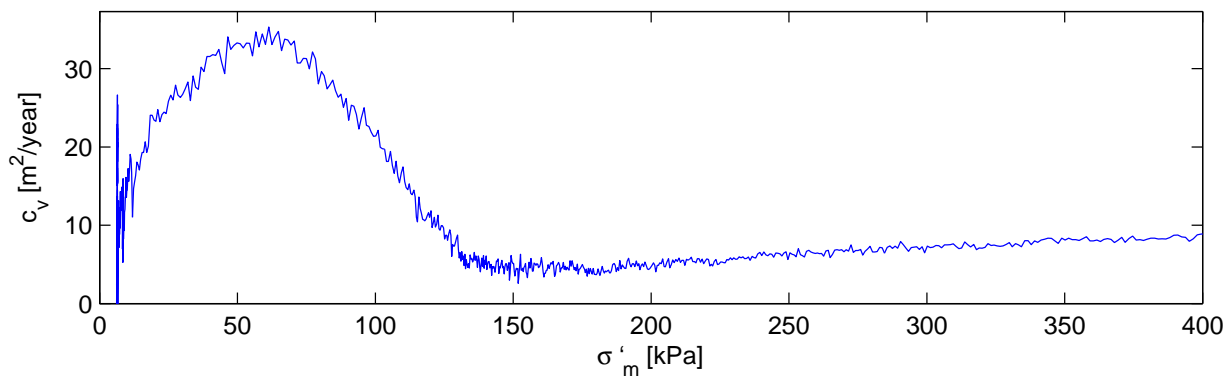
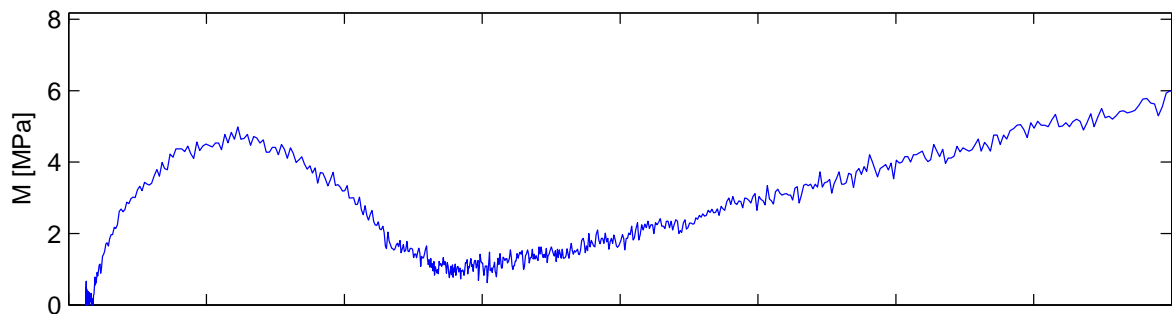
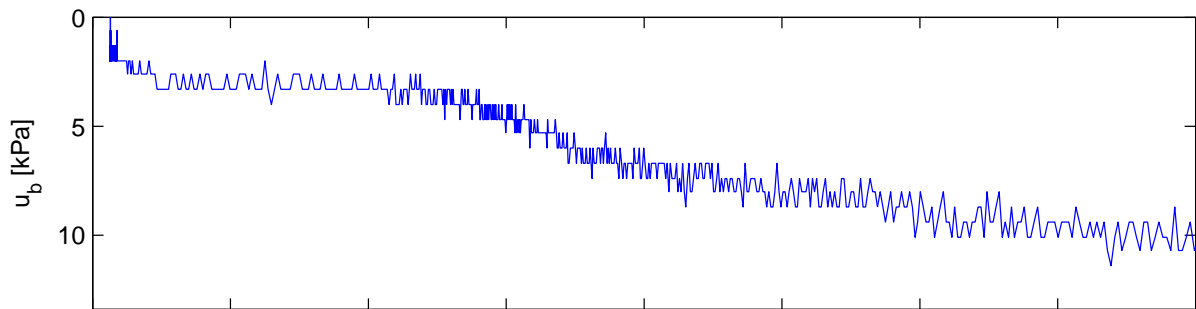
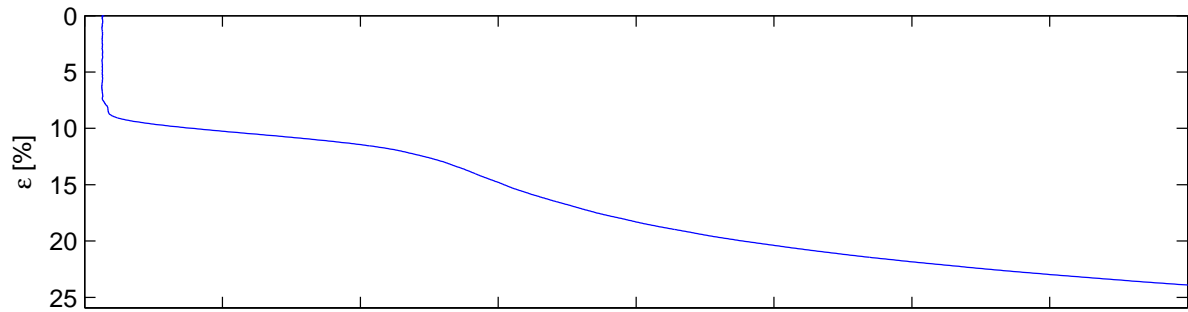
Mini block sample H2 D 3.0–3.25 m

Depth:	3.13 m	σ'_{vo} = 13.91 kPa	σ'_c = 130.00 kPa
Sampling date:	04.10.13	w = 38.70 %	M_{oc} = 5.98 MPa
Installed in storage cell:	4.12.13	γ = 18.33 kN/m ³	m = 22.05
Opening of the block sample:	16.10.13	OCR = 9.35	σ'_{ref} = 74.52 kPa
Testing date:	16.10.13		c_v = 40.00 m ² /year
Strain rate:	1.5%/hr		



Dragvoll CRS Test 1

Depth:	3.1 m	$\sigma_{vo} = 5.00$ kPa	$\sigma_c = 1.00$ kPa
Sampling date:	30.11.12	$w = 2.00$ %	$M_{oc} = 4.99$ MPa
Opening of the block sample:	30.12.12	$\gamma = 3.00$ kN/m ³	$m = 21.47$
Testing date:	30.12.12	OCR = 0.20	$\sigma'_{ref} = 60.15$ kPa
Strain rate:	1.5%/hr		$c_v = 9.06$ m ² /year



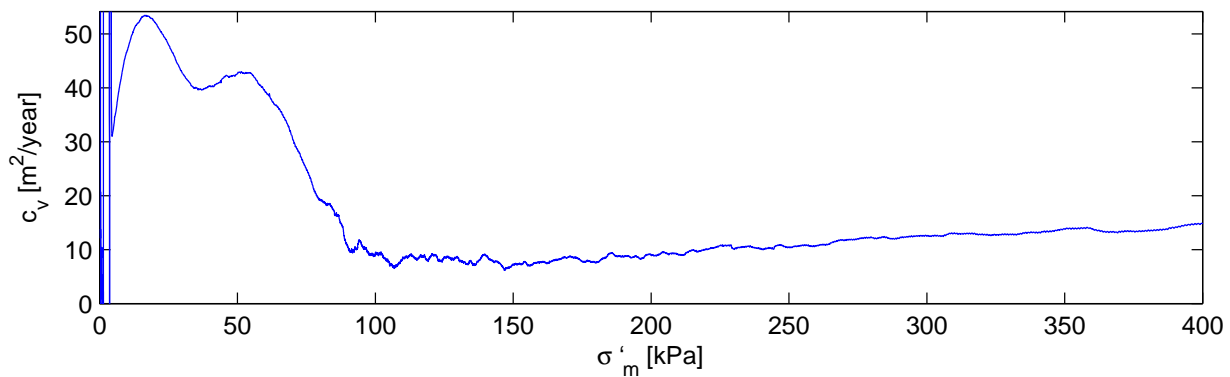
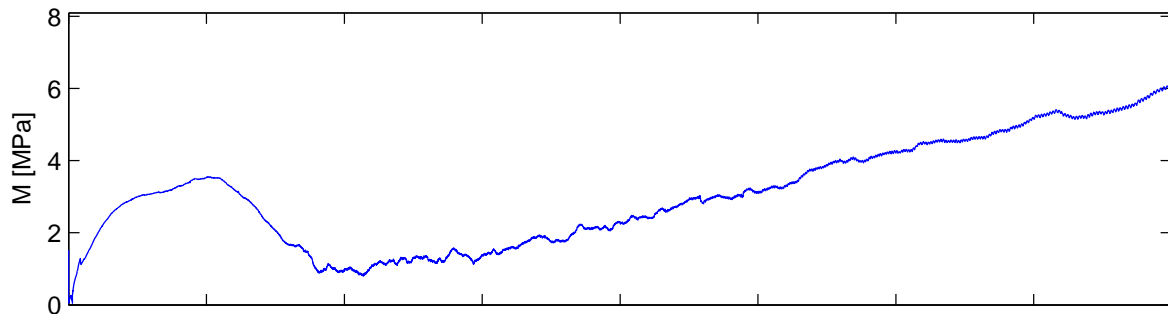
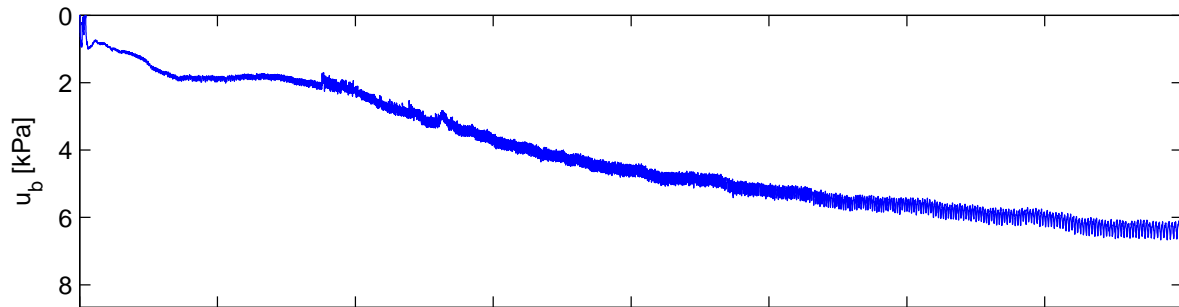
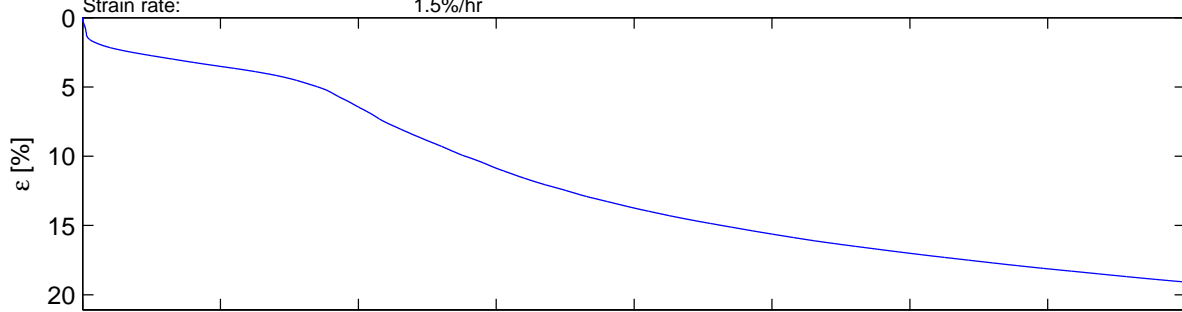
Dragvoll CRS

Mini block sample H2 D 3.25–3.5 m

Depth: 3.34 m
Sampling date: 04.10.13
Installed in storage cell: 4.12.13
Opening of the block sample: 14.11.13
Testing date: 14.11.13
Strain rate: 1.5%/hr

σ'_{vo} = 23.38 kPa
 w = 45.40 %
 γ = 17.80 kN/m³
OCR = 3.42

σ'_c = 80.00 kPa
 M_{oc} = 3.55 MPa
 m = 17.78
 σ'_{ref} = 50.15 kPa
 c_v = 45.00 m²/year



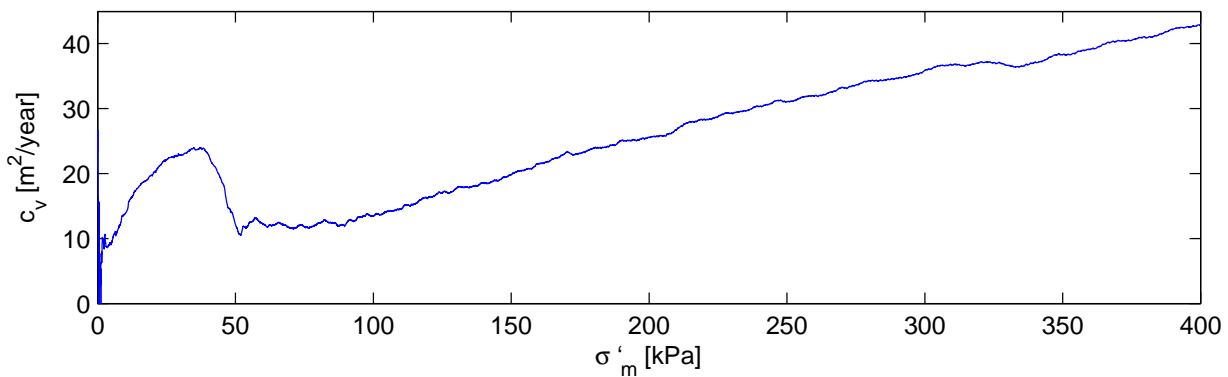
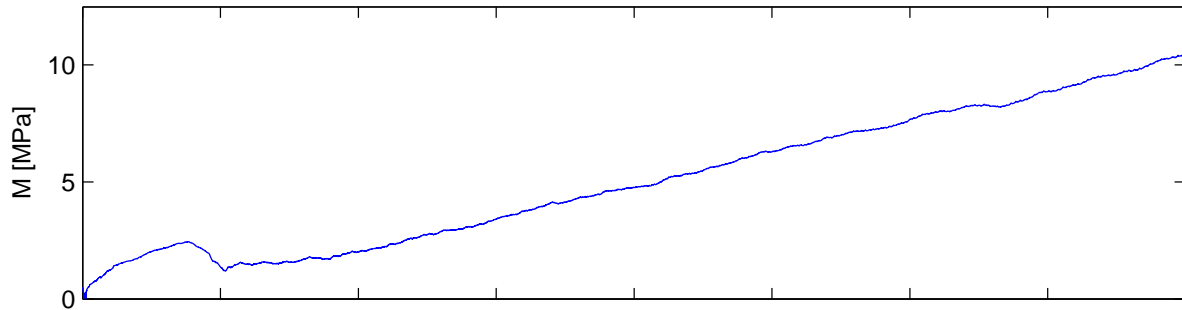
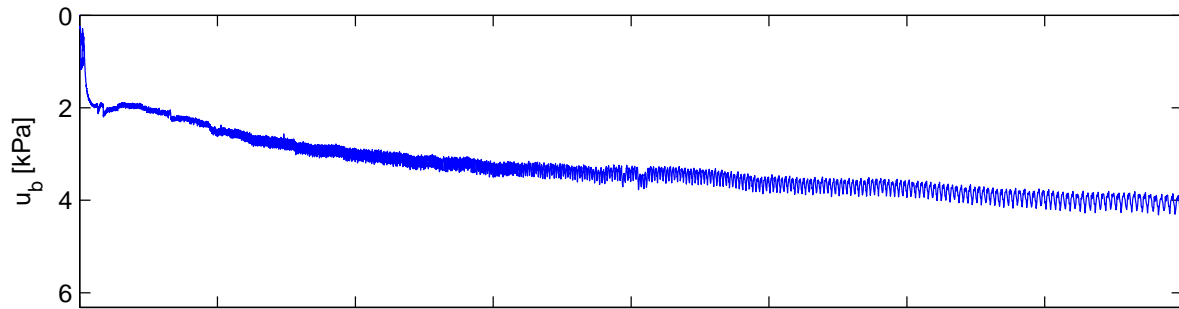
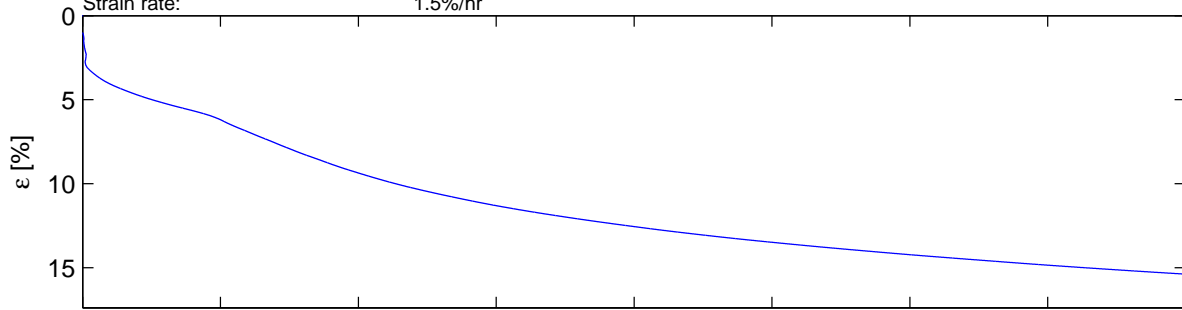
Dragvoll CRS

Mini block sample H2 D 4.0–4.25 m

Depth: 4.21 m
 Sampling date: 04.10.13
 Installed in storage cell: 4.12.13
 Opening of the block sample: 18.11.13
 Testing date: 18.11.13
 Strain rate: 1.5%/hr

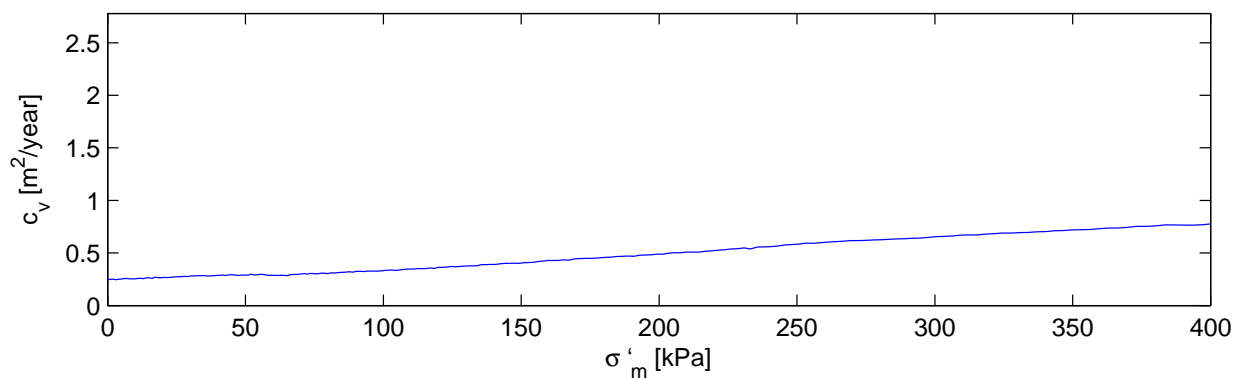
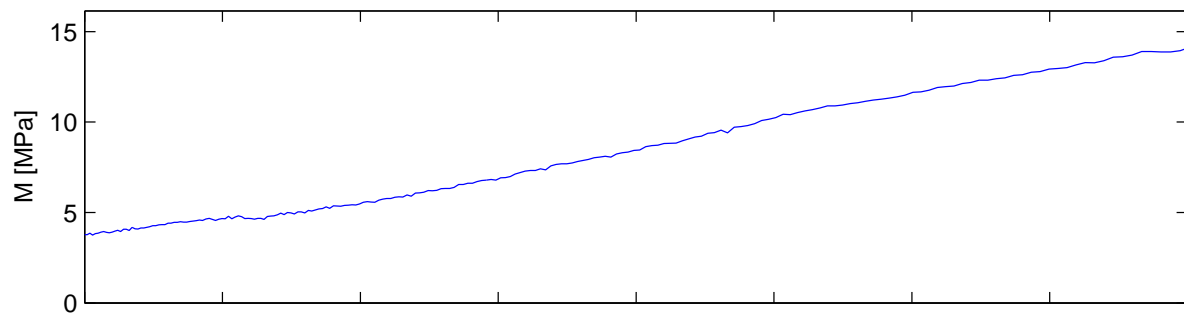
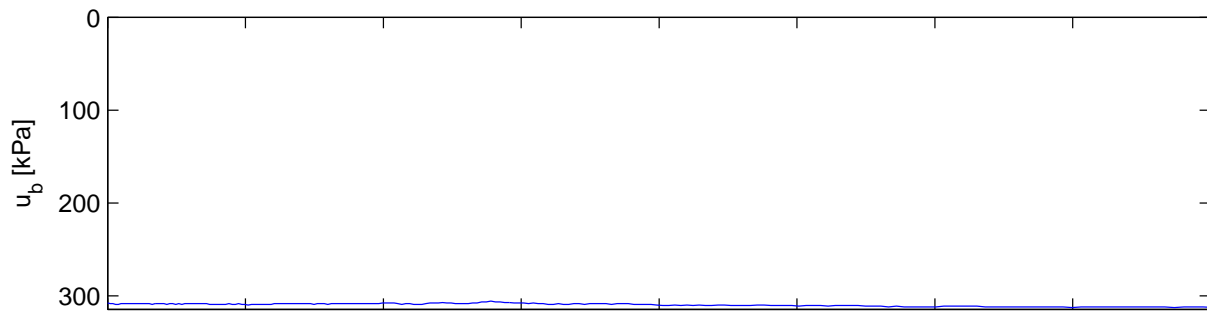
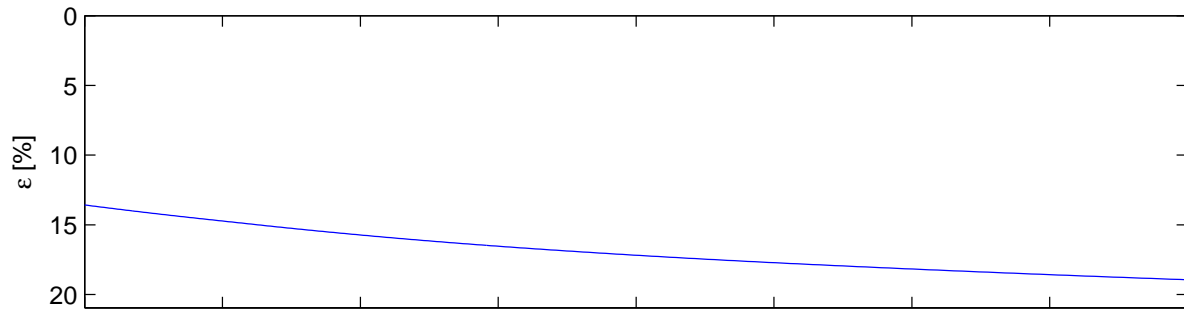
σ'_{vo} = 29.47 kPa
 w = 35.50 %
 γ = 18.77 kN/m³
 OCR = 1.70

σ'_c = 50.00 kPa
 M_{oc} = 2.09 MPa
 m = 26.62
 σ'_{ref} = 26.51 kPa
 c_v = 23.00 m²/year



Dragvoll CRS Test 1

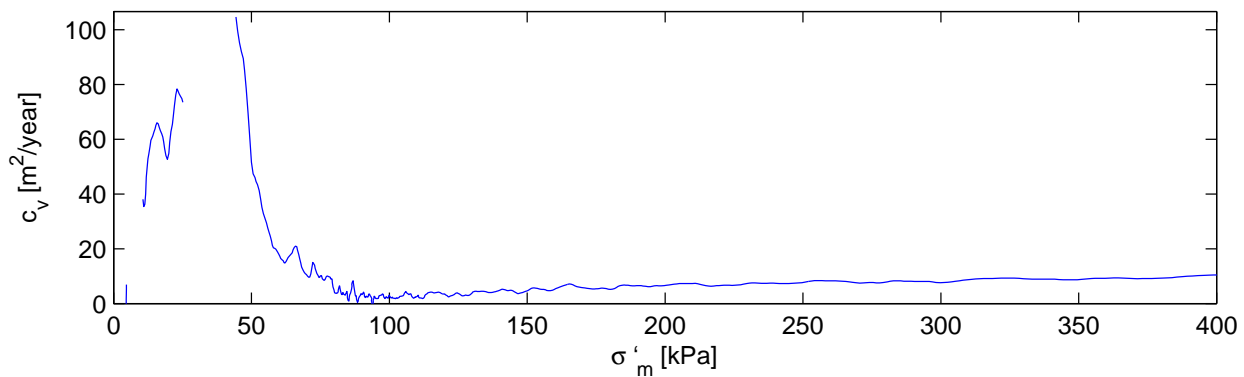
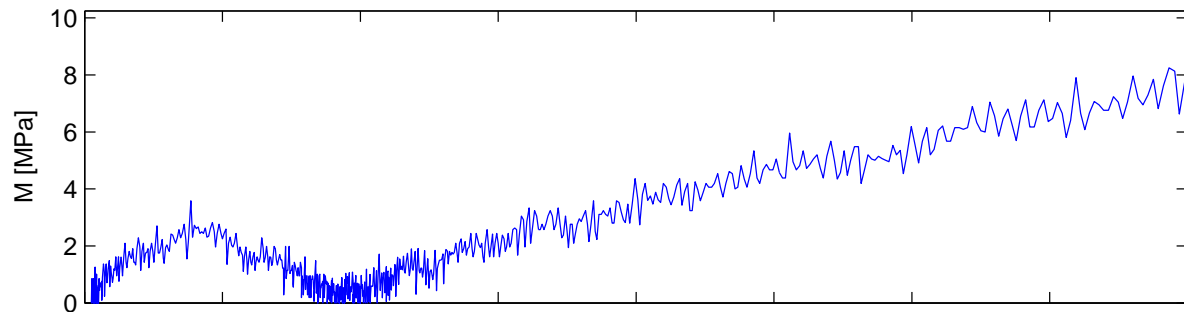
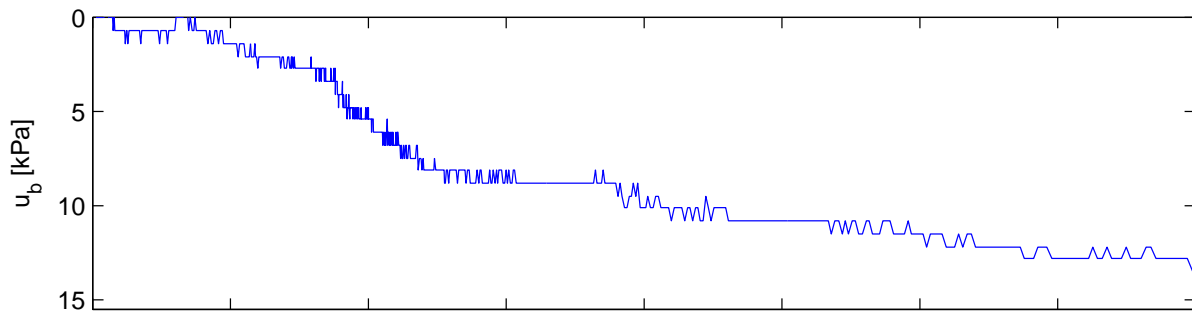
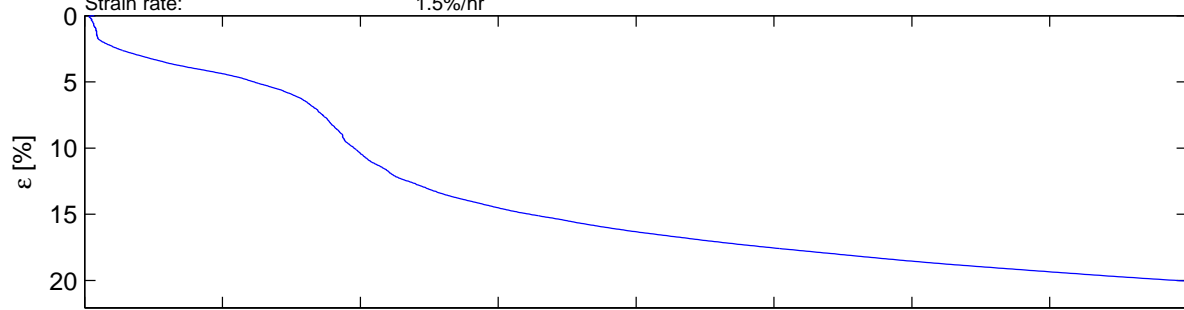
Depth:	3.1 m	$\sigma_{vo} = 5.00$ kPa	$\sigma_c = 1.00$ kPa
Sampling date:	30.11.12	$w = 2.00$ %	$M_{oc} = 2.38$ MPa
Opening of the block sample:	30.12.12	$\gamma = 3.00$ kN/m ³	$m = 26.93$
Testing date:	30.12.12	OCR = 0.20	$\sigma'_{ref} = -155.27$ kPa
Strain rate:	1.5%/hr		$c_v = 0.78$ m ² /year



Dragvoll CRS

Mini block sample H2 D 4.5–4.75 m

Depth:	4.71 m	$\sigma'_{vo} = 32.97$ kPa	$\sigma'_c = 70.00$ kPa
Sampling date:	04.10.13	$w = 39.70$ %	$M_{oc} = 1.94$ MPa
Installed in storage cell:	4.12.13	$\gamma = 18.14$ kN/m ³	$m = 27.90$
Opening of the block sample:	25.11.13	OCR = 2.12	$\sigma'_{ref} = 27.15$ kPa
Testing date:	25.11.13		$c_v = 16.00$ m ² /year
Strain rate:	1.5%/hr		



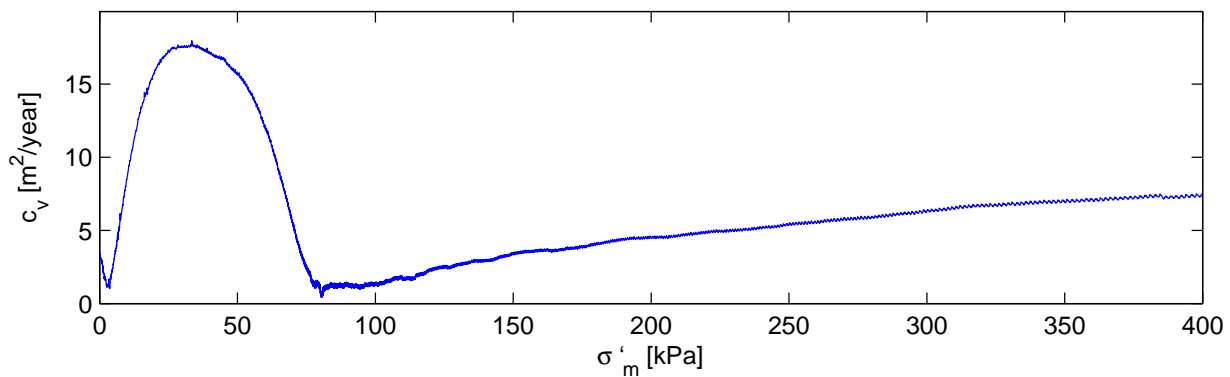
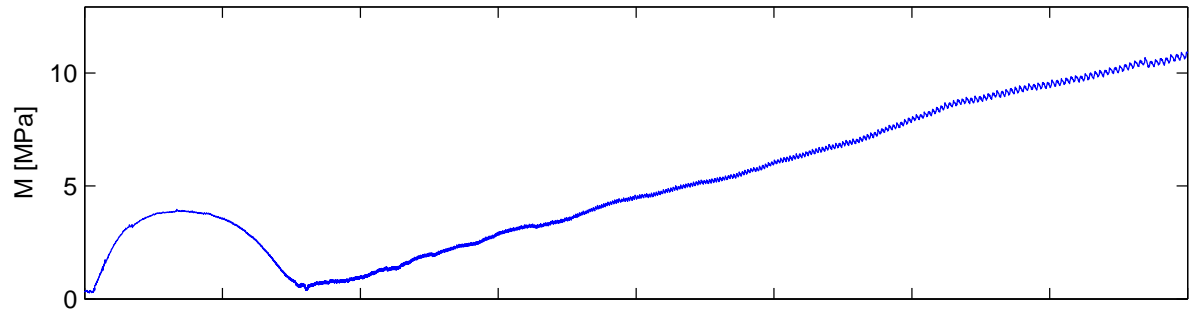
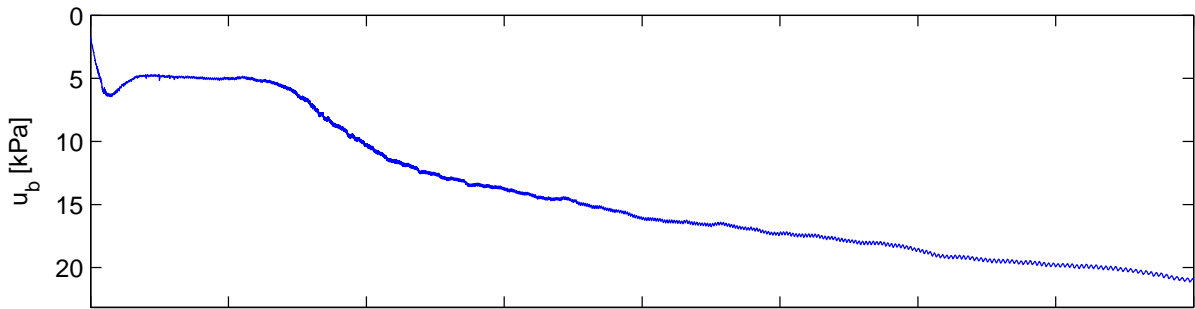
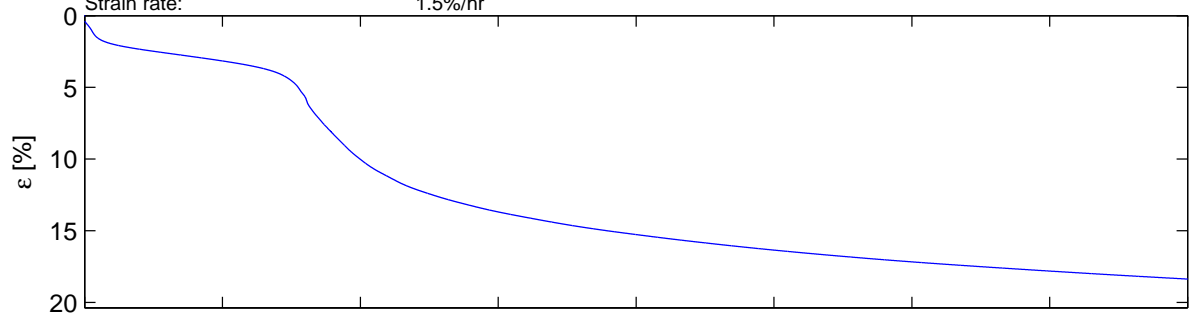
Dragvoll CRS

Mini block sample H1 D 5.0–5.25 m

Depth: 5.15 m
 Sampling date: 27.09.13
 Installed in storage cell: 4.12.13
 Opening of the block sample: 1.09.13
 Testing date: 1.09.13
 Strain rate: 1.5%/hr

σ'_{vo} = 32.05 kPa
 w = 37.30 %
 γ = 18.22 kN/m³
 OCR = 2.34

σ'_c = 75.00 kPa
 M_{oc} = 3.97 MPa
 m = 32.80
 σ'_{ref} = 33.43 kPa
 c_v = 17.00 m²/year



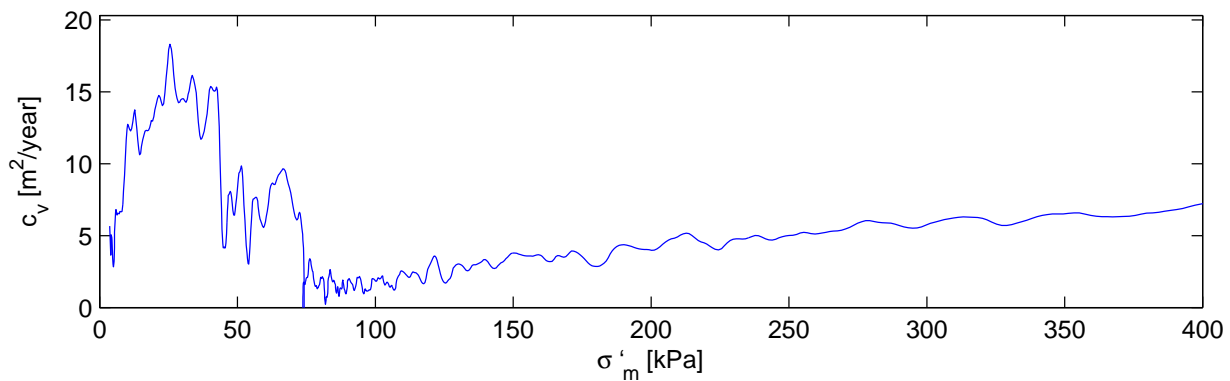
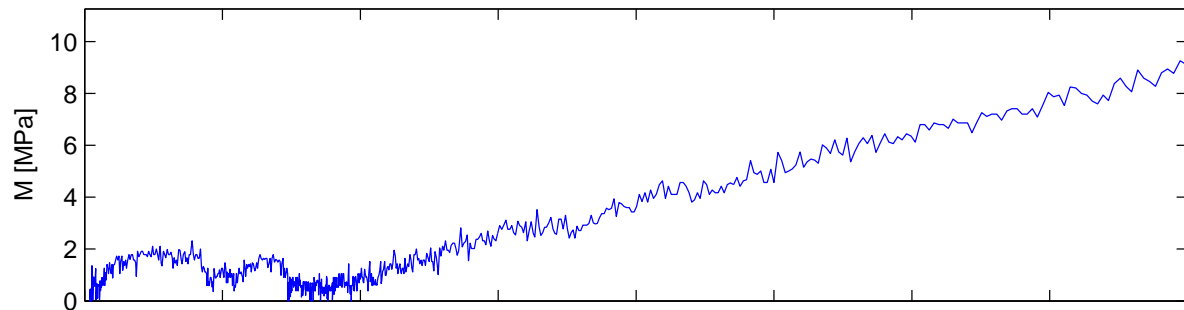
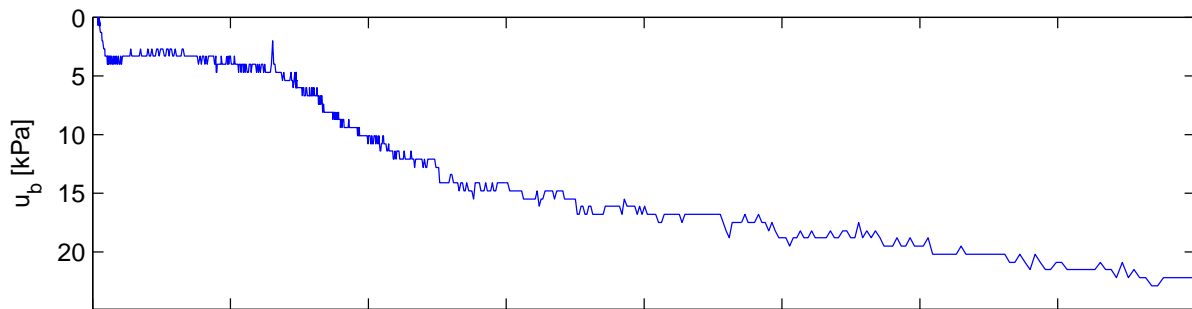
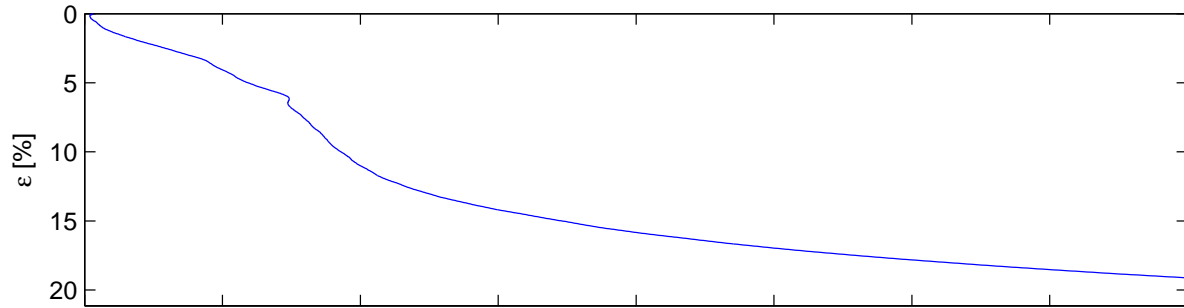
Dragvoll CRS

Mini block sample H1 D 5.0–5.25 m

Depth: 5.17 m
Sampling date: 27.09.13
Opening of the block sample: 1.09.13
Testing date: 1.09.13
Strain rate: 1.5%/hr

σ'_{vo} = 36.19 kPa
 w = 39.20 %
 γ = 18.50 kN/m³
OCR = 1.93

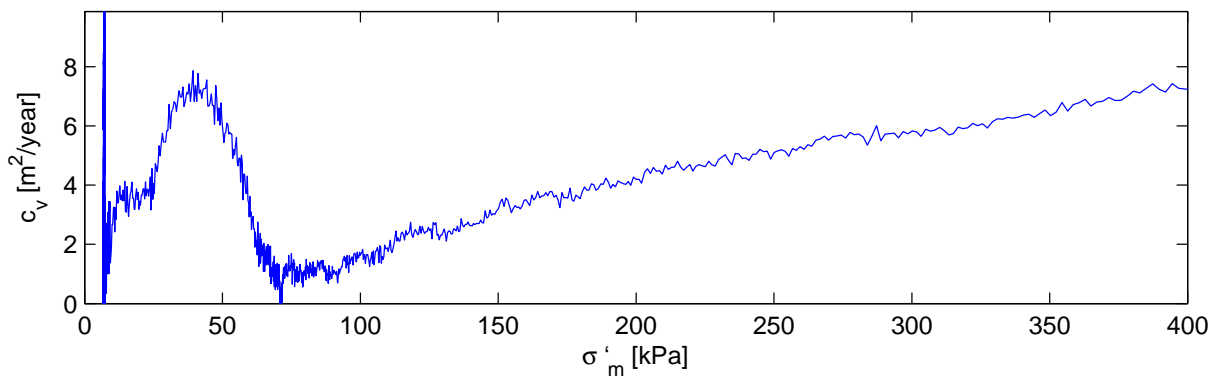
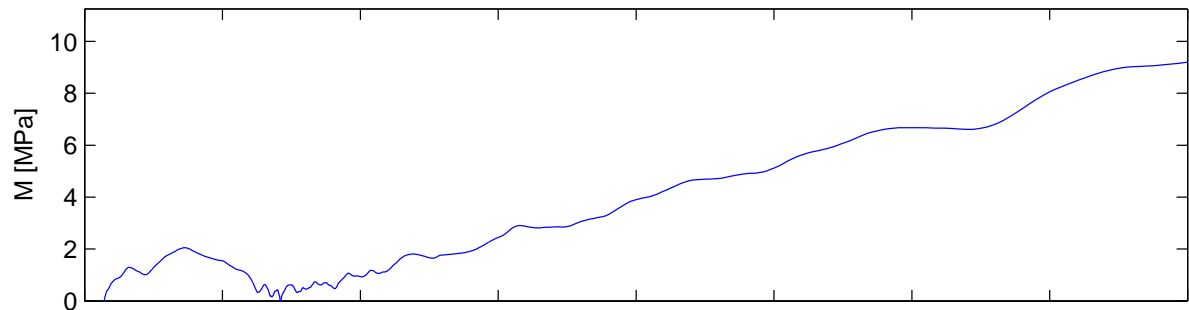
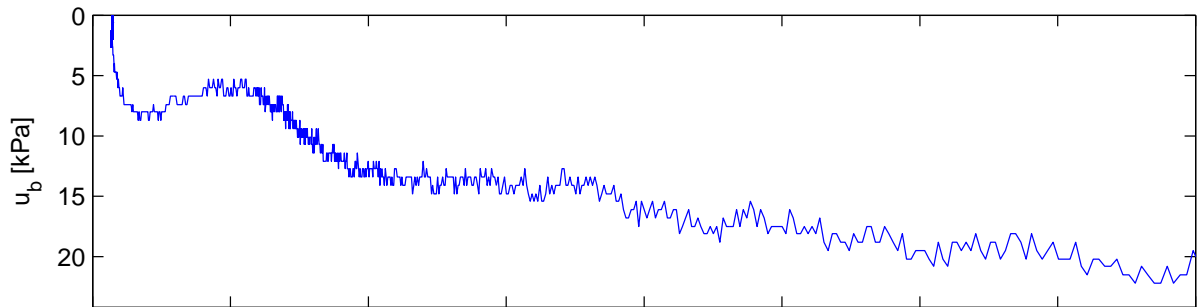
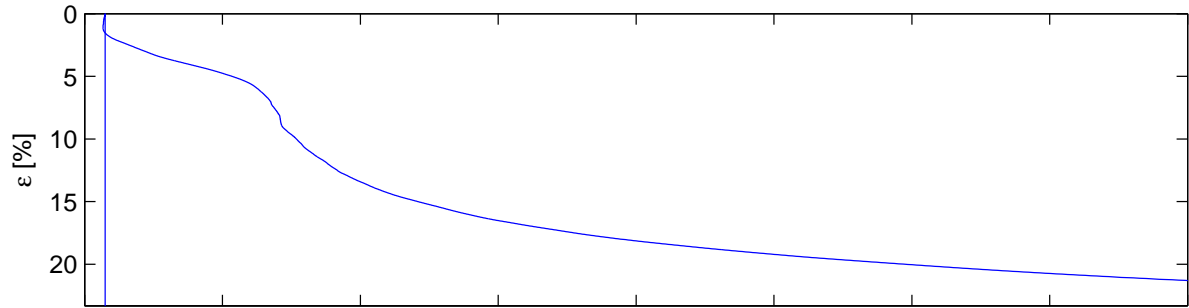
σ'_c = 70.00 kPa
 M_{oc} = 2.32 MPa
 m = 27.99
 σ'_{ref} = 38.41 kPa
 c_v = 7.27 m²/year



Dragvoll CRS

Mini block sample H1 D 5.0–5.25 m

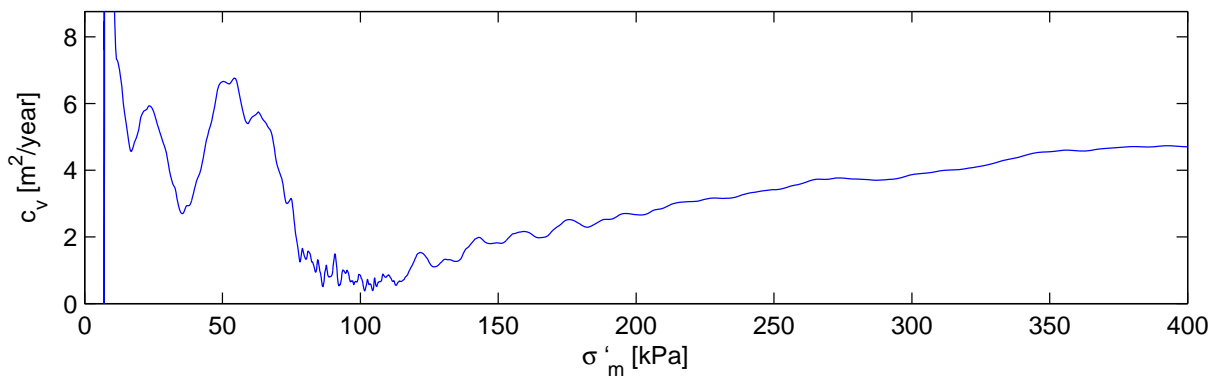
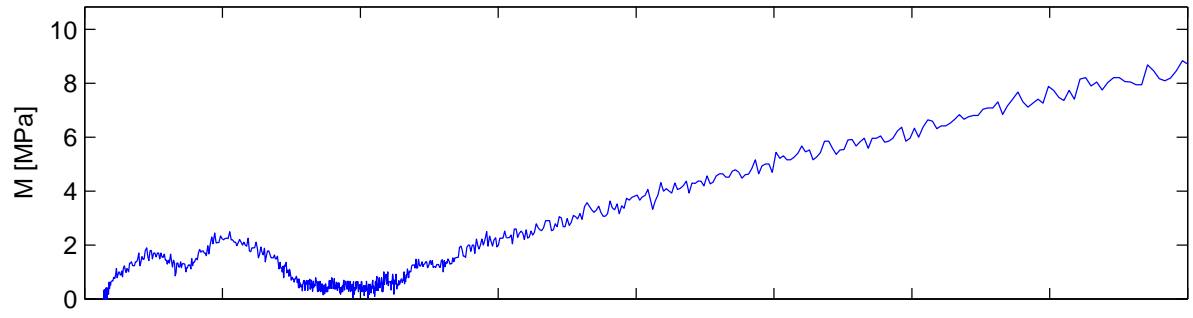
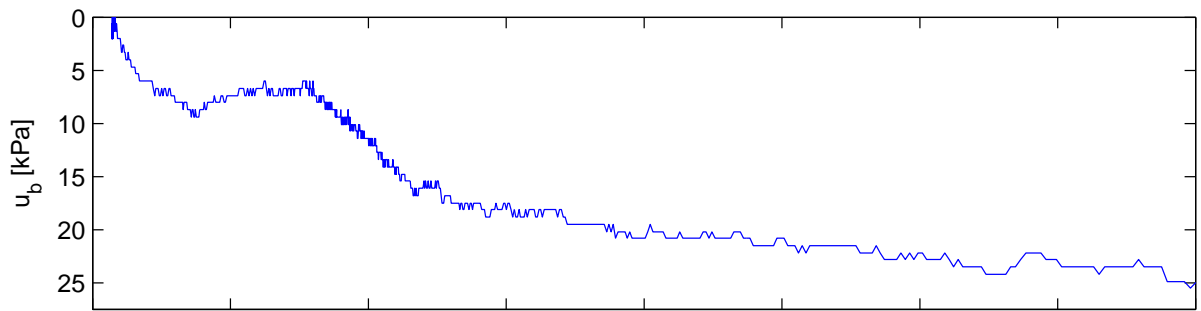
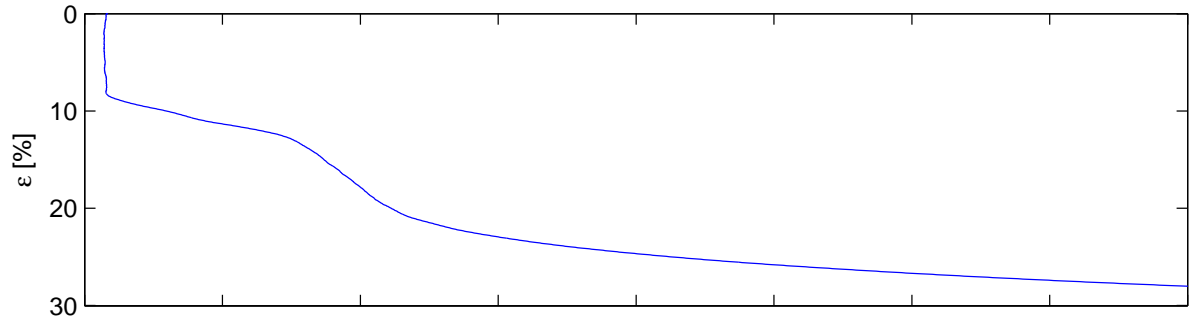
Depth:	5.19 m	σ'_{vo} = 36.33 kPa	σ'_c = 70.00 kPa
Sampling date:	27.09.13	w = 39.90 %	M_{oc} = 2.05 MPa
Opening of the block sample:	1.09.13	γ = 18.37 kN/m ³	m = 28.14
Testing date:	1.09.13	OCR = 1.93	σ'_{ref} = 36.08 kPa
Strain rate:	1.5%/hr		c_v = 7.08 m ² /year



Dragvoll CRS

Mini block sample H1 D 6.0–6.25 m

Depth:	6.105 m	$\sigma'_{vo} = 42.74$ kPa	$\sigma'_c = 75.00$ kPa
Sampling date:	30.09.13	$w = 39.30$ %	$M_{oc} = 2.49$ MPa
Opening of the block sample:	1.09.13	$\gamma = 18.33$ kN/m ³	$m = 27.68$
Testing date:	11.10.13	OCR = 1.75	$\sigma'_{ref} = 52.04$ kPa
Strain rate:	1.5%/hr		$c_v = 4.71$ m ² /year



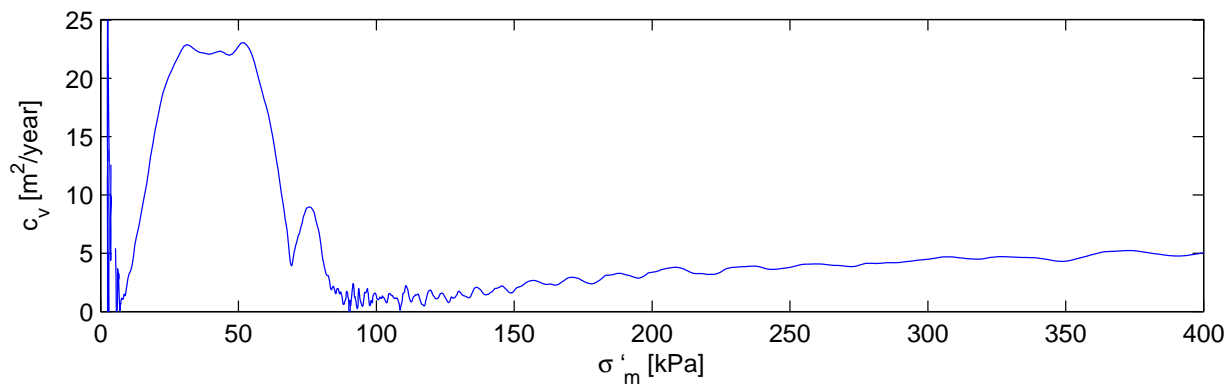
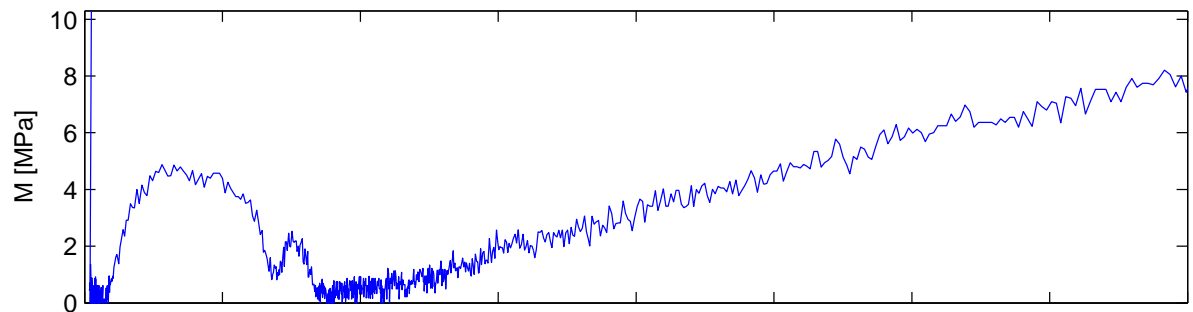
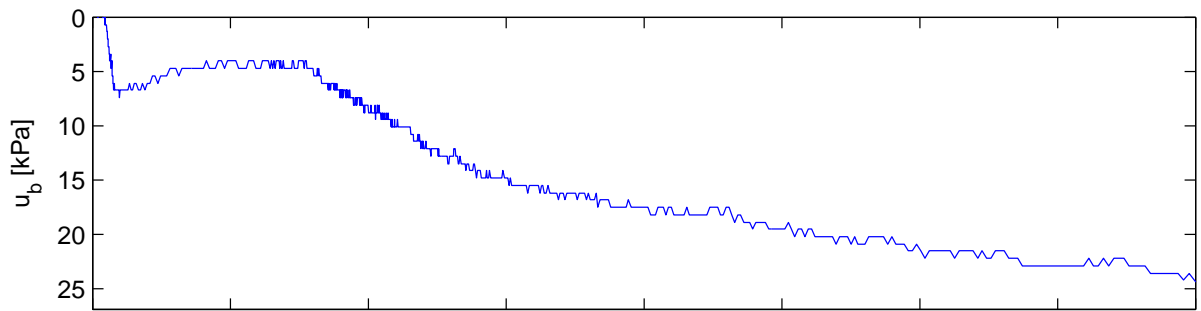
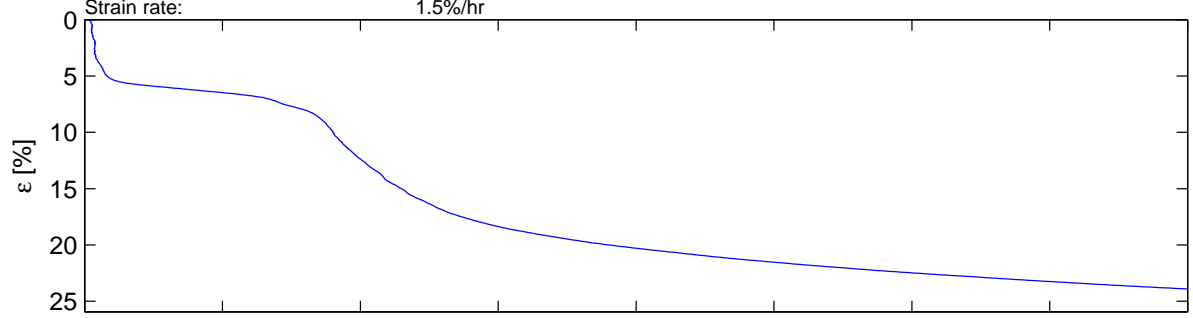
Dragvoll CRS

Mini block sample H1 D 6.0–6.25 m

Depth: 6.145 m
 Sampling date: 30.09.13
 Installed in storage cell: 4.12.13
 Opening of the block sample: 1.09.13
 Testing date: 11.09.13
 Strain rate: 1.5%/hr

σ'_{vo} = 43.00 kPa
 w = 38.90 %
 γ = 18.21 kN/m³
 OCR = 1.74

σ'_c = 75.00 kPa
 M_{oc} = 4.57 MPa
 m = 25.01
 σ'_{ref} = 45.59 kPa
 c_v = 15.00 m²/year



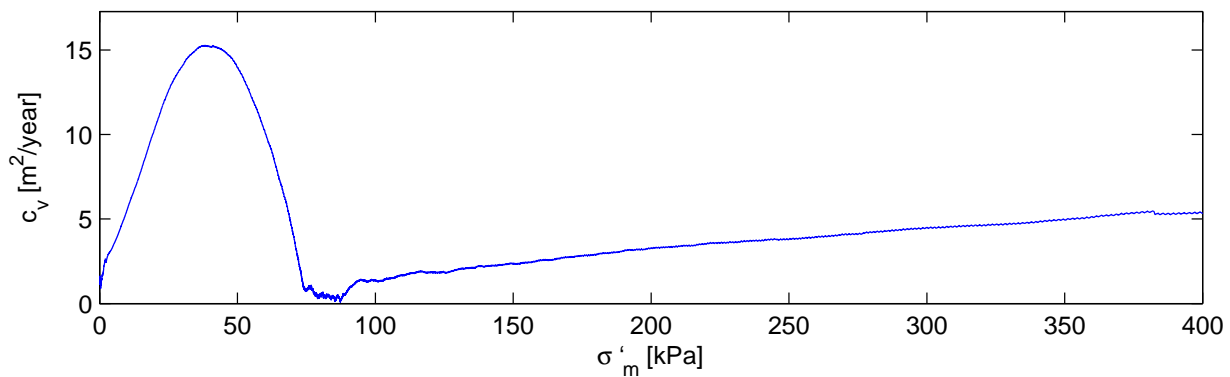
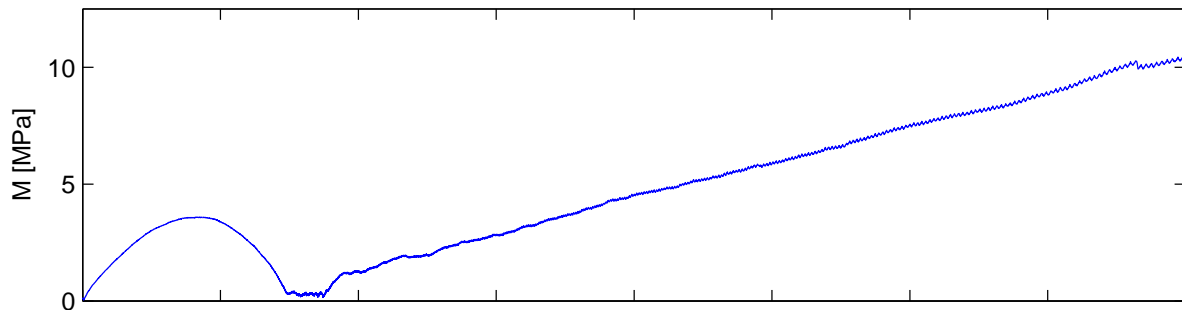
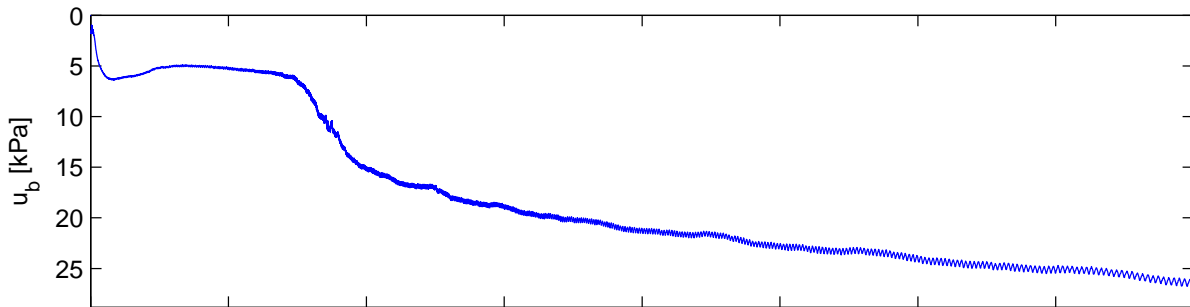
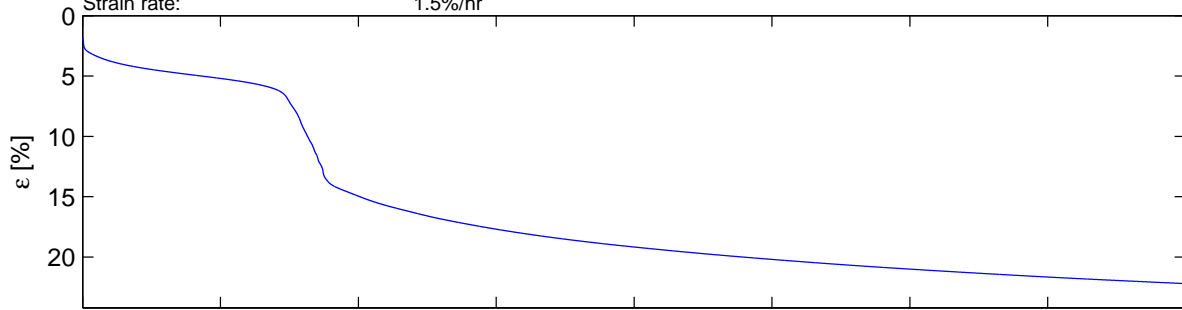
Dragvoll CRS

Mini block sample H1 D 6.0–6.25 m

Depth: 6.225 m
 Sampling date: 30.09.13
 Installed in storage cell: 4.12.13
 Opening of the block sample: 11.10.13
 Testing date: 12.10.13
 Strain rate: 1.5%/hr

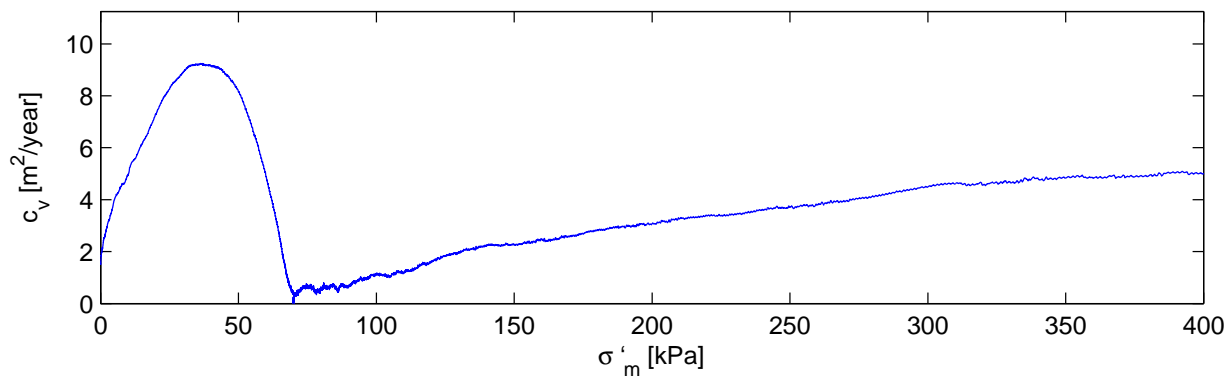
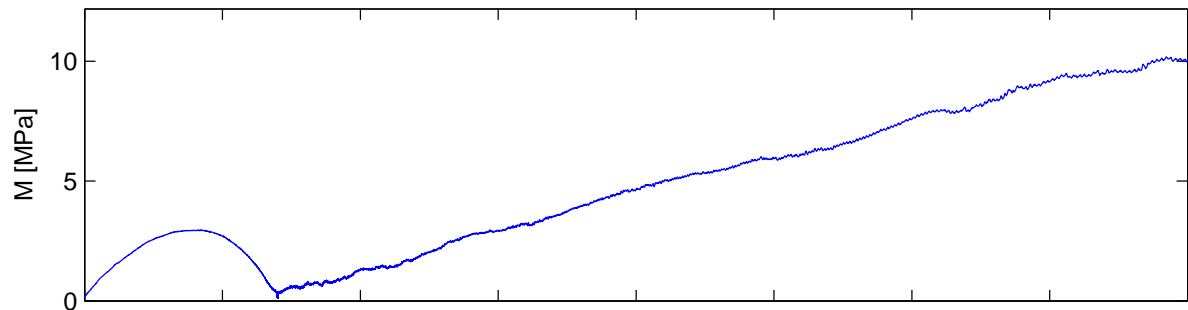
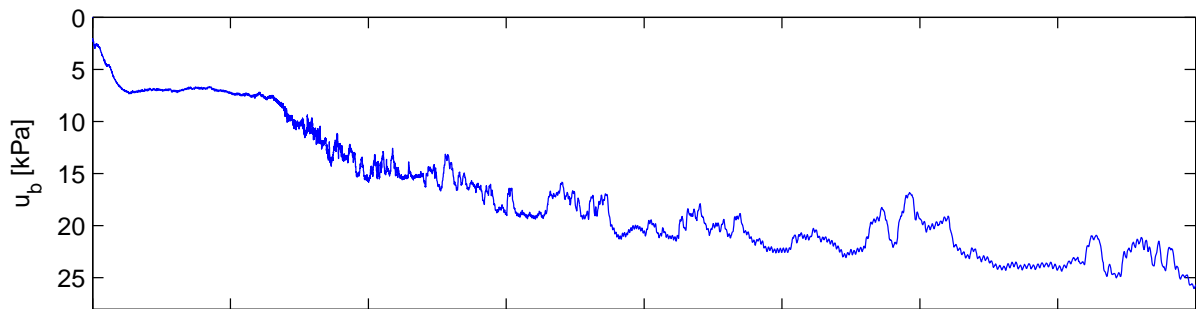
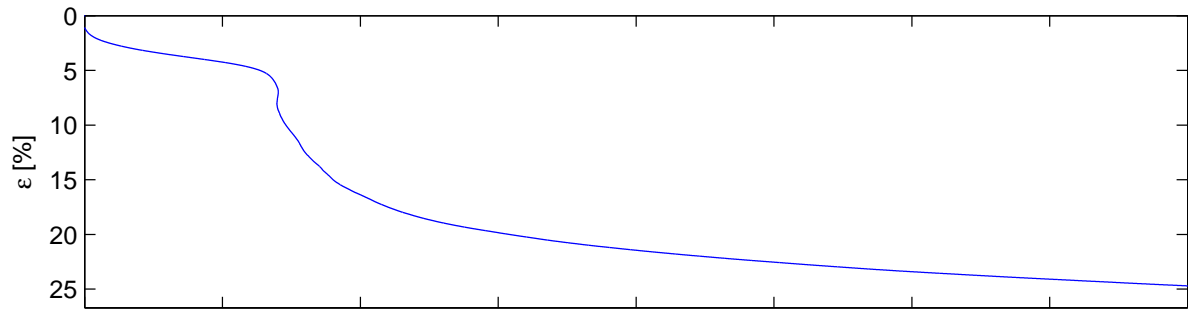
σ'_{vo} = 43.58 kPa
 w = 41.10 %
 γ = 18.14 kN/m³
 OCR = 1.72

σ'_c = 75.00 kPa
 M_{oc} = 3.59 MPa
 m = 32.58
 σ'_{ref} = 41.04 kPa
 c_v = 16.00 m²/year



Dragvoll CRS Test 1

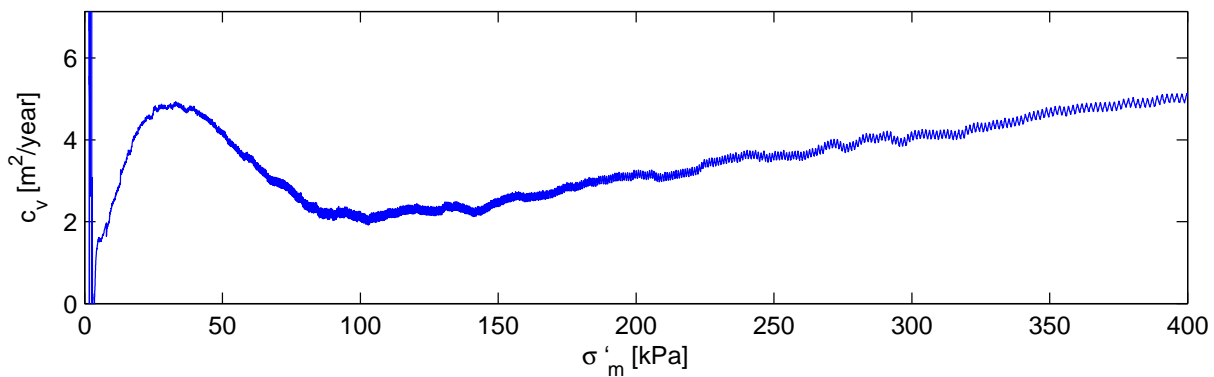
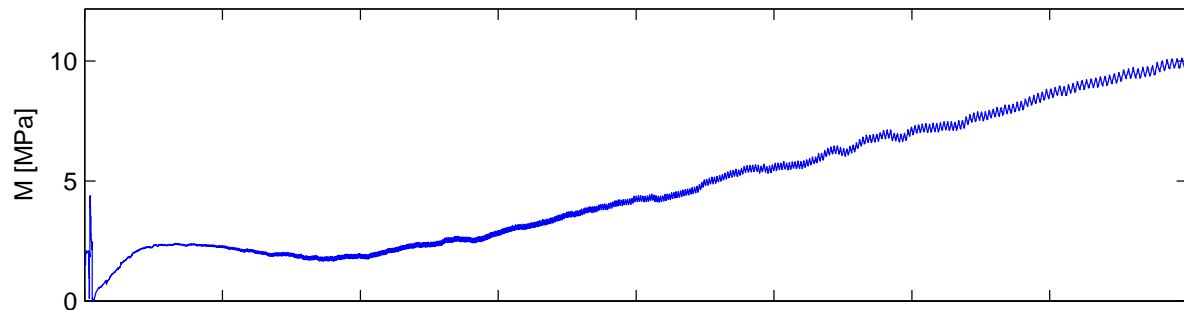
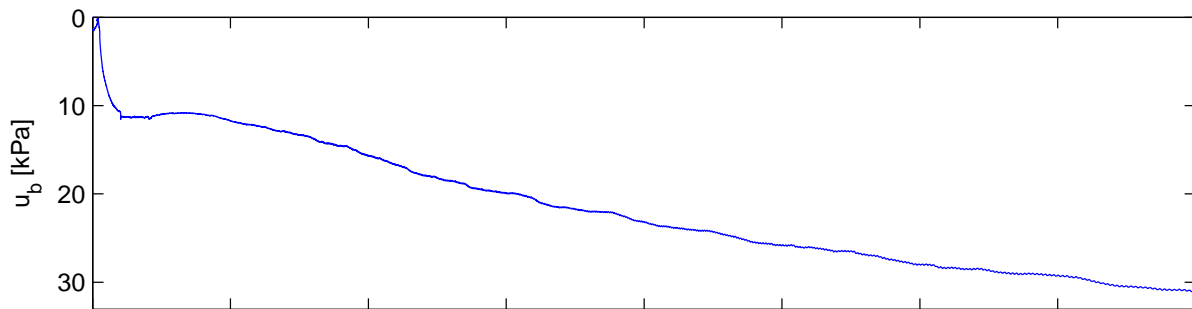
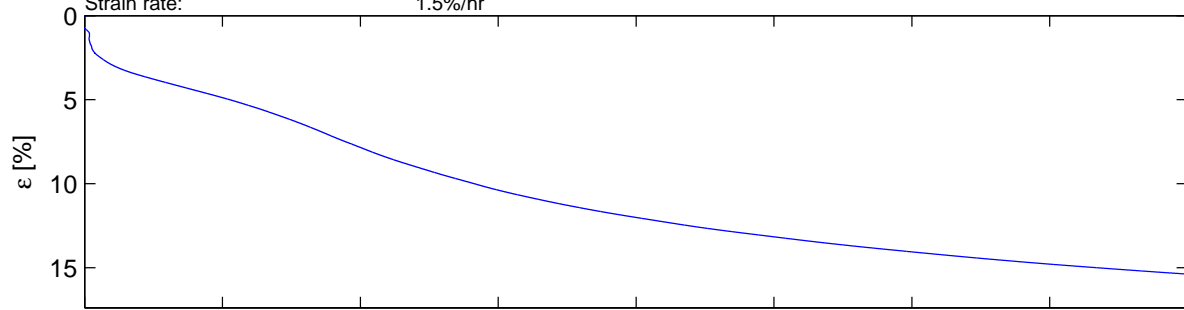
Depth:	3.1 m	$\sigma_{vo} = 5.00$ kPa	$\sigma_c = 1.00$ kPa
Sampling date:	30.11.12	$w = 2.00$ %	$M_{oc} = 2.96$ MPa
Opening of the block sample:	30.12.12	$\gamma = 3.00$ kN/m ³	$m = 30.04$
Testing date:	30.12.12	OCR = 0.20	$\sigma'_{ref} = 42.50$ kPa
Strain rate:	1.5%/hr		$c_v = 5.02$ m ² /year



Dragvoll CRS

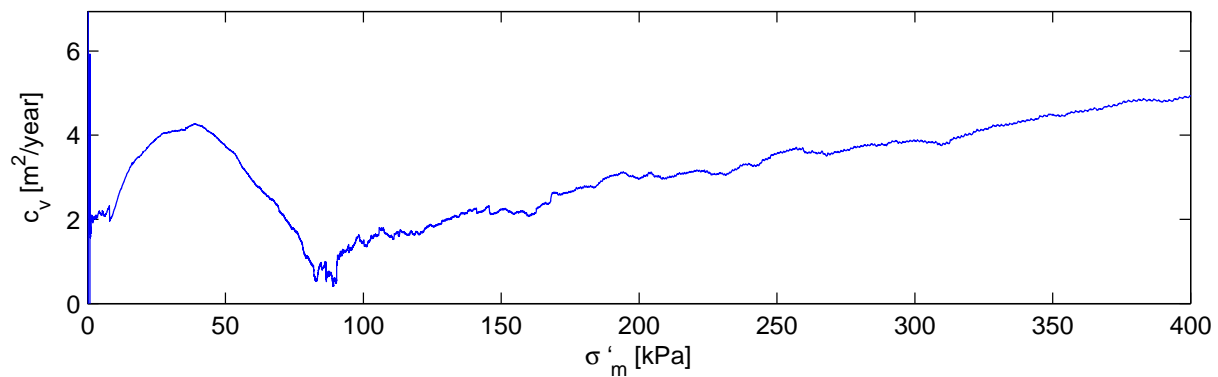
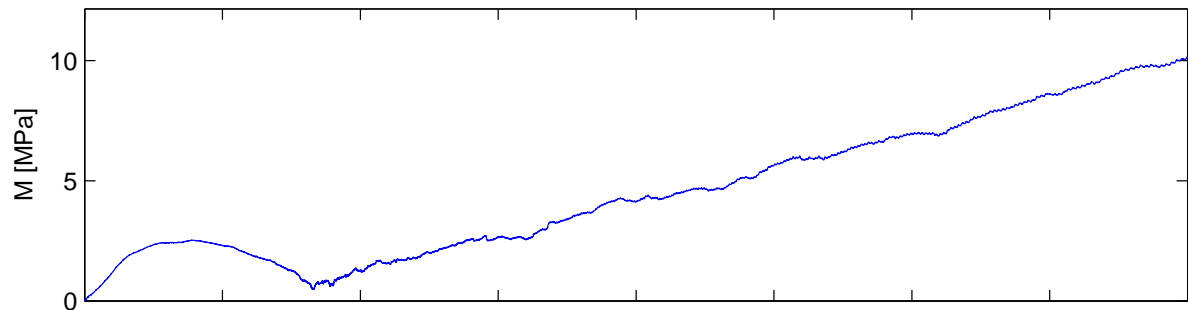
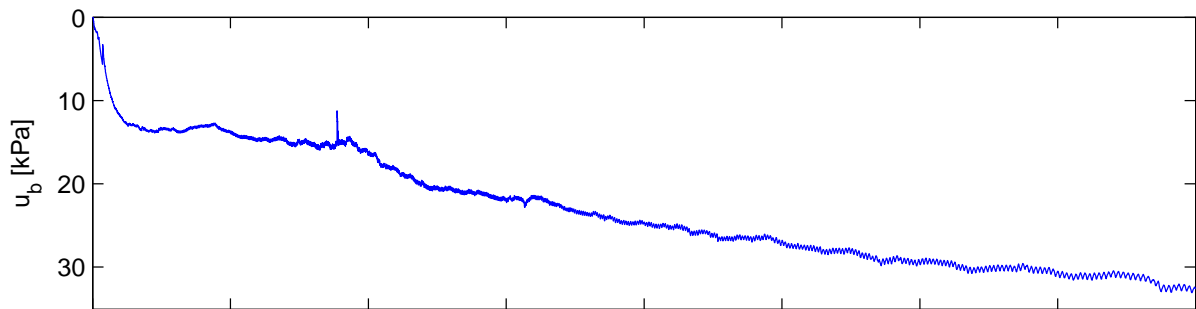
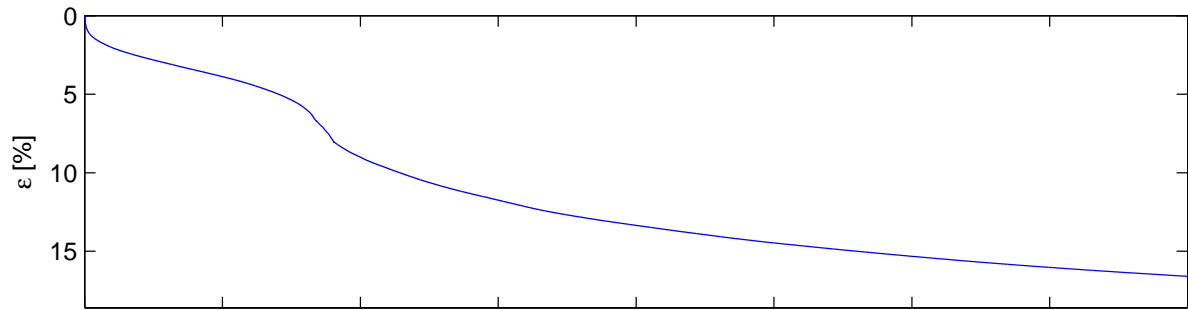
Mini block sample H2 D 8.45–8.70 m

Depth:	8.55 m	σ'_{vo} = 59.85 kPa	σ'_c = 70.00 kPa
Sampling date:	05.11.13	w = 35.00 %	M_{oc} = 2.40 MPa
Installed in storage cell:	4.12.13	γ = 18.81 kN/m ³	m = 26.31
Opening of the block sample:	08.11.13	OCR = 1.17	σ'_{ref} = 33.00 kPa
Testing date:	08.11.13		c_v = 3.00 m ² /year
Strain rate:	1.5%/hr		



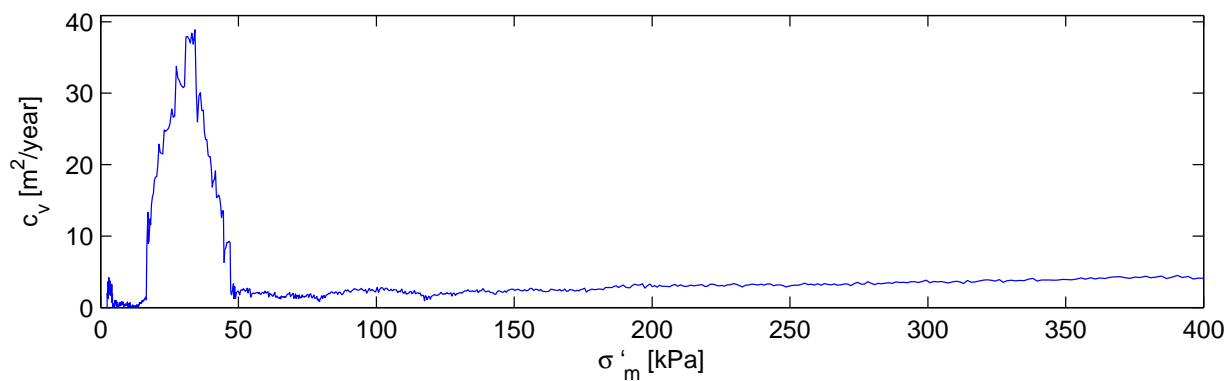
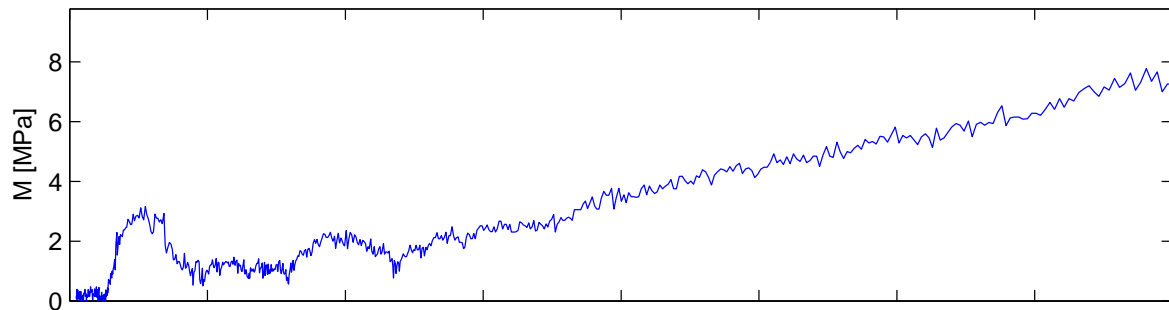
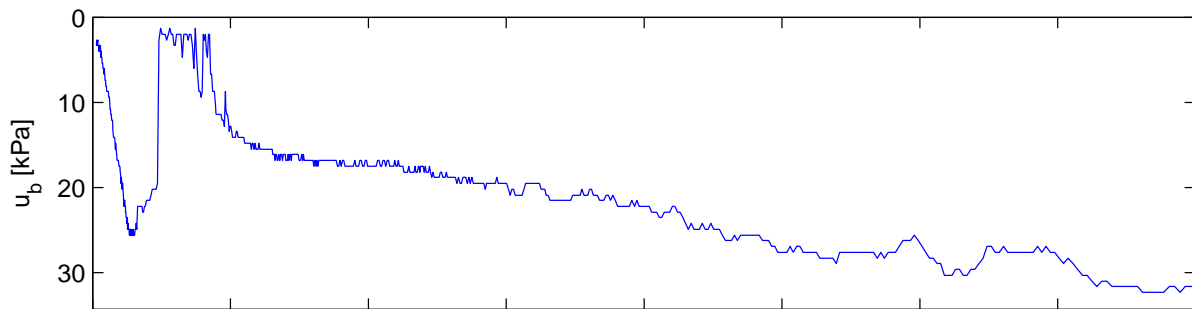
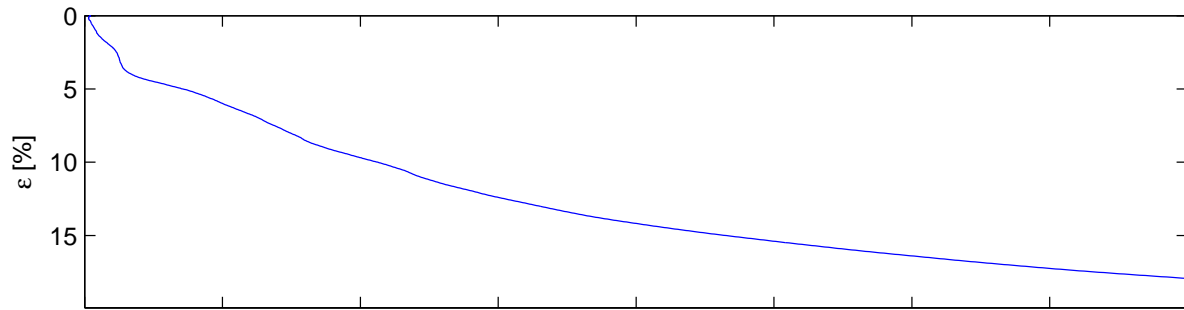
Dragvoll CRS Test 1

Depth:	3.1 m	$\sigma_{vo} = 5.00$ kPa	$\sigma_c = 1.00$ kPa
Sampling date:	30.11.12	$w = 2.00$ %	$M_{oc} = 2.53$ MPa
Opening of the block sample:	30.12.12	$\gamma = 3.00$ kN/m ³	$m = 30.38$
Testing date:	30.12.12	OCR = 0.20	$\sigma'_{ref} = 39.03$ kPa
Strain rate:	1.5%/hr		$c_v = 4.93$ m ² /year



Dragvoll CRS Test 1

Depth:	3.1 m	$\sigma_{vo} = 5.00$ kPa	$\sigma_c = 1.00$ kPa
Sampling date:	30.11.12	$w = 2.00$ %	$M_{oc} = 1.91$ MPa
Opening of the block sample:	30.12.12	$\gamma = 3.00$ kN/m ³	$m = 19.54$
Testing date:	30.12.12	OCR = 0.20	$\sigma'_{ref} = 36.20$ kPa
Strain rate:	1.5%/hr		$c_v = 4.29$ m ² /year



Appendix E

Oedometer tests on samples stored in water and KCl solution

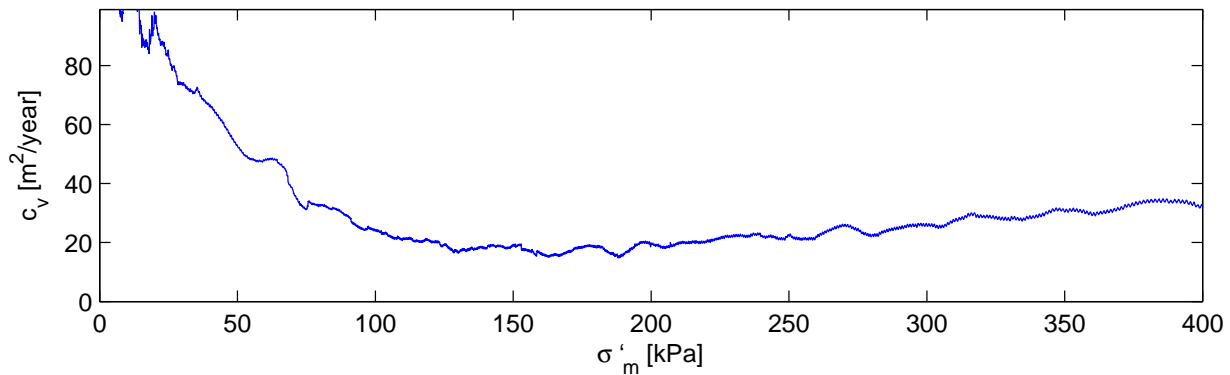
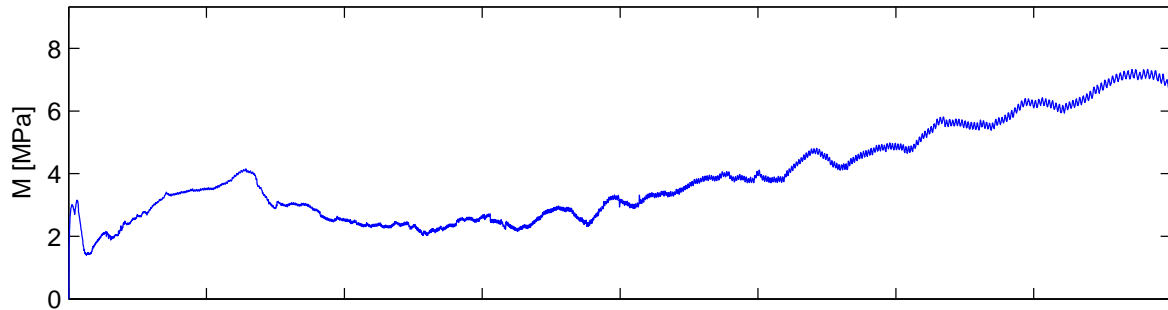
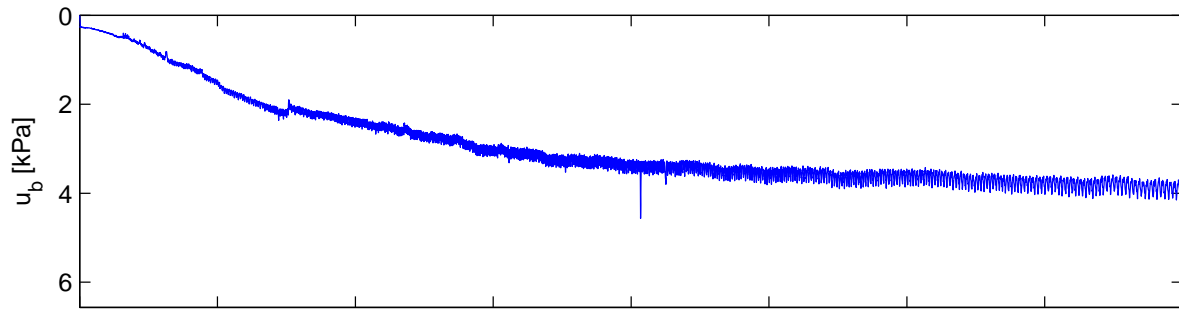
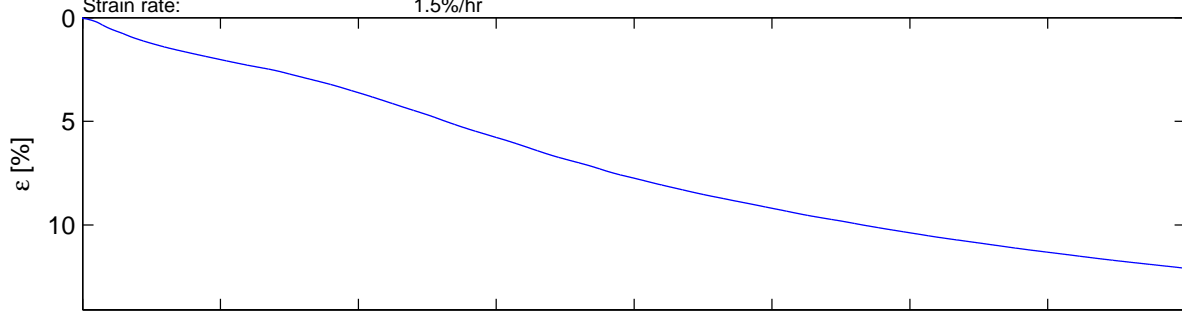
Dragvoll CRS

Mini block sample H2 D3,5–3,75m Potassium chloride

Depth: 3.65 m
Sampling date: 4.10.13
Installed in storage cell: 4.12.13
Opening of the block sample: 15.1.14
Testing date: 19.1.14
Strain rate: 1.5%/hr

σ'_{vo} = 25.55 kPa
 w = 36.70 %
 γ = 18.96 kN/m³
OCR = 3.52

σ'_c = 90.00 kPa
 M_{oc} = 4.15 MPa
 m = 17.82
 σ'_{ref} = 64.24 kPa
 c_v = 32.11 m²/year



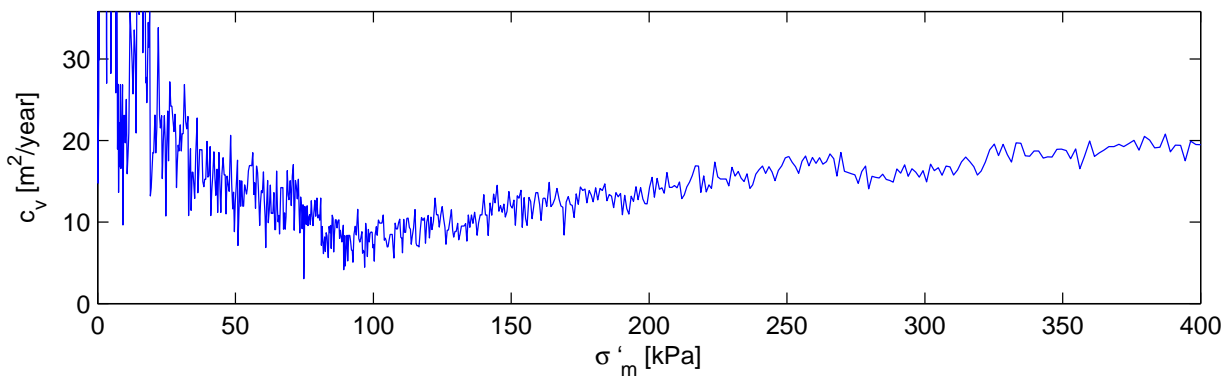
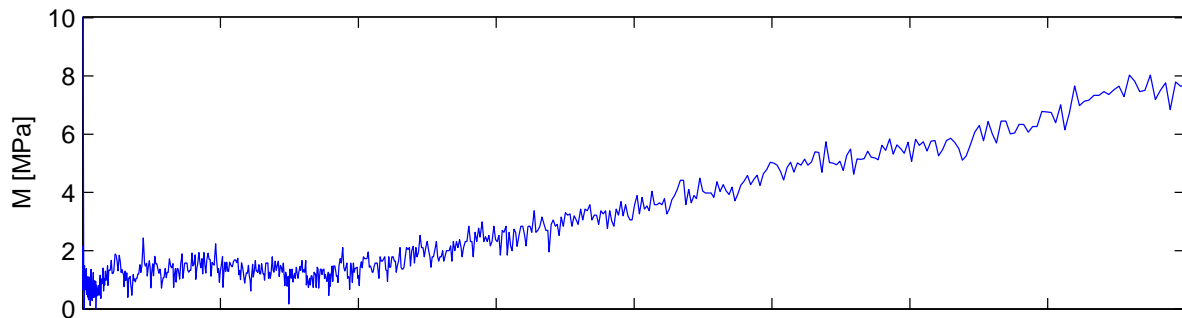
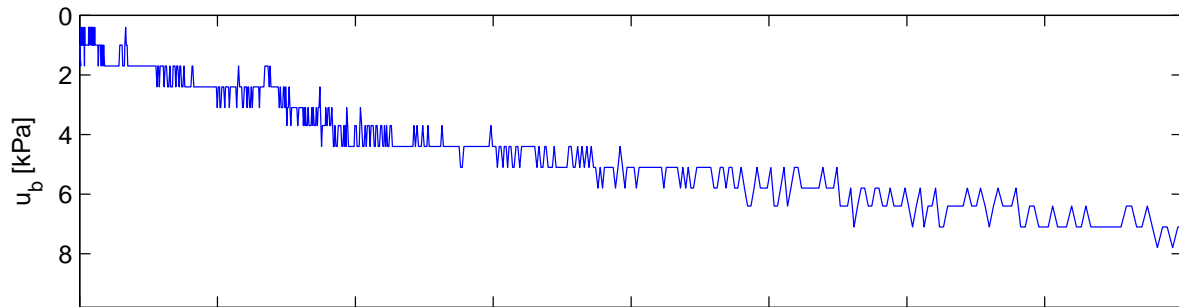
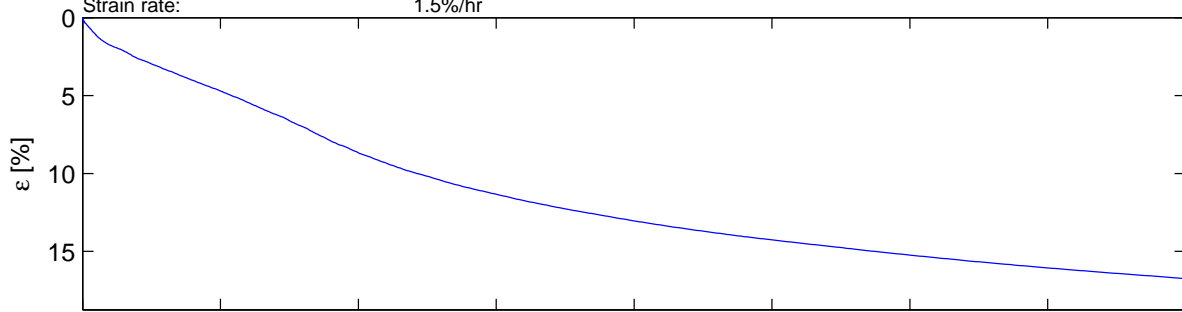
Dragvoll CRS

Mini block sample H2 D3,75–4,0m Water

Depth: 3.905 m
 Sampling date: 4.10.13
 Installed in storage cell: 4.12.13
 Opening of the block sample: 20.1.14
 Testing date: 20.1.14
 Strain rate: 1.5%/hr

σ'_{vo} = 27.34 kPa
 w = 40.66 %
 γ = 18.38 kN/m³
 OCR = 2.56

σ'_c = 70.00 kPa
 M_{oc} = 30.69 MPa
 m =
 σ'_{ref} = 1538.16 kPa
 c_v = 19.84 m²/year



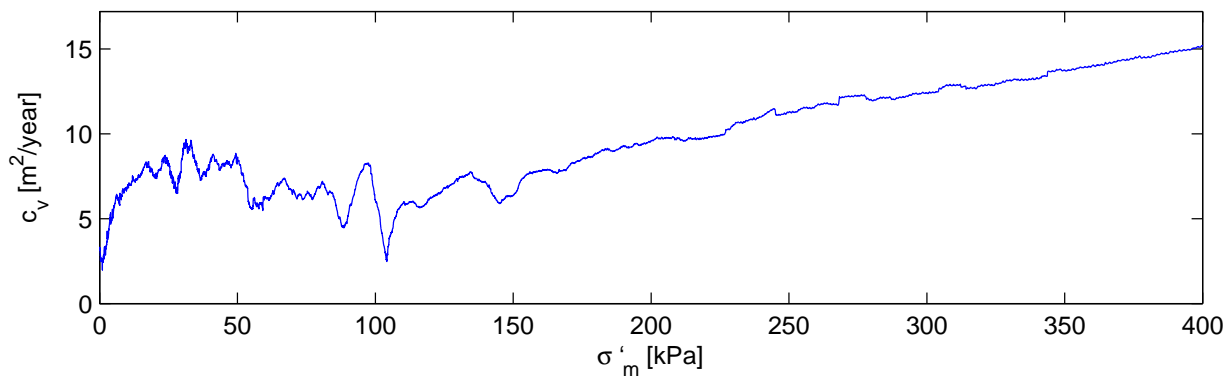
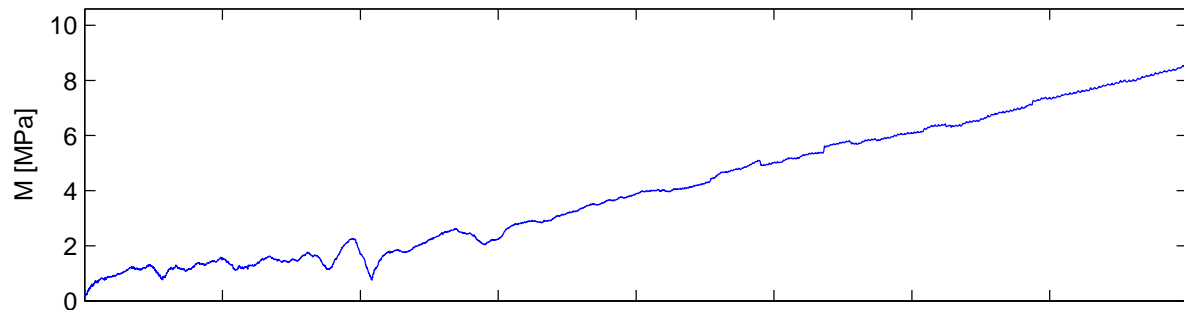
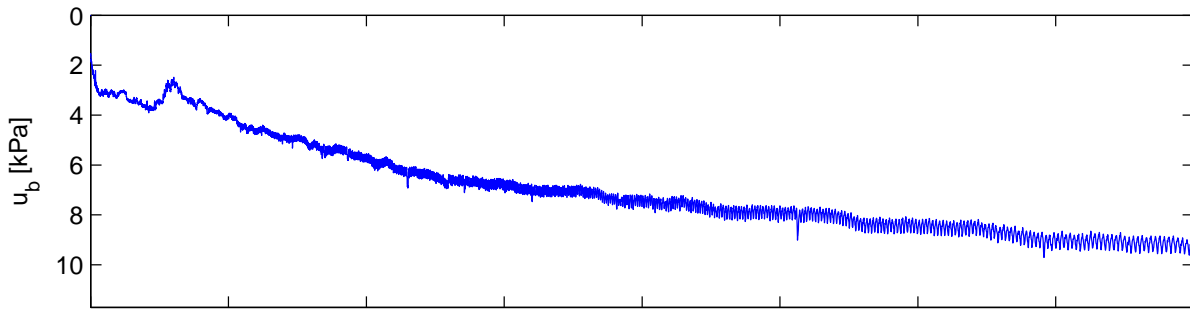
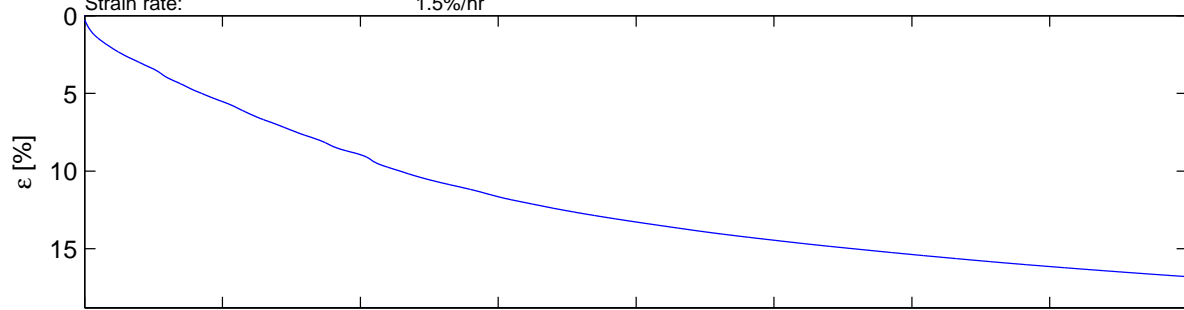
Dragvoll CRS

Mini block sample H2 D3,75–4,0m Water

Depth: 3.955 m
 Sampling date: 4.10.13
 Installed in storage cell: 4.12.13
 Opening of the block sample: 20.1.14
 Testing date: 20.1.14
 Strain rate: 1.5%/hr

σ'_{vo} = 27.67 kPa
 w = 40.75 %
 γ = 18.12 kN/m³
 OCR = -

σ'_c = -
 M_{oc} = 1.56 MPa
 m = 26.36
 σ'_{ref} = 50.01 kPa
 c_v = 15.15 m²/year



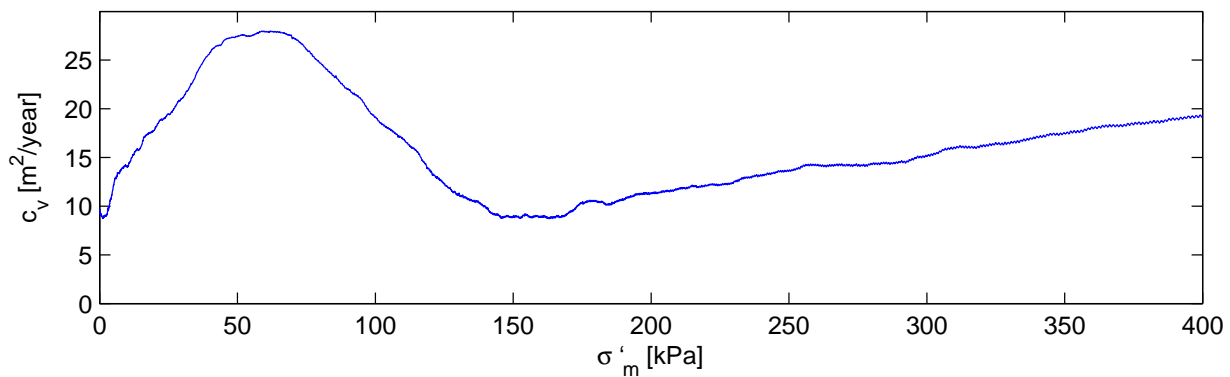
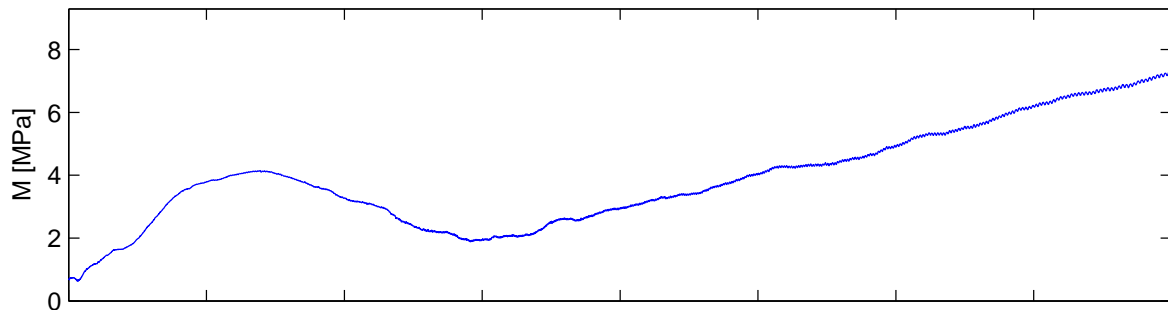
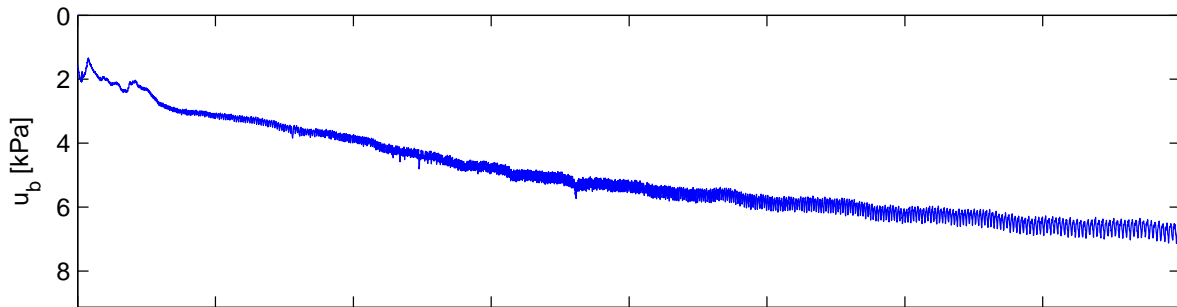
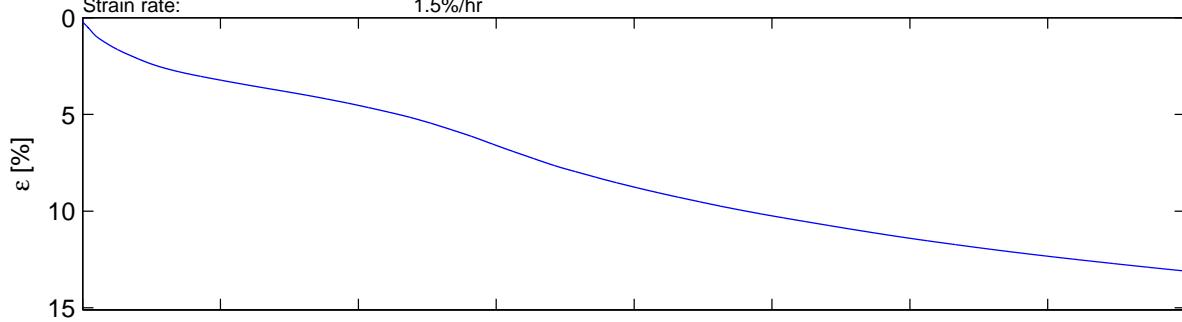
Dragvoll CRS

Mini block sample H2 D4,25–4,5m Potassium chloride

Depth: 4.315 m
Sampling date: 4.10.13
Installed in storage cell: 4.12.13
Opening of the block sample: 4.2.14
Testing date: 6.2.14
Strain rate: 1.5%/hr

σ'_{vo} = 30.20 kPa
 w = 37.80 %
 γ = 18.67 kN/m³
OCR = 3.81

σ'_c = 115.00 kPa
 M_{oc} = 4.08 MPa
 m = 21.07
 σ'_{ref} = 74.24 kPa
 c_v = 19.21 m²/year



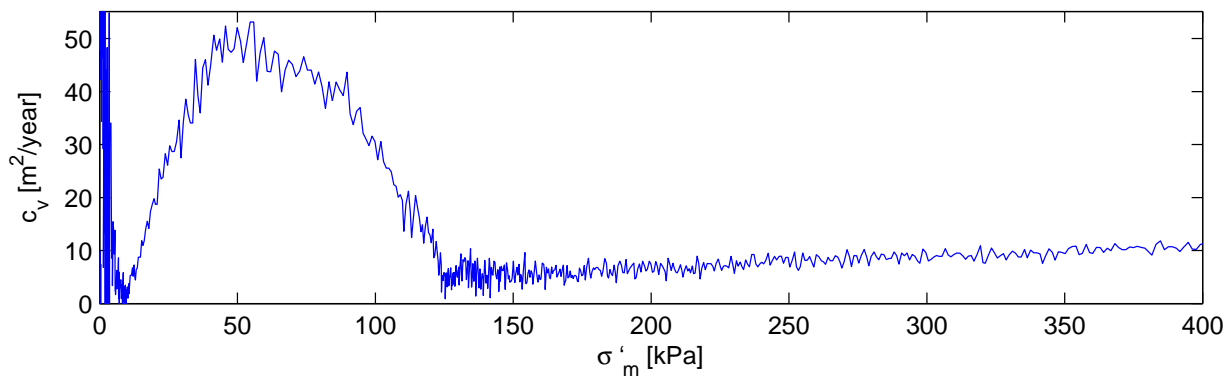
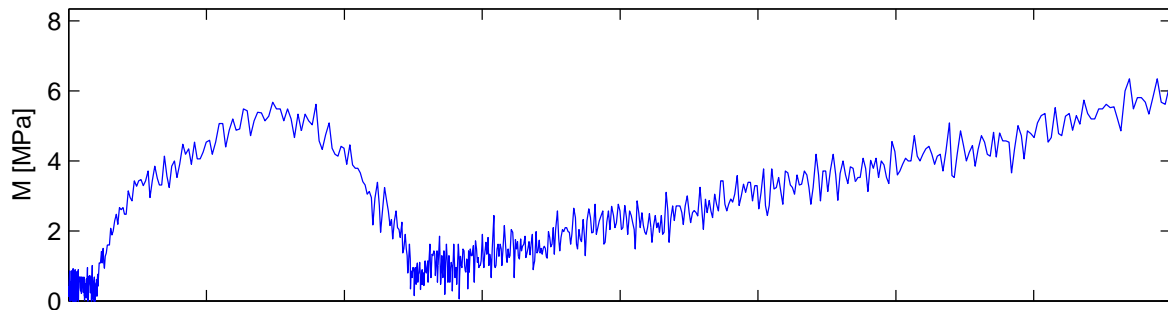
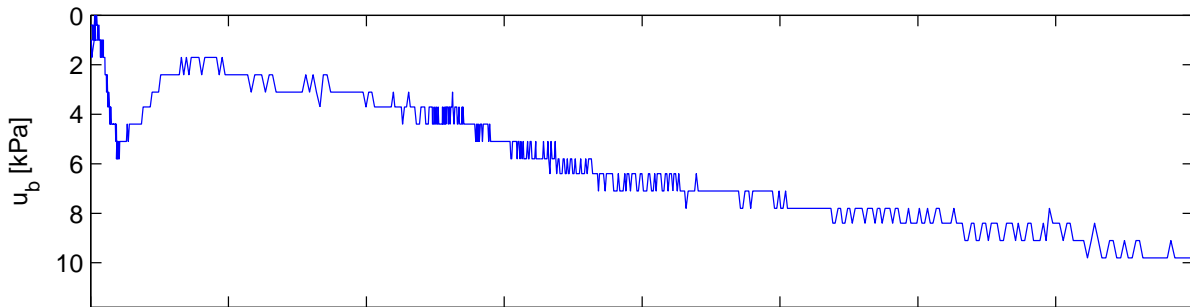
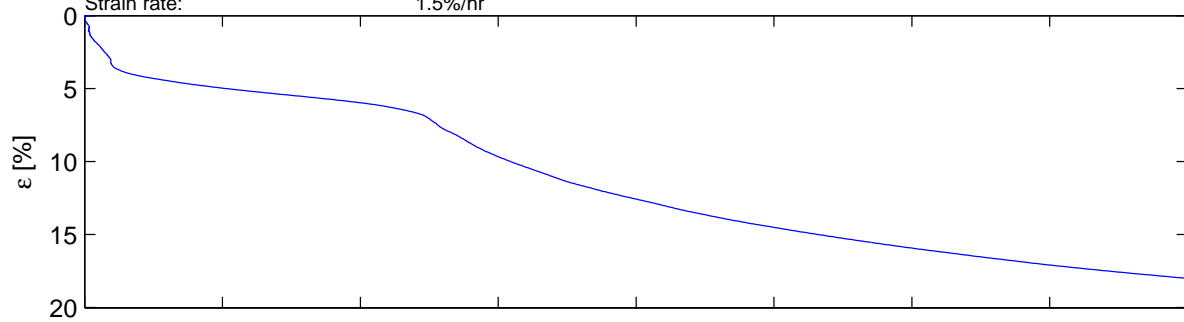
Dragvoll CRS

Mini block sample H2 D4,25–4,5m Potassium chloride

Depth: 4.355 m
Sampling date: 4.10.13
Installed in storage cell: 4.12.13
Opening of the block sample: 4.2.14
Testing date: 6.2.14
Strain rate: 1.5%/hr

σ'_{vo} = 30.49 kPa
 w = 40.78 %
 γ = 18.67 kN/m³
OCR = 3.94

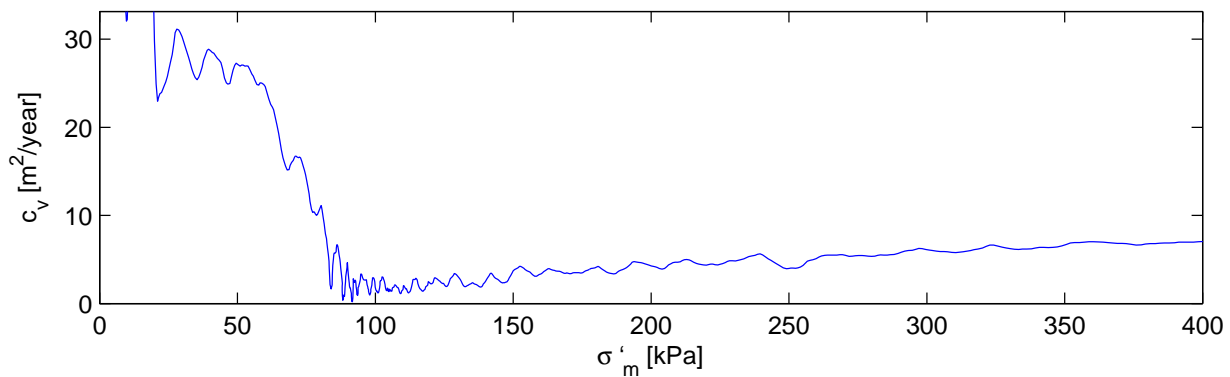
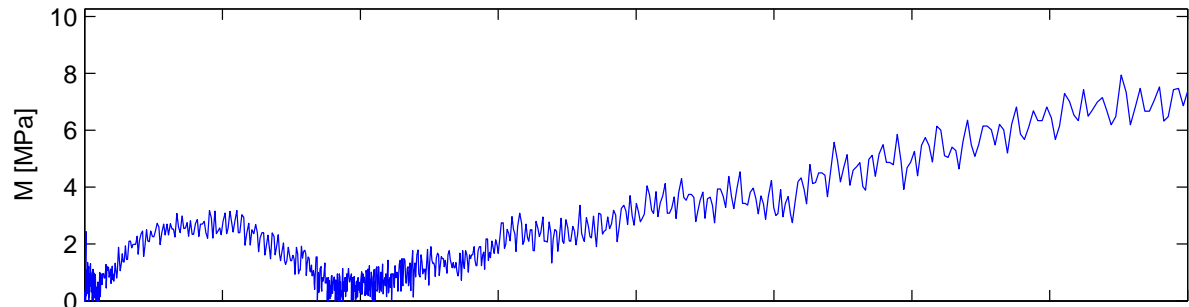
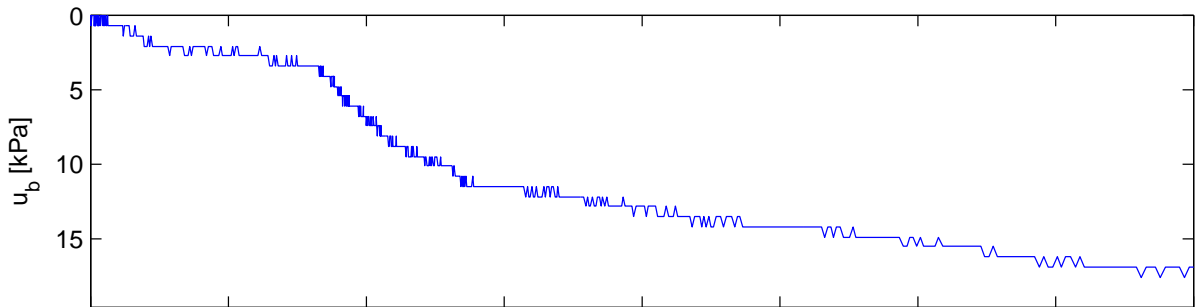
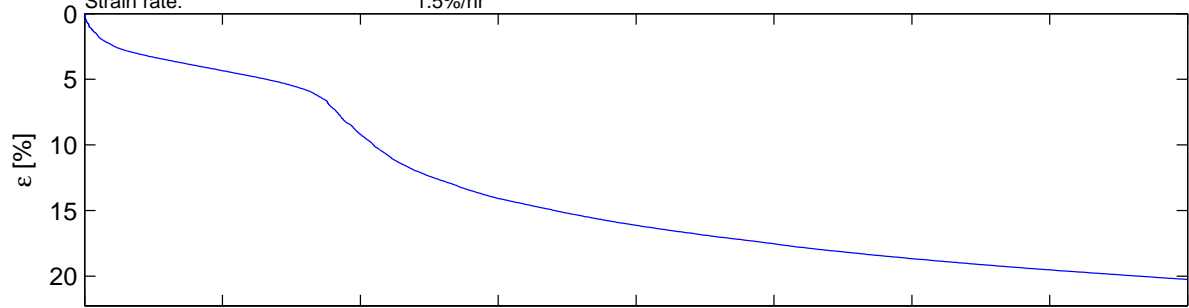
σ'_c = 120.00 kPa
 M_{oc} = 5.49 MPa
 m = 21.69
 σ'_{ref} = 75.38 kPa
 c_v = 11.41 m²/year



Dragvoll CRS

Mini block sample H2 D4,75–4,0m Water

Depth:	4.95 m	$\sigma'_{vo} = 32.65$ kPa	$\sigma'_c = 80.00$ kPa
Sampling date:	24.10.13	$w = 41.42$ %	$M_{oc} = 24.40$ MPa
Installed in storage cell:	4.12.13	$\gamma = 18.00$ kN/m ³	$m =$
Opening of the block sample:	10.2.14	OCR = 2.45	$\sigma'_{ref} = 1204.08$ kPa
Testing date:	12.2.14		$c_v = 7.09$ m ² /year
Strain rate:	1.5%/hr		



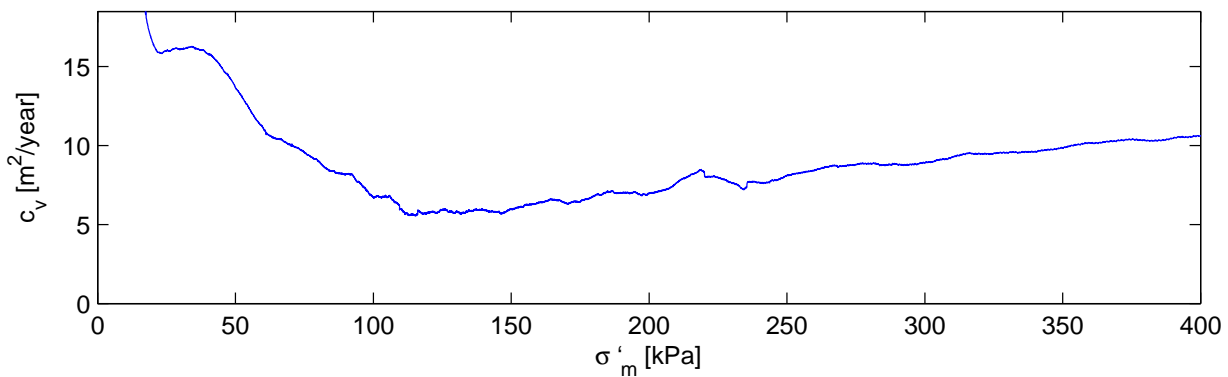
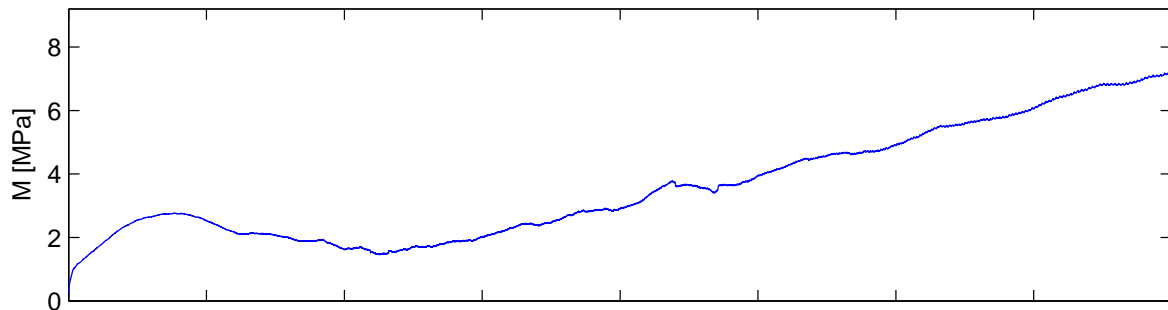
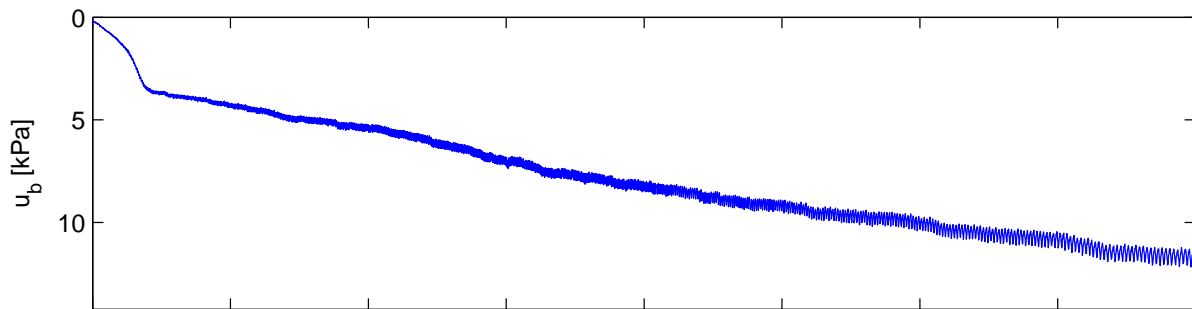
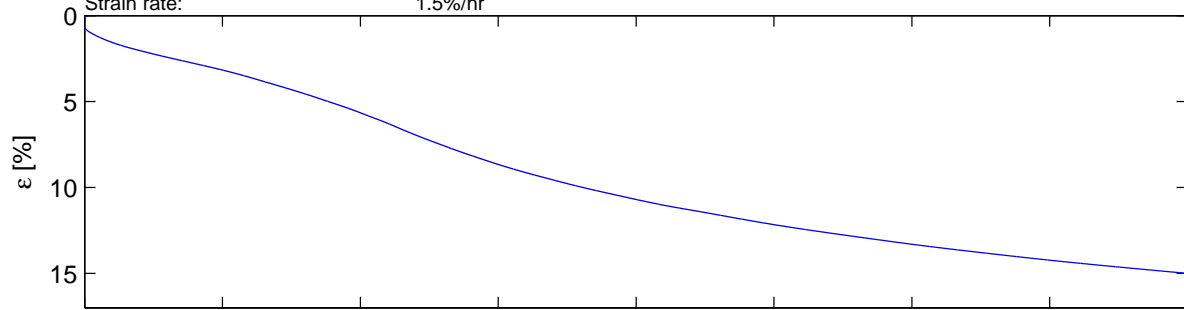
Dragvoll CRS

Mini block sample H2 D5,05–5,3m Potassium chloride

Depth: 5.19 m
Sampling date: 24.10.13
Installed in storage cell: 4.12.13
Opening of the block sample: 18.2.14
Testing date: 20.2.14
Strain rate: 1.5%/hr

σ'_{vo} = 36.33 kPa
 w = 38.04 %
 γ = 18.97 kN/m³
OCR = 2.20

σ'_c = 80.00 kPa
 M_{oc} = 2.53 MPa
 m = 19.93
 σ'_{ref} = 49.81 kPa
 c_v = 10.64 m²/year



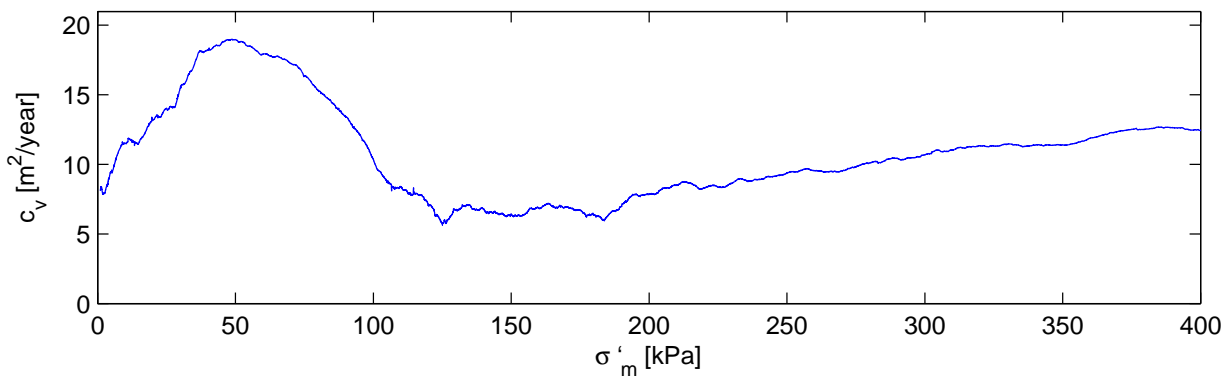
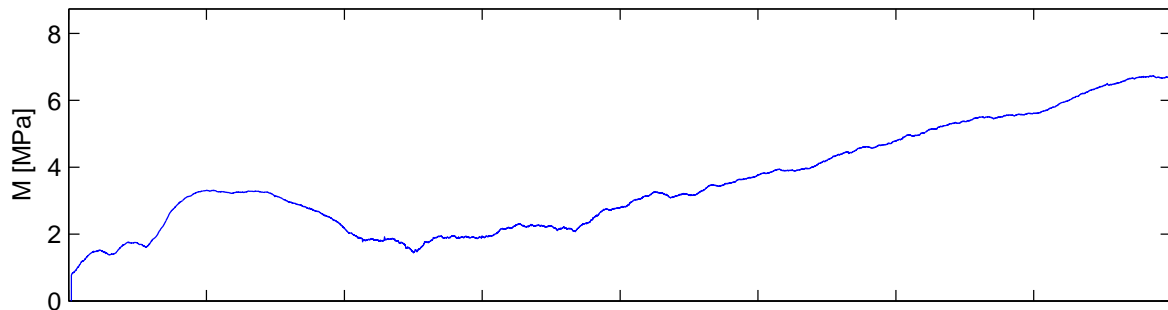
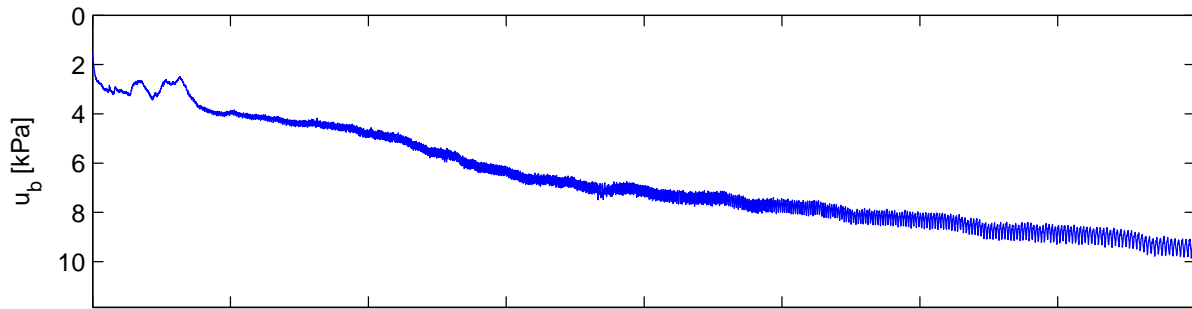
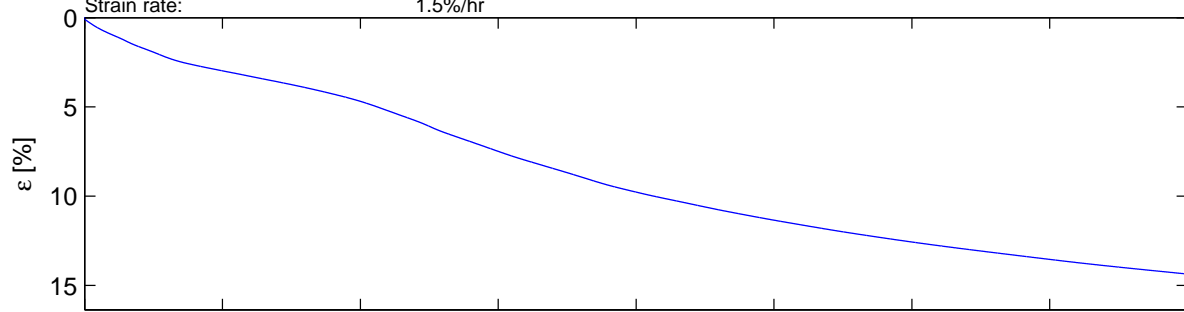
Dragvoll CRS

Mini block sample H2 D5,05–5,3m Potassium chloride

Depth: 5.27 m
Sampling date: 24.10.13
Installed in storage cell: 4.12.13
Opening of the block sample: 18.2.14
Testing date: 24.2.14
Strain rate: 1.5%/hr

σ'_{vo} = 36.89 kPa
 w = 38.55 %
 γ = 18.94 kN/m³
OCR = 2.71

σ'_c = 100.00 kPa
 M_{oc} = 2.93 MPa
 m = 18.97
 σ'_{ref} = 81.41 kPa
 c_v = 12.44 m²/year



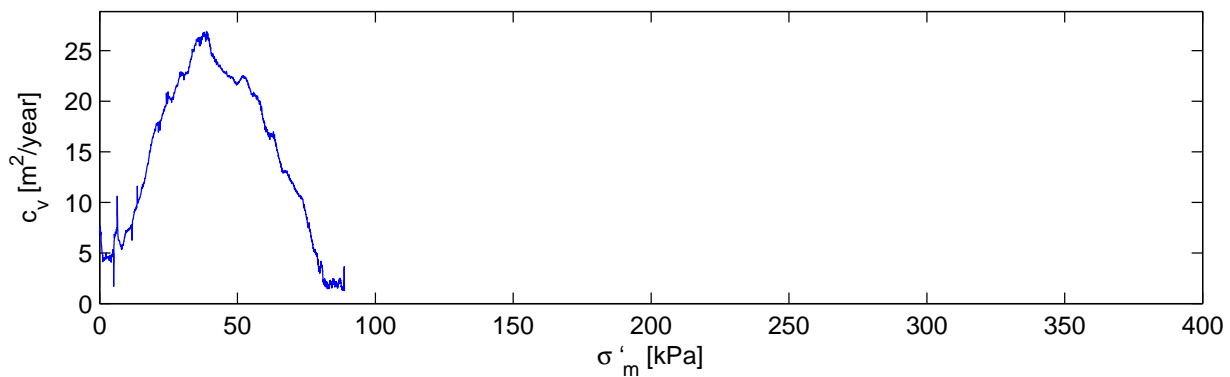
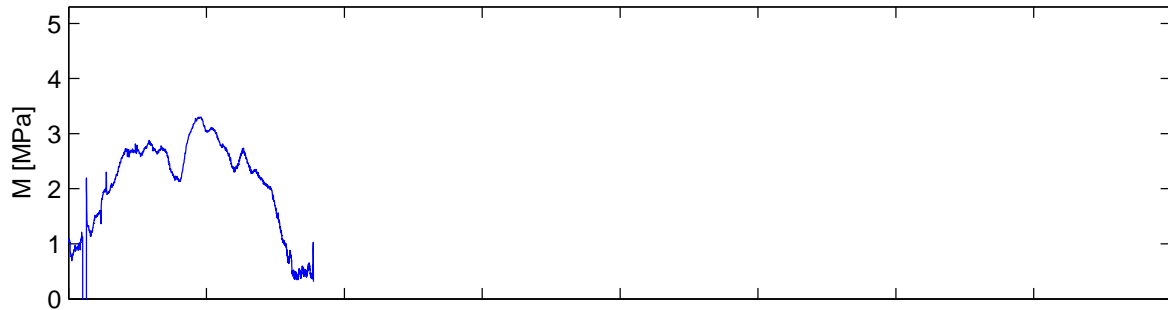
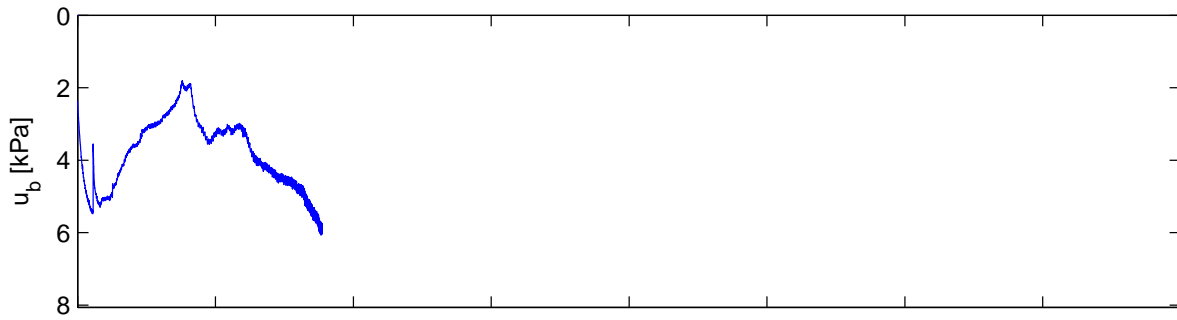
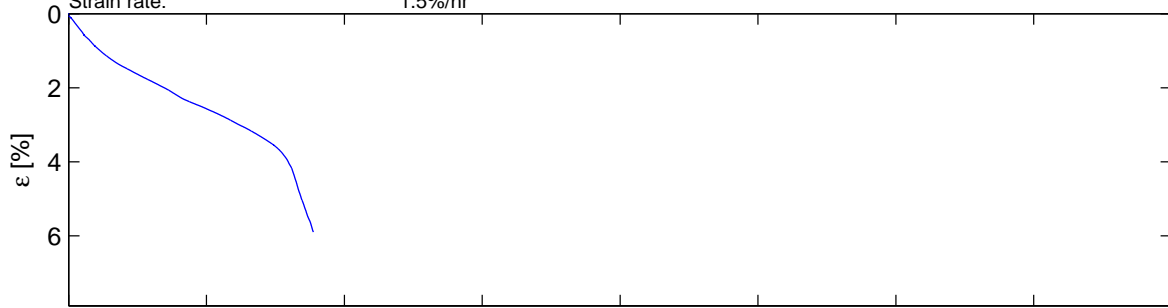
Dragvoll CRS

Mini block sample H2 D5,55–5,8m Water

Depth: 5.705 m
Sampling date: 24.10.13
Installed in storage cell: 4.12.13
Opening of the block sample: 25.2.14
Testing date: 28.2.14
Strain rate: 1.5%/hr

σ'_{vo} = 39.94 kPa
 w = 0.00 %
 γ = 18.47 kN/m³
OCR = 1.88

σ'_c = 75.00 kPa
 M_{oc} = 3.30 MPa
 m = 0.00
 σ'_{ref} = kPa
 c_v = 0.00 m²/year



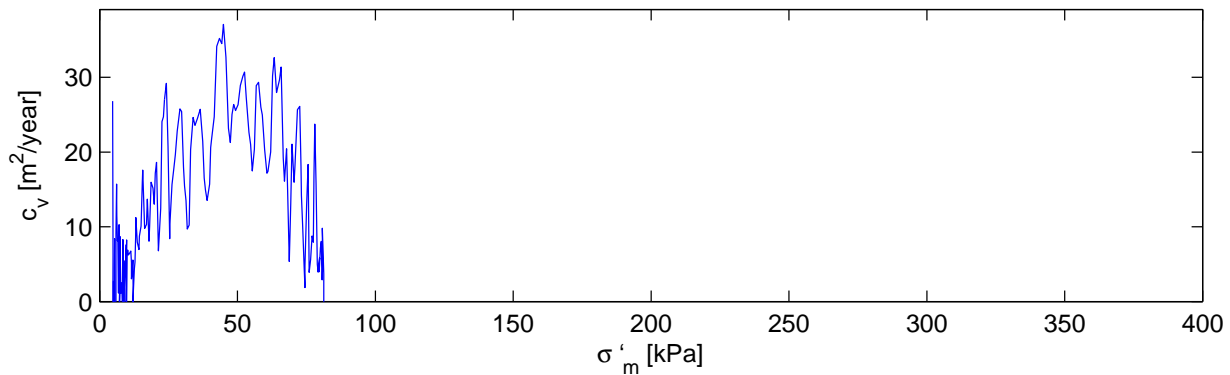
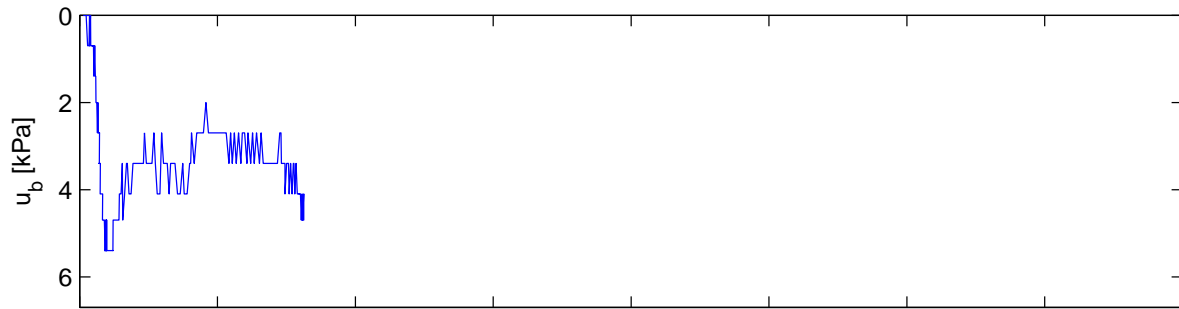
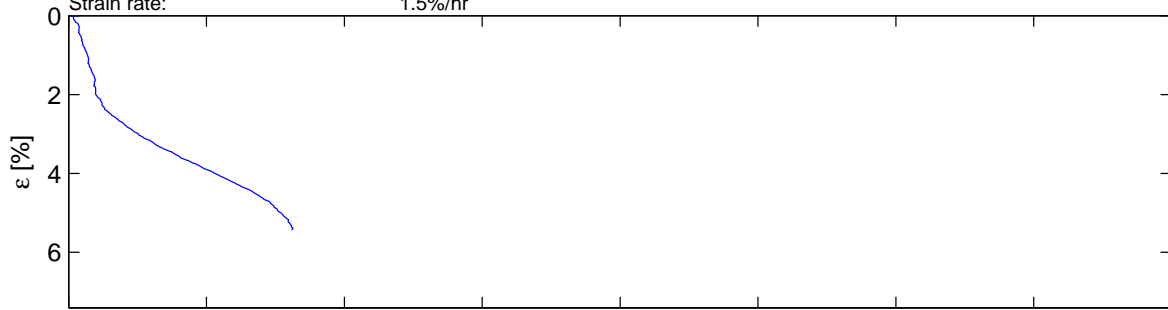
Dragvoll CRS

Mini block sample H2 D5,55–5,8m Water

Depth: 5.735 m
Sampling date: 24.10.13
Installed in storage cell: 4.12.13
Opening of the block sample: 25.2.14
Testing date: 28.2.14
Strain rate: 1.5%/hr

σ'_{vo} = 40.15 kPa
 w = 0.00 %
 γ = 18.34 kN/m³
OCR = 1.87

σ'_c = 75.00 kPa
 M_{oc} = 3.50 MPa
 m = 0.00
 σ'_{ref} = kPa
 c_v = 0.00 m²/year



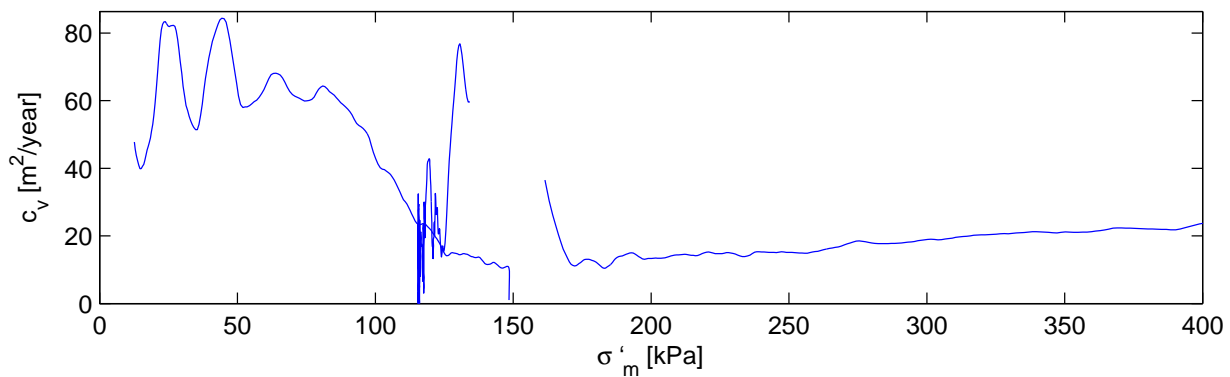
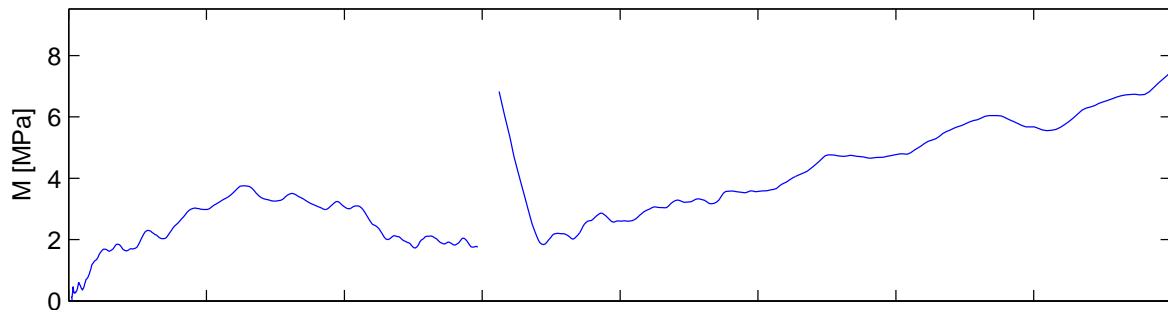
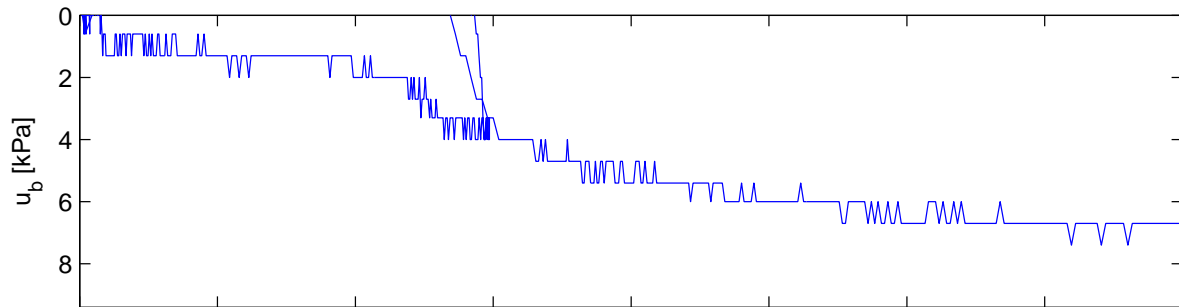
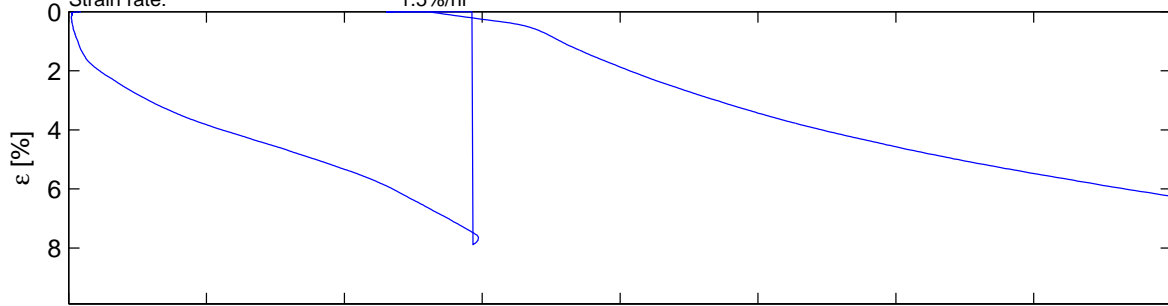
Dragvoll CRS

Mini block sample H2 D7,45–7,7m Potassium chloride

Depth: 7.575 m
Sampling date: 30.10.13
Installed in storage cell: 4.12.13
Opening of the block sample: 10.3.14
Testing date: 11.3.14
Strain rate: 1.5%/hr

σ'_{vo} = 53.02 kPa
 w = -
 γ = 19.57 kN/m³
OCR = 2.17

σ'_c = 115.00 kPa
 M_{oc} = 3.27 MPa
 m = 21.06
 σ'_{ref} = 75.21 kPa
 c_v = 23.89 m²/year



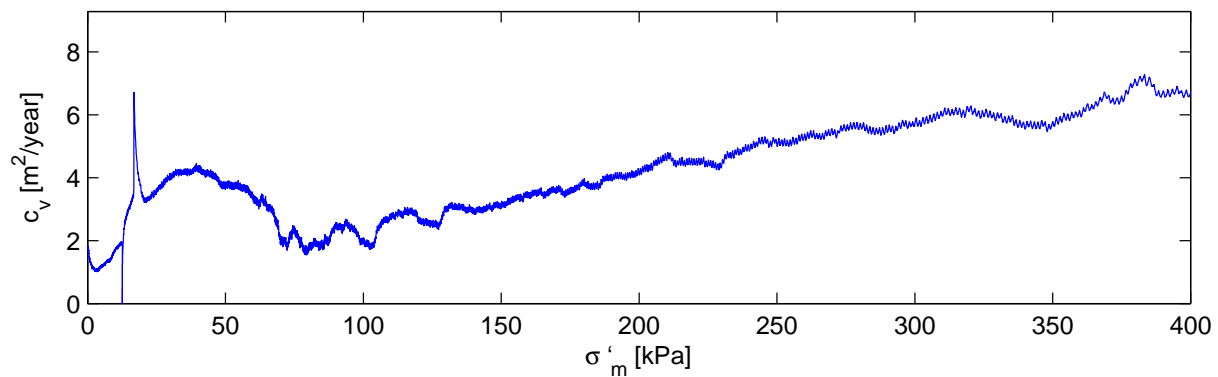
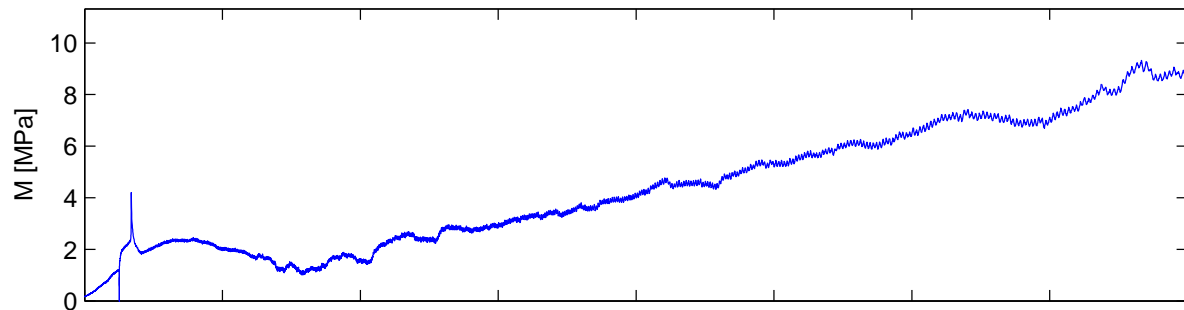
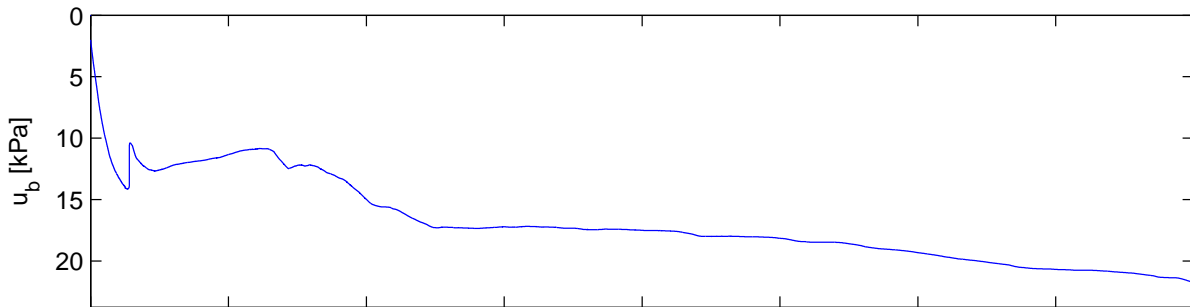
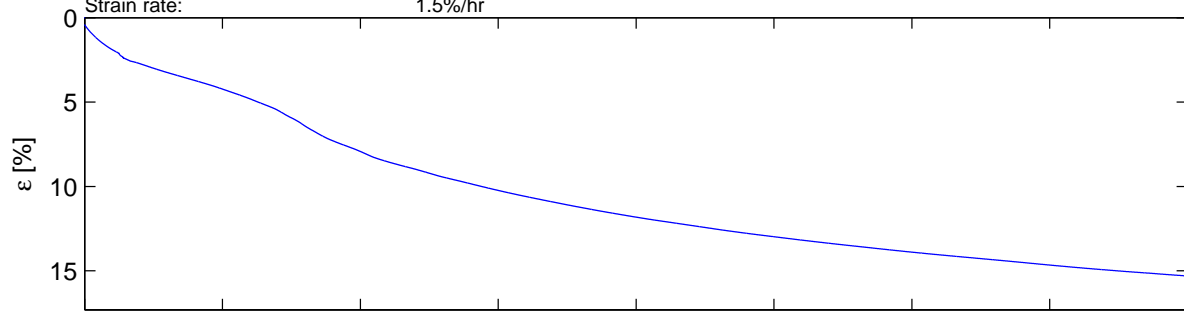
Dragvoll CRS

Mini block sample H2 D8,2–8,45m Water

Depth: 8.355 m
 Sampling date: 30.10.13
 Installed in storage cell: 4.12.13
 Opening of the block sample: 16.3.14
 Testing date: 16.3.14
 Strain rate: 1.5%/hr

σ'_{vo} = 58.49 kPa
 w = 34.13 %
 γ = 19.33 kN/m³
 OCR = 1.20

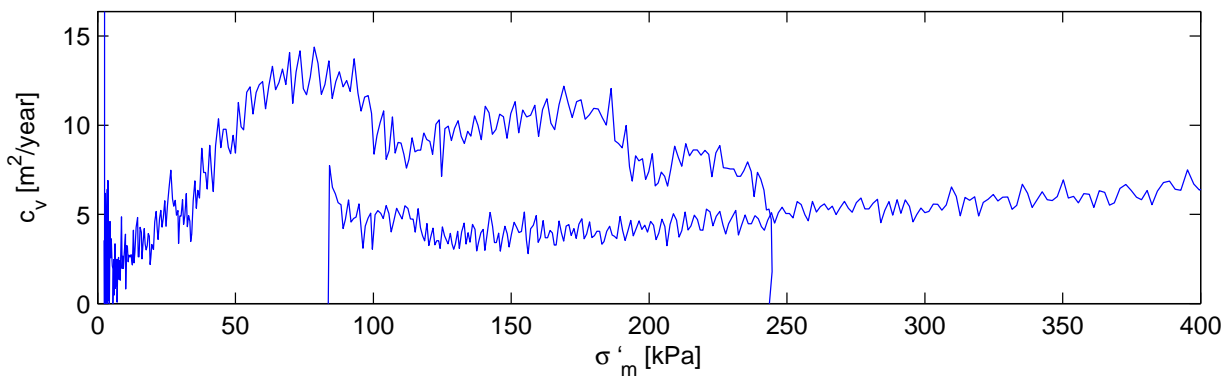
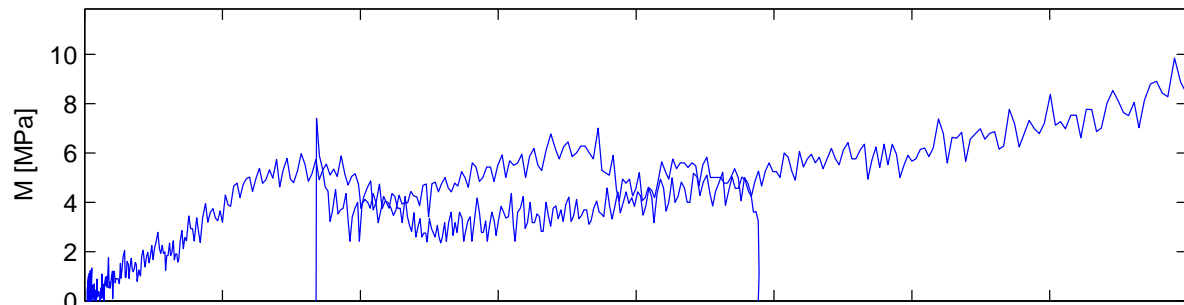
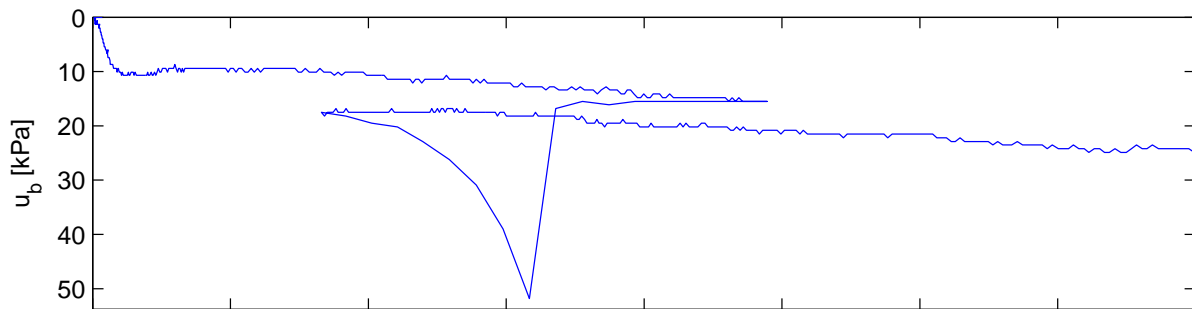
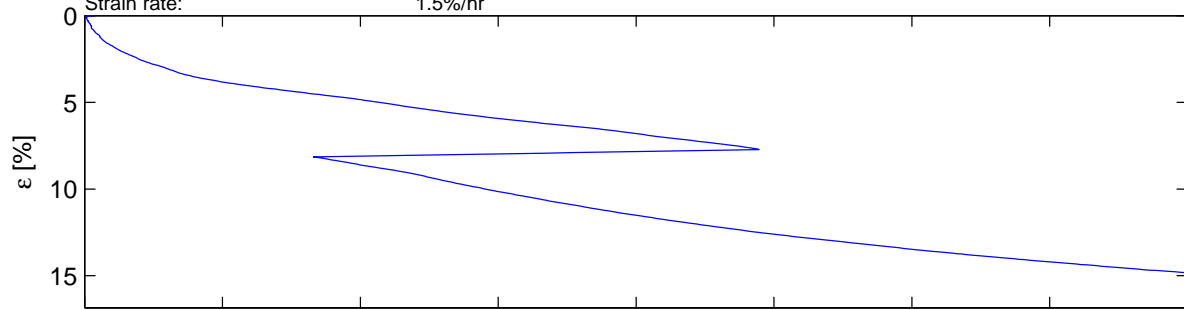
σ'_c = 70.00 kPa
 M_{oc} = 2.33 MPa
 m = 24.40
 σ'_{ref} = 40.01 kPa
 c_v = 6.69 m²/year



Dragvoll CRS

Mini block sample H2 D8,2-8,45m Water

Depth:	8.385 m	σ'_{vo} = 58.69 kPa	σ'_c = 80.00 kPa
Sampling date:	30.10.13	w = 35.18 %	M_{oc} = 3.90 MPa
Installed in storage cell:	4.12.13	γ = 18.57 kN/m ³	m = 296.86
Opening of the block sample:	16.3.14	OCR = 1.36	σ'_{ref} = 51.07 kPa
Testing date:	16.3.14		c_v = 7.07 m ² /year
Strain rate:	1.5%/hr		



Appendix F

Triaxial test on reference samples

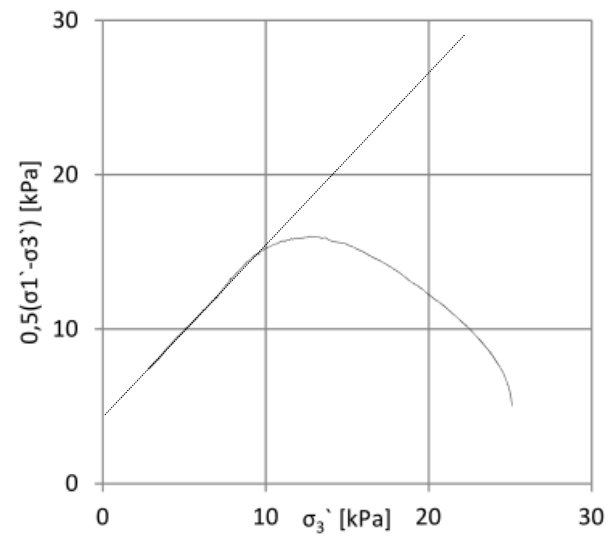
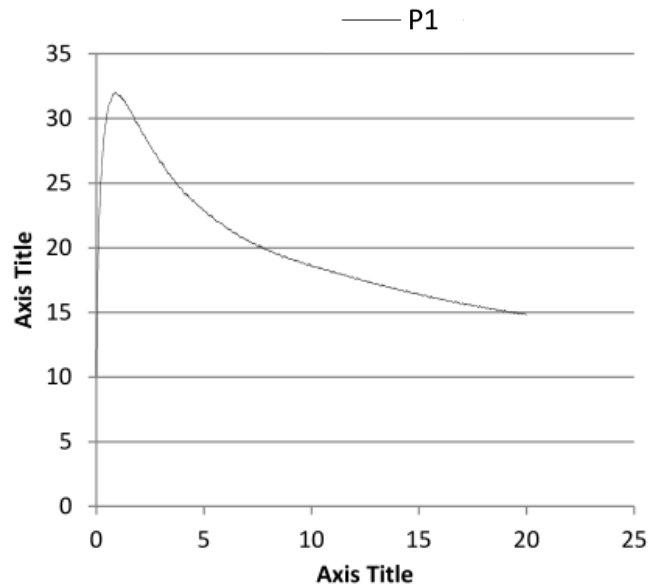
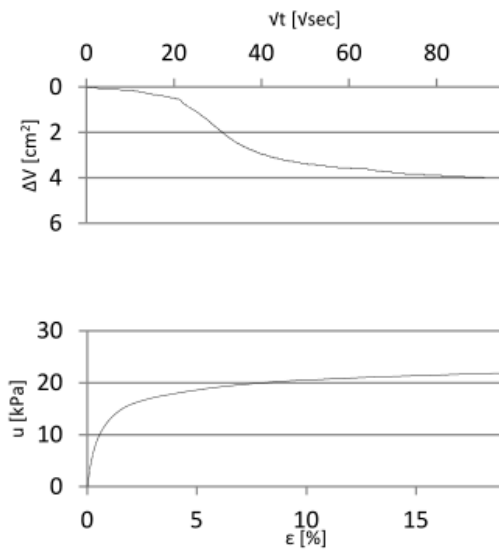
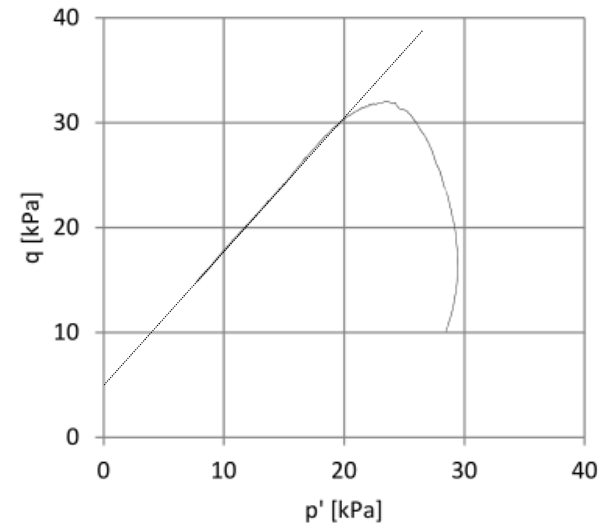
All plots taken from Bryntesen [9].

Dragvoll Bore Hole 1

Mini Block specimen D 5,0-5,25m

Triax depth: 5,07 m

$p'_{o'}$ - Consolidated
Test date: 1.10.2013
 $\sigma'_{vo} = 35$ kPa
 $w = 41,0\%$
 $\gamma = 18,85$ kN/m³
 $\Delta V = 3,97$ cm³
 $\epsilon_f = 0,7\%$
 $S_u = 15,9$ kPa
 $\tan \phi = 0,62$
 $a = 3,64$ kPa
 $D = +0,27$

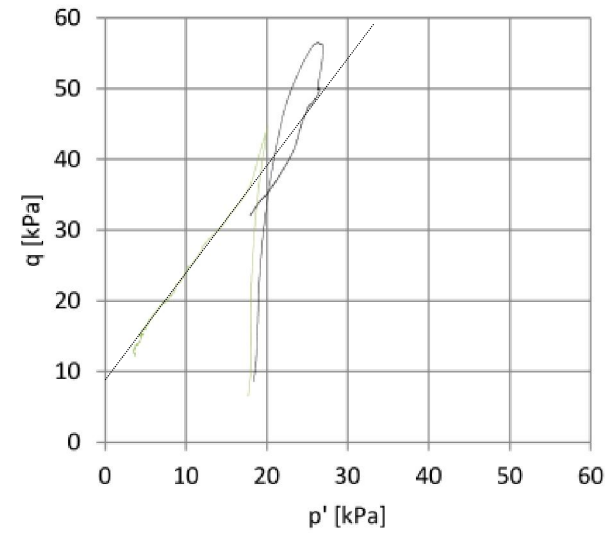


Dragvoll Bore Hole 2

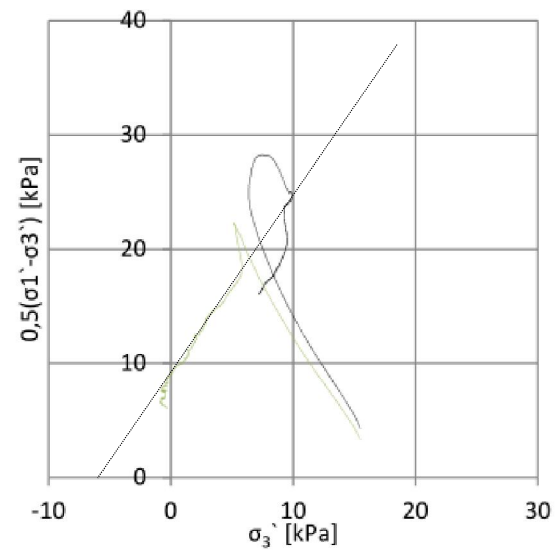
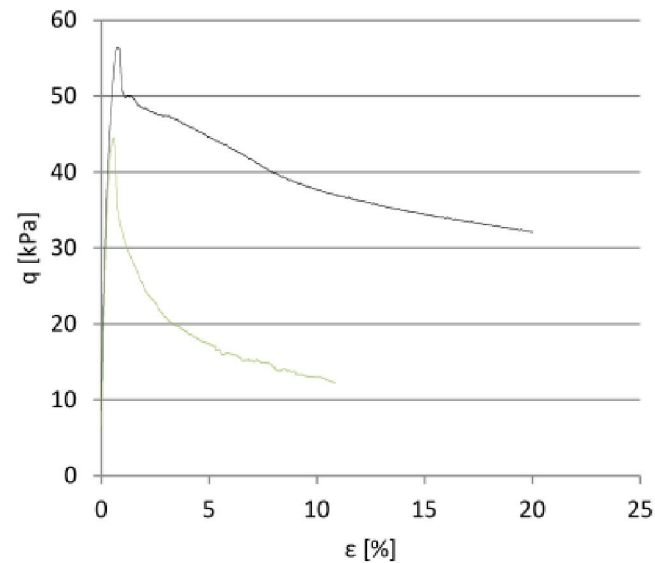
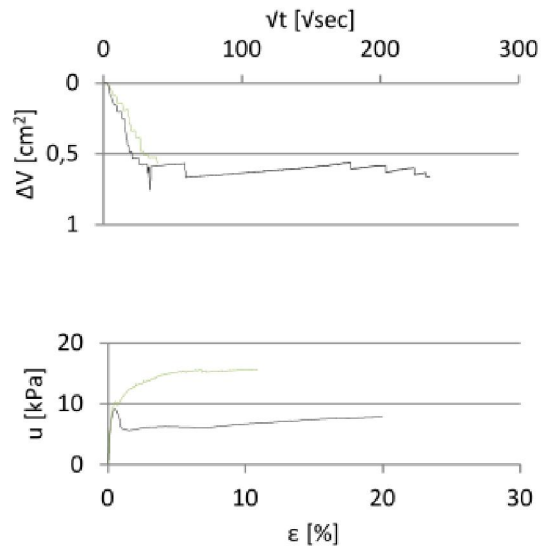
Mini Block specimen D 3,0-3,25m

Triax depth: 3,17 m

P1	P2
p' ₀ - Consolidated	p' ₀ - Consolidated
Test date: 16.10.2013	Test date: 16.10.2013
σ' _{vo} = 22,5 kPa	σ' _{vo} = 22,5 kPa
w = 45,6 %	w = --
γ = 17,45 kN/m ²	γ = 17,24 kN/m ²
ΔV = 0,59 cm ³	ΔV = 0,52 cm ³
ε _f = 0,67 %	ε _f = 0,7 %
S _u = 28,19 kPa	S _u = 21,6 kPa
φ = --	Tan φ = 0,73
a = --	a = 5,8 kPa
D = +0,03	D = +0,04



— P1 — P2

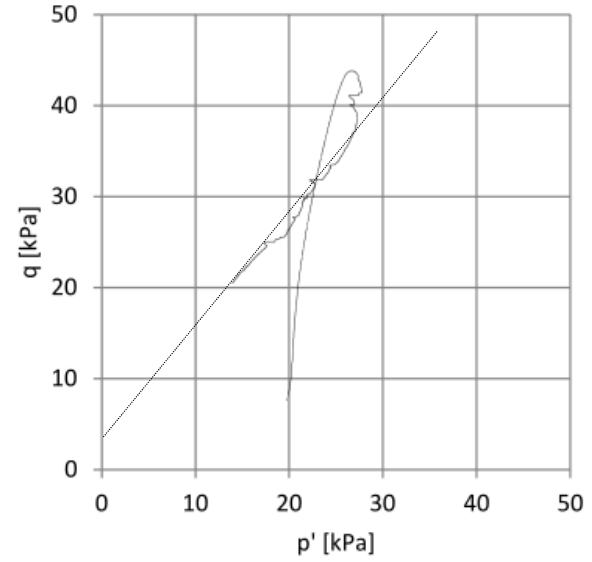


Dragvoll Bore Hole 2

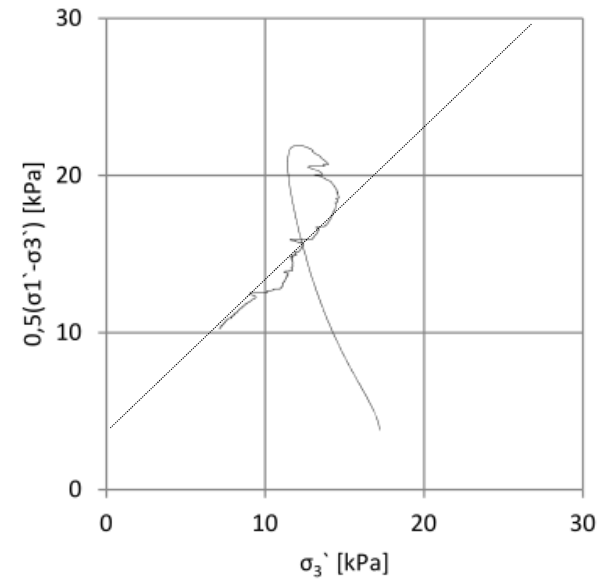
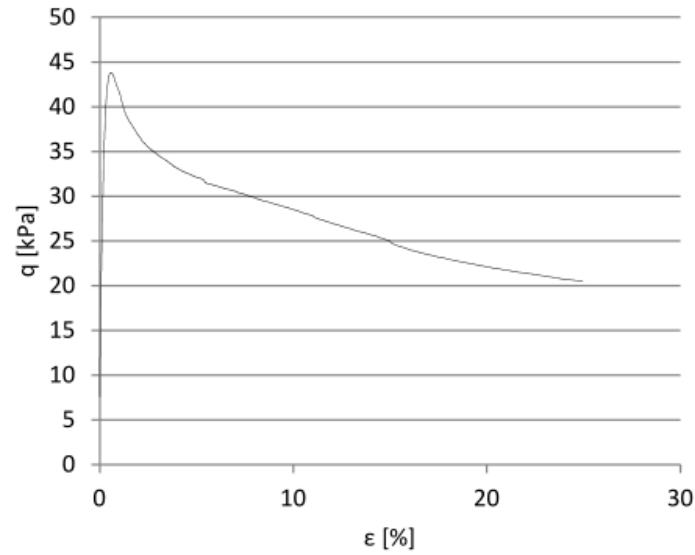
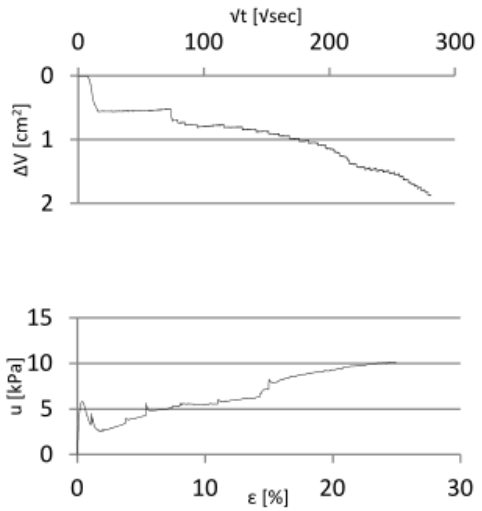
Mini Block specimen D 3,25-3,50m

Triax depth: 3,378 m

p'_0 - Consolidated
 Test date: 14.11.2013
 σ'_{vo} = 23,6 kPa
 w = --
 γ = --
 ΔV = 0,80 cm³
 ϵ_f = 0,66 %
 S_u = 21,88 kPa
 $\tan \phi$ = 0,58
 a = 2,8 kPa
 D = +0,09



— P1

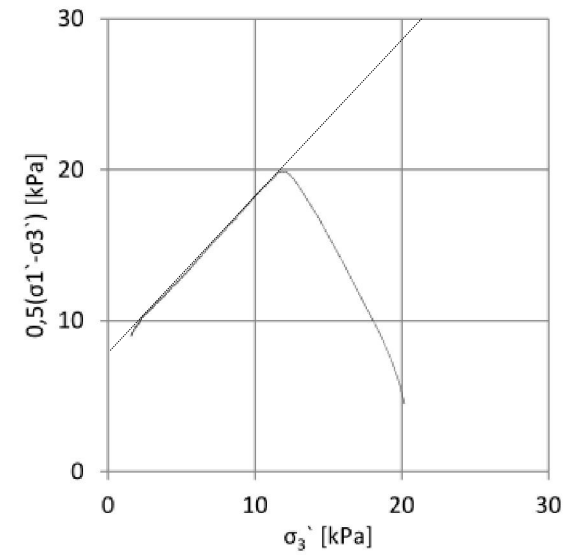
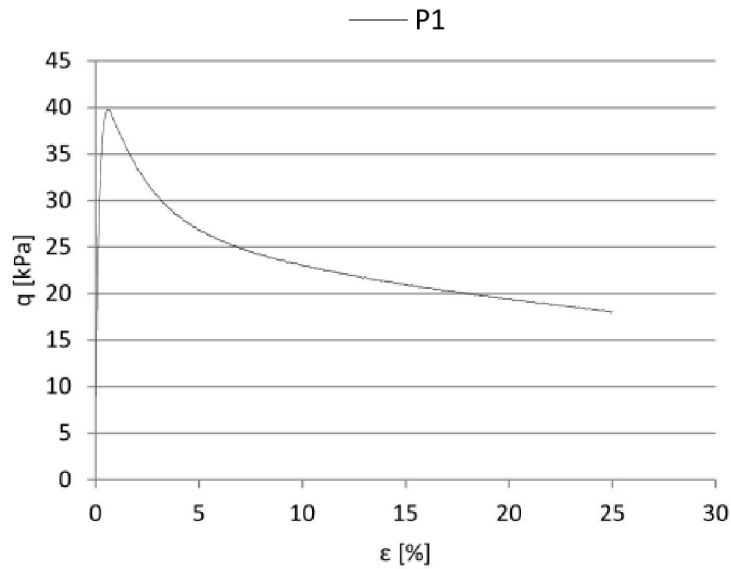
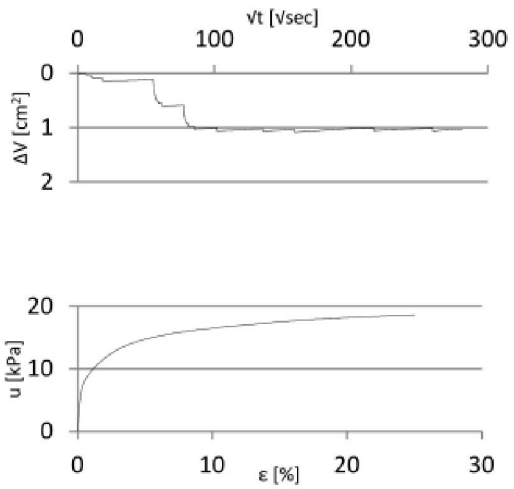
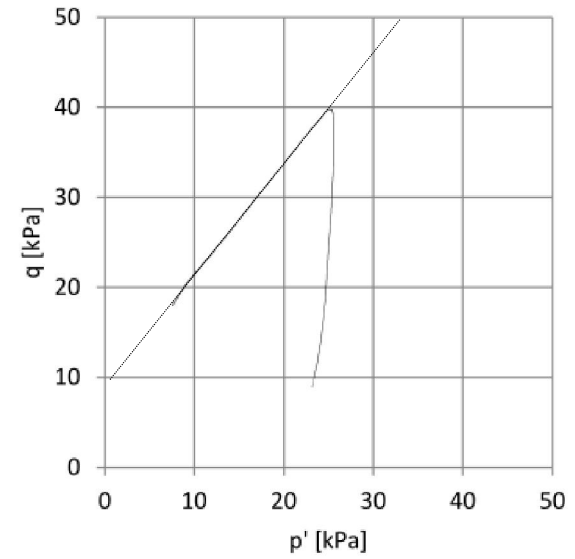


Dragvoll Bore Hole 2

Mini Block specimen D 4,0-4,25m

Triax depth: 4,172 m

p'_0 - Consolidated
 Test date: 18.11.2013
 σ'_{vo} = 29,19 kPa
 w = 38,4 %
 γ = 17,2 kN/m²
 ΔV = 1,03 cm³
 ϵ_f = 0,46 %
 S_u = 19,81 kPa
 $\tan \phi$ = 0,61
 a = 7,2 kPa
 D = +0,18



Dragvoll Bore Hole 2

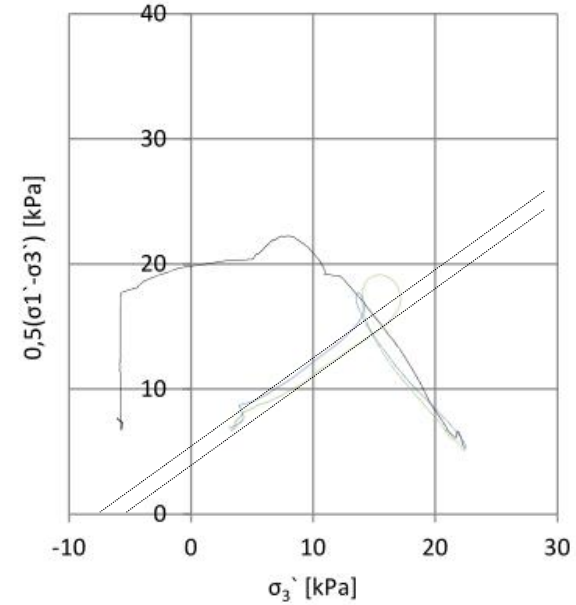
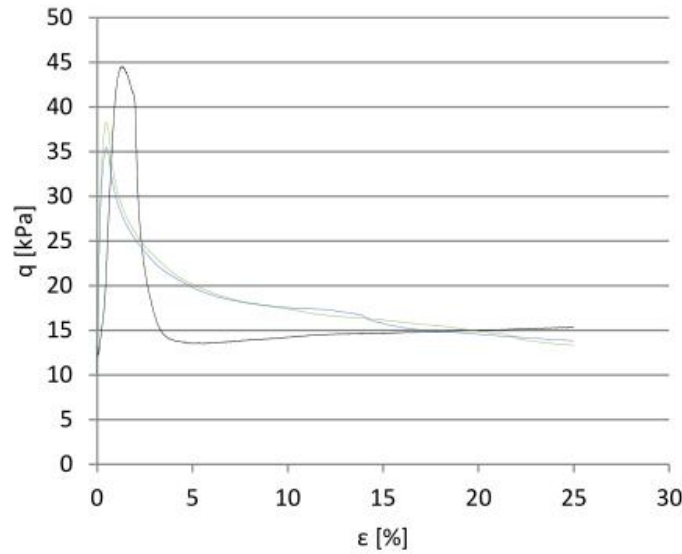
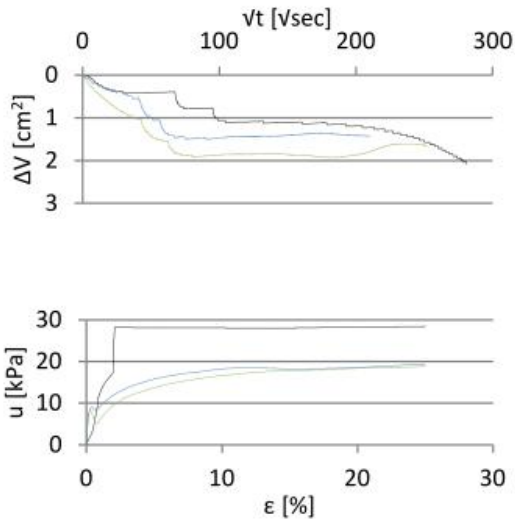
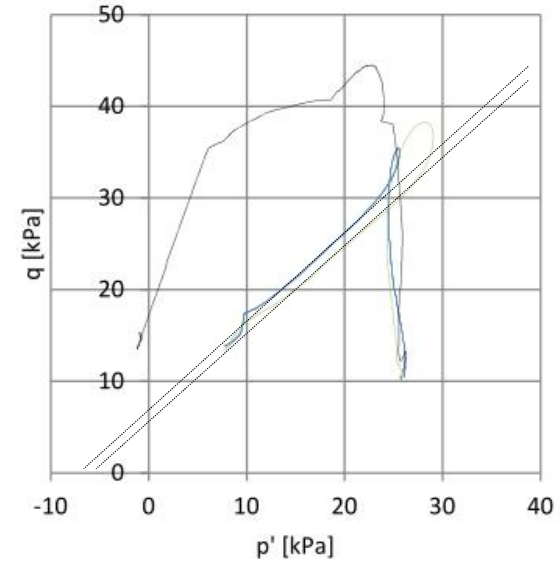
Mini Block specimen D 4,50-4,75m

Triax depth: 4,663 m

P1	P2	P3
$p'_{o'}$ - Consolidated	$p'_{o'}$ - Consolidated	$p'_{o'}$ - Consolidated
Test date: 25.11.2013	Test date: 29.11.2013	Test date: 1.12.2013
σ'_{vo} = 32,6 kPa	σ'_{vo} = 32,6 kPa	σ'_{vo} = 32,6 kPa
w = 41,8 %	w = 41,1 %	w = 41,4 %
γ = 18,66 kN/m ²	γ = 17,48 kN/m ²	γ = 18,68 kN/m ²
ΔV = 1,14 cm ³	ΔV = 1,91 cm ³	ΔV = 1,48 cm ³
ϵ_f = 1,27 %	ϵ_f = 0,38 %	ϵ_f = 0,37 %
S_u = --	S_u = 19,09 kPa	S_u = 17,00 kPa
Tan ϕ = --	Tan ϕ = 0,47	Tan ϕ = 0,47
a = --	a = 6,4 kPa	a = 8,2
		D = +0,01



— P1 — P2 — P3

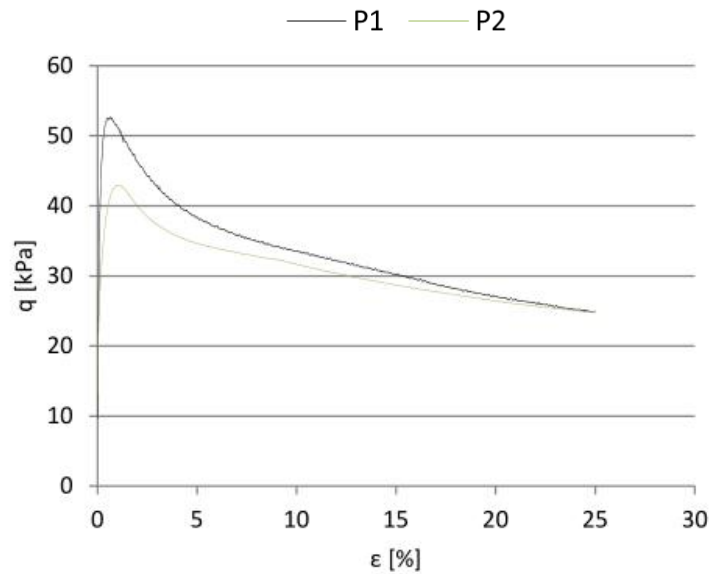
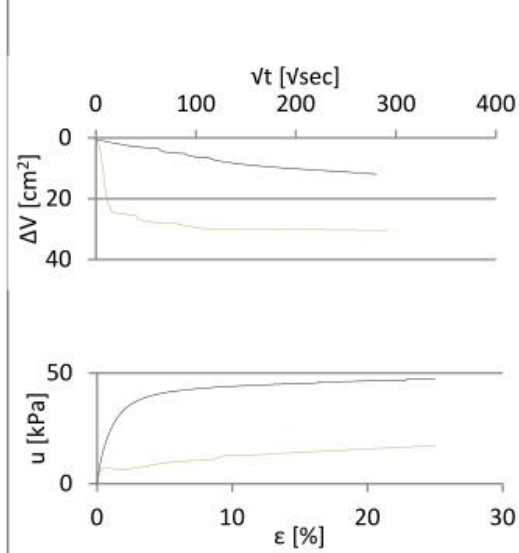
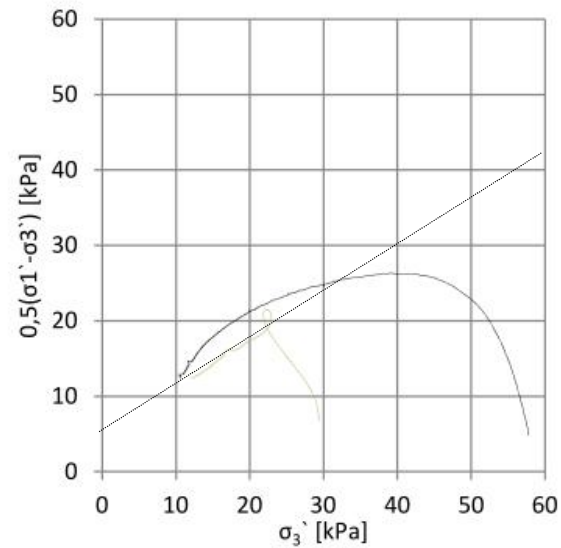
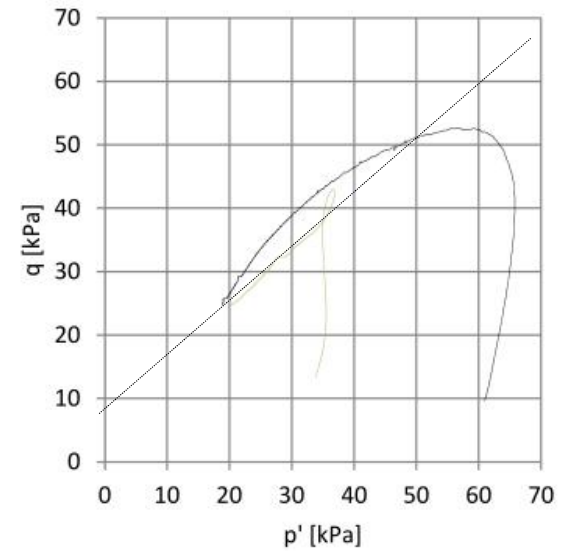
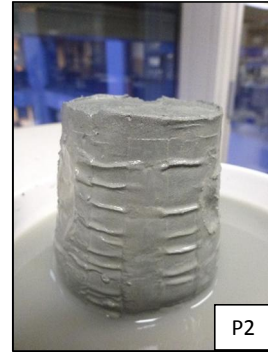


Dragvoll Bore Hole 2

Mini Block specimen D 8,45-8,70m

Triax depth: 8,468 m

P1	P2
p'_{o-} Consolidated	0,5 p'_{o-} Consolidated
Test date: 8.11.2013	Test date: 8.11.2013
σ'_{vo} = 59,3 kPa	σ'_{vo} = 59,3 kPa
w = 35,2 %	w = 35,3 %
γ = 19,37 kN/m ²	γ = 19,66 kN/m ²
ΔV = 11,6 cm ³	ΔV = 30,3 cm ³
ϵ_f = 0,21 %	ϵ_f = 0,77 %
S_u = 26,2 kPa	S_u = 21,0 kPa
ϕ = --	Tan ϕ = 0,43
a = --	a = 11,2 kPa
D = +0,22	D = +0,32

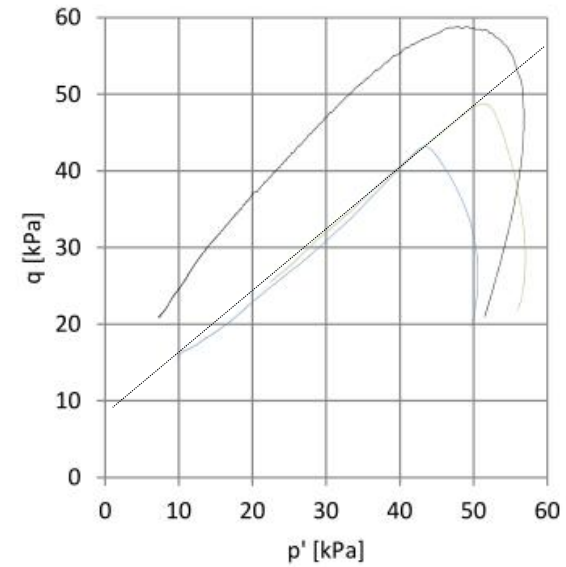


Dragvoll Bore Hole 2

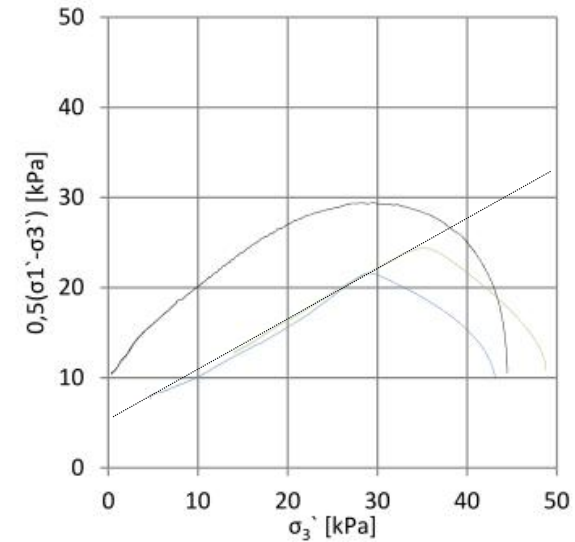
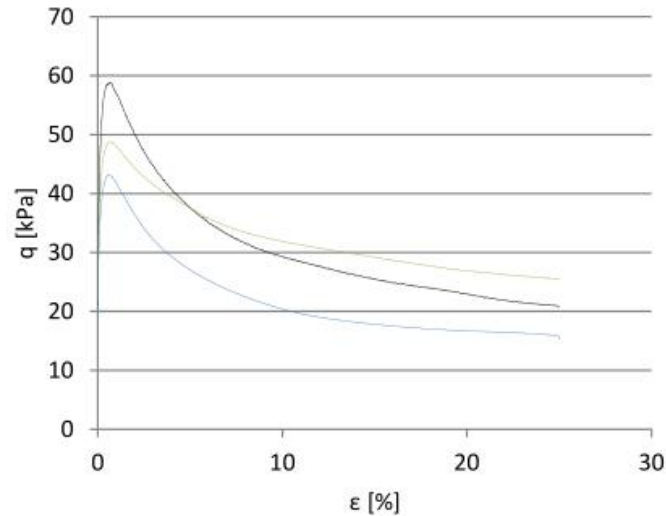
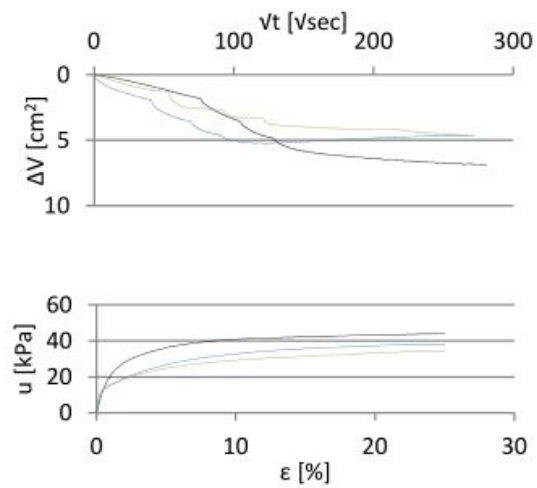
Mini Block specimen D 8,70-9,00m

Triax depth: 8,828 m

P1	P2	P3
1,1 p' ₀ - Consolidated	p' ₀ - Consolidated	p' ₀ - Consolidated
Test date: 25.11.2013	Test date: 12.11.2013	Test date: 7.12.2013
σ' _{vo} = 61,8 kPa	σ' _{vo} = 61,8 kPa	σ' _{vo} = 61,8 kPa
w = 33,1 %	w = 37,5 %	w = 38,1 %
γ = 19,5 kN/m ²	γ = 19,6 kN/m ²	γ = 19,46 kN/m ²
ΔV = 5,0 cm ³	ΔV = 4,0 cm ³	ΔV = 5,25 cm ³
ε _f = 0,44 %	ε _f = 0,44 %	ε _f = 0,4 %
S _u = 29,3	S _u = 24,2 kPa	S _u = 21,5 kPa
φ = --	Tan φ = 0,43	Tan φ = 0,43
a = --	a = 9,8 kPa	a = 9,8 kPa
D = +0,26	D = +0,23	D = +0,23



— P1 — P2 — P3



Appendix G

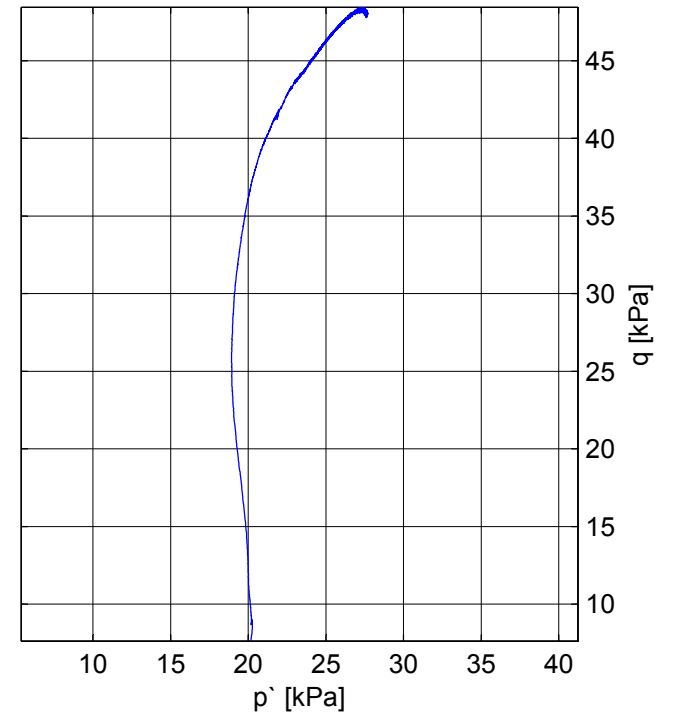
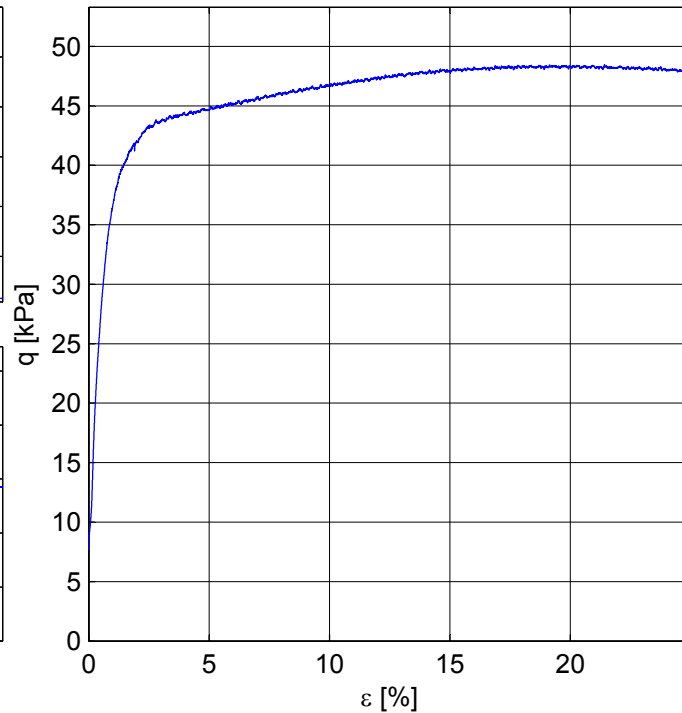
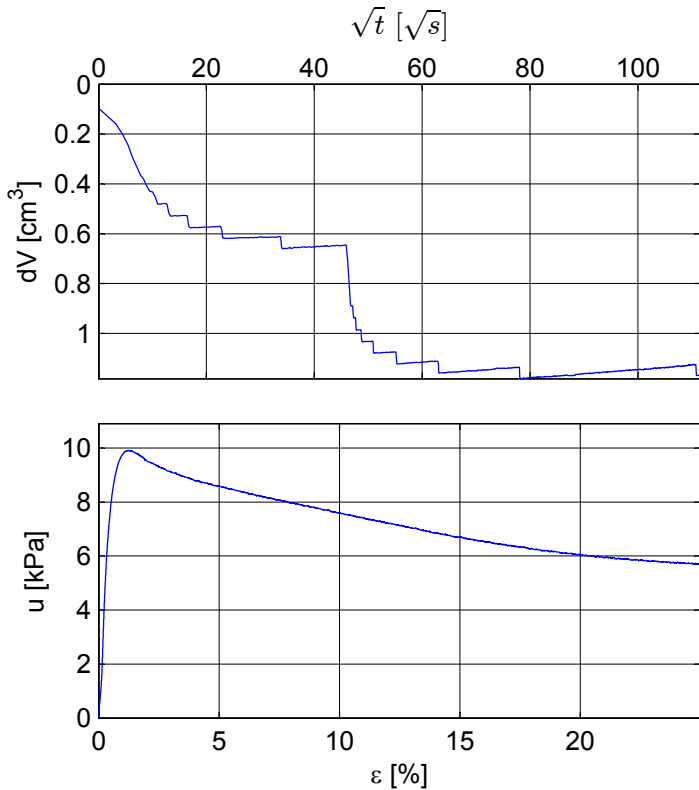
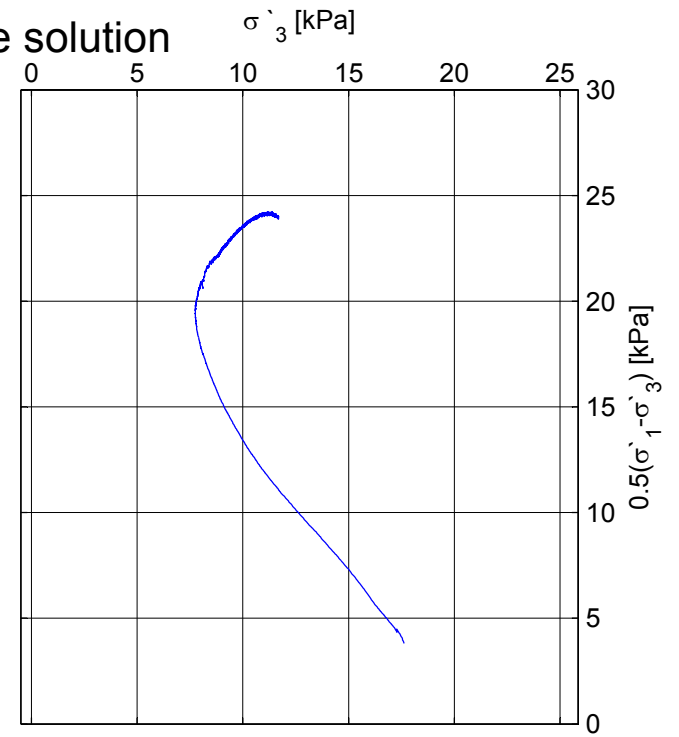
Triaxial test on samples stored in water and KCl solution

Treaxial test, Dragvoll bore hole 2. Stored in saturated potassium chloride solution

Mini Block sample D 3,5-3,75m

Depth: 3,690m
 Sampling date: 4.10.13
 Installed in storage cell: 4.12.13
 Opening date of block sample: 15.1.14
 Test date: 15.1.14
 strain rate: 1,5 %/hour
 p'_0 -consolidation

σ'_{vo}	= 25.83 kPa	σ'_c	= 90 kPa
w	= 34.26 %	OCR	= 3.72
γ	= 19.08 kN/m ³	D	= -0.08
ΔV	= 1.18 cm ³		
ε_v	= 0.51 %		
S_u	= 24.22 kPa		
ε_f	= 2.50 %		

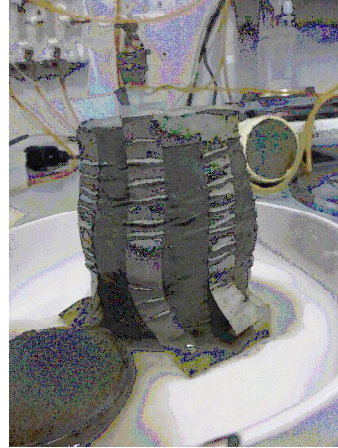


Treaxial test, Dragvoll bore hole 2. Stored in saturated potassium chloride solution

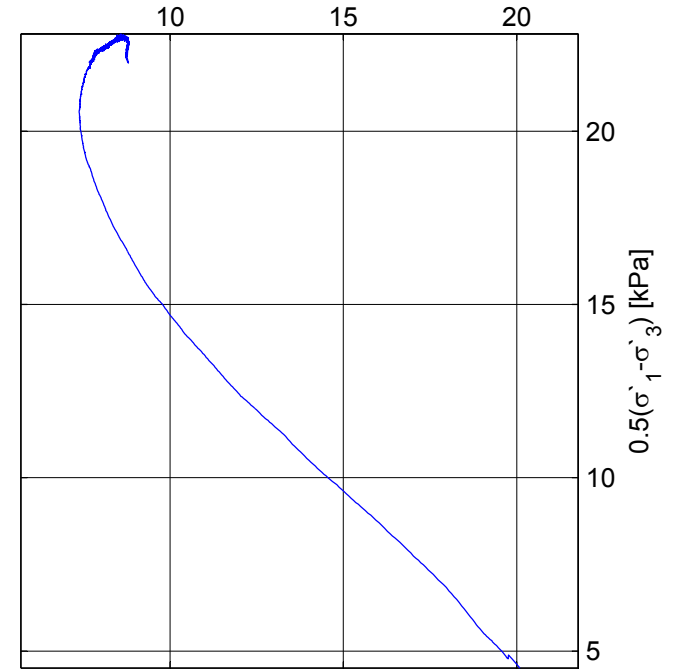
Mini Block sample D 3,5-3,75m

Depth: 3,690m
 Sampling date: 4.10.13
 Installed in storage cell: 4.12.13
 Opening date of block sample: 15.1.14
 Test date: 19.1.14
 strain rate: 1,5 %/hour
 1,1 σ'_0 -consolidation

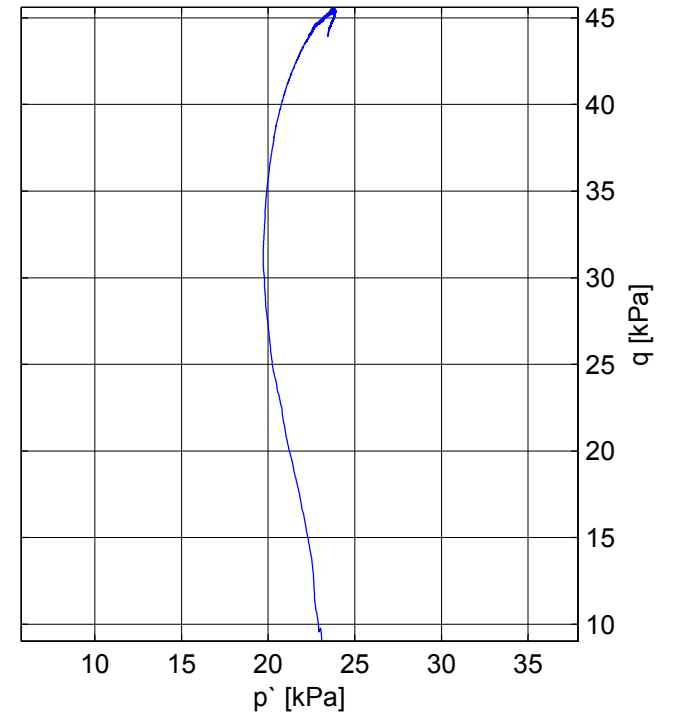
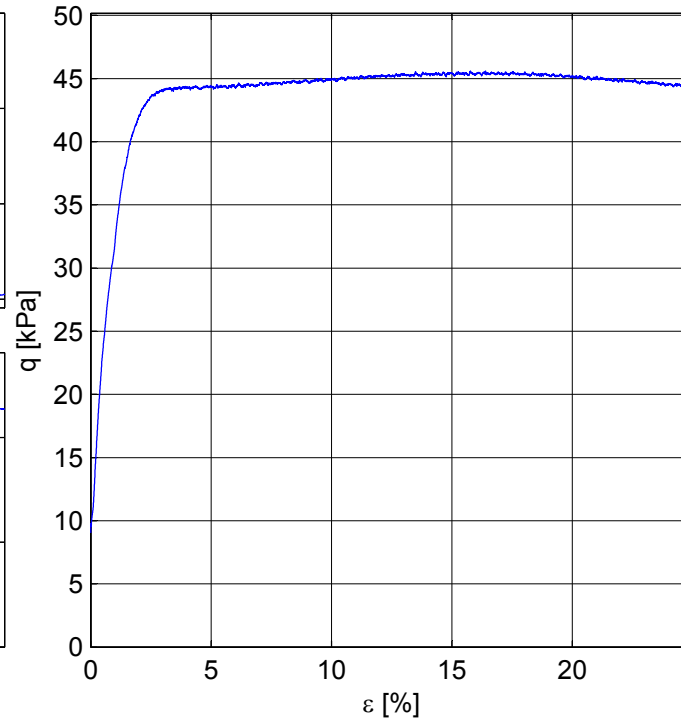
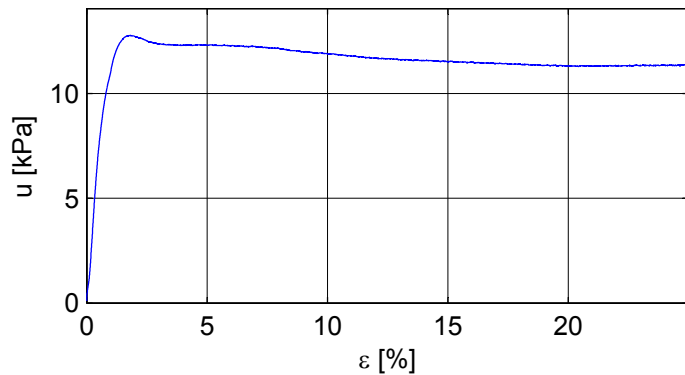
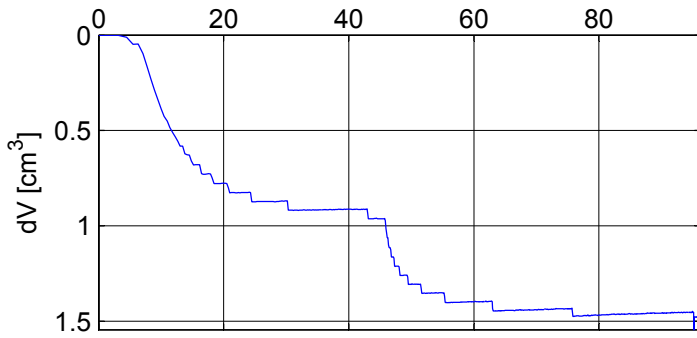
σ'_{vo}	= 25.83 kPa	σ'_c	= 90 kPa
w	= 33.48 %	OCR	= 3.72
γ	= 19.31 kN/m ³	D	= -0.34
ΔV	= 1.55 cm ³		
ϵ_v	= 0.67 %		
S_u	= 22.81 kPa		
ϵ_f	= 2.50 %		



σ'_3 [kPa]



\sqrt{t} [\sqrt{s}]



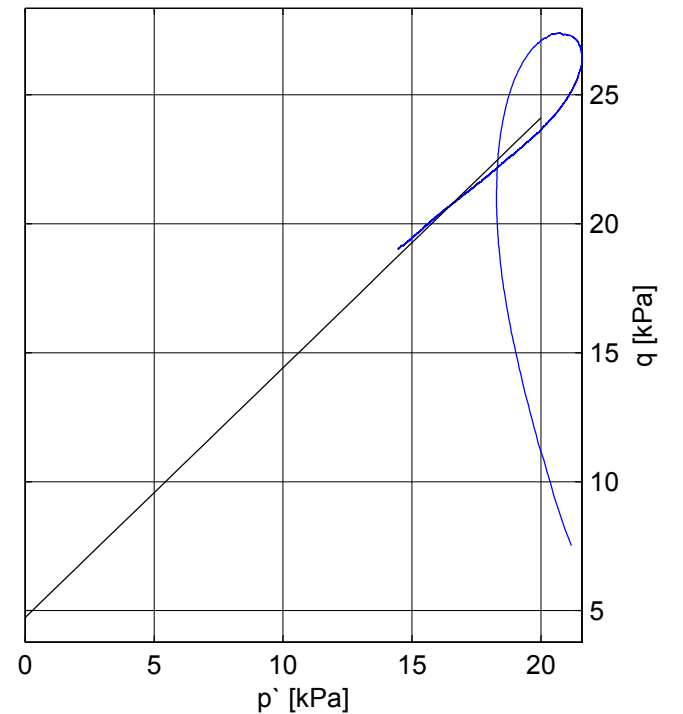
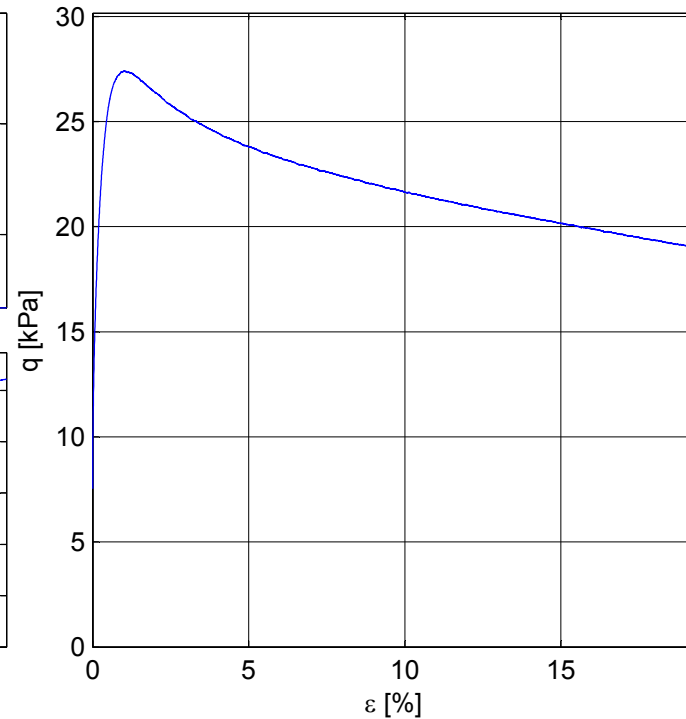
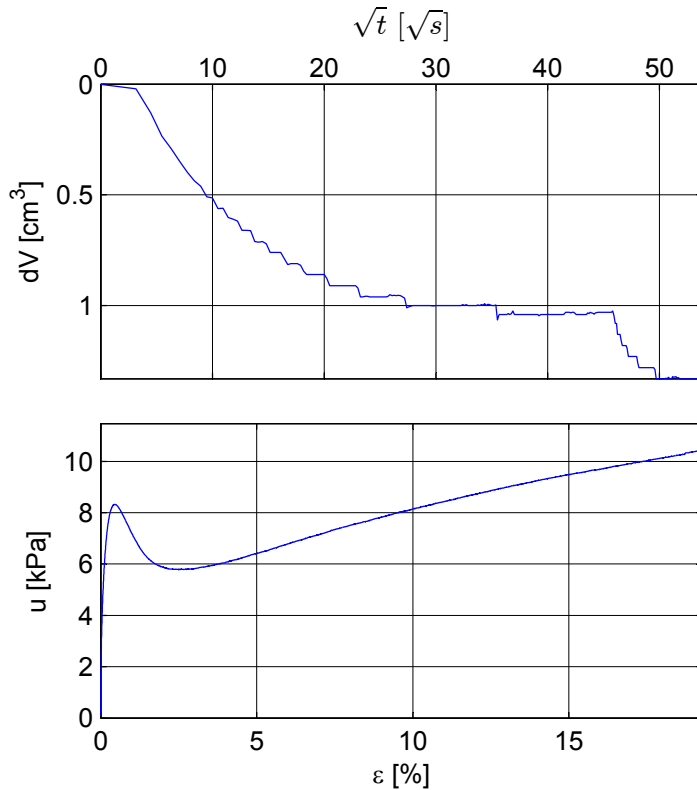
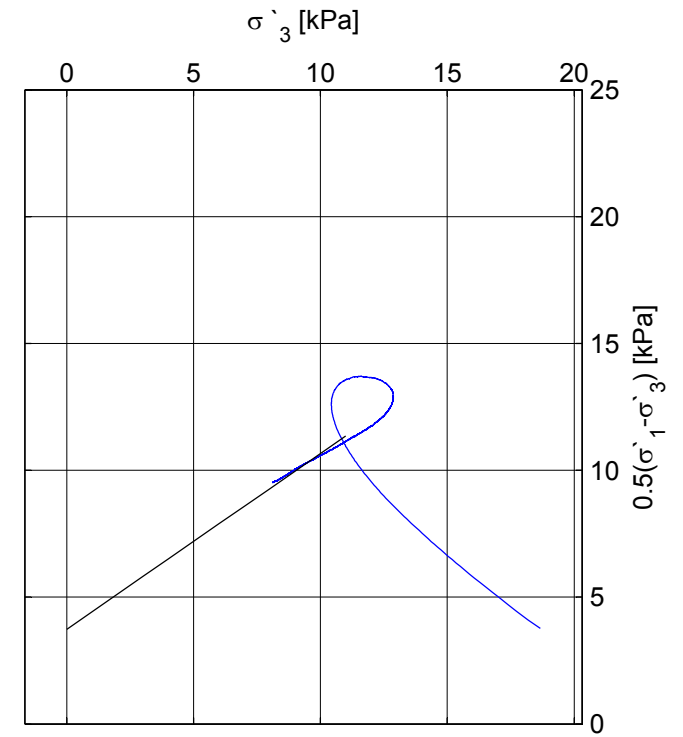
Treaxial test, Dragvoll bore hole 2. Stored in oxygen free distilled water

Mini Block sample D 3,75-4,0m

Depth: 3,922m
 Extraction date of specimen: ?
 Installed in water cell: 4.12.13
 Opening date of block sample: 20.1.14
 Test date: 20.1.14
 strain rate: 1,5 %/hour
 p'_0 -consolidation



σ'_{vo}	= 83.00 kPa	σ'_c	= 70 kPa
w	= 35.20 %	OCR	= 1.17
γ	= 19.37 kN/m ³	tan ϕ	= 0.45
ΔV	= 1.33 cm ³	ϕ	= 24.17 °
ε_v	= 0.57 %	a	= 5 kPa
S_u	= 13.71 kPa	D	= -0.32
ε_f	= 1.05 %	S_f	= 0.69
E_0	= 28.92 MPa	M_f	= 0.97



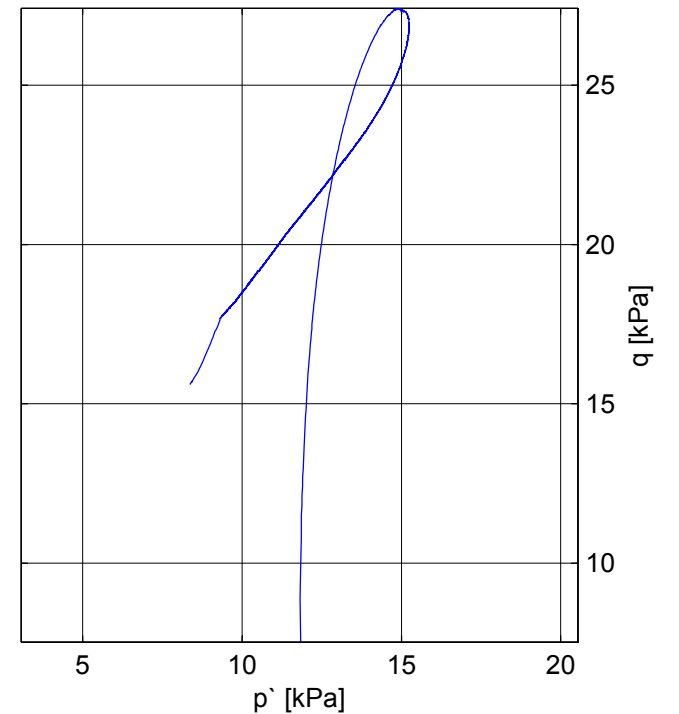
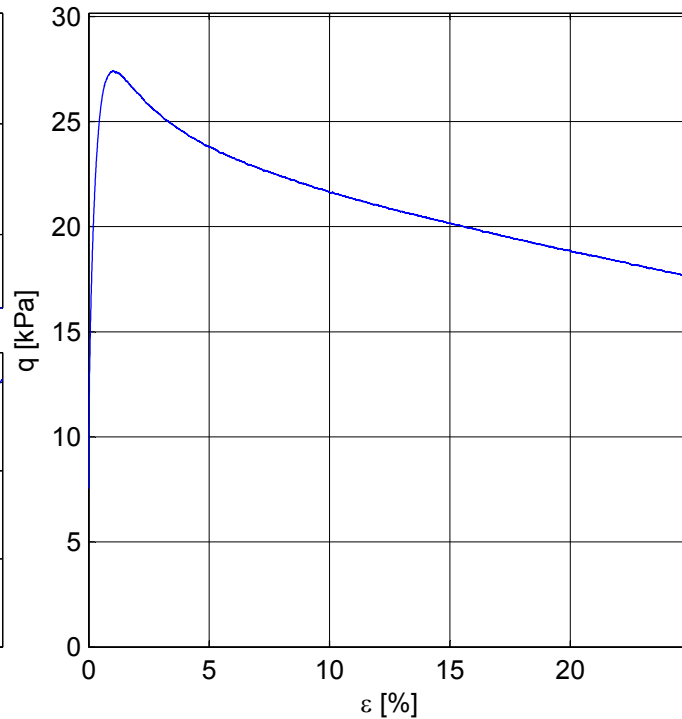
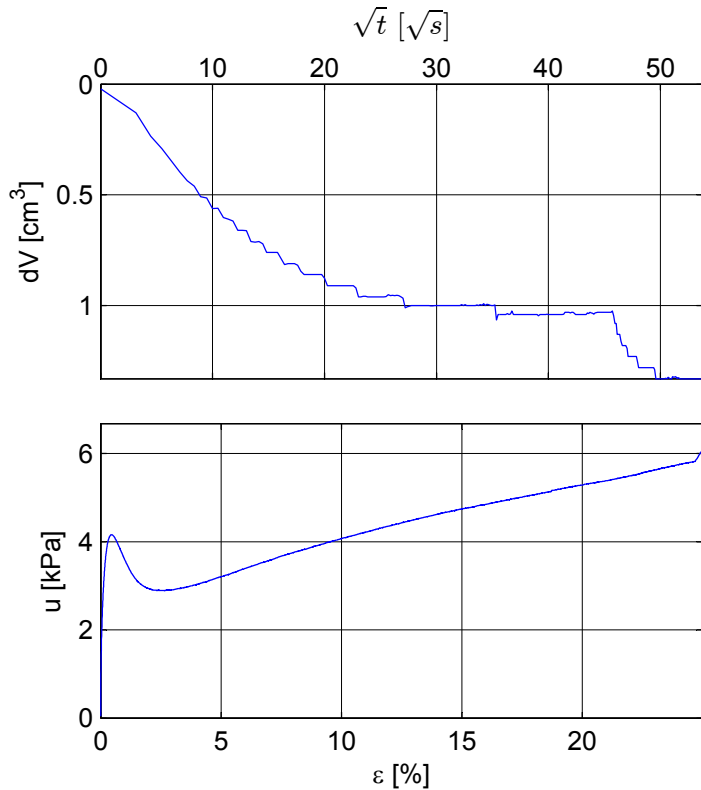
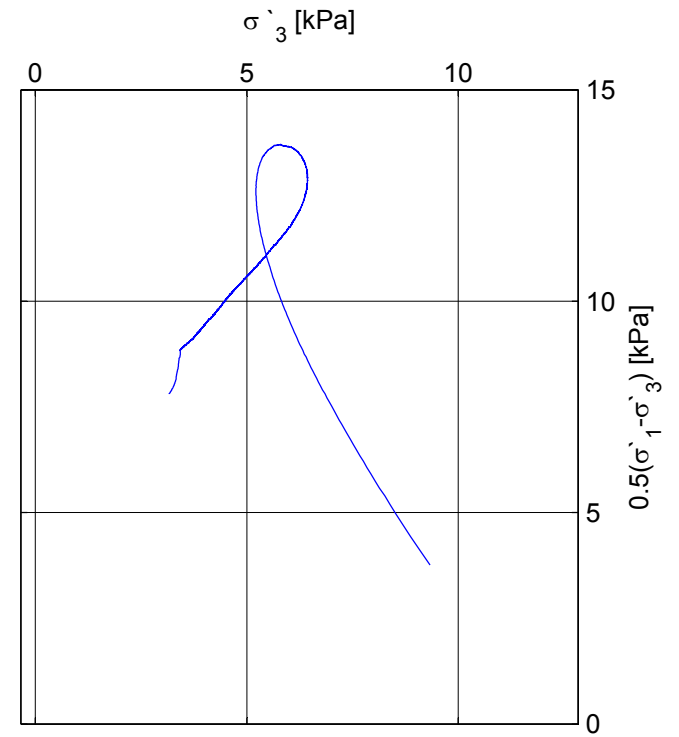
Treaxial test, Dragvoll bore hole 2. Stored in oxygen-free, distilled water

Mini Block sample D 3,75-4,0m

Depth: 3,922m
 Sampling date: 4.10.13
 Installed in storage cell: 4.12.13
 Opening date of block sample: 20.1.14
 Test date: 20.1.14
 strain rate: 1,5 %/hour
 p'_0 -consolidation
 Note: Equipment error.



σ'_{vo}	= 27.45 kPa	σ'_c	= 70 kPa
w	= 29.81 %	OCR	= 2.56
γ	= 18.19 kN/m ³	D	= 0.03
ΔV	= 1.33 cm ³		
ε_v	= 0.57 %		
S_u	= 13.71 kPa		
ε_f	= 1.05 %		

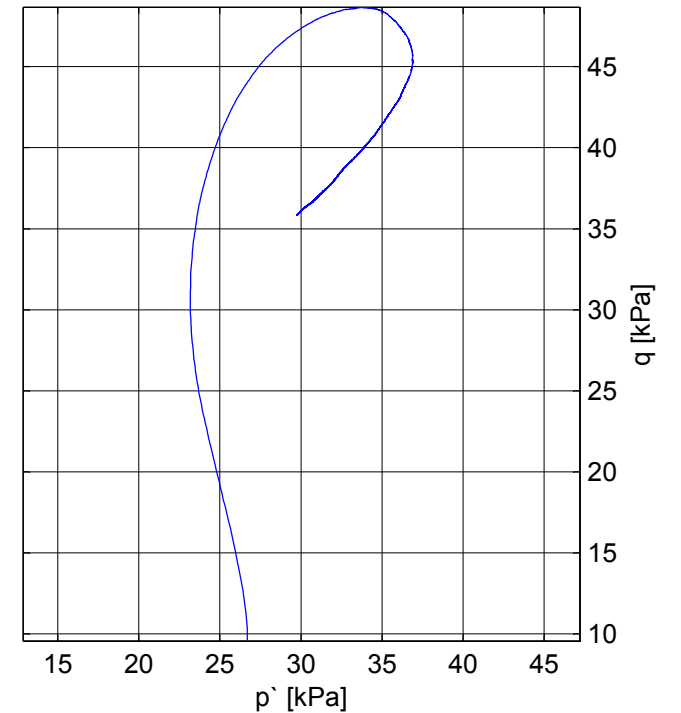
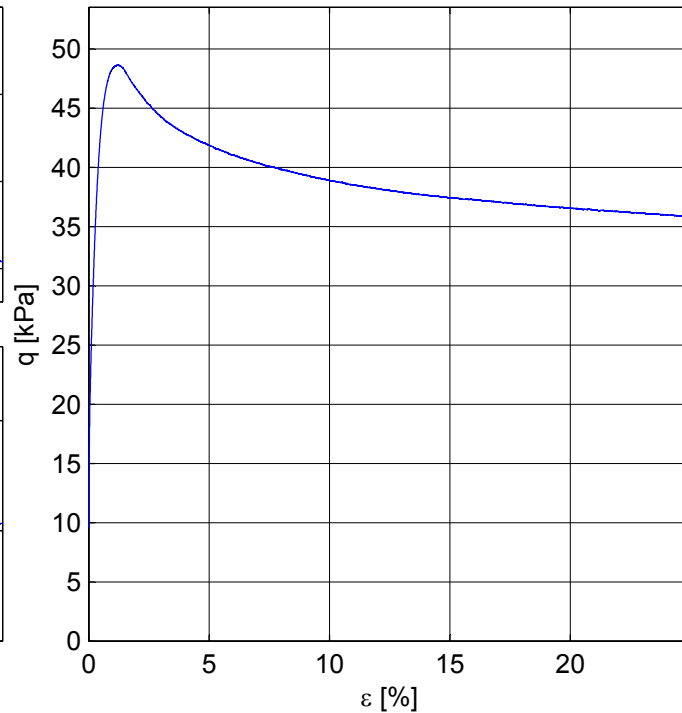
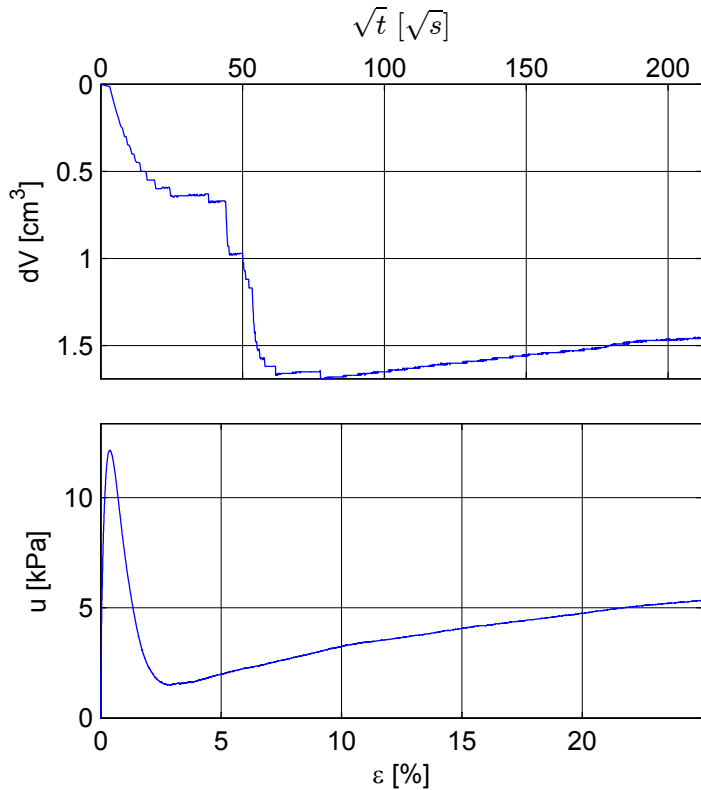
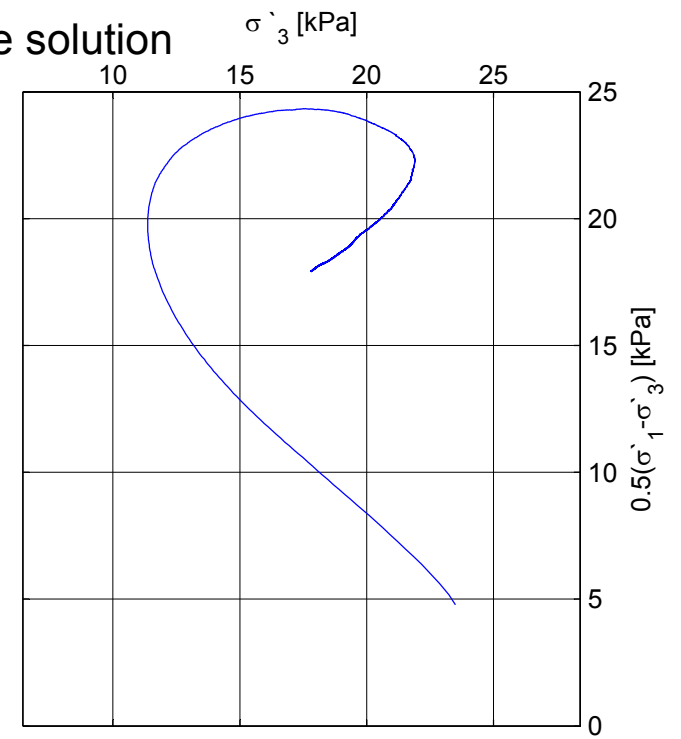


Treaxial test, Dragvoll bore hole 2. Stored in saturated potassium chloride solution

Mini Block sample D 4,25-4,5m

Depth: 4,35m
 Sampling date: 4.10.13
 Installed in storage cell: 4.12.13
 Opening date of block sample: 4.2.14
 Test date: 6.2.14
 strain rate: 1,5 %/hour
 1,1 ρ_0 -consolidation

σ'_{vo}	= 30.45 kPa	σ'_c	= 115 kPa
w	= - %	OCR	= 3.81
γ	= - kN/m ³	D	= -0.09
ΔV	= 1.69 cm ³		
ϵ_v	= 0.73 %		
S_u	= 24.33 kPa		
ϵ_f	= 1.20 %		

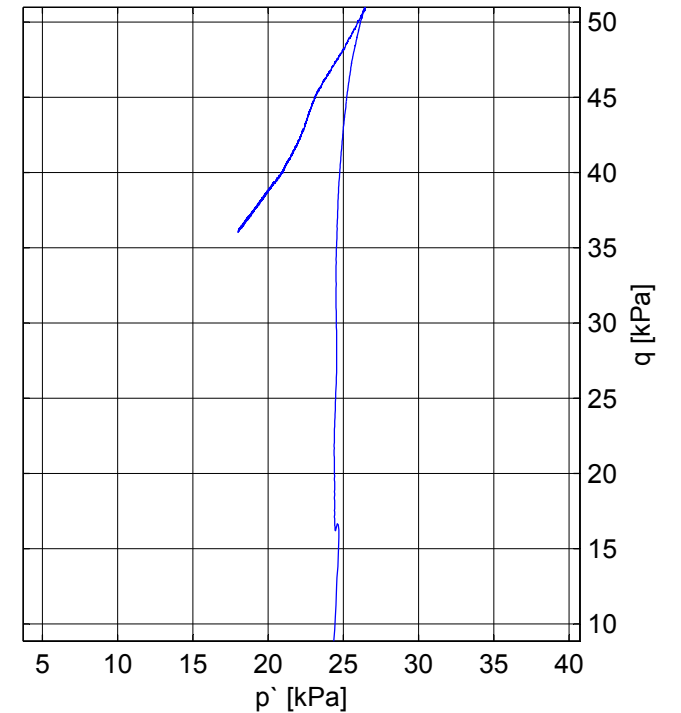
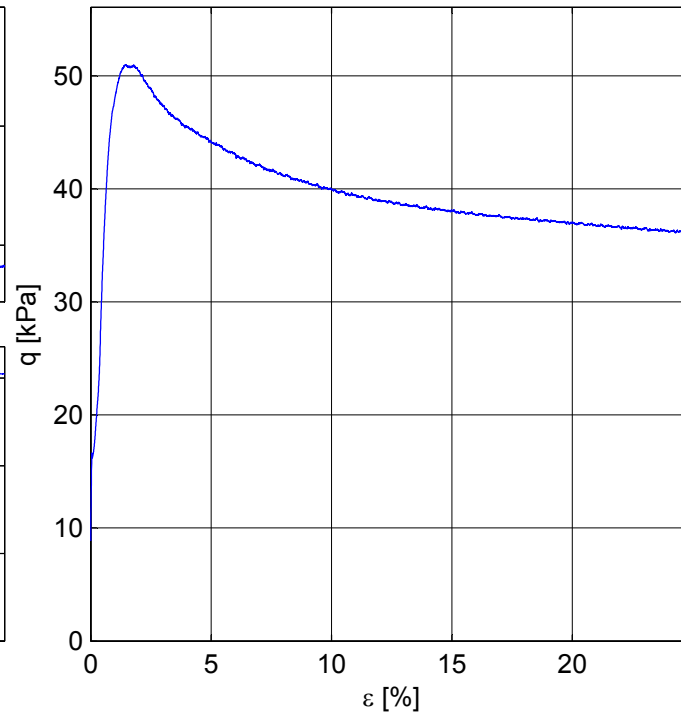
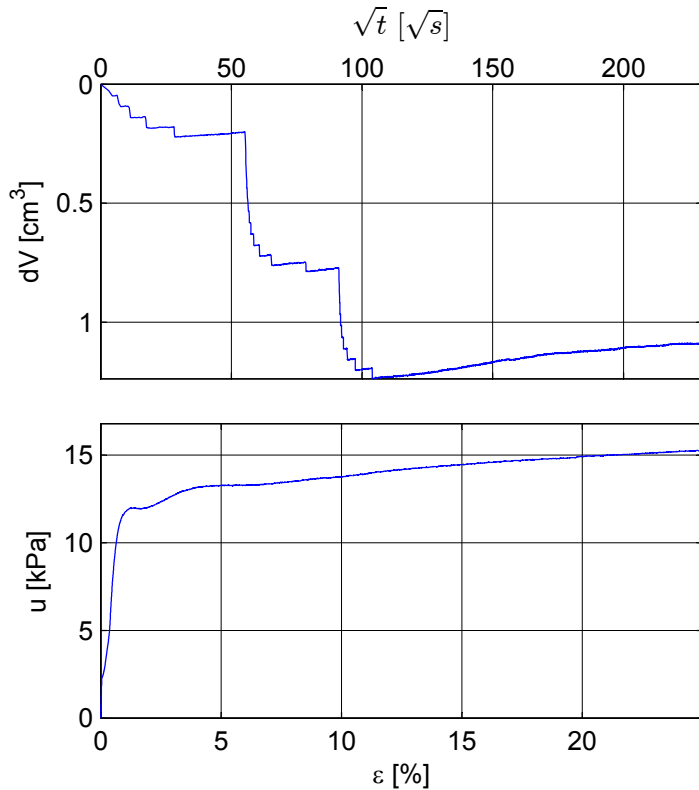
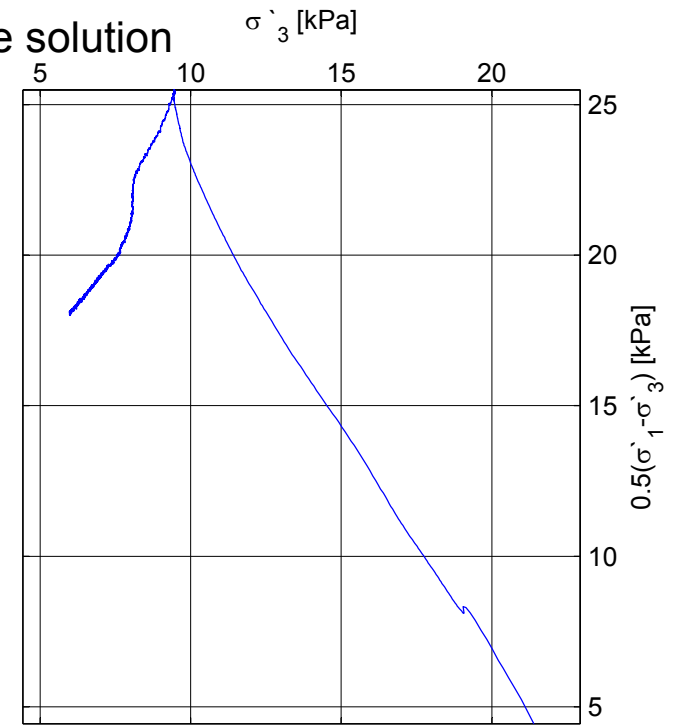


Treaxial test, Dragvoll bore hole 2. Stored in saturated potassium chloride solution

Mini Block sample D 4,25-4,5m

Depth: 4,35m
 Sampling date: 4.10.13
 Installed in storage cell: 4.12.13
 Opening date of block sample: 4.2.14
 Test date: 6.2.14
 strain rate: 1,5 %/hour
 p'_0 -consolidation

σ'_{vo}	= 30.45 kPa	σ'_c	= 115 kPa
w	= 35.87 %	OCR	= 3.81
γ	= 18.92 kN/m ³	D	= 0.05
ΔV	= 1.24 cm ³		
ϵ_v	= 0.53 %		
S_u	= 25.49 kPa		
ϵ_f	= 1.47 %		

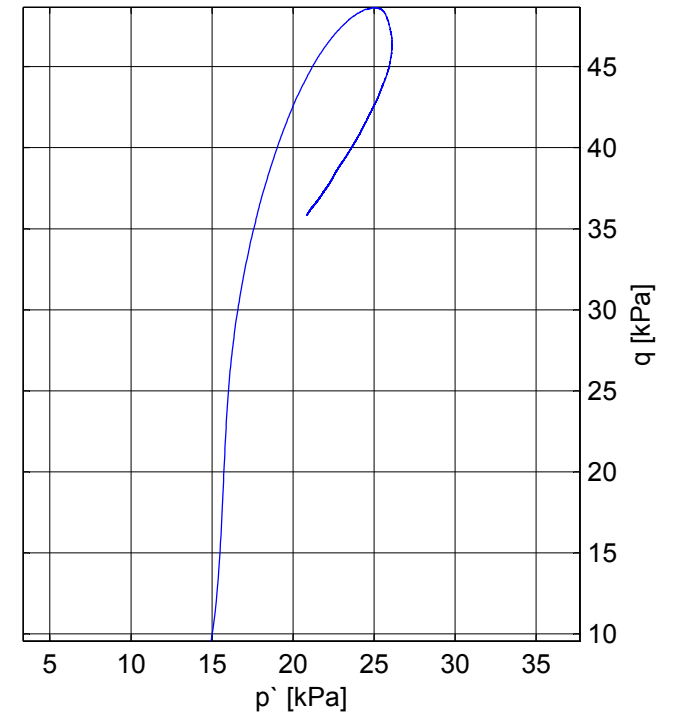
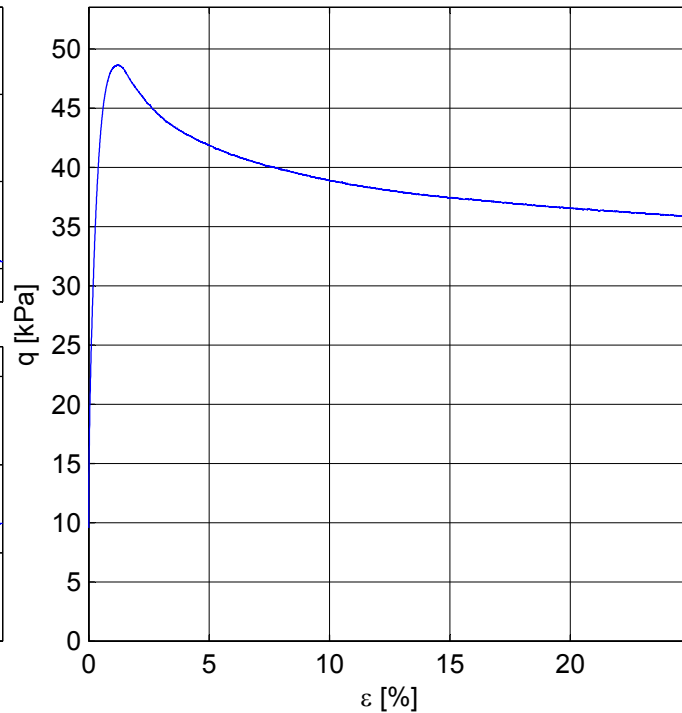
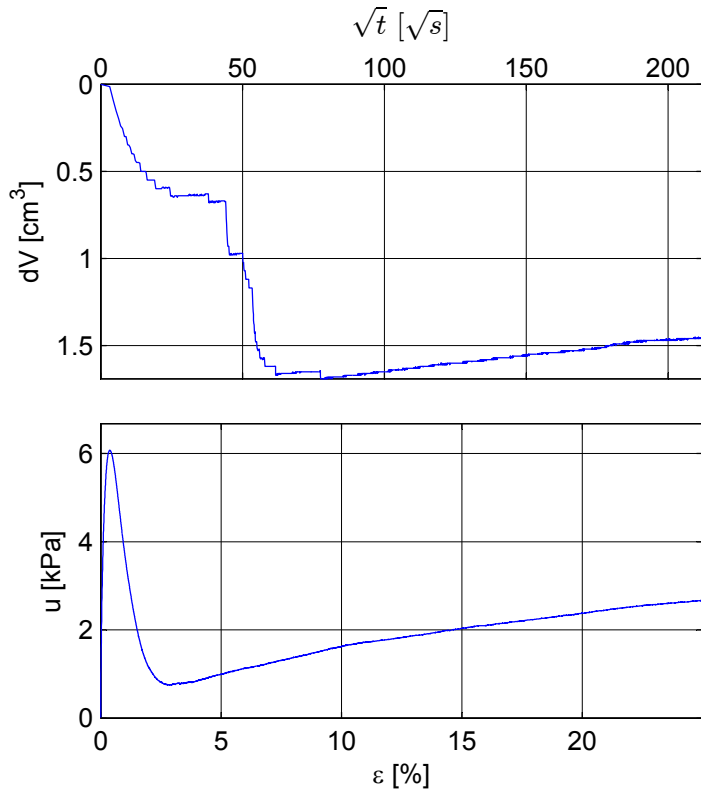
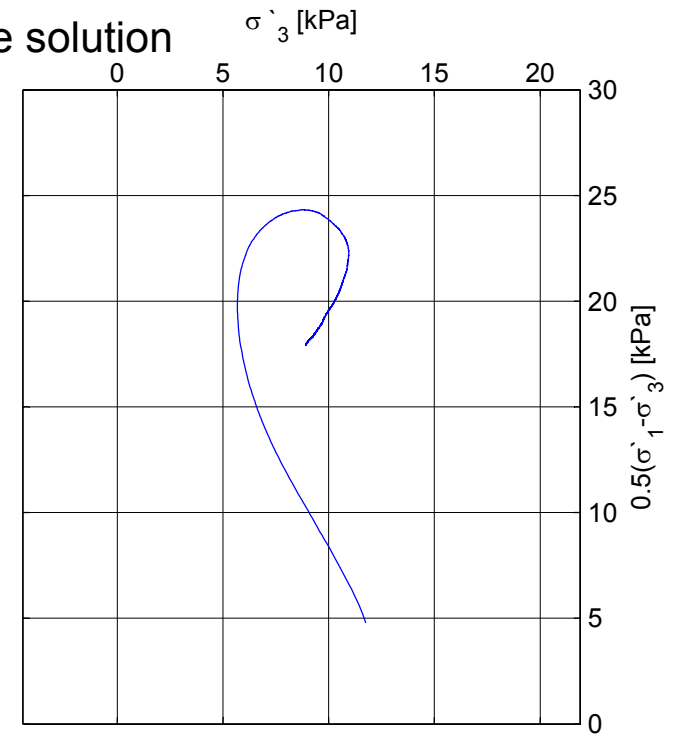


Treaxial test, Dragvoll bore hole 2. Stored in saturated potassium chloride solution

Mini Block sample D 4,25-4,5m

Depth: 4,35m
 Sampling date: 4.10.13
 Installed in storage cell: 4.12.13
 Opening date of block sample: 4.2.14
 Test date: 6.2.14
 strain rate: 1,5 %/hour
 1,1p₀-consolidation
 Note: Equipment error.

σ'_{vo}	= 30.45 kPa	σ'_c	= 115 kPa
w	= - %	OCR	= 3.81
γ	= - kN/m ³	D	= 0.07
ΔV	= 1.69 cm ³		
ϵ_v	= 0.73 %		
S_u	= 24.33 kPa		
ϵ_f	= 1.20 %		

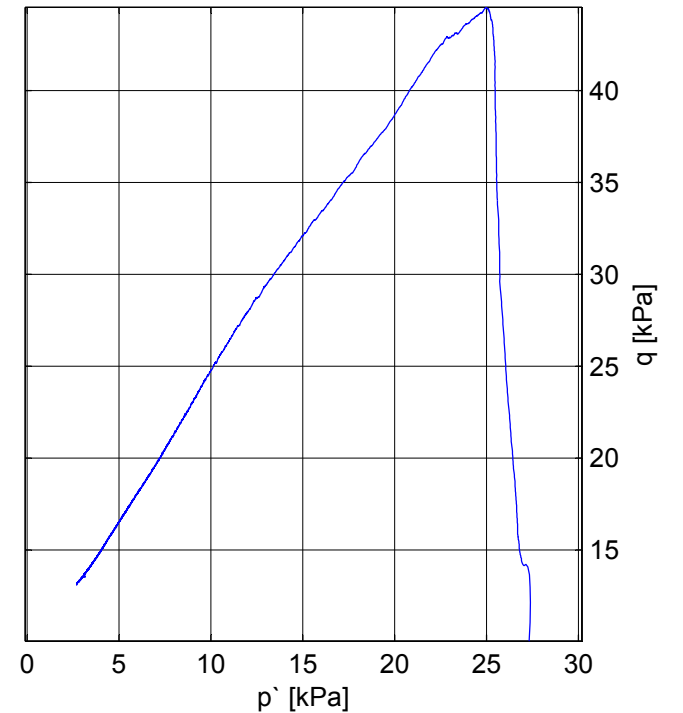
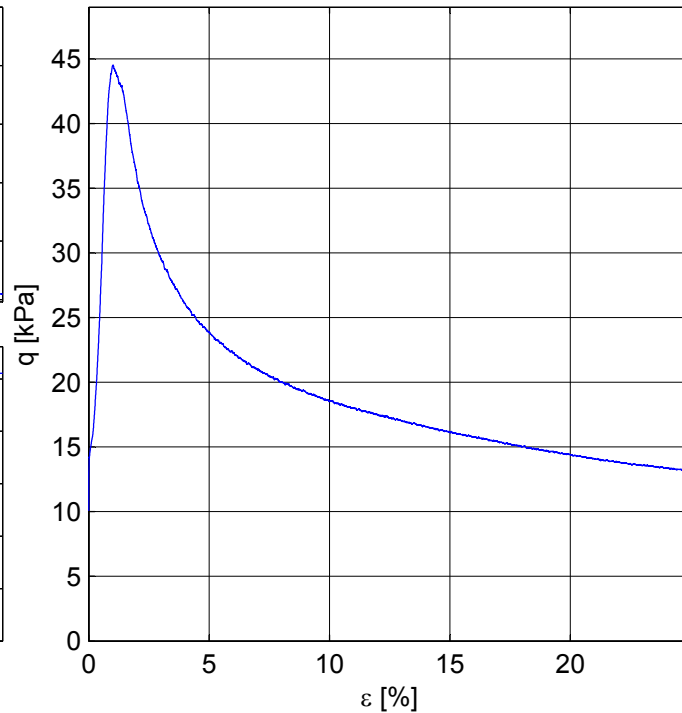
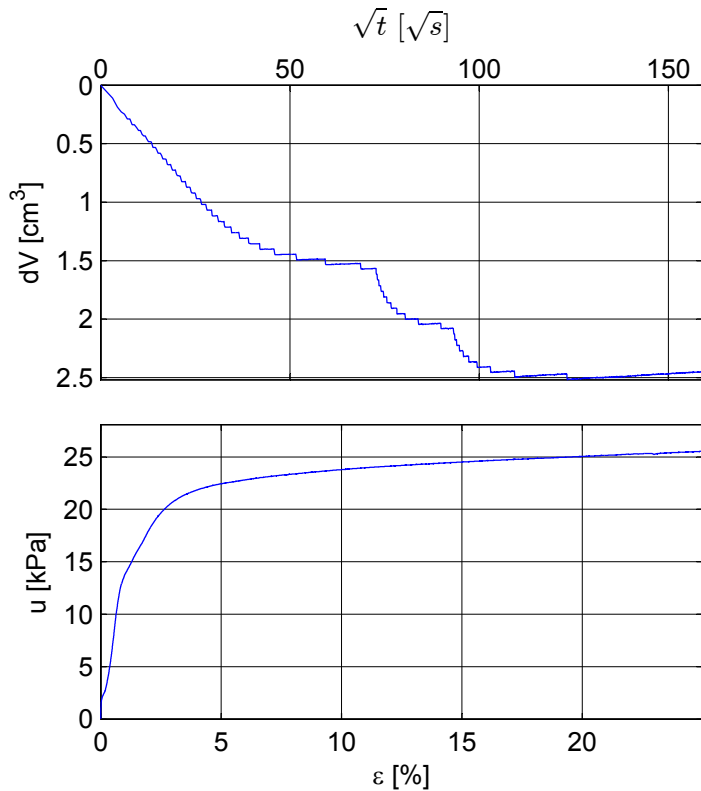
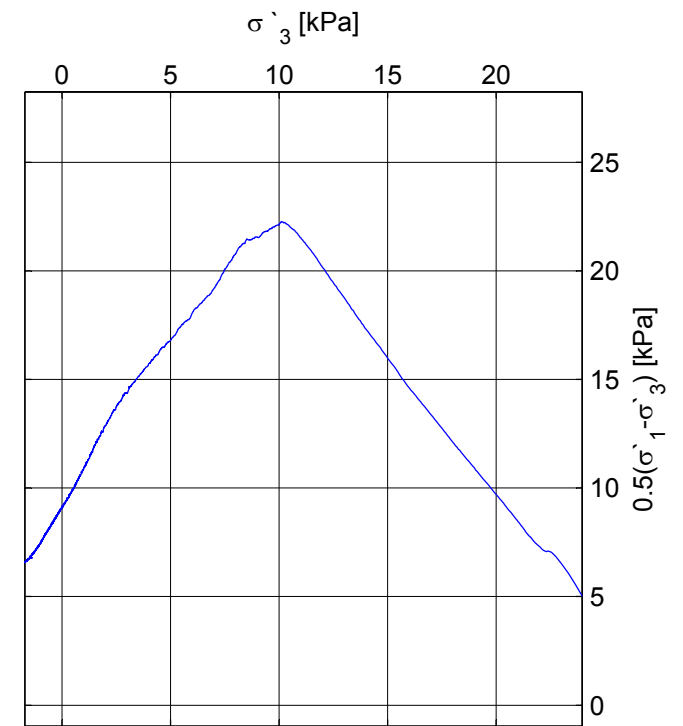


Treaxial test, Dragvoll bore hole 2. Stored in oxygen-free, distilled water

Mini Block sample D 4,75-5,0m

Depth: 4,895m
 Sampling date: 24.10.13
 Installed in storage cell: 4.12.13
 Opening date of block sample: 10.2.14
 Test date: 12.2.14
 strain rate: 1,5 %/hour
 p'_0 -consolidation

σ'_{vo}	= 34.27 kPa	σ'_c	= 80 kPa
w	= 39.64 %	OCR	= 2.45
γ	= 18.75 kN/m ³	D	= 0.03
ΔV	= 2.52 cm ³		
ε_v	= 1.09 %		
S_u	= 22.27 kPa		
ε_f	= 1.02 %		



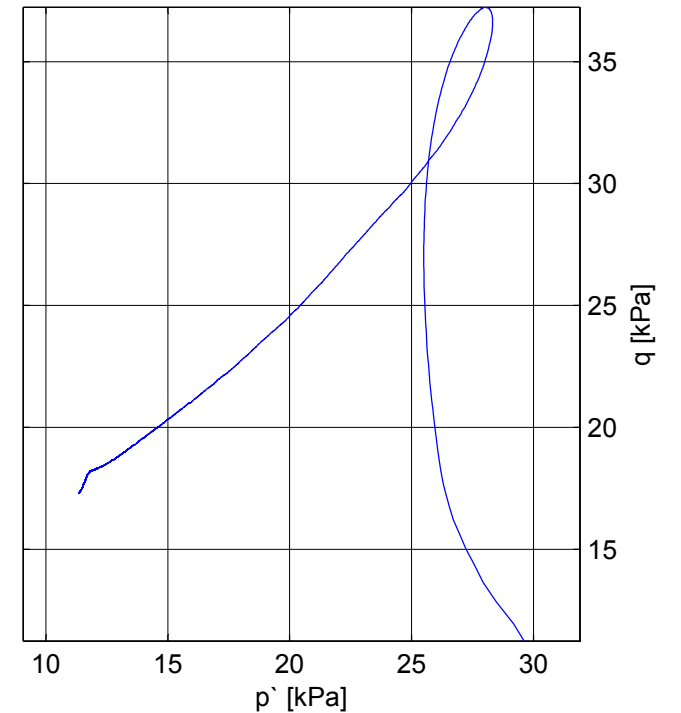
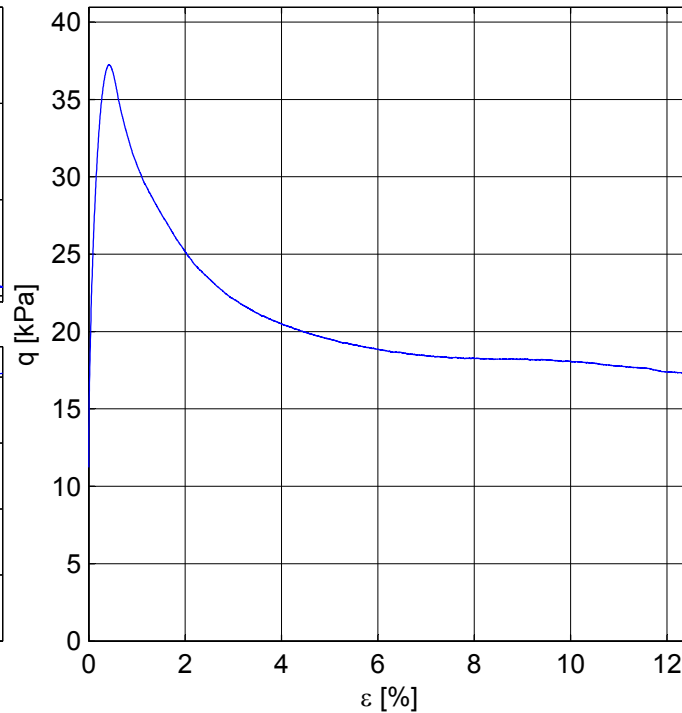
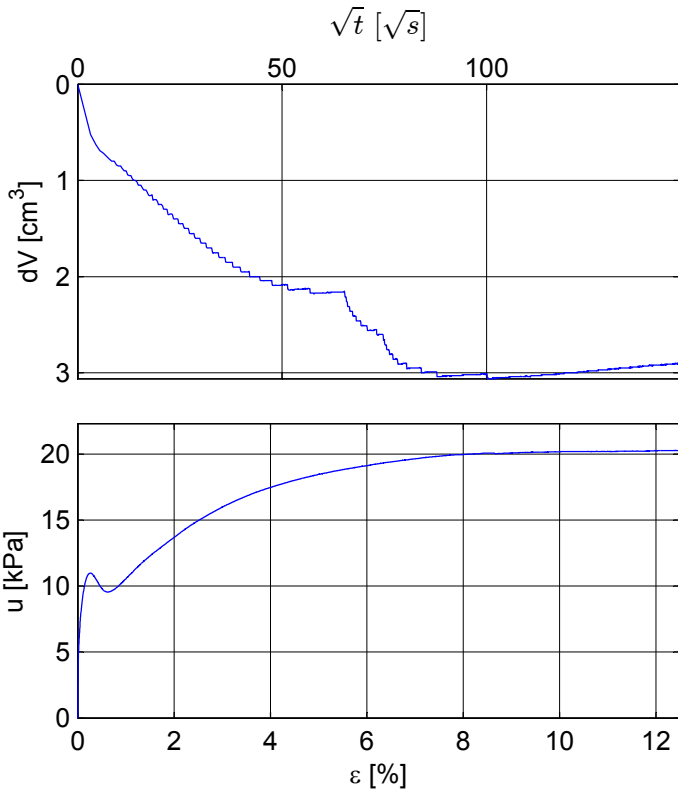
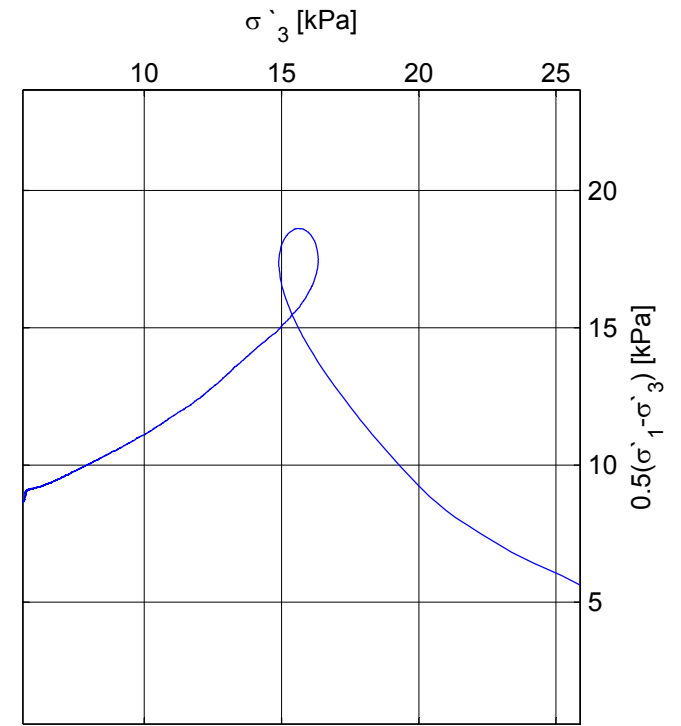
Treaxial test, Dragvoll bore hole 2. Stored in oxygen free distilled water

Mini Block sample D 4,75-5,0m

Depth: 4,895m
 Extraction date of specimen: 24.10.13
 Installed in water cell: 4.12.13
 Opening date of block sample: 10.2.14
 Test date: 12.2.14
 strain rate: 1,5 %/hour
 1,1p₀-consolidation test 2



σ'_{vo}	= 34.27 kPa	σ'_c	= 80 kPa
w	= 41.87 %	OCR	= 2.45
γ	= 18.96 kN/m ³	D	= -0.71
ΔV	= 3.06 cm ³		
ε_v	= 1.32 %		
S _u	= 18.62 kPa		
ε_f	= 0.43 %		



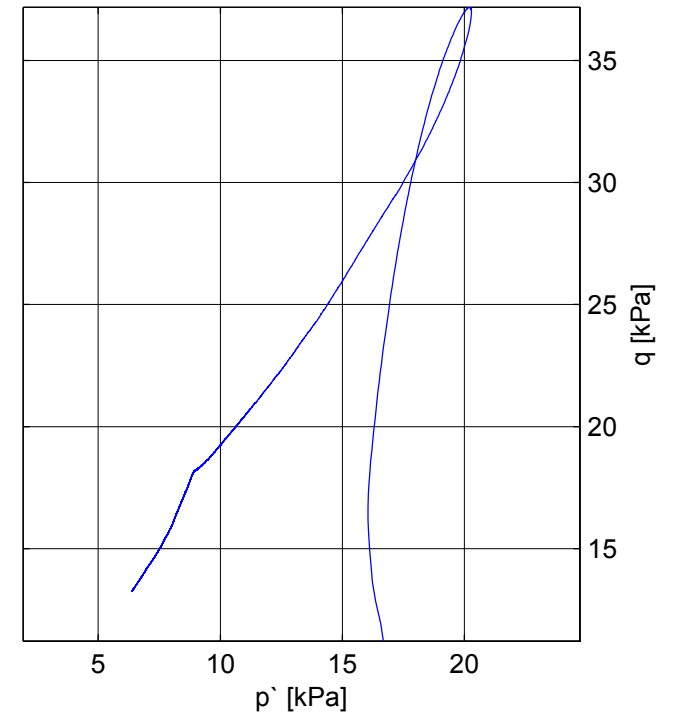
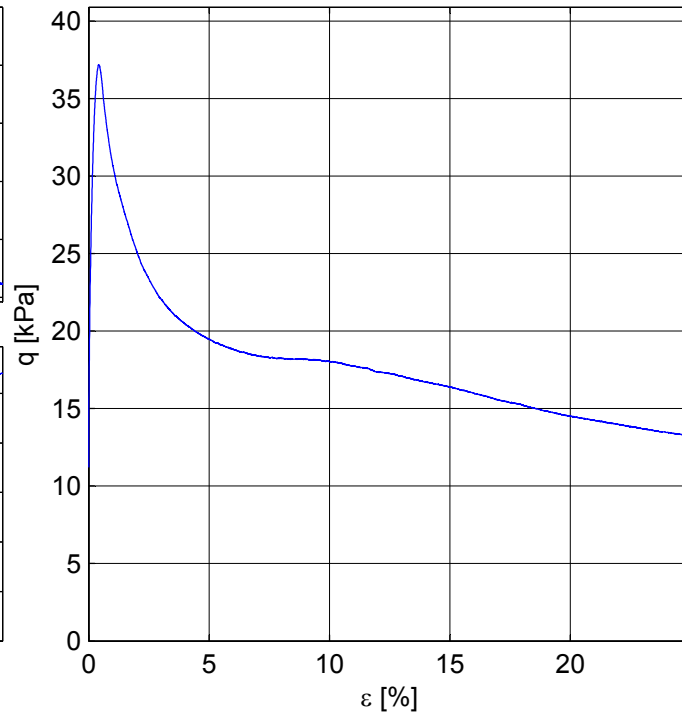
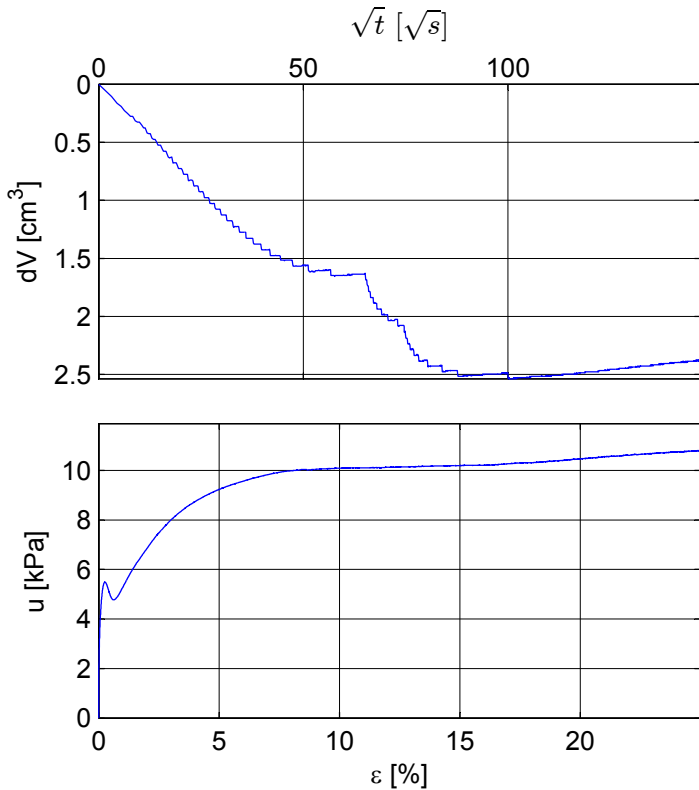
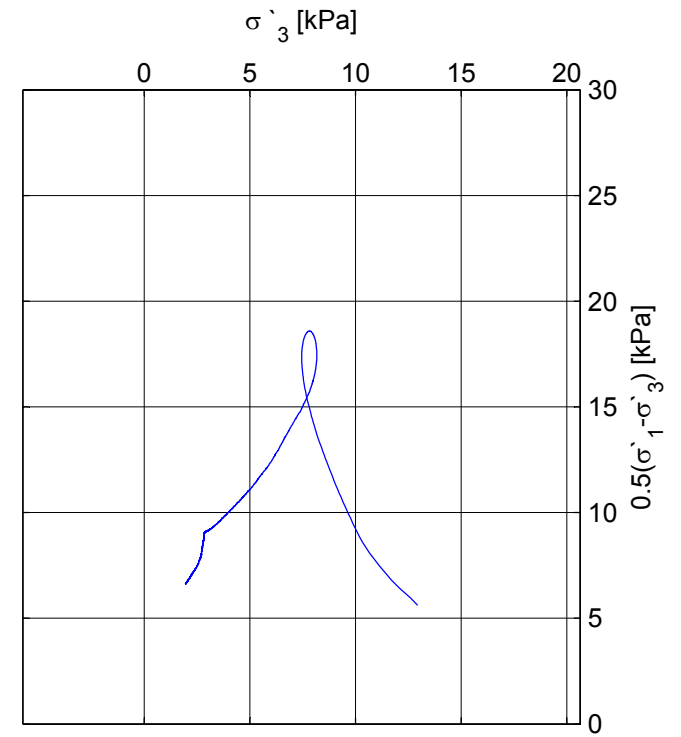
Treaxial test, Dragvoll bore hole 2. Stored in oxygen-free, distilled water

Mini Block sample D 4,75-5,0m

Depth: 4,895m
 Sampling date: 24.10.13
 Installed in storage cell: 4.12.13
 Opening date of block sample: 10.3.14
 Test date: 12.3.14
 strain rate: 1,5 %/hour
 1,1p₀-consolidation
 Note: Equipment error.



σ'_{vo}	= 34.27 kPa	σ'_c	= 80 kPa
w	= 41.87 %	OCR	= 2.45
γ	= 18.96 kN/m ³	D	= -0.22
ΔV	= 2.54 cm ³		
ϵ_v	= 1.09 %		
S _u	= 18.59 kPa		
ϵ_f	= 0.43 %		



Treaxial test, Dragvoll bore hole 2. Stored in oxygen-free, distilled water

Mini Block sample D 5,55-5,8m

Depth: 5,73m

Sampling date: 24.10.13

Installed in storage cell: 4.12.13

Opening date of block sample: 24.2.14

Test date: 24.2.14

strain rate: 1,5 %/hour

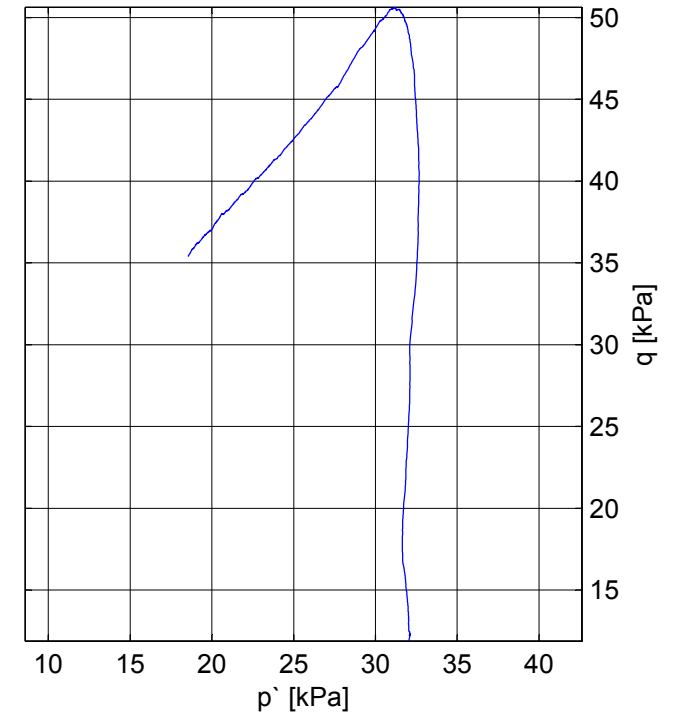
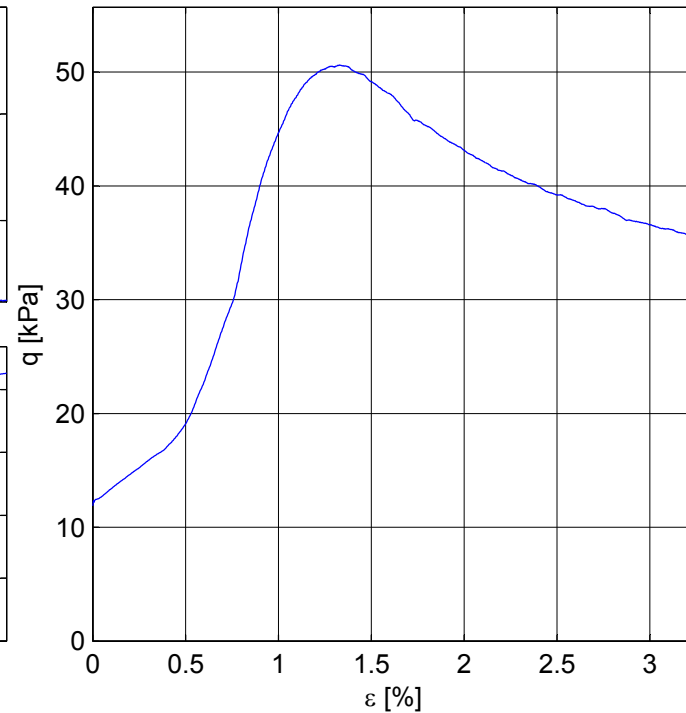
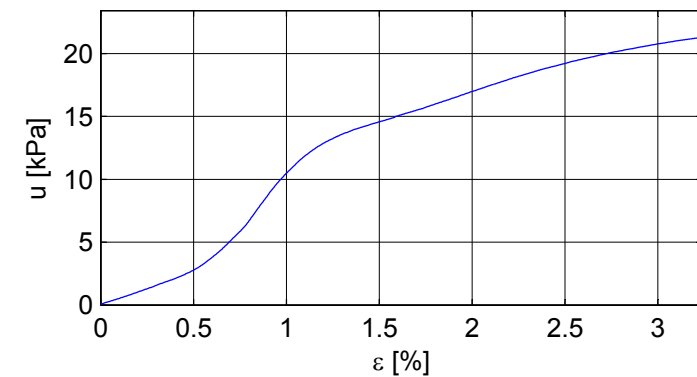
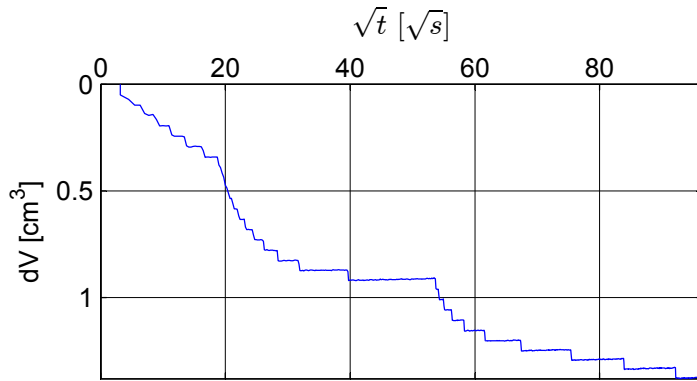
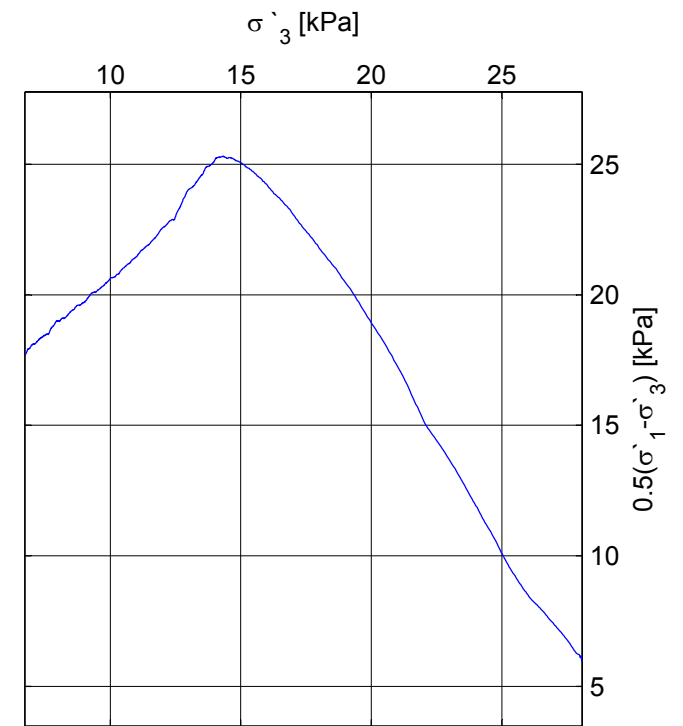
p'_0 -consolidation

Note: Power brakeage during shear phase.

σ'_{vo}	= 40.11 kPa	σ'_c	= 75 kPa
w	= - %	OCR	= 2.00
γ	= 18.79 kN/m ³	D	= -0.09

ΔV	= 1.38 cm ³
ε_v	= 0.60 %
S_u	= 25.32 kPa

ε_f = 1.33 %



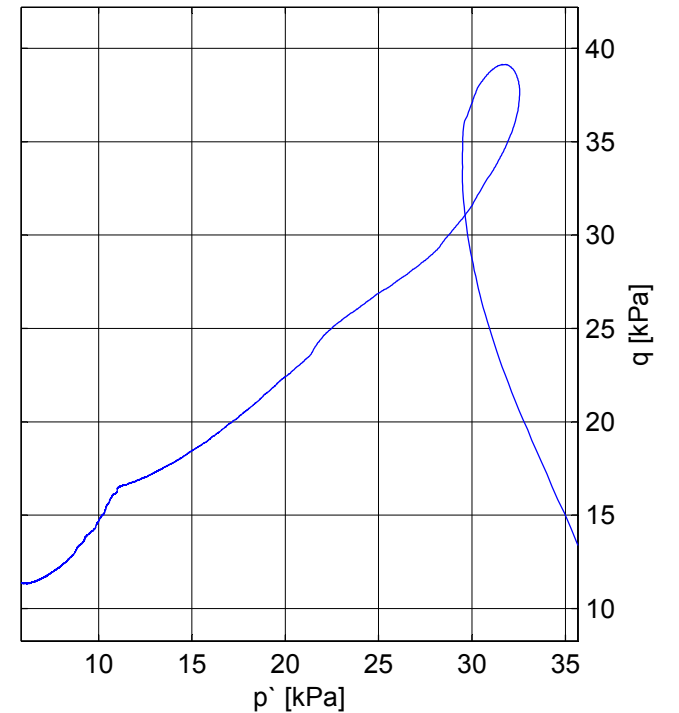
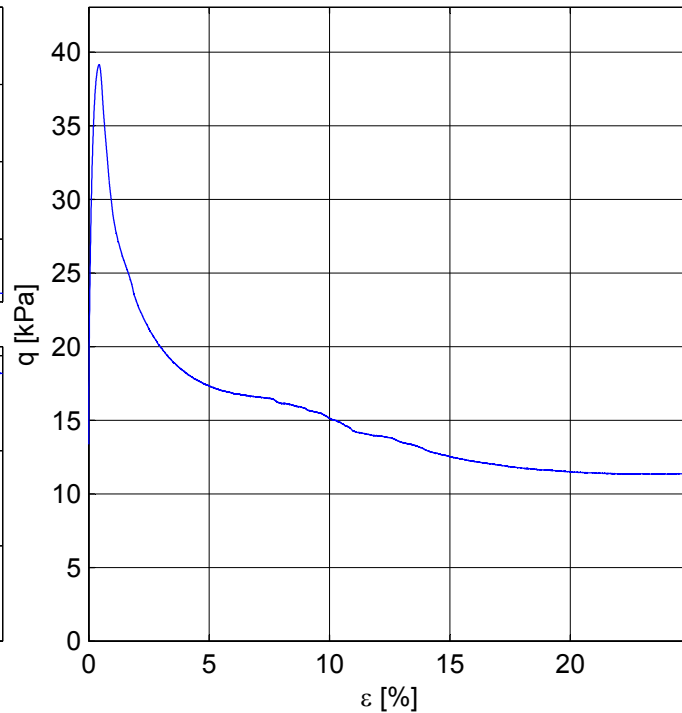
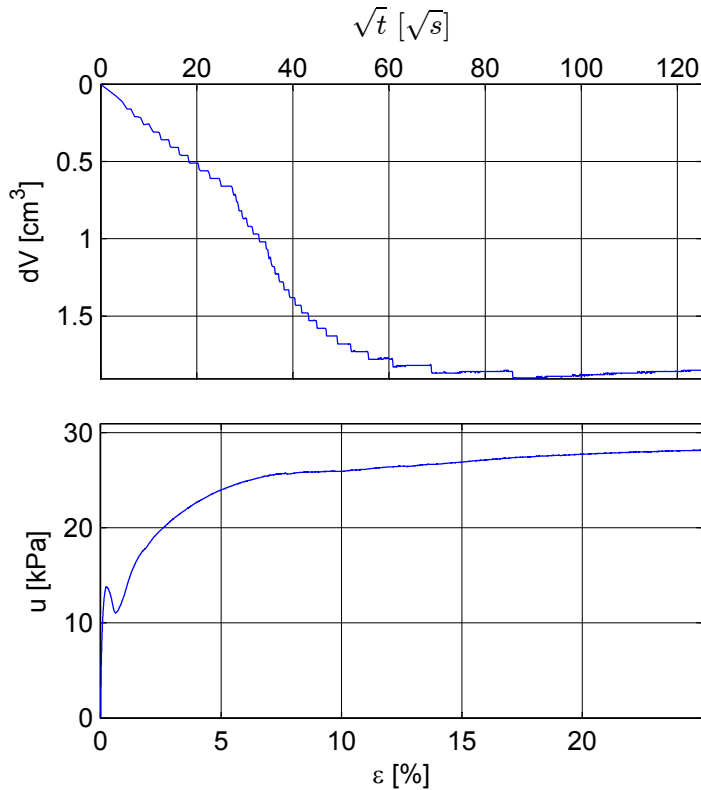
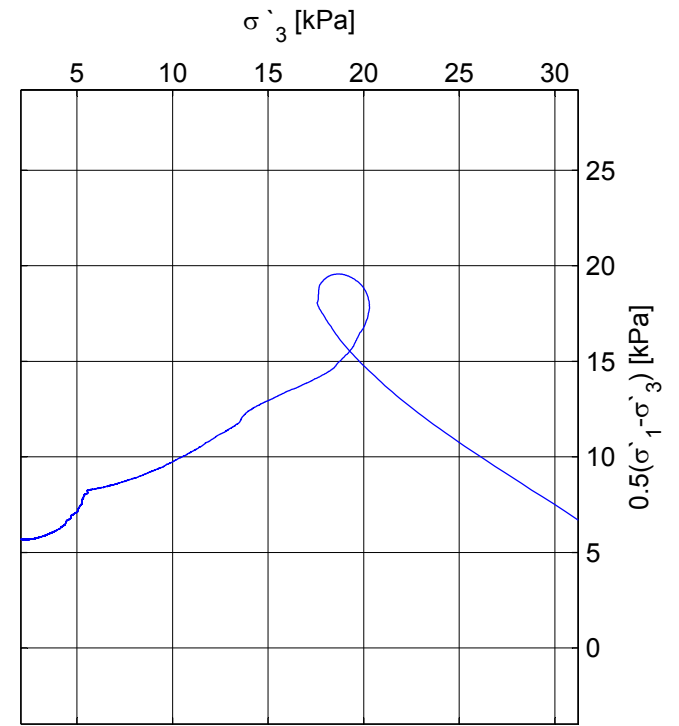
Treaxial test, Dragvoll bore hole 2. Stored in oxygen-free, distilled water

Mini Block sample D 5,55-5,8m

Depth: 5,73m
 Sampling date: 24.10.13
 Installed in storage cell: 4.12.13
 Opening date of block sample: 24.2.14
 Test date: 24.2.14
 strain rate: 1,5 %/hour
 1,1p₀-consolidation



σ'_{vo}	= 40.11 kPa	σ'_c	= 75 kPa
w	= 41.08 %	OCR	= 2.00
γ	= 18.89 kN/m ³	D	= -0.44
ΔV	= 1.91 cm ³		
ϵ_v	= 0.82 %		
S_u	= 19.57 kPa		
ϵ_f	= 0.44 %		



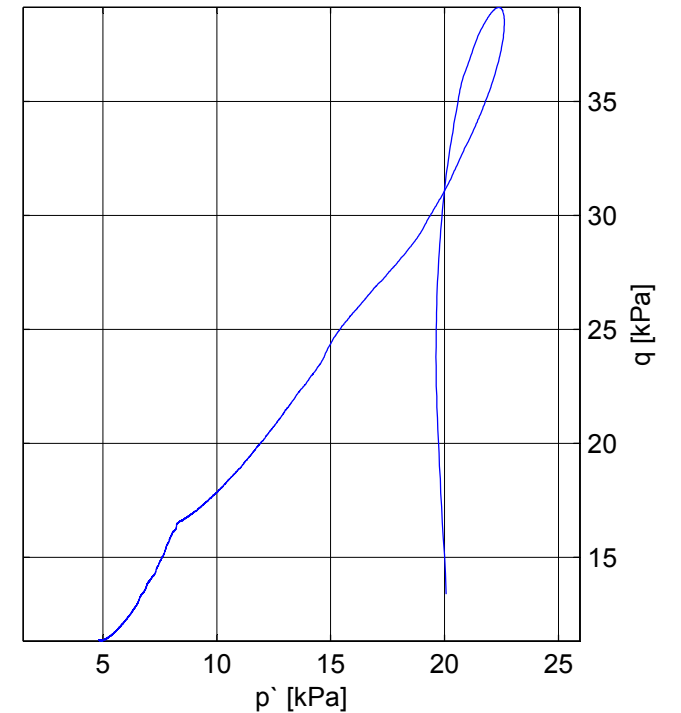
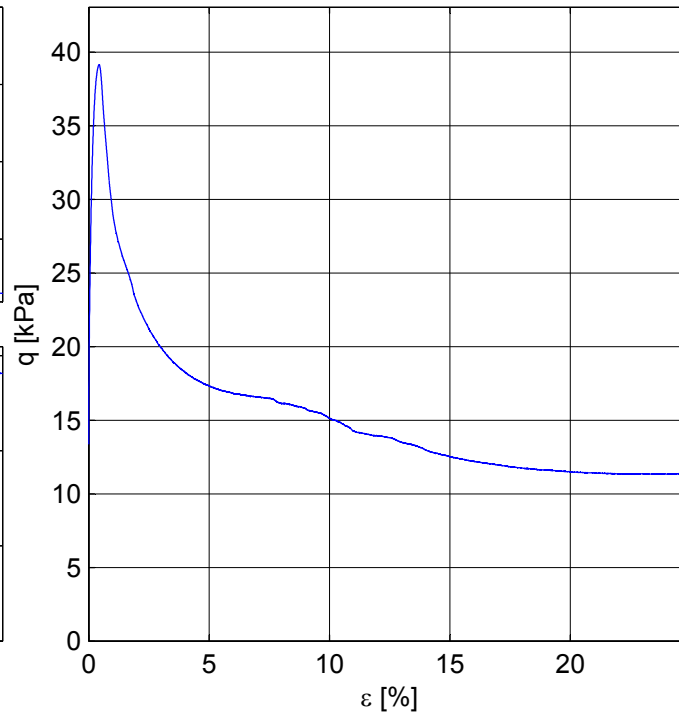
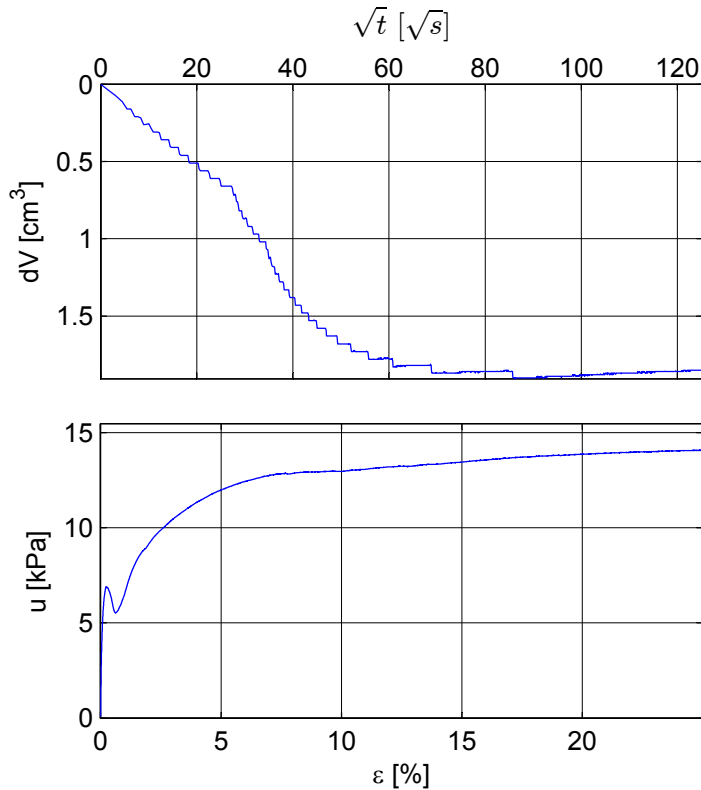
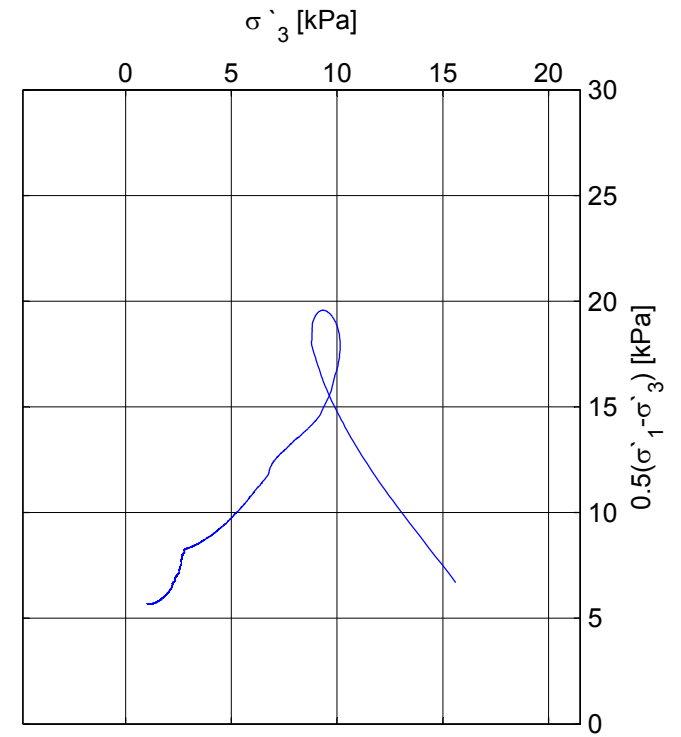
Treaxial test, Dragvoll bore hole 2. Stored in oxygen-free, distilled water

Mini Block sample D 5,55-5,8m

Depth: 5,73m
 Sampling date: 24.10.13
 Installed in storage cell: 4.12.13
 Opening date of block sample: 24.2.14
 Test date: 24.2.14
 strain rate: 1,5 %/hour
 1,1p₀-consolidation
 Note: Equipment error.



σ'_{vo}	= 40.11 kPa	σ'_c	= 75 kPa
w	= 41.08 %	OCR	= 1.88
γ	= 18.89 kN/m ³	D	= -0.05
ΔV	= 1.91 cm ³		
ϵ_v	= 0.82 %		
S _u	= 19.57 kPa		
ϵ_f	= 0.44 %		

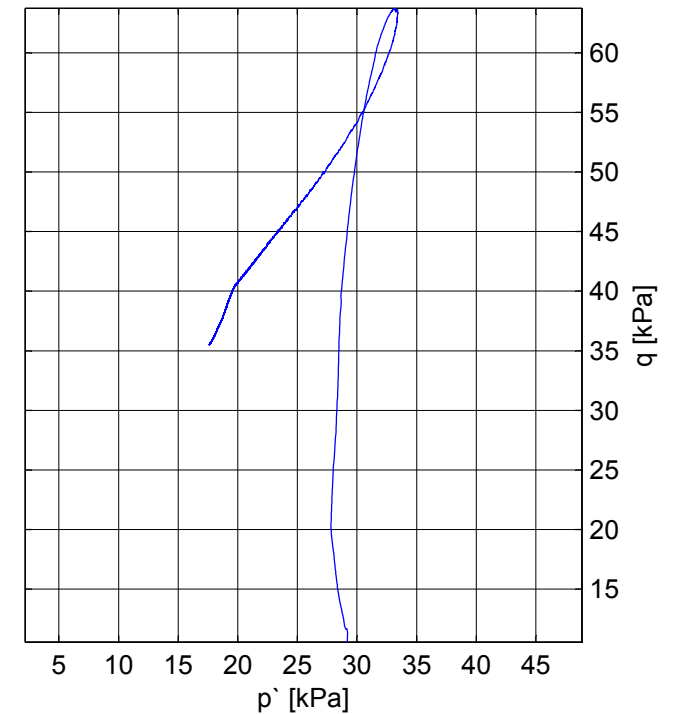
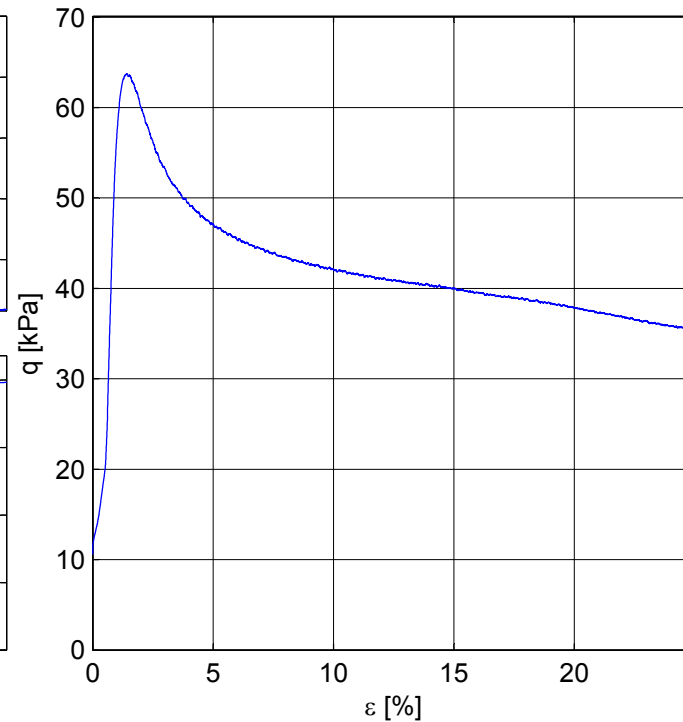
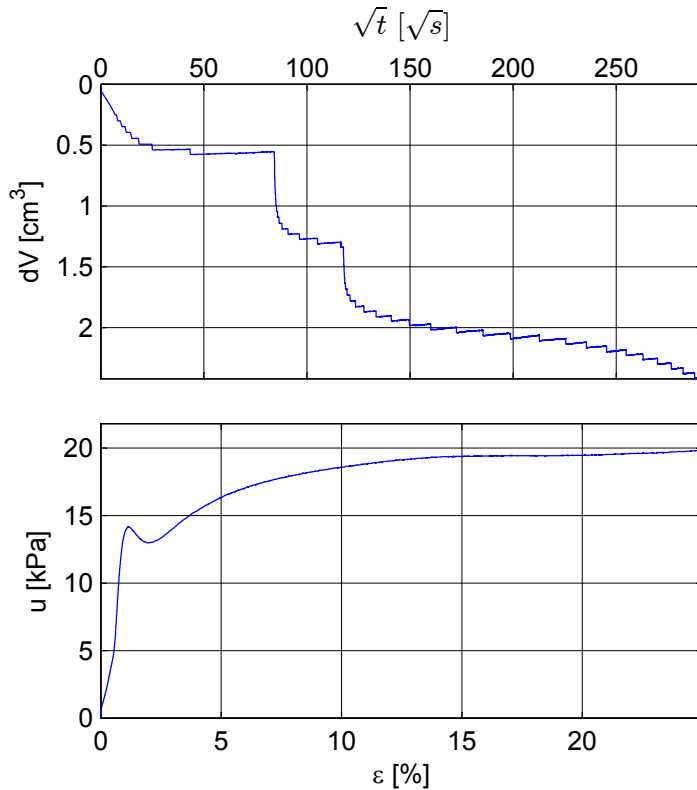
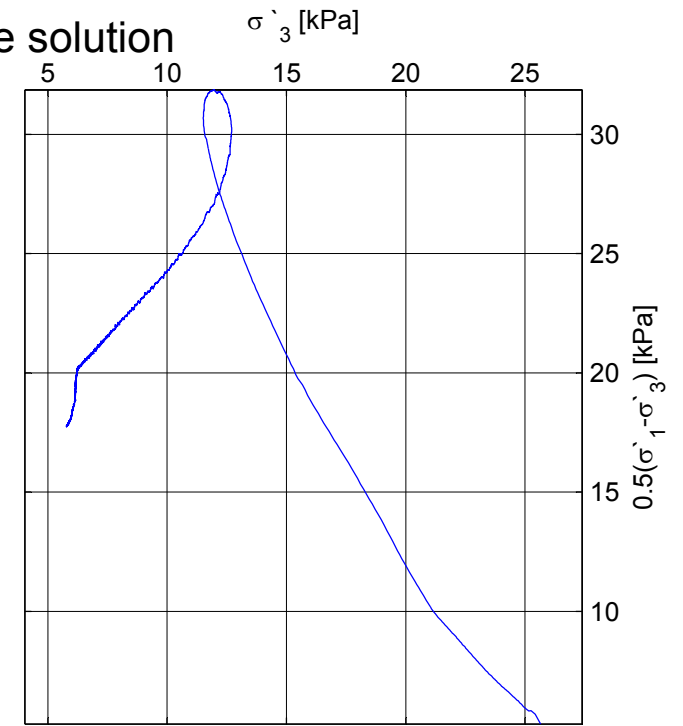
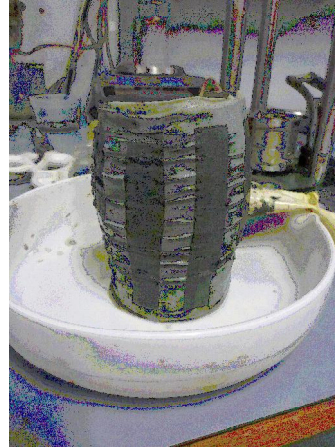


Treaxial test, Dragvoll bore hole 2. Stored in saturated potassium chloride solution

Mini Block sample D 5,05-5,3m

Depth: 5,245m
 Sampling date: 24.10.13
 Installed in storage cell: 4.12.13
 Opening date of block sample: 18.2.14
 Test date: 19.2.14
 strain rate: 1,5 %/hour
 p'_0 -consolidation

σ'_{vo}	= 36.72 kPa	σ'_c	= 100 kPa
w	= 34.26 %	OCR	= 2.71
γ	= 19.52 kN/m ³	D	= -0.29
ΔV	= 2.42 cm ³		
ε_v	= 1.04 %		
S_u	= 31.87 kPa		
ε_f	= 1.42 %		

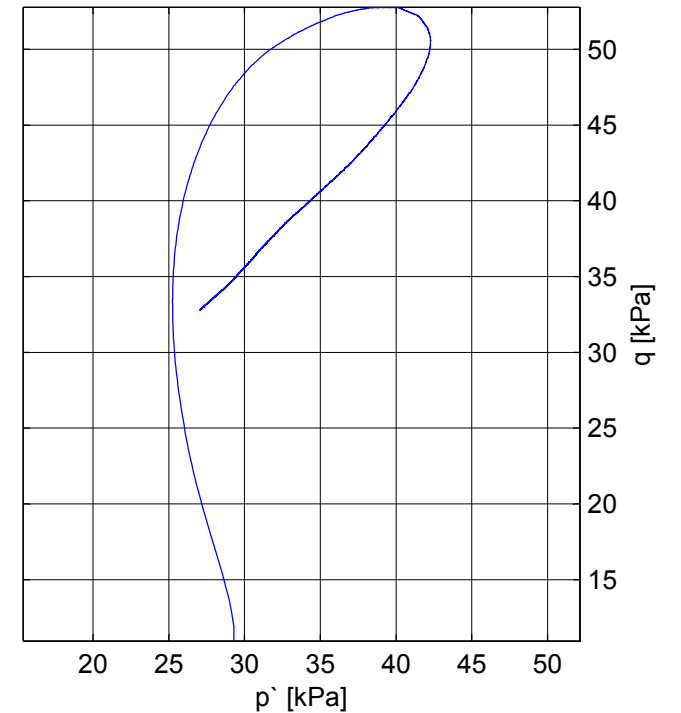
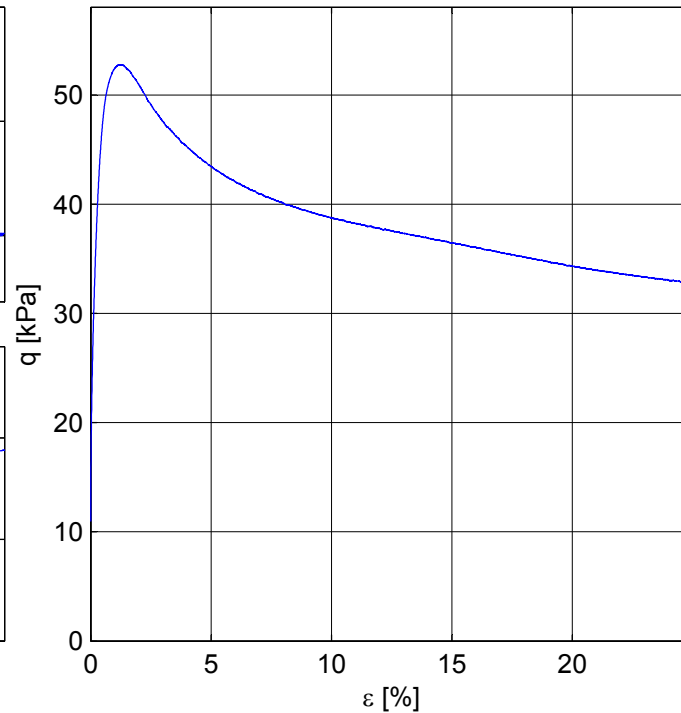
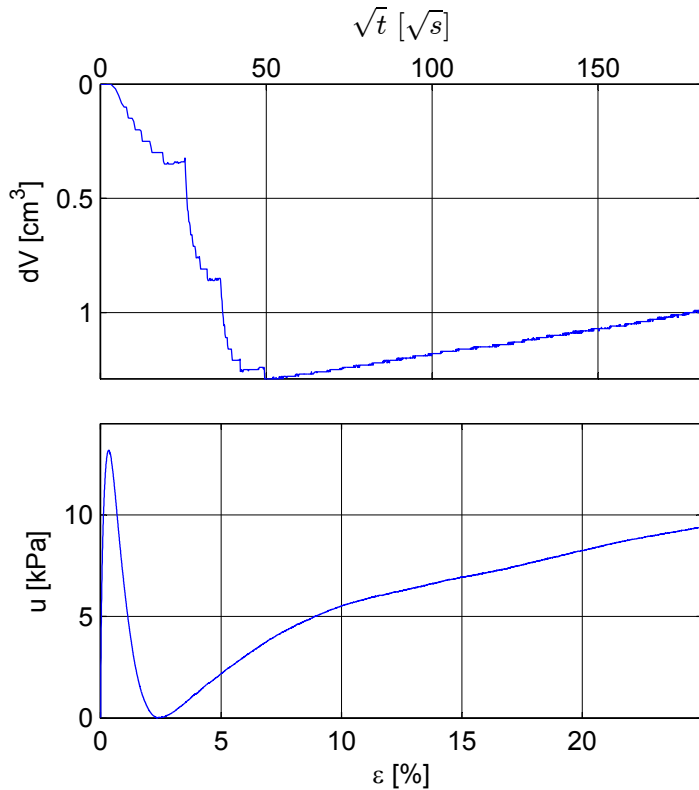
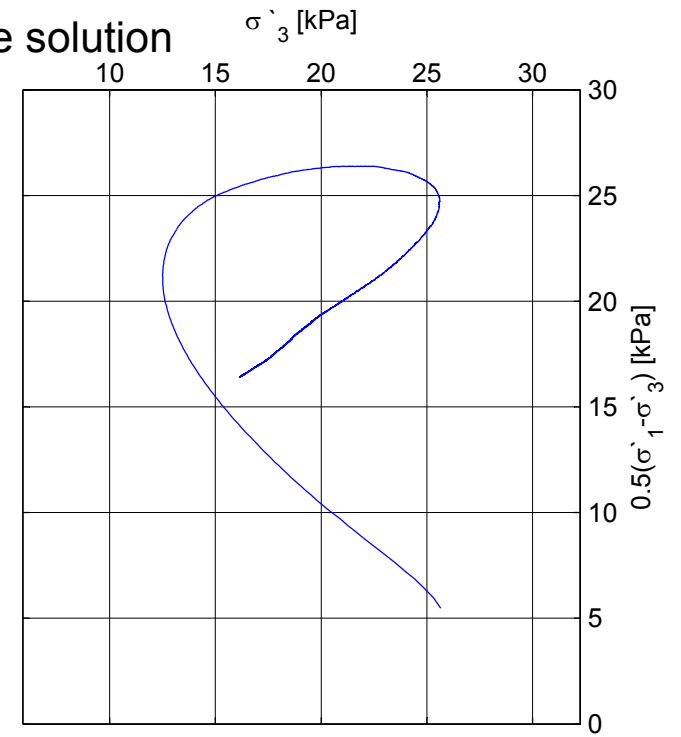


Treaxial test, Dragvoll bore hole 2. Stored in saturated potassium chloride solution

Mini Block sample D 5,05-5,3m

Depth: 5,245m
 Sampling date: 24.10.13
 Installed in storage cell: 4.12.13
 Opening date of block sample: 18.2.14
 Test date: 19.2.14
 strain rate: 1,5 %/hour
 p'_0 -consolidation

σ'_{vo}	= 36.72 kPa	σ'_c	= 100 kPa
w	= 34.26 %	OCR	= 2.71
γ	= 19.52 kN/m ³	D	= -0.13
ΔV	= 1.29 cm ³		
ε_v	= 0.56 %		
S_u	= 26.39 kPa		
ε_f	= 1.28 %		

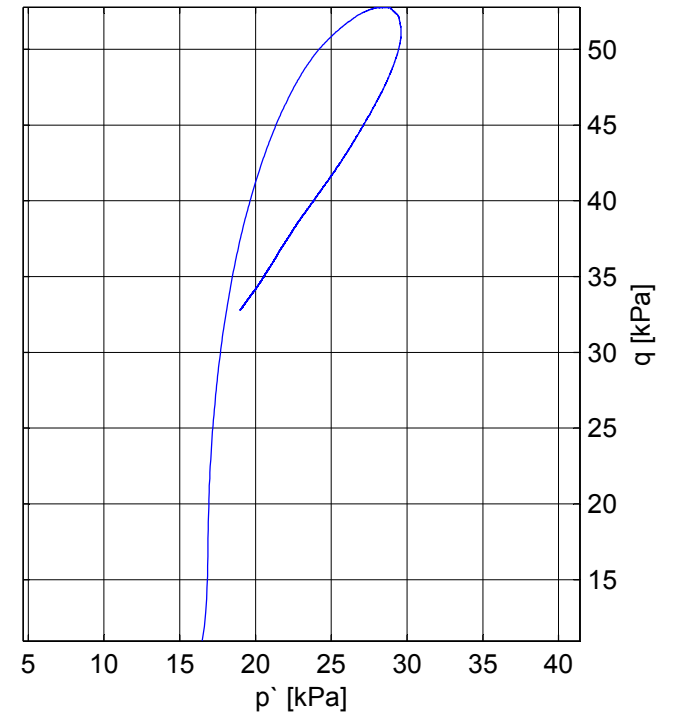
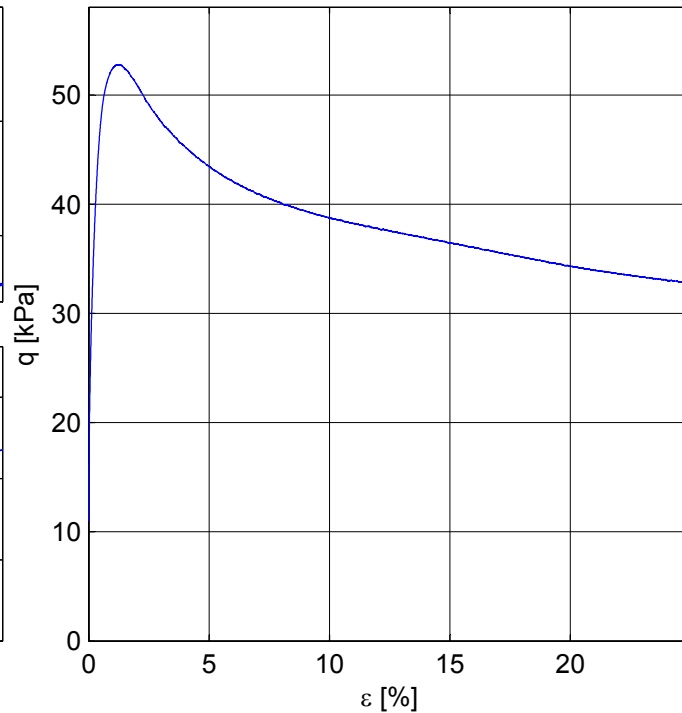
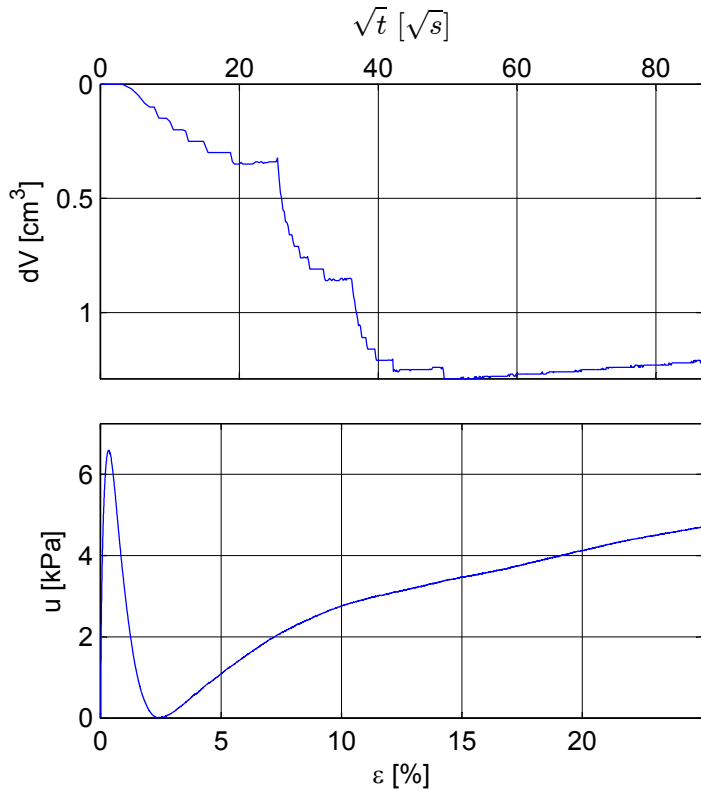
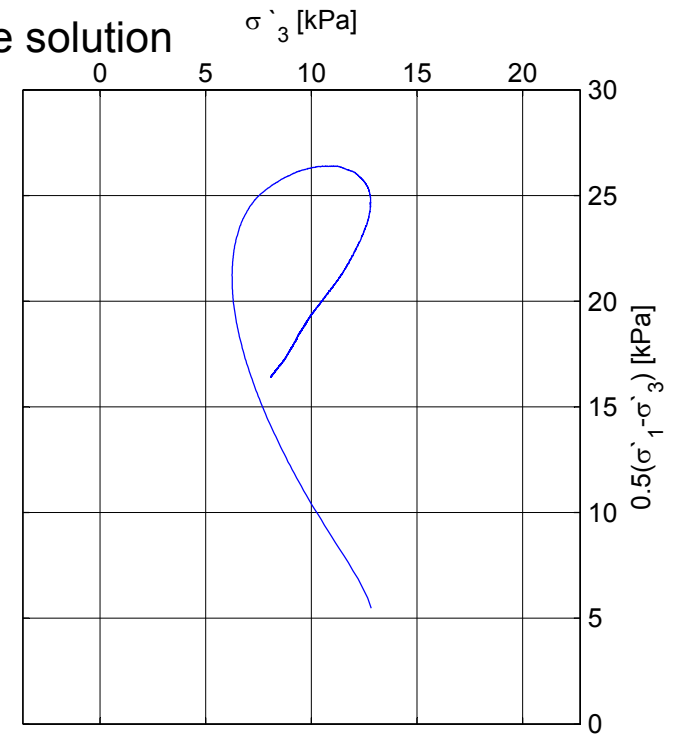


Treaxial test, Dragvoll bore hole 2. Stored in saturated potassium chloride solution

Mini Block sample D 5,05-5,3m

Depth: 5,245m
 Sampling date: 24.10.13
 Installed in storage cell: 4.12.13
 Opening date of block sample: 18.2.14
 Test date: 19.2.14
 strain rate: 1,5 %/hour
 p'_0 -consolidation
 Note: Equipment error.

σ'_{vo}	= 36.72 kPa	σ'_c	= 100 kPa
w	= 34.26 %	OCR	= 2.71
γ	= 19.52 kN/m ³	D	= 0.04
ΔV	= 1.29 cm ³		
ϵ_v	= 0.56 %		
S_u	= 26.39 kPa		
ϵ_f	= 1.28 %		



Treaxial test, Dragvoll bore hole 2. Stored in saturated potassium chloride solution

Mini Block sample D 7,45-7,7m

Depth: 7,615m

Sampling date: 30.10.13

Installed in storage cell: 4.12.13

Opening date of block sample: 10.3.14

Test date: 11.3.14

strain rate: 1,5 %/hour

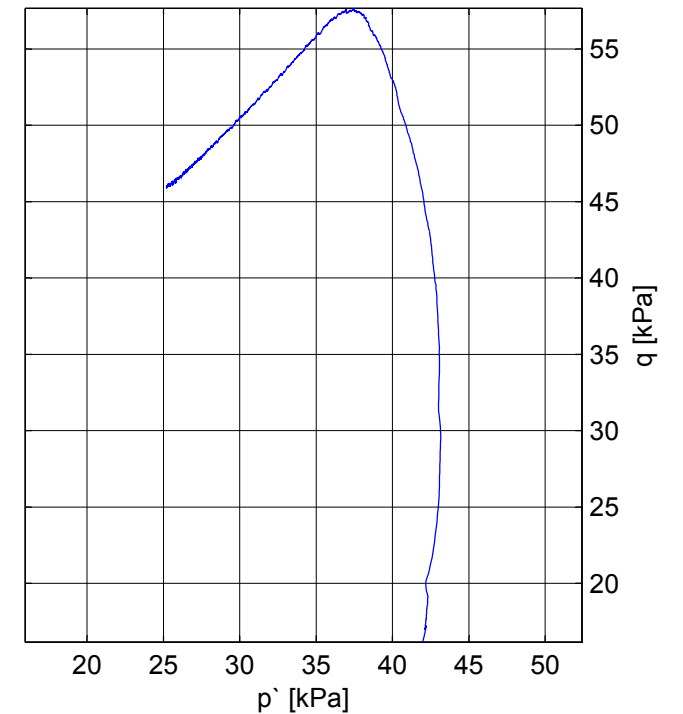
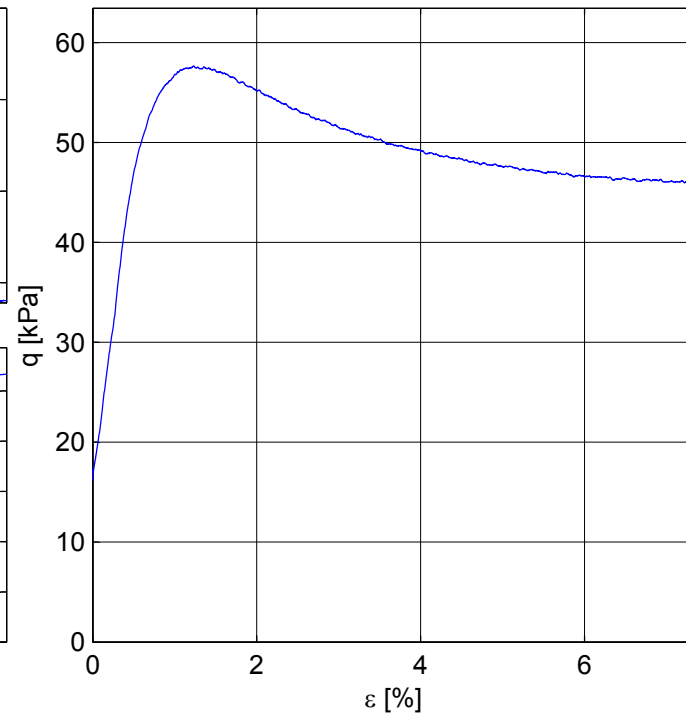
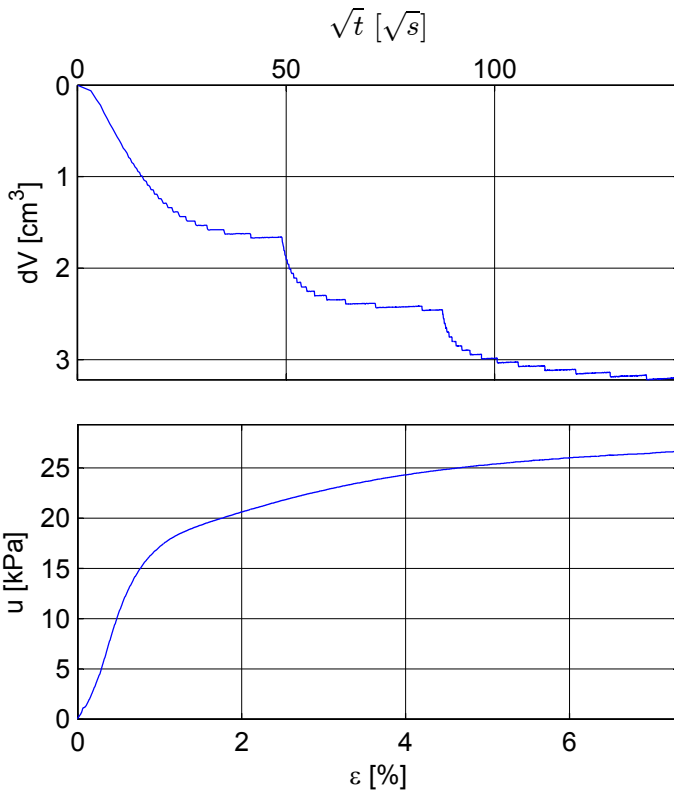
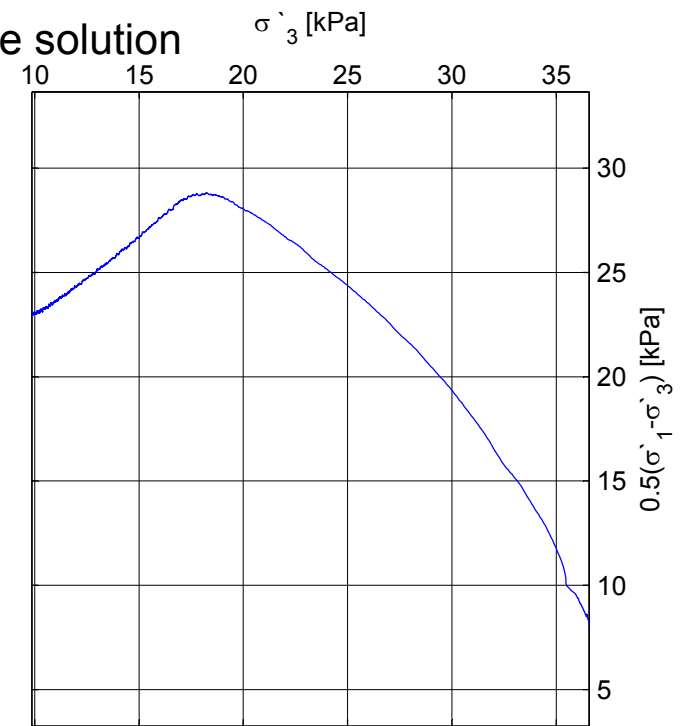
p'_0 -consolidation

Note: Power brakeage during shear phase.

σ'_{vo}	= 53.31 kPa	σ'_c	= 115 kPa
w	= 30.68 %	OCR	= 1.89
γ	= 19.90 kN/m ³	D	= 0.10

ΔV	= 3.22 cm ³
ε_v	= 1.39 %
S_u	= 28.84 kPa

ε_f = 1.23 %

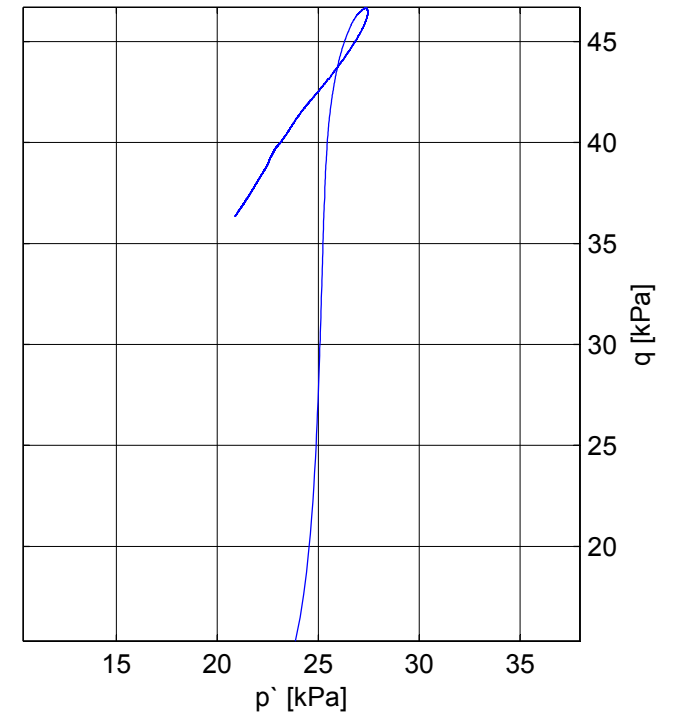
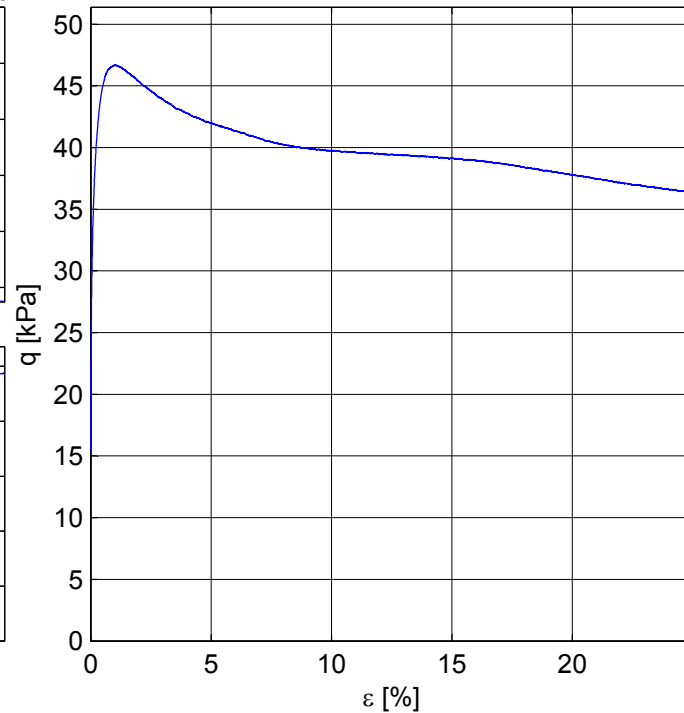
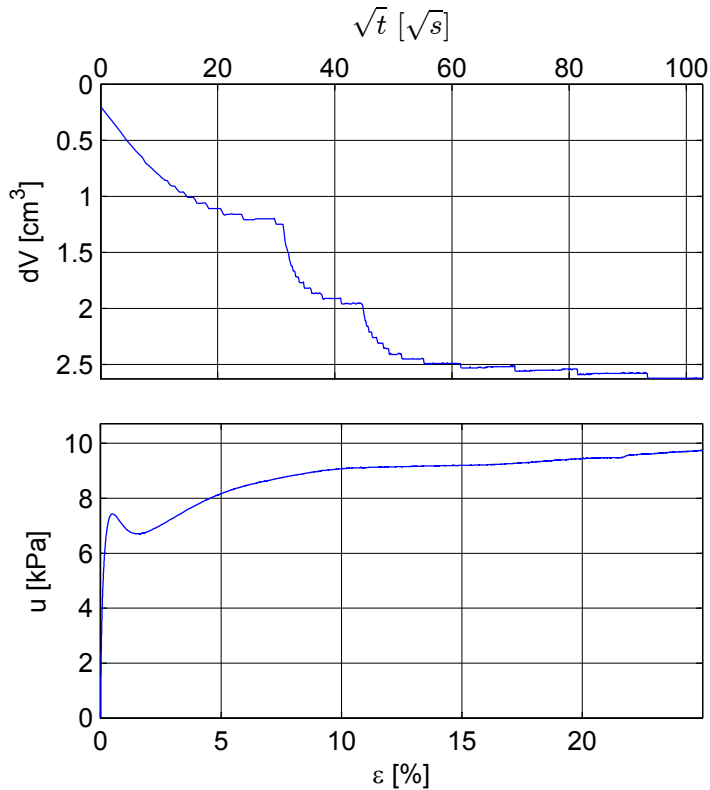
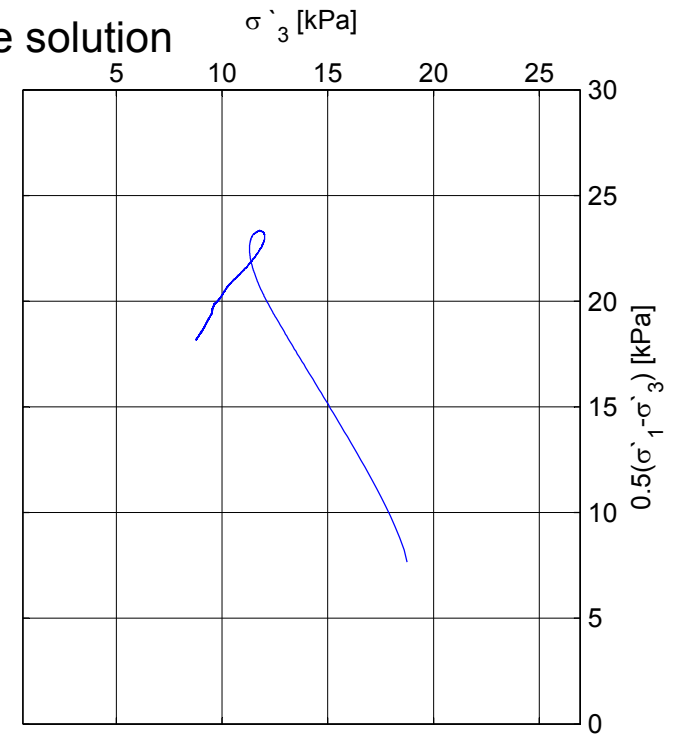


Treaxial test, Dragvoll bore hole 2. Stored in saturated potassium chloride solution

Mini Block sample D 7,45-7,7m

Depth: 7,615m
 Sampling date: 30.10.13
 Installed in storage cell: 4.12.13
 Opening date of block sample: 10.3.14
 Test date: 11.3.14
 strain rate: 1,5 %/hour
 p₀-consolidation test 2
 Note: Equipment error.

σ'_{vo}	= 53.31 kPa	σ'_c	= 115 kPa
w	= 29.79 %	OCR	= 1.89
γ	= 20.20 kN/m ³	D	= 0.09
ΔV	= 2.63 cm ³		
ϵ_v	= 1.13 %		
S_u	= 23.35 kPa		
ϵ_f	= 0.99 %		



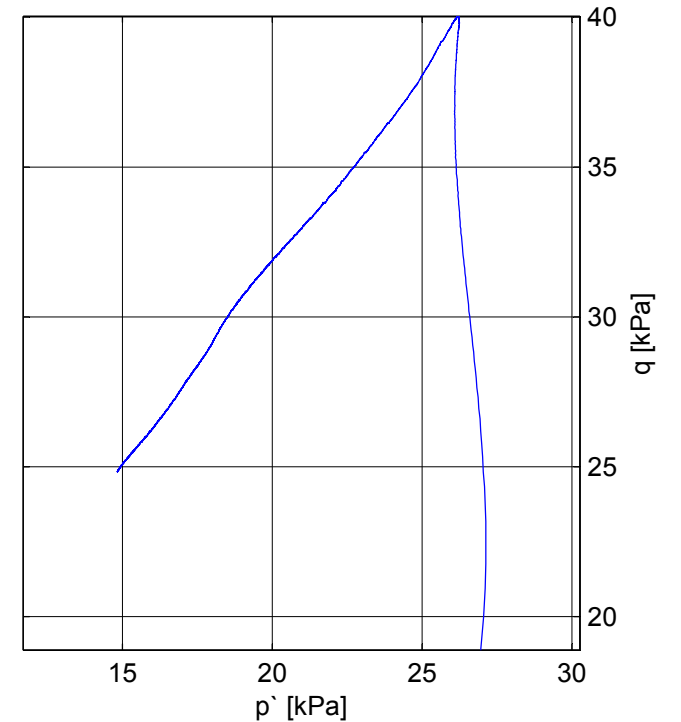
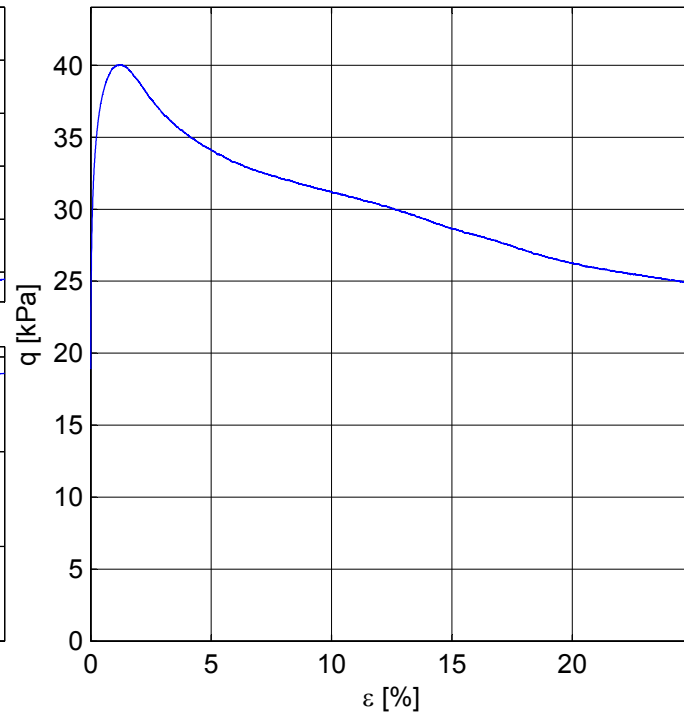
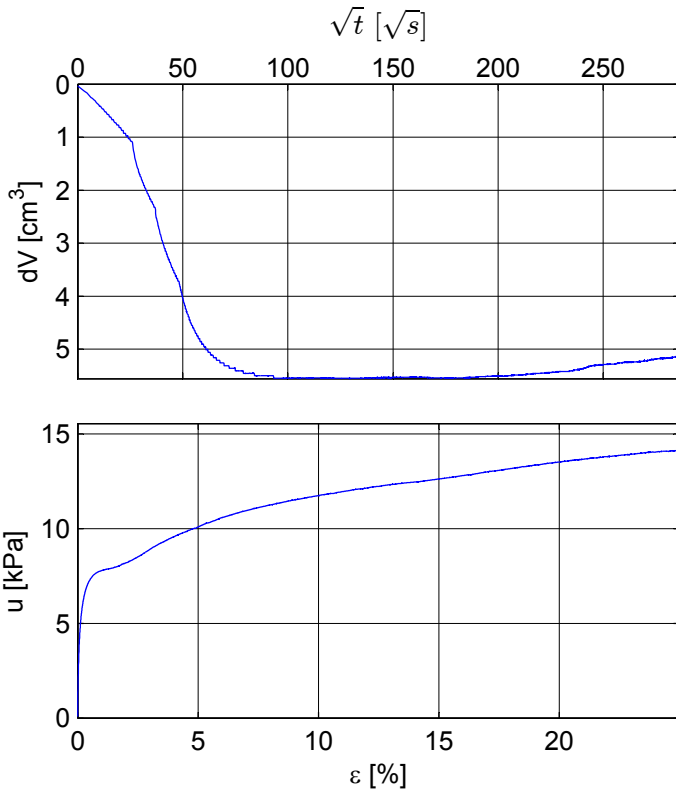
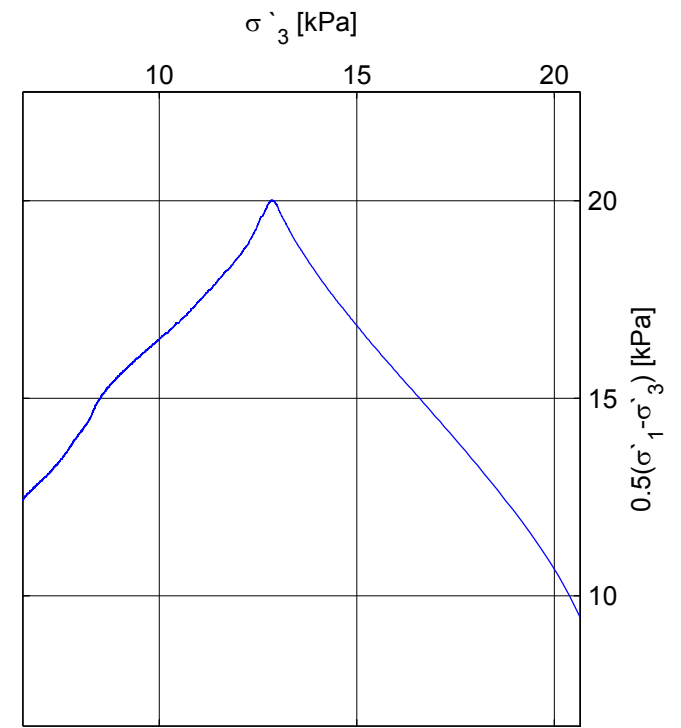
Treaxial test, Dragvoll bore hole 2. Stored in oxygen-free, distilled water

Mini Block sample D 8,2-8,45m

Depth: 8,39m
 Sampling date: 30.10.13
 Installed in storage cell: 4.12.13
 Opening date of block sample: 16.3.14
 Test date: 16.3.14
 strain rate: 1,5 %/hour
 p₀-consolidation test 2
 Note: Equipment error.



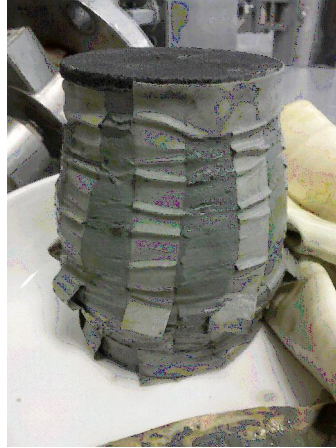
σ'_{vo}	= 58.73 kPa	σ'_c	= 70 kPa
w	= 32.07 %	OCR	= 1.20
γ	= 19.61 kN/m ³	D	= -0.06
ΔV	= 5.56 cm ³		
ε_v	= 2.40 %		
S _u	= 20.02 kPa		
ε_f	= 1.21 %		



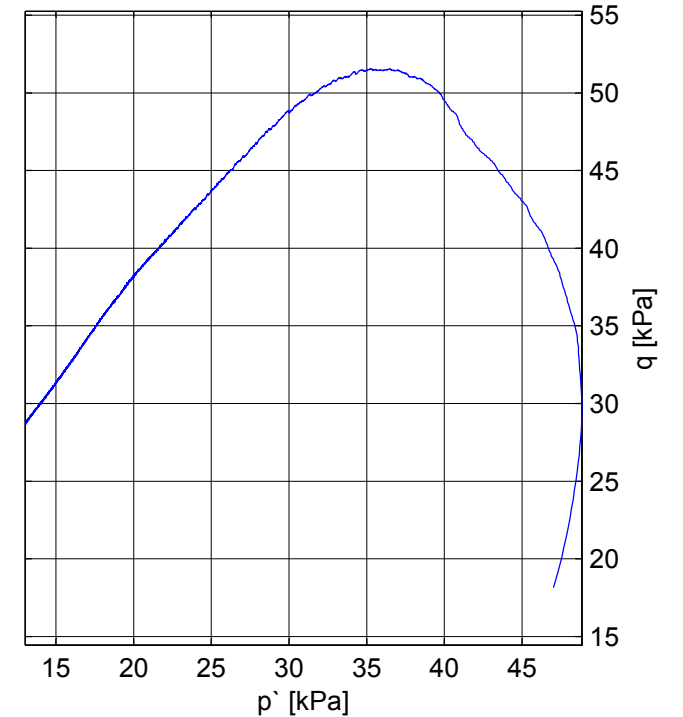
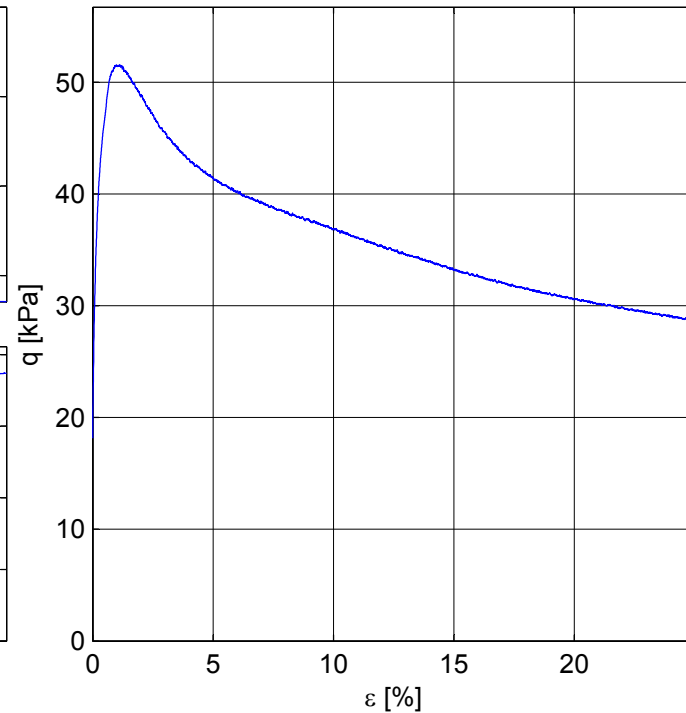
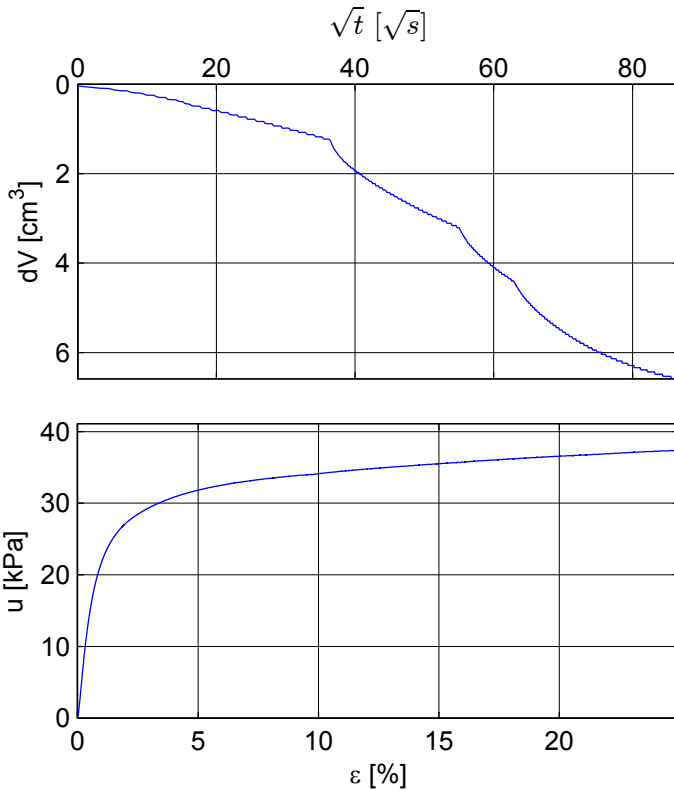
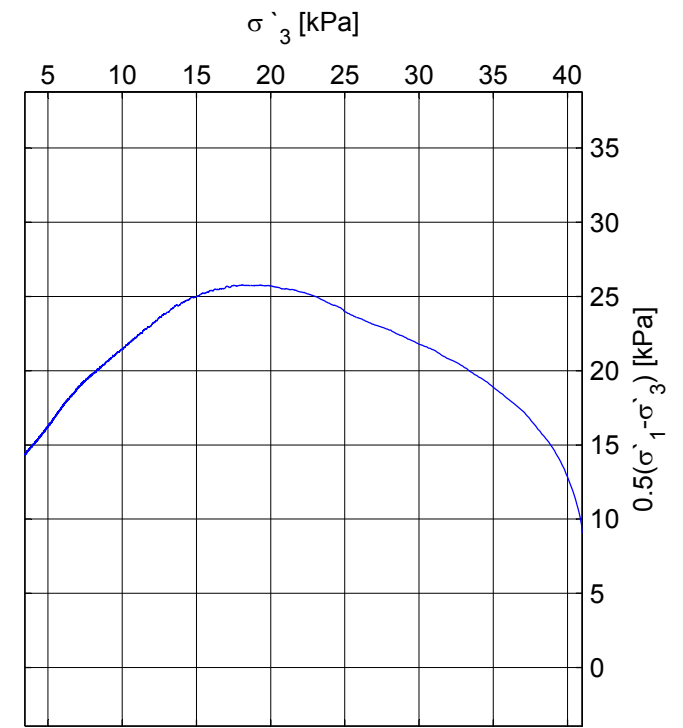
Treaxial test, Dragvoll bore hole 2. Stored in oxygen-free, distilled water

Mini Block sample D 8,2-8,45m

Depth: 8,39m
 Sampling date: 30.10.13
 Installed in storage cell: 4.12.13
 Opening date of block sample: 16.3.14
 Test date: 16.3.14
 strain rate: 1,5 %/hour
 p'_0 -consolidation



σ'_{vo}	= 58.73 kPa	σ'_c	= 70 kPa
w	= 34.27 %	OCR	= 1.20
γ	= 19.48 kN/m ³	D	= 0.17
ΔV	= 6.59 cm ³		
ε_v	= 2.84 %		
S_u	= 25.78 kPa		
ε_f	= 1.12 %		



Appendix H

Oedometer comparison

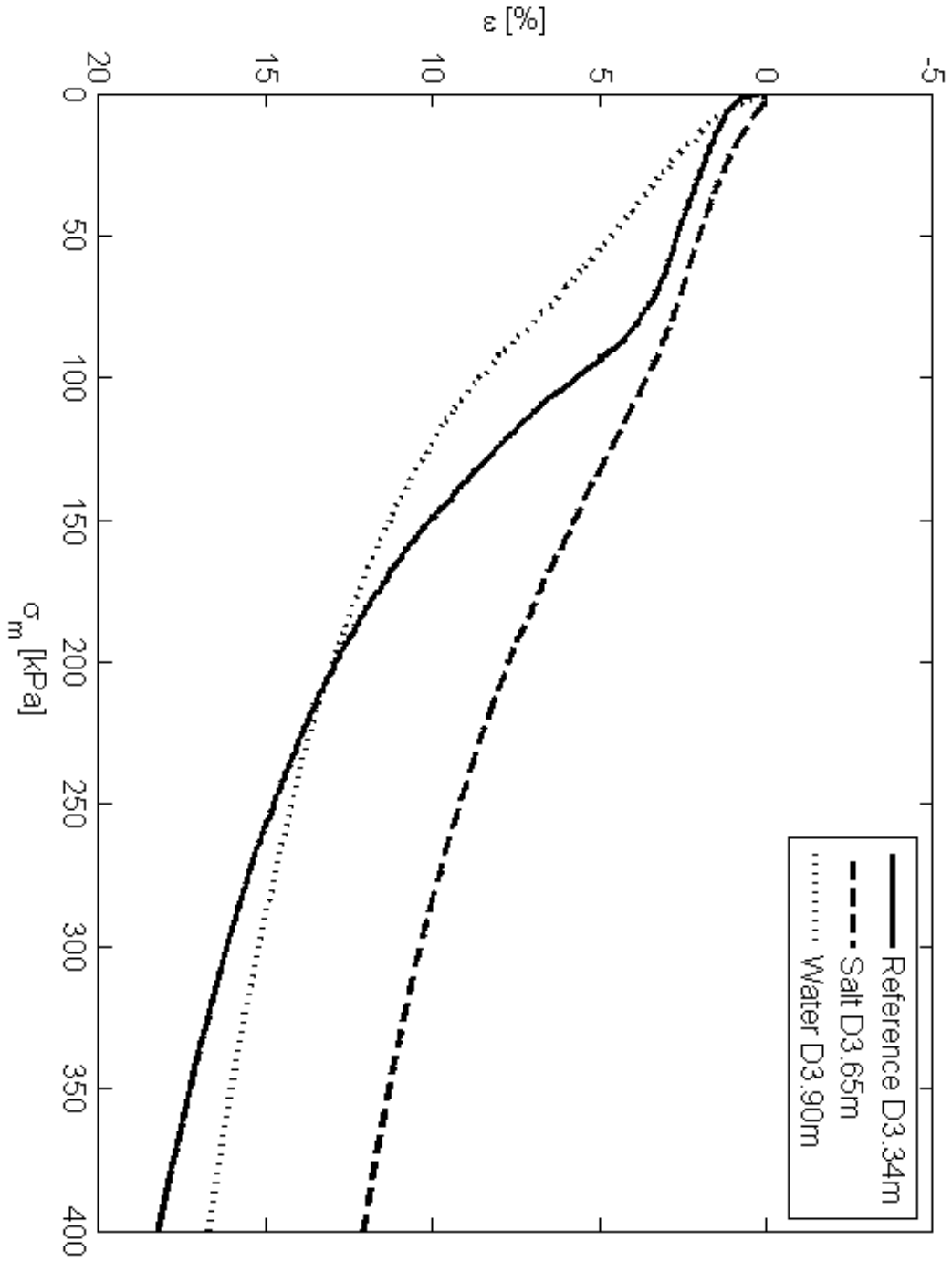


Figure H.1: Comparison of storage method, preconsolidation pressure

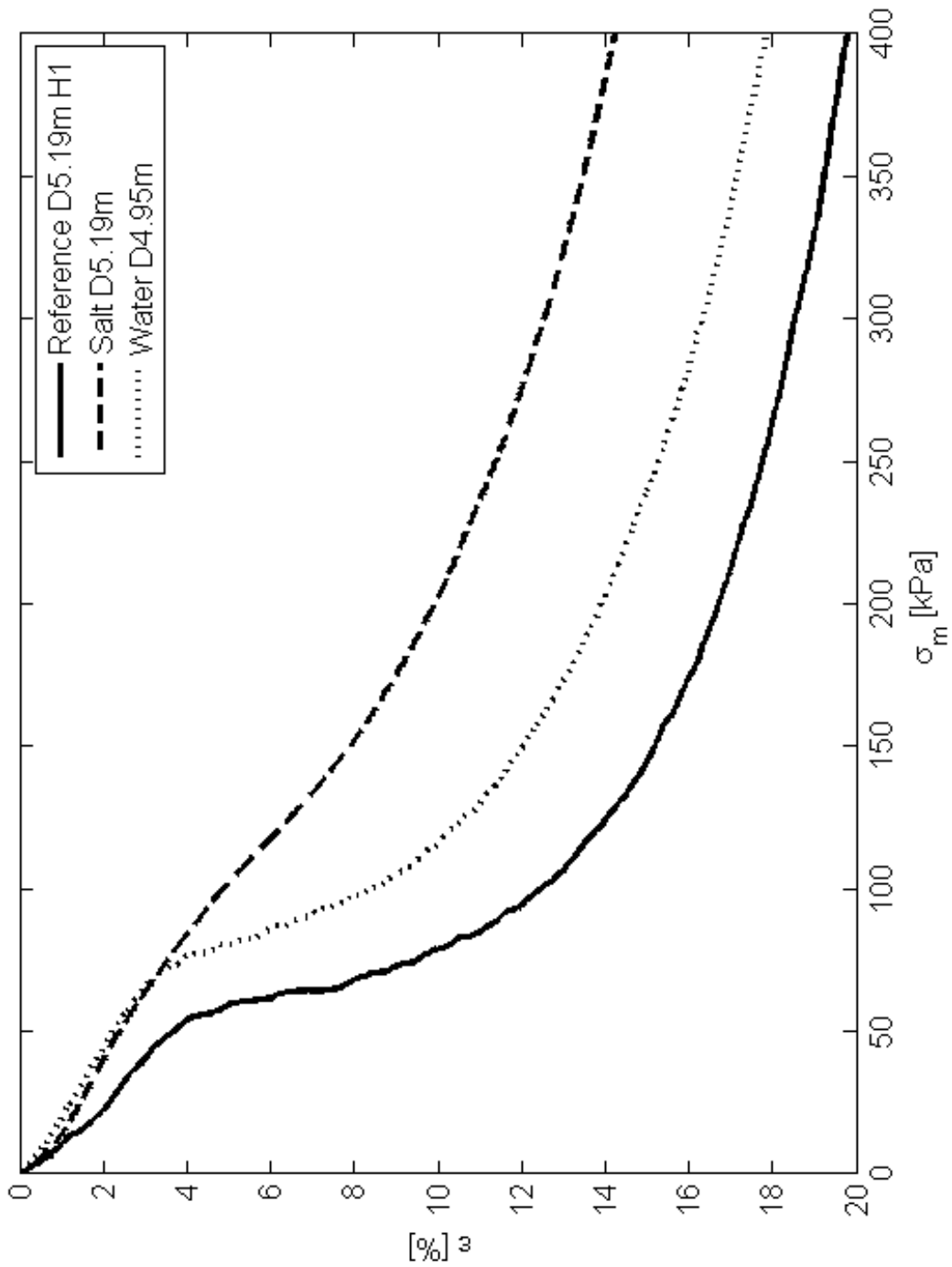


Figure H.2: Comparison of storage method, preconsolidation pressure

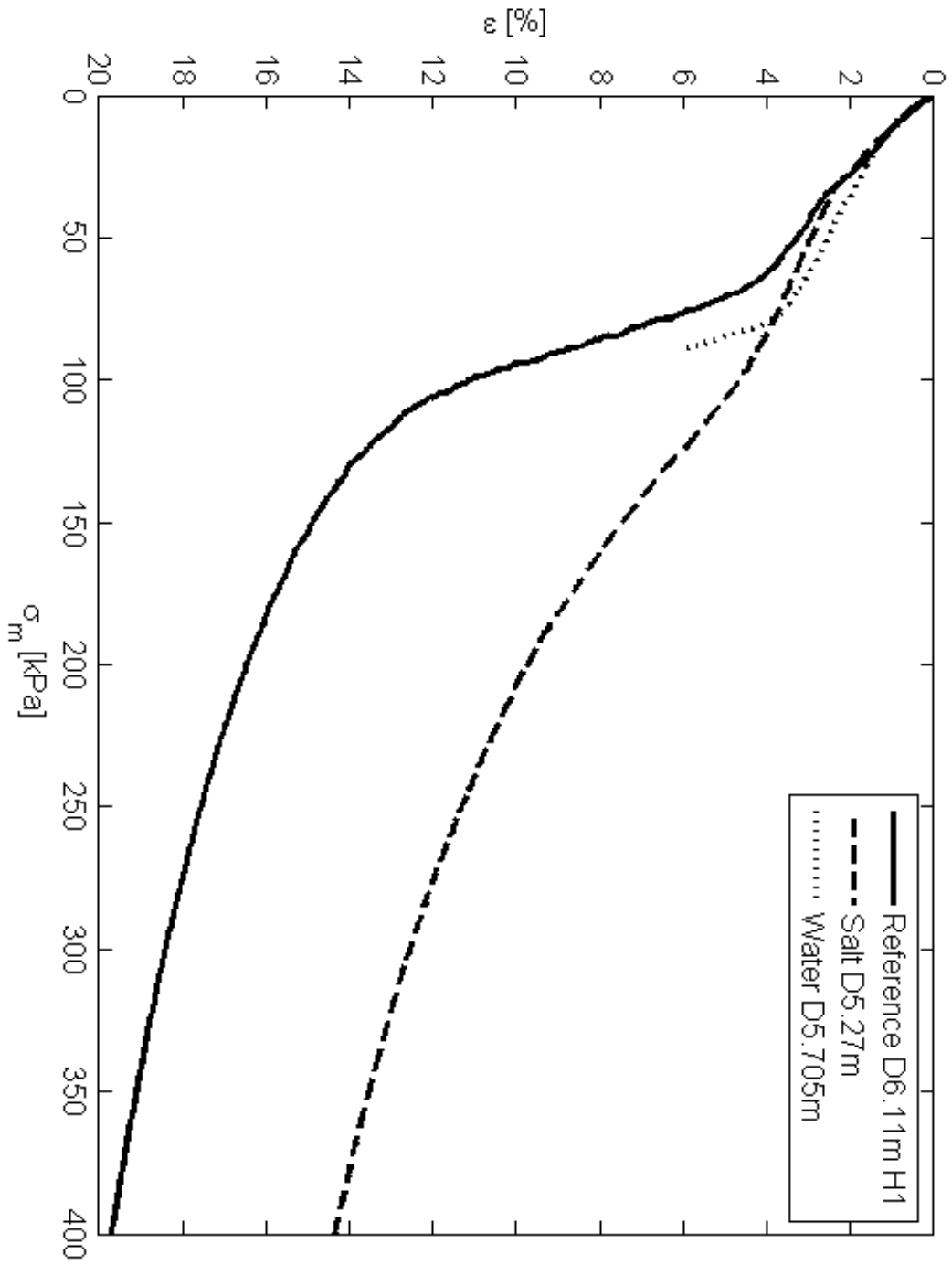


Figure H.3: Comparison of storage method, preconsolidation pressure

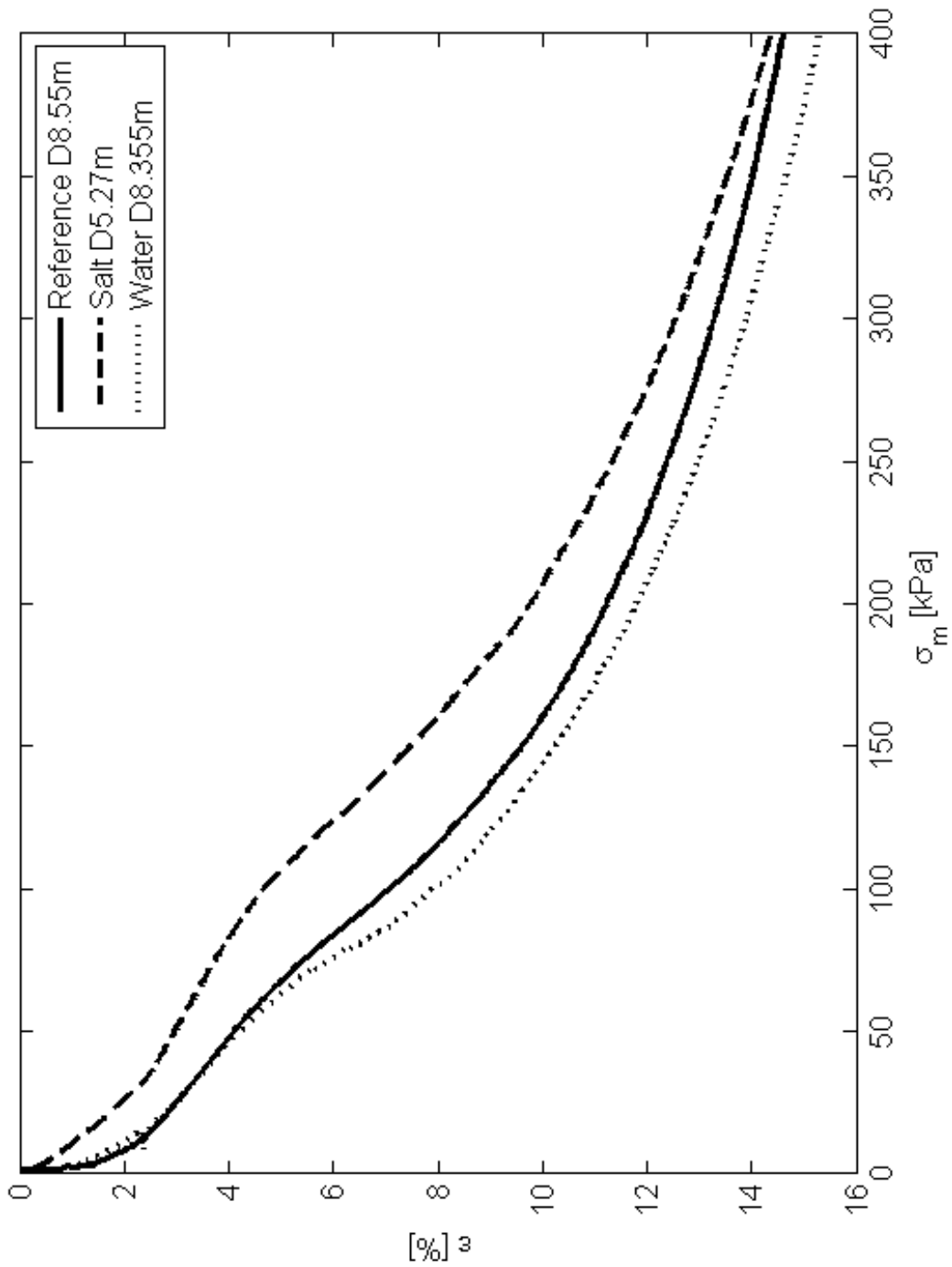


Figure H.4: Comparison of storage method, preconsolidation pressure

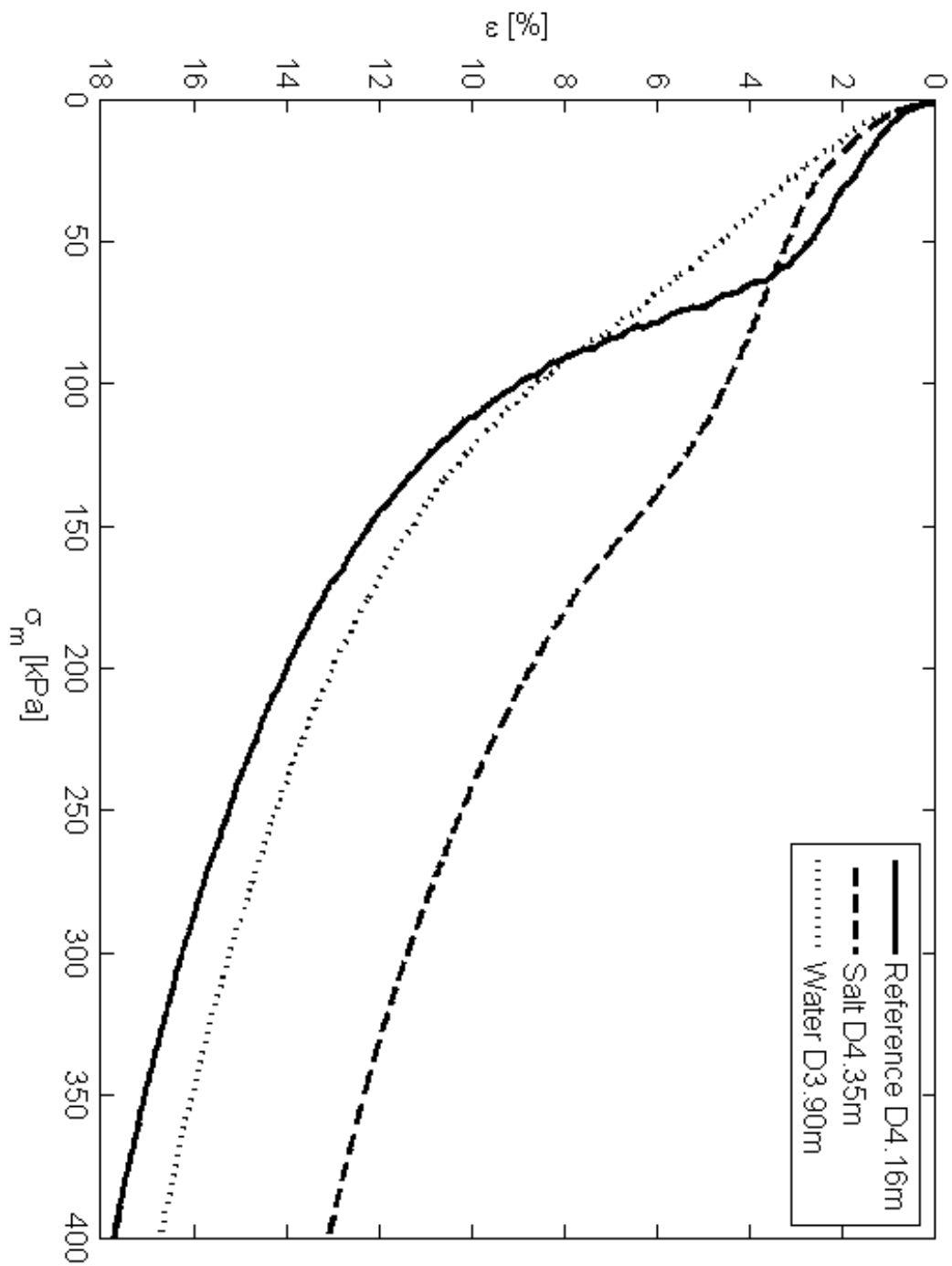


Figure H.5: Comparison of storage method, preconsolidation pressure